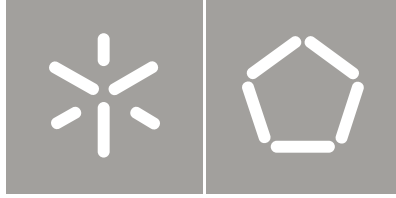Universidade do Minho
Escola de Engenharia

Ana Cristina Magalhães Ferreira

Numerical Optimization and Economic
Analysis in the design of a Micro-CHP System
with a Stirling engine and a Solar Collector

April, 2014

Universidade do Minho
Escola de Engenharia

Ana Cristina Magalhães Ferreira

Numerical Optimization and Economic
Analysis in the design of a Micro-CHP System
with a Stirling engine and a Solar Collector

Otimização Numérica e Análise Económica
na Conceção de uma Micro-Cogeração com
motor Stirling e Concentrador Solar

Doctoral Thesis for PhD degree in Industrial and
Systems Engineering

Work performed under the supervision of:
Professor Senhorinha de Fátima Capela Fortunas
Teixeira

Professor Luís António de Sousa Barreiros Martins

Professor Manuel José Lopes Nunes

April, 2014

Acknowledgments

Sem trabalho, nada se consegue!

António Henrique Ferreira, meu pai

Abstract

Numerical Optimization and Economic Analysis in the design of a Micro-CHP System with a Stirling engine and a Solar Collector

The micro-CHP systems are a promising technology for improving the energy efficiency of small energy conversion units, located near the end user. The combined heat and power production allows the optimal use of the primary energy sources and significant reductions in carbon emissions. Its use, still incipient, has a great potential for applications in the residential sector. This study aims to develop a methodology for the thermal-economic optimization of micro cogeneration units using Stirling cycle engine as prime mover and concentrated solar energy as the heat source.

A detailed thermodynamic study was carried out to define the model for the physical characterization of the Stirling engine. The study of the physical model includes three types of analysis: ideal isothermal, ideal adiabatic and non-ideal adiabatic analyses. The latter includes limitations in the heat transfer processes and losses due pumping effects. These analyses were performed through numerical simulations by developing a code in MatLab® programming language, based on the model developed by Urieli and Berchowitz. The mathematical modelling was modified, improved and adapted to adjust the configuration of the Stirling engine for cogeneration applications. Subsequently to its implementation, several sensitivity analyses on the operational and geometric parameters were conducted in order to understand which of them have the highest relevance in the Stirling engine performance. The definition of these criteria is crucial in the choice of the decision variables for the thermal-economic optimization model.

After characterizing the physical model, a purchase cost equation representative of each system component was defined: a cost equation for each one of the heat exchangers (i.e. heater, regenerator and cooler) and a cost equation representative of the engine bulk. Each cost equation is based on physical parameters, taking into account the sizing of the system. Through data collected from market available Stirling systems, the most appropriate cost coefficients were defined and the cost equations were validated.

After the validation of both physical and economic models, the thermal-economic optimization was formulated. The maximization of the annual worth from the system operation was defined as the objective function, subjected to a set of nonlinear thermodynamic and economic constraints in order to give significance to the numerical results. The model was formulated considering a cost/benefit approach, where the terms of the objective function represent a balance between costs and revenues. The decision variables correspond to geometric and operational parameters with the highest relevance in the system operation. The Pattern Search algorithm was implemented to achieve the numerical solution, using different search methods, i.e., the Nelder-Mead and genetic algorithm method

The optimization model was effective in the determination of the optimal solution and a positive annual worth was obtained for the defined input simulation conditions. The thermal-economic model yielded the combination of decision variables that defines the best configuration for maximum economic benefit. Through the economic assessment of the best solution obtained for the micro-CHP system, and considering the costs for installing a solar concentrator collector, it can be that such a system is economically attractive, with a payback period of approximately 9 years.

Resumo |

Otimização Numérica e Análise Económica na Conceção de uma Micro-Cogeração com motor Stirling e Concentrador Solar

Os sistemas de micro-cogeração são uma tecnologia muito promissora para a melhoria da eficiência energética das pequenas unidades de conversão de energia localizadas junto ao utilizador final. A produção combinada de calor e eletricidade permite a otimização da utilização das fontes de energia primária e significativas reduções nas emissões de carbono. A sua utilização, ainda incipiente, possui um grande potencial para as aplicações no sector residencial. Este estudo visa o desenvolvimento de uma metodologia de otimização termo-económica dedicada ao desenvolvimento de unidades de micro-cogeração usando como tecnologia os motores de ciclo Stirling e a energia solar como fonte de calor.

O trabalho iniciou-se com um estudo detalhado sobre o modelo termodinâmico para a caracterização física do motor Stirling. O estudo do modelo físico incluiu três tipos de análises: a análise ideal isotérmica, a análise ideal adiabática e a análise não ideal onde foram incluídas as limitações na transferência de calor e as perdas devido a efeitos de bombagem. O estudo das diferentes análises foi efetuado através de simulações numéricas com o desenvolvimento de um código de programação em linguagem MatLab®, tendo como base o modelo desenvolvido por Urieli e Berchowitz. Este foi modificado, melhorado e adaptado no sentido de a adequar à configuração do motor Stirling para aplicações em cogeração. Após a sua implementação, foram efetuadas várias análises de sensibilidade a parâmetros, quer operacionais quer geométricos, de modo a compreender quais os critérios mais influentes na performance do motor Stirling. A identificação destes critérios foi fundamental para a definição das variáveis de decisão a usar no modelo de otimização termo-económica.

Após a caracterização do modelo físico, procedeu-se à definição das equações dos custos de investimento para cada um dos componentes do sistema. Assim, foram definidas quatro equações de custo: uma equação para cada um dos permutadores de calor (i.e. permutador de aquecimento, arrefecimento e regenerador) e uma equação representativa do corpo do motor. Cada uma das equações de custo foi definida com base em parâmetros físicos, tendo em consideração o dimensionamento do sistema. Através de dados recolhidos de sistemas Stirling já comercializados, foram definidos os coeficientes de custo mais adequados e procedeu-se à sua validação.

Foi desenvolvido e implementado o modelo de otimização termo-económica. A maximização do lucro anual decorrente da operação do sistema foi definida como a função objetivo, estando sujeita a um conjunto de restrições não lineares de natureza termodinâmica e económica, com vista a dar significância aos resultados numéricos. O modelo foi formulado numa abordagem custo/benefício em que os termos da função-objetivo representam um balanço entre custos e receitas. O conjunto de variáveis de decisão que correspondem às variáveis geométricas e operacionais de maior relevância no sistema. Foi usado o algoritmo Pattern Search do Matlab® com uso de diferentes métodos de procura, isto é, o Nelder-Mead e os algoritmos genéticos, na resolução numérica do modelo.

O modelo de otimização mostrou-se eficaz na determinação da solução ótima, tendo sido obtido lucros na operação do sistema para as condições de simulação definidas, assim como, a combinação ótima para as variáveis de decisão que definem a melhor configuração para o máximo benefício económico. Através da avaliação económica de aquisição deste sistema de micro-cogeração, e considerando os custos de instalação de um concentrador solar, verificou tratar-te de um projeto economicamente atrativo, com retorno de investimento de aproximadamente 9 anos.

Table of contents |

List of tables

Chapter 7

List of Figures

Chapter 4

Chapter 6

Chapter 7

Nomenclature|

Latin Symbols

Symbol	Description	Unit
A	Area	m^2
AW	Annual Worth	$€/year$
C	Cost	$€$
C_f	Friction Coefficient	-
$c_i(x)$	Constraint Function	-
$Cons_{dhw}$	Domestic Hot Water Consumption	$L.m^{-2}.day^{-1}$
c_p	Specific Heat Capacity at constant pressure	$kJ.kg^{-1}K^{-1}$
C_{ref}	Reference Cost Coefficient	$€/m^2$ $€/cm^3.bar$
C_{su}	Sutherland Constant	-
c_v	Specific Heat Capacity at constant volume	$kJ.kg^{-1}K^{-1}$
d	Diameter	mm
$d^{(j)}$	Search Direction Vector	-
E	Energy	
FE_{CO2}	Equivalent CO_2 Emission Factor	$gCO_2.kWh^{-1}$
F_m	Sizing Factor of Purchase Cost Equations	-
F_T	Temperature Factor of Purchase Cost Equations	-
$f(x)$	Objective Function	-
G	Power density of the incident sunlight	$W.m^{-2}$
h	Convective heat transfer coefficient	$W.m^{-2}.K^{-1}$
$h_j(x)$	Inequality Constraints	-
I_1, I_2, I_3	Winter Climatic Zones	-
i_e	Effective Rate of Return	-
k	Thermal Conductivity	$W.m^{-1}.K^{-1}$
L	Length	mm
$L(x, \lambda)$	Lagrange Function	-
m	Mass of Gas	kg
$M(x, \lambda)$	Merit Function	-
nt	Number of Tubes of the Heat Exchangers	-
Nu	Nusselt Number	

P	Pressure	bar
ΔP	Pressure Drop	bar
$P(x,r)$	Penalty Function for Constraints Violation	-
Pr	Prandtl Number	
p	Price	$€$
Q	Thermal Energy	$J/cycle$
$\dot{Q}$	Thermal Power	W
Q_{dhw}	Thermal Domestic Hot Water	$kWh.m^2.day^{-1}$
$Q_{r,ideal}$	Adiabatic Heat Transferred between Regenerator Matrix and Working Gas	$J/cycle$
$Q_{r,hlss}$	Regenerator Housing Thermal Conductance	$J/cycle$
Q_{rloss}	Heat-transfer Reduction at Regenerator	$J/cycle$
Rev	Revenue	$€$
R	Gas Constant	$kJ.kg^{-1}K^{-1}$
Re	Reynolds Number	
r	Penalty Function Factor	-
r_v	Volume/Compression Ratio	-
s	Schmidt Analysis variable	-
S_D	Distance between Staggered Tubes	mm
S_L	Horizontal Distance between Tubes In-line	mm
S_T	Vertical Distance between Tubes In-line	mm
St	Stanton Number	-
S_k	Simplex Polyhedron	-
t	Number of Operating Hours	$hours$
T	Temperature	K
$\overline{T}$	Mean Temperature	K
u	Velocity	$m.s^{-1}$
V	Volume	cm^3
W	Work	$J/cycle$
$\dot{W}$	Electrical Power	W
$x^{(j)}$	Solution Approximation	-
$x*$	Local Minimum	-
$\overline{X}$	Simplex Centroid	-
$X_{1,2,3,n}$	Simplex Vertices	-
X_{contr_int}	Contracted to Interior Vertex	-

X_{exp}	Expanded Vertex	-
X_{new}	New Simplex Vertices	-
X_{reflec}	Reflected Vertex	-
$Y(\theta)$	Vector of Unknown Functions solved by Runge-Kutta	-

Greek Symbols

Symbol	Description	Unit
α	Thermal Diffusivity	$m^2.s$
β_p	Penalty Parameter	-
β	Schmidt Analysis Triangle Angle	^{o}
γ	Specific Heat Ratio	-
δ	Simplex Expansion Size	-
δW	Mechanical Work done on the Environment	$J / cycle$
ε	Effectiveness	%
η	Multipliers Vector	-
η_{el}	Electrical Efficiency	%
η_{th}	Thermal Efficiency	%
η_{Carnot}	Carnot Efficiency	%
θ	Crank Angle	^{o}
ϑ	Schmidt Analysis Variable	-
λ^T	Lagrange Multiplier Vector	-
λ	Heat-to-Power Ratio	-
μ	Dynamic Viscosity	$kg.m^{-1}.s^{-1}$
ξ	Convergence Tolerance	-
ρ	Density	$kg.m^{-3}$
$\sigma^{(j)}$	Step Length	-
τ	Wall Shear Stress	Pa
Φ	Porosity	-
Γ_0	Solar irradiation	$W.m^{-2}$
$\Theta(x,r)$	Penalty Function	-
ΔW	Work Loss	$J / cycle$
χ	Building Temperature Ratio	-
ψ	Coefficient of Residual Equipment Cost	-
ω	Advance Phase Angle of Expansion Cylinder	^{o}

Superscripts

Symbol	Description
b	Sizing Exponent of Purchase Cost Equations
n	Number of Years

Subscripts

Symbol	Description
a	Non-Heated Air
amb	Ambient Air
avoided	Avoided
b	Boiler
c	Compression Space
c/k	Interface between Compression Space and Cooler
co_2	Carbon Emissions
d	Dead Volume
e	Expansion Space
el	Electrical
eng	Engine Bulk
exit	Outlet
fuel	Fuel Source
h	Heater
h/e	interface between Heater and Expansion Space
hydraulic	Hydraulic Diameter
i	i^{th} component
ideal	Referent to the Ideal Adiabatic Analysis
in	Inlet
inner	Internal Diameter
inside	Inside Air
inv	Investment
j	iteration
k	Cooler

Numerical Optimization and Economic Analysis in the Design of a micro-CHP System with a Stirling Engine and a Solar Collector

XXIII

k/r	Interface between Cooler and Regenerator
m	Maintenance
matrix	Matrix Regenerator
max	Maximum
min	Minimum
out	Outer Diameter
overall	Overall Efficiency
p	Produced
r	Regenerator
r/h	Interface between Regenerator and Heater
ref	Reference
res	Residual
sell	Selling Electricity
sw	Swept Volume
th	Thermal
w	Wetted Heat Transfer Area
w0	Void Regenerator Wetted Area
wall	Wall
water	Referent to the Coolant Mass flow Water
wire	Regenerator Wire Diameter

Abbreviations

Symbol	Description
AFC	Alkaline Fuel Cell
AC	Alternate Current
CES	Carbon Emission Savings
CF	Cash Flow
CHP	Combined Heat and Power Production
CRF	Capital Recovery Factor
DSC	Davis, Swann and Campey method
DC	Direct Current
DL	Decree Law
DMFC	Direct Methanol Fuel Cell
DGEG	Directorate-General for Energy and Geology
DHW	Domestic Hot Water
DFPSE	Double Free Piston Stirling Engine
EED	Energy Efficiency Directive
EFA	Engineering Functional Approach
EPBD	Energy Performance Buildings Directive
ERSE	Energy Services Regulatory Authority
EU	European Union
EA	Evolutionary Algorithm
EEA	Exergoeconomic Analysis
FIT	Feed-in-Tariffs
FF	Form Factor
GT	Gas Turbine
GPS	Generalized Patter Search
GSS	Generalized Set Search
GA	Genetic Algorithm
HDD	Heating Degree Days
ICE	Internal Combustion Engine
IEA	International Energy Agency
KKT	Karush-Kuhn -Tucker conditions
LFP	Linear Free Piston
LPG	Liquefied petroleum gas

LHV	Lower Heating Value
MADS	Mesh Adaptive Direct Search
MCFC	Molten Carbonate Fuel Cell
MOEA	Multi-Objective Evolutionary Algorithms
NES	National Electric System
NG	Natural Gas
NM	Nelder-Mead Algorithm
NPV	Net Present Value
NTU	Number of Transfer Units
ORC	Organic Rankine Cycle
PAFC	Phosphoric Acid Fuel Cell
PEM	Polymer Electrolyte Membranes Fuel Cell
PES	Primary Energy Saving
PSO	Particle Swarm Optimization
QP	Quadratic Problem
RCCTE	Regulamento das Características do Comportamento Térmico de Edifícios (Portuguese Regulation of Thermal Behaviour of Buildings)
ERSE	Regulatory Entity of the Electric Sector
RES	Renewable Energy Sources
R&D	Research and Development
SQP	Sequential Quadratic Programming
SOFC	Solid Oxide Fuel Cell
STT	Structural Theory of Thermoeconomics
TEC	Theory of Exergetic Cost
TECD	Theory of Exergetic Cost-Disaggregating
TPDC	Thermal Power Duration Curve
TFA	Thermoeconomic Functional Analysis
WHD	Winter Heating Demanding

1

Introduction |

1.1. Motivation

This research project aims the development of numerical optimization methods for a thermal-economic analysis in the design of a micro-cogeneration unit. The main idea is to take into account the energy requirements for individual and multi residential buildings. The innovation of this work is correlated with the application of numerical optimization techniques in the economic evaluation of a new cogeneration system, taking into consideration the restrictions of Portuguese market. The cogeneration system applies a new technology and uses a renewable energy source, i.e., a solar powered Stirling cycle engine.

1.1.1. Cogeneration Systems versus Conventional Energy conversion

In modern society few goods are as important as energy. However, the energy needs are mostly accomplished by using fossil fuels such as oil, coal and natural gas. In this sense, several measures have been presented to promote the use of energy in a more sustainable way. The sustainable development consists on the rational use of energy, satisfying energy demands without compromising the future of mankind. The idea of cogeneration is almost as old as the Industrial Revolution and was introduced when steam was the main source of energy in industry and electricity was giving the first steps in power and lighting usage. In 1882, the first commercial power station, built by Thomas Edison, was a cogeneration plant that distributed both electricity and thermal energy to neighbouring buildings (WADE, 2014). As

electrical power became more widely diffused, steam driven mechanisms were replaced, creating a transition from mechanically to electrically powered systems (Alanne & Saari, 2004). The increase of centralized power facilities and reliable utility grids drove electricity costs down, and industrial large scale units began buying electricity and ceased the generation of their own power. This lead to a decrease in the importance of cogeneration plants until the first oil crisis of 1973. However, in the last decades, systems that are efficient and have the ability to use alternative energy sources have begun to be commercialized. This situation was driven by the increase in energy prices, the uncertainty in fuel supplies, energy grid reliability issues and growing environmental concerns.

Combined Heat and Power (CHP) or cogeneration is defined as the simultaneous production of useful thermal energy (usually heat in the form of hot water and/or steam) and mechanical energy from a single primary energy source. The mechanical energy is usually converted into electricity. The thermal energy can be used in a direct heating process or indirectly in the production of hot water or steam (Praetorius & Schneider, 2006). Cogeneration is an excellent technology for improving the overall efficiency of energy conversion systems. As can be seen in Figure 1.1, when compared to the conventional separate production of electricity (in a centralised power station) and heat (in a local boiler), the combined production of heat and power in a single unit can result in a significant reduction in the total fuel consumption. The single CHP unit allows the recovery of thermal energy from the electricity generation, which contributes to higher global efficiency.
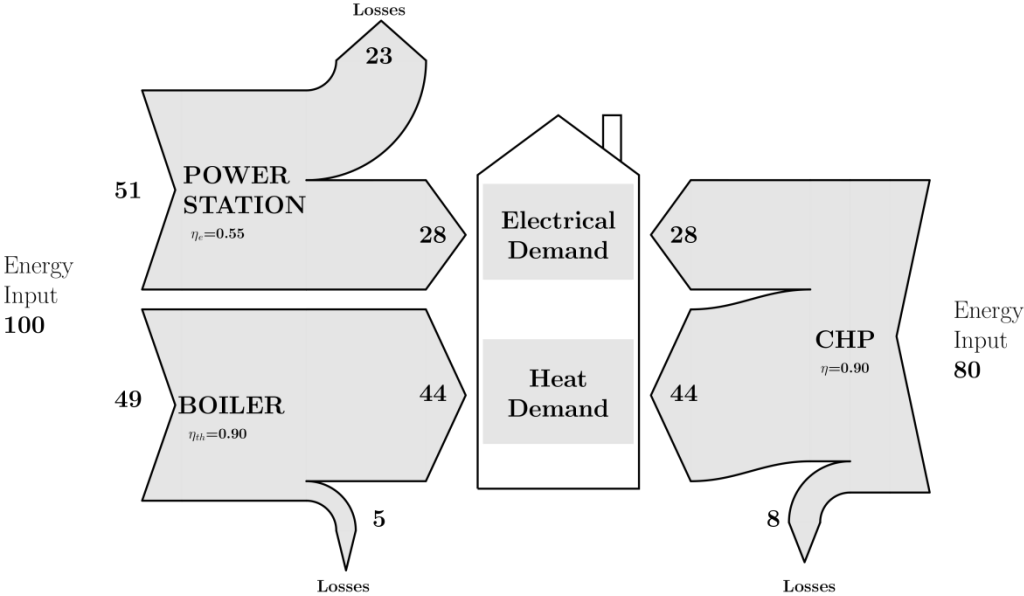
Figure1.1 Energy flows of conventional separate production versus the CHP alternative.

Small-scale CHPs also referred as Micro CHPs have found niche markets in domestic and building applications due to the ability to rapidly vary their electrical load and to adjust the thermal output.

Cogeneration has been worldwide considered as the major alternative to traditional systems in terms of energy saving and environmental conservation (Cao, Mohamed, Hasan, & Sirén, 2014).

The potential of cogeneration systems is mainly seen in buildings with central heating systems. This generally means that electricity generators with heat exchanger(s) and storage boilers replace conventional heating systems. The heat produced is used for space and water heating and possibly cooling, while the electricity is used within the building or fed into the grid to supply electrical power, as presented by Figure 1.2.
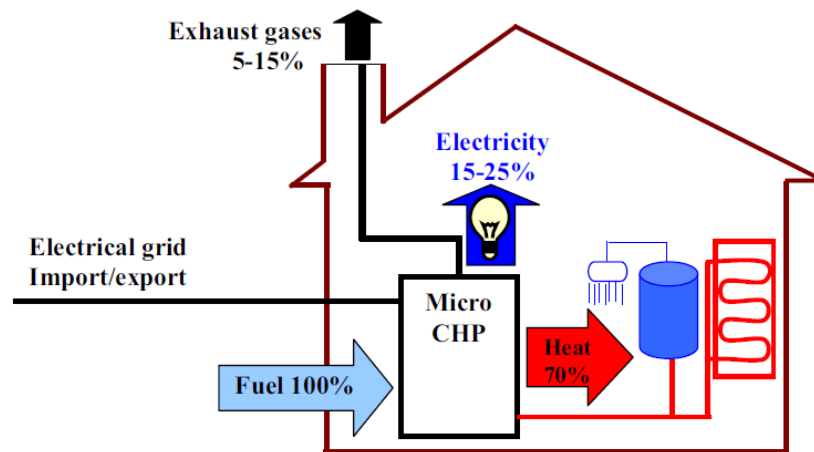
Figure 1.2 A general schematic of domestic micro CHP system. Adapted from (Maghanki, Ghobadian, Najafi, & Galogah, 2013)

CHP systems present flexible solutions to produce thermal and electrical energies which reduce both primary energy consumption as well as the overall investment costs. Therefore, and despite the general use of auxiliary boilers, the additional cost of a full separate installation to generate all the thermal energy is avoided (Dentice d'Accadia, Sasso, Sibilio, & Vanoli, 2003; Onovwiona & Ugursal, 2006). The improved efficiency in energy conversion corresponds to a reduction in the amount of energy for a given energy level output and, therefore, to a decrease in greenhouse and pollutant gas emissions. The use of cogeneration reduces the demand for limited natural resources (e.g. coal, natural gas, and oil) and improves the nation's energy security (Chicco & Mancarella, 2009).

The cogeneration market is still dominated by large-scale units but new technologies are emerging for small- and micro-scale systems. Such plants have great potential for applications in small and medium-sized buildings. The main target market for small-scale and micro-CHP systems is the massive residential sector as a replacement for conventional boilers. The micro-CHP plants shall operate according to the 'heat-demand' profile of the residential buildings (Onovwiona, Ugursal & Fung, 2007).

In the conventional energy flow-path the primary source is converted, usually in a large-scale plant, and then transmitted to the end-user to satisfy energy demands. The bulk of electricity is delivered by centralized power plants, most of them using large fossil fuel combustion or nuclear reactions to produce

steam to drive steam turbine generators. In many cases, the energy is converted in a decentralized energy conversion plant, located near to the end-user, and then distributed to the final appliances, as shown in Figure 1.3.
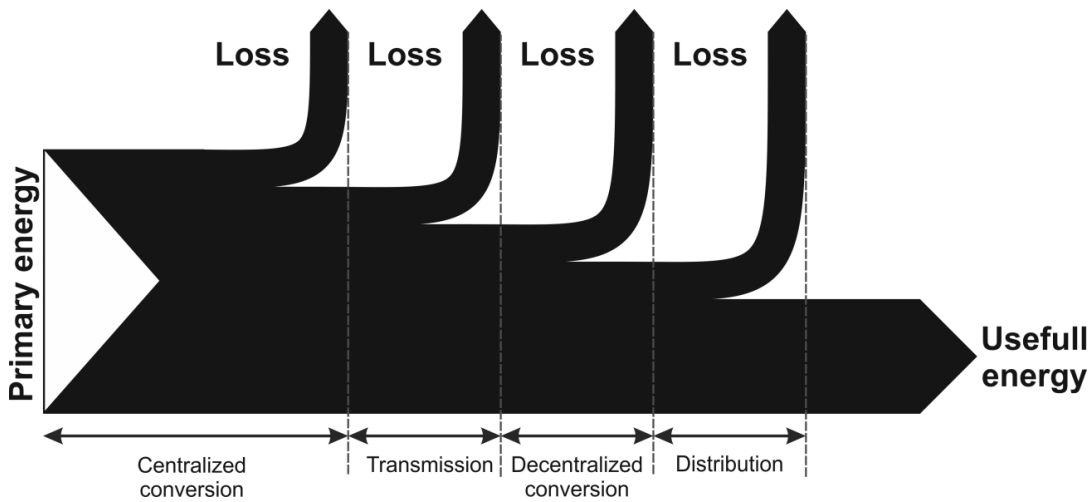
Figure1.3 *Grassman* diagram of energy conversion processes.

Decentralized energy conversion includes the use of small-scale generators, located near to the end-user, or in an isolated place where the connection to the grid is remote. Providing electrical power through decentralized energy plants on those locations allows a reduction of transmission and distribution losses, and so, costs are minimized.

In the design of technical systems and in order to introduce them into the market, it is important to reduce costs, improve the system performance and its reliability. The use of rigorous methods in decision-making (such as numerical optimization methods) is an effective tool for finding optimal solutions. To make use of this tool, the objective function must be defined a correlation that quantitatively measures the performance of the system under study. This objective function can be a single variable, such as the profit, or a combination of variables that can be numerically quantified. To achieve an optimal solution, it is necessary to find the best combination for the input decision variables that optimize the objective function taking into account the physical limitations and problem constrains. The identification of the objective function, decision variables and the constraints allows the construction of an appropriated optimization model that is complex enough to give feasible solutions.

The choice of the most appropriate algorithm depends on the application. In many cases, there are mathematical expressions, known as optimality conditions, for checking if the defined set of variables is indeed the solution of the problem. The verification of the optimal conditions gives useful information on how the approximation to the solution can be improved. Therefore, the model may be improved by applying techniques, such as sensitivity analysis, which reveals the stability of the solution to changes in

the model and data. The interpretation of the solution may also suggest directions for which the model can be improved. The solution obtained from the mathematical model must be feasible.

The development of favourable policies in using cogeneration technologies and renewable energy sources, and the application of numerical optimization methods to solve complex mathematical models are intrinsically connected with the motivation for the development of this work. In this particular project, the mathematical model of a new technology (i.e. a thermal energy system) involves the problem of plant optimization and must take into account both the technical and the economic aspects. The integration of these two fields is the subject of thermal-economics. The aim is to minimize the total costs, including those related with the thermodynamic inefficiencies and so to define the key parameters of each plant-component that lead to the optimal design of the technology. Thus far, numerical methods of optimization have been used for the thermodynamic and economic optimization of large scale systems (Abusoglu & Kanoglu, 2009; Feng, Chen, & Sun, 2011; Tsatsaronis, 1993; Valero et al., 1994). Studies involving the comparison of different cogeneration technologies are also commonly available, often assuming a fixed design.

Summarizing, growing concern about the depletion of fossil energy resources and environmental issues have led to policies favouring the introduction of distributed/decentralized energy production systems (Bruckner, Morrison, & Wittmann, 2005). CHP has gained attention because of decreased fuel consumption and lower gas emissions. Small-scale cogeneration systems are an example of distributed energy production suitable for the building sector. Dentice d'Accacia and co-workers, in 2003 reported on the possibilities of residential micro-CHP systems and presented a general survey of market and technological perspectives. The authors concluded that the introduction of micro-CHP for domestic applications would be subject to the availability of the technology, the matching of electrical and thermal load profiles, and gas and electricity prices (Dentice d'Accadia et al., 2003). Also, the implementation of micro-CHP systems aims to replace the boiler in the conventional central heating system and the production of electricity as a by-product (De Paepe & Mertens, 2007; Praetorius & Schneider, 2006).

The most used CHP technologies are those based on the internal combustion engine, micro gas turbine, organic Rankine cycle and Stirling engine. Internal combustion engines are the most well established technology for small- and micro-CHP applications. Regarding the development of micro turbines, the major technical factors that challenge the development of systems with less than 10 kW of capacity are related to the small-scale impacts (e.g. high heat and mechanical losses, as well as, increased specific costs). The Micro CHP systems based on Rankine cycles, with a power size of up to 10 kW, are mostly available on the market at a prototype level only.

Fuel-cell micro-CHP achieves lower electrical efficiency levels and the effective use of the heat production is unable to compete with efficient central power plants. Despite several potential markets, these systems face a number of competing technologies and the price projections based on learning curves for fuel cells

reveal that without economies of scale, they can hardly reach the markets without subsidies before 2025. Cogeneration systems based on Stirling engine as prime movers have an electric power ranging from 1 kW to 9 kW and a corresponding thermal power size from 5 kW to 25 kW, which may also represent a good alternative to household boilers. The electric efficiency ranges from 13% to 28% with the CHP efficiency higher than 80%, which may even go beyond 95% (Maghanki et al., 2013). Comparing all these technologies, Stirling engines seems to be a good alternative to supply the energy needs of small and medium size buildings. From an energy point of view, this system should satisfy most of the thermal and electric energy demand, with a primary energy saving index higher than 20%. Regarding the economic feasibility, it is accepted that a reasonable target for the marginal cost of a CHP system for household heating is approximately 3000 €/kW$_{el}$ (Barbieri, Spina, & Venturini, 2012).

The use of renewable energy sources and efficient energy conversion systems - such is the case of cogeneration – is considered, currently, a priority. The market trends correspond to the decentralized energy generation and the increasing replacement of boilers and other conventional systems by small- and micro-scale cogeneration units able to produce the same amounts of useful energies. The micro scale cogeneration systems (<50 kW$_{el}$) have been developed as ideal solutions to meet the energy needs for the building sector in urban areas. Small and micro-cogeneration units represent a great opportunity to decentralize the production of electricity.

1.1.2. Where is the research opportunity?

The research opportunity is related with the possibility of optimizing a renewable-based cogeneration system for houses, by using numerical optimization tools. The increase of energy demands in the building sector, the innovative nature of the technology, the favourable legislation (e.g. with the opportunity for selling electricity to the grid by benefiting from attractive feed-in-tariffs) justify the proposed research work. In Portugal, during 2012, the cogeneration installed power capacity reached a value around 1 300 MW, spread over various technologies. Most of those technologies use Natural Gas (NG) as fuel. Accordingly to data from Cogen Portugal, in 2012, cogeneration installations were responsible for the production of 14% of the electricity consumed in the country.

A significant part of the energy consumptions is related to buildings. It is estimated that buildings use about 40% of the primary energy needs in Europe. In that way, buildings, including households, play a major role in the energy consumptions in Europe. Electricity consumption per capita has increased steadily in Portugal and in the EU15 since the sixties.

Accordingly to the most recent data from International Energy Agency (IEA), in 2009 the Portuguese residential sector is the third highest consumer of final energy in the country. The sector is responsible for the consumption of almost 30% of electricity in a total of 47 855 GWh (see Figure 1.4).
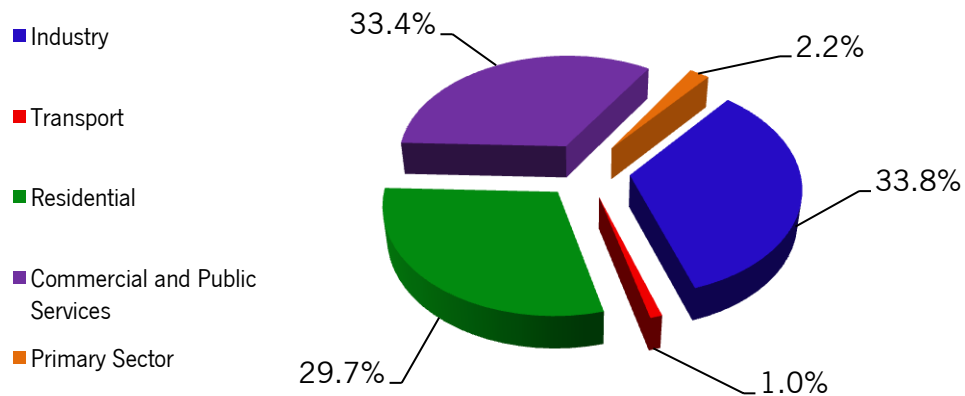
Figure1.4 Electricity consumption by activity sector (International Energy Agency - IEA, 2012).

In the Portuguese household sector the consumption of electricity has been growing in the last decades due to the new consumption habits of the population. The continuous growing of electricity consumption in Portuguese residential buildings leads to a major role of this energy source in the domestic sector, which is directly related with the increasing use of electrical equipment but also with the use of electricity for heating. This can explain why electricity registered a growth in consumption when compared with other energy sources. There is also a significant amount of energy used for hot water needs and for heating and spaces. Still, there are a significant number of buildings in Portugal and in Europe built in a period of time in which thermal regulations were not in force.

1.2. Scope and Objectives

The main objective of this project is to develop a thermo-economic optimization model for facilities based on a new micro-cogeneration system. This system applies a new technology and uses a renewable energy source, i.e., the powered solar Stirling cycle engine. The implementation of a numerical optimization method allows the determination of the optimal solution and ensuring the design of a facility that represents an economically viable solution.

The specific objectives of the project are:

- Study and definition of the thermodynamic model for the physical characterization of the Stirling engine;
- Definition of the thermal power duration curve representative of both heating and domestic hot water needs for a residential building.
- Definition of the purchase cost equations for each system component and the development of a complete nonlinear optimization model (objective function and constraints);

- Implementation of the thermo-economic model, using numerical optimization techniques. The numerical model will be implemented in MatLab with the possibility of comparing the performance of different techniques for non-linear optimization problems. Validation of the optimal solution should be performed through a sensitivity analysis by varying physical, economic and numerical parameters;

- Study the economic viability of CHP facilities concerning the Portuguese market, taking into account the most relevant variables to the target customers. The variables should include the study of energy consumption profiles, purchase and sale prices of electricity;

- Identification of the main attractive features of this type of equipment that may lead to the viability of its commercialization in the Portuguese market.

1.3. Structure of the Thesis

The present thesis is organized in eight chapters: (1) Introduction; (2) Literature review; (3) Energy consumption profiles; (4) Analysis and characterization of the physical model; (5) Development and validation of the thermo-economic optimization model; (6) Results and discussion; (7) Economic viability of micro-CHP system; (8) Conclusions and future work.

In the first chapter, the general motivation for this research work is presented and the framework is provided. The objectives and contributions of the present study are also offered.

The second chapter concerns a literature review. The state-of-the-art of the different technologies that are applied on micro-cogeneration systems is described. In particular, the study should be further explored in the analysis of the Stirling engine cycle; relevant legislation about energy systems; profiles of energy consumption for the residential sector in Portugal; and the identification of critical factors for the diffusion of micro-CHP in the Portuguese market. The review also includes the study of the tools and methods used in the thermal-economic optimization and a brief review of the optimization models.

In chapter three, a study is presented to define the energy consumption profiles for single and/or multi-family residences, determining the appropriate relationship with thermal storage demands. The evaluation of the energy consumptions is very important to minimize electricity demand from the network grid and to maximize the efficiency of the CHP unit.

The fourth chapter reports the thermodynamic analysis of the physical system considering: the definition of the equations which describe the Stirling cycle considering three distinct thermodynamic analysis; sizing of the heat exchangers. Subsequently, the thermal fluid analysis is also presented. The analysis and the characterization of the physical model are concluded with the definition of the thermodynamic model.

The aim of chapter five is the development of the thermo-economic optimization procedure. The objective function and constrains of thermo-economic optimization model that maximizes the revenues of the new

cogeneration system are presented. After the development of the mathematical model in which the thermodynamic equations are determined, the equations of the purchase costs of the main components of the micro-cogeneration are disclosed. The cost equations are based on physical parameters and quality and sizing parameters are included in the definition of the purchase cost equations. Four representative purchase cost equations were defined to estimate the system cost. The non-linear optimization model will be defined considering a single objective function, which corresponds to the maximization of the annual worth from the system operation. In the maximization of the annual worth, income/profits from selling the electricity to the grid network are included in the mathematical model. The economic operation of CHP systems requires both limitation of operational performance and power demands Therefore, the aim is the determination of the total cost per year, including the fuel cost, the initial investment, the operation and maintenance cost. In addition, a set of non-linear constrains are imposed by the operability of the system, giving physical significance to the complex mathematical model. The implementation and validation of the numerical optimization model in the MatLab environment is also described. The MatLab software was chosen due to its use as a scientific tool that allows the performance comparison of different numerical techniques, including distinct optimization tools.

Chapter six discloses the main numerical results from the study. The results were divided in four main groups. The first group concerns the results from the thermodynamic analysis, including the results from the isothermal, ideal adiabatic and non-ideal analysis for a base-case scenario were the geometrical and operational parameters are fixed values. The second group of results correspond to a sensitivity analysis focused on the impact of each geometrical and physical parameter in the performance of the Stirling engine. The third group of results regards the cost estimation of each system component and the sensitivity of the purchase cost regarding the parameters variation. The fourth group of results concerns the thermal-economic from the application of the optimization model.

The study concerning the economic viability of the new micro-CHP system in the Portuguese market is presented in chapter seven. The study is based on a cost/benefit analysis. The micro-economic changes that influence the feasibility of micro-CHP are discussed.

Finally, the main conclusions of the research and some suggestions for further developments are pointed out in chapter eight.

1.4. Contributions of the Work

In this project, numerical optimization tools are applied in modelling a cogeneration system based on a recent technology, the Stirling engines. Several contributions of this project were identified:

- The aim of this project is to contribute for the optimization of micro-scale cogeneration systems for residential applications. The optimization of this technology is based on the development of a

physical and economic model in order to achieve a feasible commitment between the maximization of system performance and its purchase cost. The system optimization allows reducing the amount of used primary energy and, simultaneously, improves the efficiency in the energy conversion process. The combination of both aspects increases the sustainability of these thermal systems in the market. As a consequence, these systems contribute to the reduction of fossil fuels imports and the gas emissions, which represent an economic and an environmental benefit.

- The project contributes to societal objective that promote the development and use of sustainable systems that allow the rational use of energy, fulfilling the building energy demand without compromising the security of national energy grids.

- One of the major contributions is the development of purchase cost equations for each main component of the system. These equations were formulated considering a methodology that allows estimating the total investment cost of the thermal plant considering the operational and thermodynamic parameters. These purchase cost equations are adjusted to this technology and includes quality and size parameters to better estimate the system cost.

- The integration of a physical and an economic model for thermal-economic optimization helps to improve initial system designs and enhance its operation in order to achieve the maximum profit, the minimum cost, the least energy waste. Monetary value provides a convenient measure of different objectives. In thermal systems, benefits arise from improved plant performance, such as improved yields of valuable products (i.e. produced energy), reduction of maintenance costs, less equipment wear, etc. Intangible benefits arise from proper identifying the objective, constraints and the degrees of freedom in the system operation, leading to higher quality in the design and faster and more reliable decision-making.

The fundamental problems in the design of Stirling engines are related with the time consumption in the design process and the cost of manufacturing. In most of the cases, finding the geometrical parameters of the engines is based on insufficient and costly experimental information. Therefore, improvements to the engine design are been achieved through high-cost and time-consuming trial-and-error procedures. Regarding this, numerical modelling represents a great opportunity to identify the key parameters and optimize the system under a cost effective process.

Abusoglu, A., & Kanoglu, M. (2009). Exergoeconomic analysis and optimization of combined heat and power production: A review. *Renewable and Sustainable Energy Reviews*, *13*(9), 2295–2308. doi:10.1016/j.rser.2009.05.004

Alanne, K., & Saari, A. (2004). Sustainable small-scale CHP technologies for buildings: the basis for multi-perspective decision-making. *Renewable and Sustainable Energy Reviews*, *8*(5), 401–431. doi:10.1016/j.rser.2003.12.005

Barbieri, E. S., Spina, P. R., & Venturini, M. (2012). Analysis of innovative micro-CHP systems to meet household energy demands. *Applied Energy*, *97*, 723–733. doi:10.1016/j.apenergy.2011.11.081

Bruckner, T., Morrison, R., & Wittmann, T. (2005). Public policy modeling of distributed energy technologies: strategies, attributes, and challenges. *Ecological Economics*, *54*(2-3), 328–345. doi:10.1016/j.ecolecon.2004.12.032

Cao, S., Mohamed, A., Hasan, A., & Sirén, K. (2014). Energy matching analysis of on-site micro-cogeneration for a single-family house with thermal and electrical tracking strategies. *Energy and Buildings*, *68*, 351–363. doi:10.1016/j.enbuild.2013.09.037

Chicco, G., & Mancarella, P. (2009). Distributed multi-generation: A comprehensive view. *Renewable and Sustainable Energy Reviews*, *13*(3), 535–551. doi:10.1016/j.rser.2007.11.014

Cogen Portugal. (2012). Cogeração em Portugal. *Cogeração - situação actual (in Portuguese)*. Retrieved November 11, 2012, from http://www.cogenportugal.com/

De Paepe, M., & Mertens, D. (2007). Combined heat and power in a liberalised energy market. *Energy Conversion and Management*, *48*(9), 2542–2555. doi:10.1016/j.enconman.2007.03.019

Dentice d'Accadia, M., Sasso, M., Sibilio, S., & Vanoli, L. (2003). Micro-combined heat and power in residential and light commercial applications. *Applied Thermal Engineering*, *23*(10), 1247–1259. doi:10.1016/S1359-4311(03)00030-9

Feng, H., Chen, L., & Sun, F. (2011). Exergoeconomic optimal performance of an irreversible closed Brayton cycle combined cooling, heating and power plant. *Applied Mathematical Modelling*, *35*(9), 4661–4673. doi:10.1016/j.apm.2011.03.036

International Energy Agency - IEA. (2012). International Energy Agency - Statistics of Electricity Consumption. *IEA*. Retrieved from http://www.iea.org

Maghanki, M. M., Ghobadian, B., Najafi, G., & Galogah, R. J. (2013). Micro combined heat and power (MCHP) technologies and applications. *Renewable and Sustainable Energy Reviews*, *28*, 510–524. doi:10.1016/j.rser.2013.07.053

Onovwiona, H. I., Ugursal, V., & Fung, A. S. (2007). Modeling of internal combustion engine based cogeneration systems for residential applications. *Applied Thermal Engineering*, *27*(5-6), 848–861. doi:10.1016/j.applthermaleng.2006.09.014

Onovwiona, H. I., & Ugursal, V. I. (2006). Residential cogeneration systems: review of the current technology. *Renewable and Sustainable Energy Reviews*, *10*(5), 389–431. doi:10.1016/j.rser.2004.07.005

Praetorius, B., & Schneider, L. (2006). Micro Cogeneration: Towards a Decentralized and Sustainable German Energy System? In *29th IAEE International Conference* (pp. 7–10). Potsdam.

Tsatsaronis, G. (1993). Thermoeconomic analysis and optimization of energy systems. *Progress in Energy and Combustion Science*, *19*(3), 227–257. doi:10.1016/0360-1285(93)90016-8

Valero, A., Lozano, M. A., Serra, L., Tsatsaronis, G., Pisa, J., Frangopoulus, C., & Spakovsky, M. R. (1994). CGAM Problem: Definition and Conventional Solution. *Energy*, *19*(3), 279–286.

WADE. (2014). World Alliance for Decentralized Energy. *What is decentralized energy?* Retrieved February 02, 2014, from http://www.localpower.org/deb_what.html

2

Literature Review |

2.1   Combined Heat and Power

2.2   Technologies Applied to Cogeneration

2.3   Optimization Methods

This chapter provides a brief review of the various studies and the state of the art of the technologies relevant to this research. A background review on various conversion technologies is considered. The main approaches in thermo-economic modelling approaches, as well as, their significance in this research are highlighted.

2.1. Combined Heat and Power

Cogeneration is not a new concept. Industrial plants led to the concept of cogeneration back in the 1880's, when steam was the primary source of energy in industry. The use of cogeneration became common practice as engineers replaced steam driven and pulley mechanisms with electric power and motors, moving from mechanical powered systems to electrically powered ones. The central electric power plants construction and utility grids led to the reduction in the electricity cost, and numerous industries began buying electricity, stopping their own energy production. This resulted in the reduction of cogeneration power plants in the industrial sector. Furthermore, other factors that led to the decline of cogeneration were the increasing of regulatory policies regarding electricity generation, low fuel costs and advances in technology resulting in products like packaged boilers (Dentice d'Accadia, Sasso, Sibilio, & Vanoli, 2003).

However, the descending trend started to revert after the first fuel crisis in 1973. Because of the increase of energy price and uncertainty in fossil fuel supply, efficient power plants and systems able to run with alternative fuels started drawing attention.

In the beginning of the 20th century, most electricity generation was from coal fired boilers and steam turbine generators, with the exhaust steam used for industrial heating applications.

These reasons led various governments especially in Europe, US, Canada and Japan to take leading roles in establishing and/or promoting the increased use of cogeneration applications not only in the industrial sector but also in other sectors including the residential one (Pehnt et al., 2004).

As mentioned before, by definition, cogeneration is the simultaneously generation of energy in different forms by using fuel energy at optimum efficiency in a cost-effective and environmentally accountable way, allowing a reduction on primary energy consumption. The main energy flows of a CHP unit are reported in Figure 2.1.

Losses

$$(1-\eta_{el}-\eta_{th})\dot{E}_p$$

Primary Power Input $\dot{E}_p$

CHP

$$\dot{E}_{el} = \eta_{el} \cdot \dot{E}_p$$

Electric Energy

$$\dot{E}_{th} = \eta_{th} \cdot \dot{E}_p$$

Thermal Energy
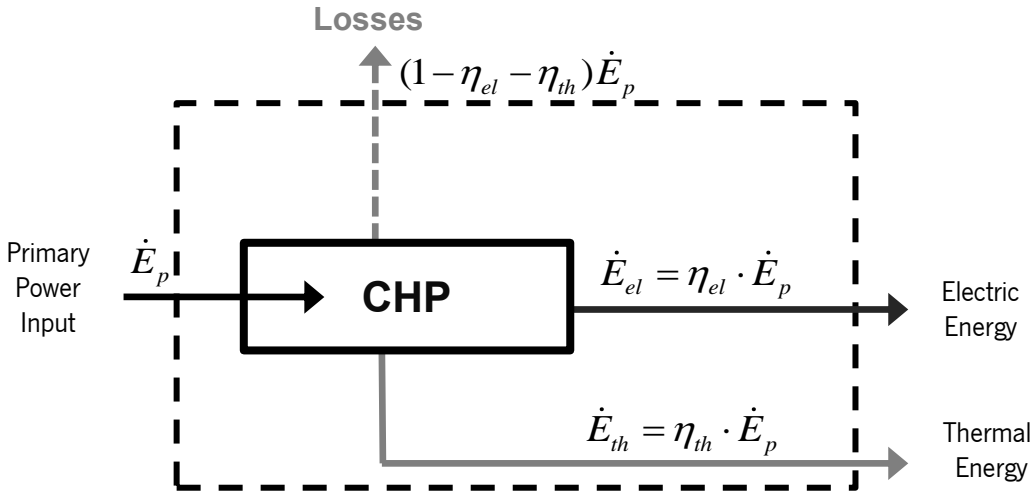
Figure 2.1 Scheme of the cogeneration energy conversion system.

The applications for cogeneration in the building sector include, for instance, hospitals, office buildings and single- and multi-family residential buildings. Specifically in the CHP applications for single-family, the design of the systems is associated with technical challenges due to the non-coincidence of thermal and electrical loads, requiring electrical/thermal storage or connection to the electrical grid (Gullì, 2006; Onovwiona & Ugursal, 2006).

CHP power plants are usually connected to the lower voltage distribution grids. Besides reducing losses in transmission and distribution, they can bring improvements to grid power quality, supplying energy when required. Moreover, applications in the residential sector offer opportunities in terms of improving energy efficiency and reduction of pollutant gas emissions. It is well believed that technologies like Stirling engines and Fuel Cells are promising for small-scale cogeneration in the near future, because of their potential to achieve high efficiency and low emissions level. Nevertheless, those technologies are still in development and they are not available at reasonable cost.

The efficiency of a cogeneration system is the best way to measure and compare it with the conventional power production. The total efficiency of a system is measured as the fraction of the input fuel that can be

converted in usefully power and heat. Most manufacturers of this kind of power plants relate efficiency to the Lower Heating Value of the input fuel (LHV). The efficiency is commonly expressed in terms of both electrical efficiency and overall efficiency, as shown by equation (2.1) and equation (2.2).

$$Electrical\ efficiency = \frac{Electrical\ ouput}{Fuel\ Input} \tag{2.1}$$

$$Overall\ efficiency = \frac{Useful\ thermal + Electrical\ output}{Fuel\ Input} \tag{2.2}$$

he overall efficiency of energy conversion in cogeneration mode increases to over 80% as compared to an average of 30–35% in conventional fossil fuel fired electricity generation systems (Onovwiona & Ugursal, 2006). The efficiency of a cogeneration system depends on the type of the prime mover, its size, and the temperature at which the recovered heat can be used.

Cogeneration systems can run with several technologies and almost all types primarily generate electricity along with making the best practical use of the heat. The conventional power plants use the high potential energy available in the fuels to generate electric power, wasting a substantial share of the low-end residual energy by rejecting the high temperature outlet gases. Otherwise, a cogeneration process uses the high potential energy to generate electric power and capitalises the low quality residual energy for heating process or similar use (Onovwiona & Ugursal, 2006). So, several benefits can be listed when regarding the potential of small- and micro-scale cogeneration plants (see Figure 2.2).

Primary energy savings: The successful implementation of CHP leads to a reduction in fuel consumption by approximately 25% compared to the convencial production of electricity.

Reduction of gas emissions: With the reduction of primary energy usage, the gas emissions are also reduced, mainly if renewable energy sources are used.

Economic benefits: End-users can obtain economic benefits, due to the possibility of selling electricity to the grid.

Increase the reliability of energy supply: The connection of cogeneration systems to the grid guarentees a continuous operation of the installation and allows the injection of energy in the national grid, improving its reliability.

Figure 2.2 Benefits from using cogeneration systems.

The advantages include economic, environmental and energy safety aspects. CHP systems can represent an effective alternative to supress some of the most relevant technological needs in the energy field. These include reducing the use of conventional fossil fuels and, therefore, reduce the costs with the energy production; reduce the pollutant gas emissions because of the reduction of fuel utilization and the use of alternative energy sources (renewable ones). Finally the possibility of recover wasted heat from systems operation is also an advantage.

When projecting or deciding for the CHP system installation, some aspects must be taken under consideration in the selection of a specific technology for a certain application:

- Normal and maximum/minimum power load in the plant, and the operation period.
- Unexpected increases and decreases in demand with their duration and response time required to provide the necessary quantity of energy.
- Type of fuel available, long-term availability of fuels and their pricing.
- Commercial availability of alternative systems, their lifetime and the corresponding expense for maintenance.
- Influence exerted by local conditions at plant site, i.e. space available, installation conditions, raw water availability, infrastructure and environment.
- Project cost and long term benefits.

2.2. Technologies Applied to Cogeneration

Various technologies are available for residential applications, i.e. single-family (<10 kW$_{el}$) and multi-family (10–50 kW$_{el}$) applications. In this size range, the technologies suitable for cogeneration systems are: Micro-turbine based cogeneration systems, Internal Combustion Engines (ICEs) based cogeneration systems, Fuel Cell based cogeneration systems, Organic Rankine cycles and reciprocating external combustion Stirling engine based cogeneration systems. Different definitions of small-size cogeneration are available in technical and scientific literature. European Directive on the promotion of cogeneration sets this value at 50 kW$_{el}$; Ugursal *et al.* (2006) analyse residential CHP systems considering applications that are suitable for single-family and multi-family households (generally covered by systems of <10 kW$_{el}$ and <25 kW$_{th}$); De Paepe *et al.* (2006) study residential applications of micro-CHP systems (<5 kW$_{el}$) for isolated single-family household (De Paepe, D'Herdt, & Mertens, 2006; H.I. Onovwiona & Ugursal, 2006).

2.2.1. Micro-Turbines

The basic components of micro-turbine systems are the compressor, turbine generator and the internal recuperator. The compressed air and the fuel are mixed and combusted in a combustion chamber. Hot

combustion gas expands turning the turbine, which drives the compressor and provides power by rotating the compressor turbine shaft. The compressor-turbine package is the heart of a micro-turbine, which is mounted on a single shaft along with the electric generator. The turbo-compressor shaft turns at high rotational speeds, of about 80 000–120 000 rpm. The physical size of components and rotational speed of micro-turbine systems are toughly influenced by the turbine and compressor design features (McDonald, 2003; Onowwiona & Ugursal, 2006).

Micro-turbines operate under the Brayton cycle. In this cycle, atmospheric air is compressed, heated, and then expanded, with the excess power produced by the expander (i.e. turbine) over that consumed by the compressor is used for power generation (Kaikko & Backman, 2007). The power produced by the turbine and consumed by the compressor is proportional to the absolute temperature of the gas passing through them. Thus, it is advantageous to operate the expansion turbine at the highest practical temperature consistent with economic materials. With the technological advance and the use of more resistant materials, it is possible to get higher turbine inlet temperatures. Plus, the optimum pressure ratio also increases. Higher temperature and pressure ratios result in higher efficiency and specific power. Thus, the trend in gas turbine advancement has been towards a combination of higher temperatures and pressures. However, micro-turbine inlet temperatures are generally limited. Accordingly to Kaikko & Backman (2007), the turbine inlet temperatures are low (1075–1275 K) to use relatively inexpensive materials for the turbine, and so, keeping the costs at a reasonable level and maintaining low-pressure ratios (3.5 to 4.0). The low inlet temperature affects the efficiency, which can be counteracted by using recuperation. As a result, micro-turbines typically apply a recuperated cycle and achieve electrical efficiencies of about 28–30%.

Micro-turbine designs include a recuperator to reduce fuel consumption, thereby substantially increasing efficiency. With a recuperator, the hot exhaust gas helps the air pre-heating as it passes from the compressor to the combustion chamber. A recuperator has two performance parameters: effectiveness and pressure drop. Higher effectiveness recuperation needs large recuperator surface area, resulting in higher-pressure drop as well as higher cost. However, increasing recuperator effectiveness raises the micro-turbine efficiency and allows fuel savings derived from pre-heating.

Additional value in cogeneration operational mode is gained when the thermal energy from the exhaust gases is recovered to supply local heat. Commonly, an integrated heat exchanger is used to extract heat from the exhaust gas before their release to the atmosphere. Depending on the application, hot water in the 70–90 °C temperature range or steam may be produced. In this case the use of recuperation may not be economically justified. In combined heat and power (CHP) generation, the overall efficiencies of the micro-turbines, as claimed by manufactures can reach values in the range 75–85%. The total investment costs for micro-turbine-based CHP applications are estimated to vary from 1000 to 1700 EUR/kW$_{el}$.

Capstone Corporation® is one of the most important manufacturers of micro-turbines for cogeneration applications (Figure 2.3). Capstone makes various sizes of micro-turbines: 30 kW, 65 kW, and 200 kW, which can be used in distributed power generation and can operate on: Natural Gas, Propane, Gas, Diesel and Kerosene.
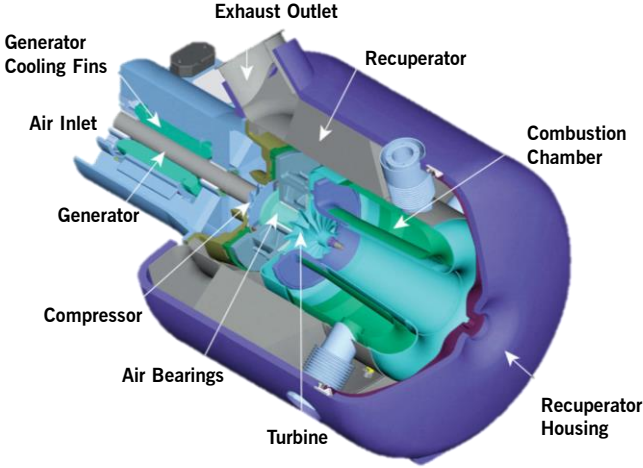
Figure 2.3 Design of the C65 Capstone MicroTurbine ("Capstone Turbine Corporation," 2012).

The Micro-turbines offer a number of potential advantages compared to other technologies for small-scale power generation. Those advantages are their compact size and low-weight per unit power, a small number of moving parts, lower noise levels, multi-fuel capabilities, as well as, opportunities for lower emissions. Micro-turbine systems range in size suitable to meet the thermal and electrical requirements of multi-family residential, commercial or institutional buildings.

2.2.2. Internal Combustion Engine (ICE)

ICE cogeneration-based systems are suitable for small-scale applications because of their robust and well-proven technology. Reciprocating ICEs are classified by their method of ignition: spark ignition, Otto engines, or compression ignition, Diesel engines. Otto engines are mainly used for smaller cogeneration applications, with their heat recovery system producing up to 160 °C hot water or steam at 20 bar. These engines can run on natural gas, although they can be set up to run on propane, gasoline or landfill gas. Diesel engines are more suitable for large-scale cogeneration, mostly running on diesel fuel or oil. They can also operate on a dual fuel mode that burns primarily natural gas with a small amount of diesel fuel (Hycienth I. Onowwiona, Ismet Ugursal, & Fung, 2007).

The interest in ICEs, as a choice of prime mover of for residential cogeneration applications is due to their robust nature, reliability, and reasonable cost.

The basic configuration of an ICE based cogeneration system comprises: the engine, the generator, the heat recovery system, the exhaust system and controls. The generator is driven by the engine, and the useful heat is recovered from the engine by the cooling systems (Onowwiona & Ugursal, 2006).

In cogeneration applications, and according to size, engines can operate at high, median or low speeds. For high-speed engines, the specific costs (EUR/kW) are lower, once the engine power output is proportional to the engine speed. ICEs have electrical efficiencies that range from 28 to 39%. In general, diesel engines are more efficient than spark ignition engines because of their higher compression ratios. In terms of overall efficiency, the value varies between 85–90% for ICE based cogeneration systems.

Concerning to heat recovery, there are four sources, where waste heat can be used: exhaust gases (between 30% and 50%), engine jacket cooling water (up to 30%), lubrication oil cooling water and turbocharger cooling. The temperature of the hot water recovered from the engine jacket is often between 85 and 90 $^{\circ}$C, whereas the engine exhaust gases temperatures can reach 120 $^{\circ}$C. The latter, can be used to produce, for instance, hot water or low-pressure steam for space heating, domestic hot water heating (Yun, Cho, Luck, & Mago, 2013). One of the most disadvantages of ICEs is the need of periodic maintenance inspections, where the most important maintenance operation involves oil changing. Some cogeneration systems based on ICEs, fuelled by natural gas, have been redesigned recently. The most important improvement is to force the oil passage through all engine surfaces. Furthermore, appropriate material quality led to the minimization of engine maintenance requirements. These engines occupy small installation space, have low noise (<60 dB(A) at 1 m), vibrations and long life service (40 000–60 000 h, corresponding to about 10 years). Several ICE based cogeneration systems, suitable for the residential sector, are currently available in the market. The main characteristics of some of those commercial systems are listed in Table 2.1. According to the data, their specific cost ranges between 2000 and 3 000€/kW$_{el}$ when electric power is higher than 5 kW$_{el}$.

Honda, and Osaka Gas have developed the Ecowill model able to produce 1 kW of electrical power and 2.80 kW of thermal output. This model was designed for single-family applications with an overall energy efficiency of 85%. The German manufacturer, Senertec®, produces a cogeneration unit of 5.0 kW electric and 12.3 kW thermal power called Dachs. This unit is based on a one-cylinder four-stroke engine that can be fuelled by natural gas, LPG, fuel oil or biodiesel. The total efficiency at full load is lower than 90%. With an optional exhaust gas heat exchanger, the thermal output could be raised to 13.3 kW and an overall efficiency of 92% is then achieved. PowerPlus Technologies®, with the Ecopower model, proposes a system based on Briggs & Stratton 5 hp engine, fuelled by natural gas or propane. Its output is of 4.7 kW of electrical power and 12.5 kW of heat for an overall efficiency of up to 92%. At the moment, gas-fired ICEs are the most mature technology available on the market.

Table 2.1 Commercially available cogeneration systems based on ICE

Specifications	Honda Ecowill	Aisin Seiki GECC 46	Ecopower	Senertec Dachs	Cogengreen Ecogen 12
Electr. Power [kW]	1.0	4.6	4.7	5.0	11.7
Therm. Power [kW]	2.8	11.7	12.5	12.3	26.5
Electr. Efficiency [%]	22.5	25.5	24.8	25.5	28.5
Therm. Efficiency [%]	63.0	58.5	66.0	62.7	64.6
Fuel	NG, LPG	NG, LPG	NG, Propane	NG	NG,LGP
Weight [Kg]	83	465	390	530	750
N° Engine Cylinders	1	3	1	1	4
Noise [dBA]	44	54	56	56	53

2.2.3. Fuel Cells

Fuel cells generate electricity through a chemical reaction without combustion and mechanical work. Concerning to principle of operation, every fuel cell has two electrodes, one positive and one negative, the anode and cathode. The reactions that produce electricity take place at the electrodes. The electrolyte carries electrically charged particles from one electrode to another, and a catalyst speeds the reactions. Hydrogen is the basic fuel, but fuel cells also require oxygen. Fuel cells generate electricity with zero pollutant emissions, since combining hydrogen and oxygen form water and heat as a by-product during the electricity production. Basically, the reaction is achieved through the electrochemical oxidation of the hydrogen and the electrochemical reduction of oxygen. The fuel cell produces an electrical current that, because of the way electricity behaves, this current returns to the fuel cell, completing an electrical circuit. Considering that the reaction is exothermic the released heat can be used for space and domestic water heating. The hydrogen used as fuel can be produced from different sources, such as, natural gas, propane, coal, or through the electrolysis of water.

Currently, there are various types of fuel cell technologies in different stages of development. These include Alkaline Fuel Cells (AFC), Polymer Electrolyte Membranes Fuel Cells (PEMFC), Phosphoric Acid Fuel Cells (PAFC), Molten Carbonate Fuel Cells (MCFC), Solid Oxide Fuel Cells (SOFC), and Direct Methanol Fuel Cells (DMFC) (Perry & Fuller, 2002).

ACF uses a solution of potassium hydroxide in water as their electrolyte. Efficiency is about 70 %, and operating temperature is 150 to 200 °C. Their output ranges from 300 W to 5 kW and require pure hydrogen fuel. MCFC uses high-temperature combinations of salt carbonates (e.g. sodium or magnesium) as the electrolyte. Efficiency ranges from 60 to 80%, and operating temperature is about 650 °C. Power plants with output up to 2 MW have been constructed, and designs exist for units up to 100 MW. Their nickel electrode-catalysts are inexpensive compared to the platinum used in ACF. But the high

temperature also limits the materials and safe uses of MCFCs in residential buildings. Efficiency of PAFCs range from 40 to 80%, and operating temperature is between 150 to 200 °C. The output of PAFCs is up to 200 kW, and 11 MW units have been tested in the last years. Platinum electrode-catalysts are needed, and internal parts must be able to withstand the corrosive acid. PEMFC works with a polymer electrolyte in the form of a thin, permeable sheet. Efficiency is about 40 to 50%, and operating temperature is about 80 °C for an output in the range from 50 to 250 kW. These cells operate at a low enough temperature to make them suitable for residential systems because the leak risk is low. However, their fuels must be purified, and a platinum catalyst is used on both sides of the membrane, which actually raise their cost.

SOFC use a hard, ceramic compound of metal oxides as electrolyte. Their efficiency is about 60%, and operating temperatures are about 1000 °C. Cells output is up to 100 kW. At such high temperatures, a reformer is not required to extract hydrogen from the fuel, and waste heat can be recycled to make additional electricity. However, the high temperature limits applications of SOFC units and they tend to be rather large (Cells2000, 2005).

Fuel cell technology is an emerging technology with potential for both electricity and thermal generation. The advantages of fuel cell cogeneration systems include low noise level, potential for low maintenance, low emissions, and a potential to achieve a high overall efficiency even with small units. With a fuel cell, carbon dioxide emissions may be reduced by up to 49%, nitrogen oxide (NOx) emissions by 91%, carbon monoxide by 68%, and volatile organic compounds by 93% (Onovwiona & Ugursal, 2006). Low emissions and noise levels make fuel cells particularly suitable for residential and small commercial applications. Figure 2.4 summarizes the main advantages and disadvantages according to fuel cell typology.

The high cost and relatively short lifetime of fuel cell systems are their main negative aspects. On-going research to solve technological problems and to develop less expensive materials and mass production processes are been developed. Fuel cell based cogeneration system consist of a system that includes: fuel cell stack; feed gas manifolds; a fuel cell processing subsystem such as fuel management controls, reformer, steam generators, shift reactors, sulphur absorbent beds, and ancillary components; a power and electronic subsystem such as solid state boost regulator, DC to AC inverters, grid interconnect switching, load management and distribution hardware, and inverter controller and overall supervisory controller; a thermal management subsystem such as stack cooling system, heat recovery and condensing heat exchangers. The components with most representative costs are: the fuel cell stack (25 to 40%) and the fuel processing subsystem, which represents 25–30% of equipment costs. The main drawback of this technology is the investment cost (Kuhn, Klemeš, & Bulatov, 2008).
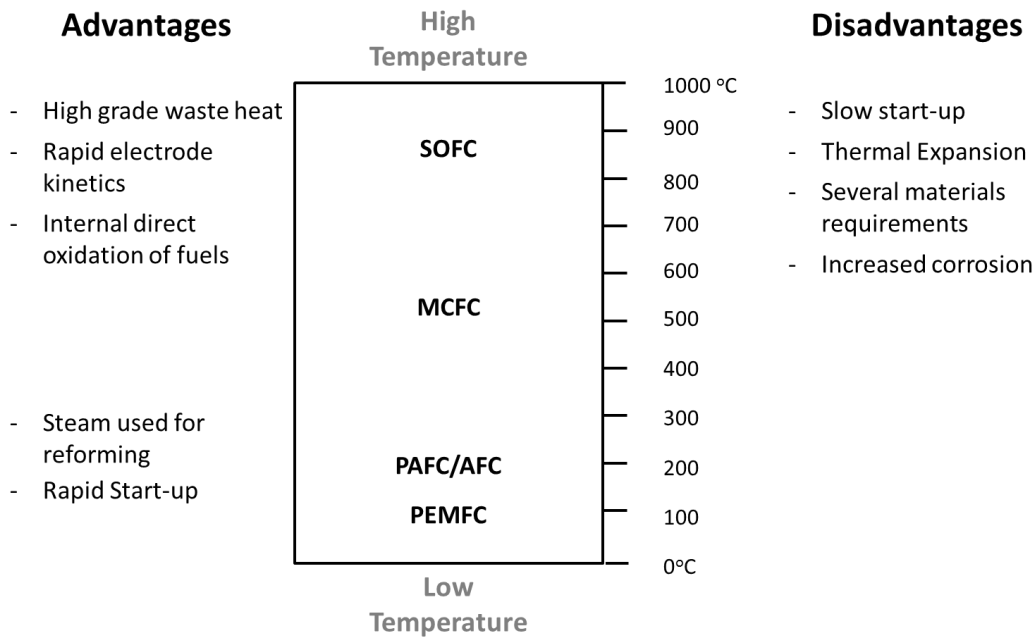
Figure 2.4 Advantages and disadvantages for different types of fuel cells and range of temperature operation.

2.2.4. Organic Rankine Cycles

Organic Rankine Cycles (ORCs) are also a emergent technology that has been prove to be suitable for low-temperature heat source applications at various scales, from several kW_{el} to over 1 MW_{el}. By using of low-temperature heat sources, the ORC has a relatively higher thermal efficiency when compared to other heat cycles. The conventional Rankine cycle comprises five components, namely, the working fluid, heater, expander (i.e. turbine), condenser and compressor (or pump). An ORC cogeneration based system uses a working fluid which is first pumped through a boiler, suffers evaporation, pass through a turbine and, finally, is condensed (Saitoh, Yamada, & Wakashima, 2007). The fluid is organic, and may have a higher boiling point than the water. Low-temperature heat can be used in the micro-CHP by converting it to work and, thus, electricity. In fact, at low temperatures, organic working fluids lead to higher cycle efficiency than water. ORC power generation systems have been used successfully in geothermal power plants for decades. In small-scale and micro-scale CHP systems, organic working fluids are desirable because the fluid mechanics leads to high efficiency. With an appropriately selected organic working fluid, the vapour can expand in the turbine in its saturated and superheated states. Some ORC engines are quite small and light, with theoretical net electrical efficiencies of up to 17%. Some units can also vary their output in response to the heating demand.

Although the specific investment cost of an ORC system is higher than conventional steam cycle, the operating cost is considerably lower due to its good controllability, high degree of automation, and low maintenance cost (Dong, Liu, & Riffat, 2009).

Key technical advantages of ORC power plants include:

- High cycle efficiency;
- Very high turbine efficiency (> 85%);
- No erosion, due to the absence of moisture in the vapour nozzles;
- Long lifetime periods;
- Simple start-stop procedures;
- Quiet operation and minimum maintenance requirements;
- Good part load performance.

In the literature, several studies have been presented concerning to ORCs optimization and experimental validation. Saitoh *et al.*(2007) reported the experimental results of a solar ORC system. Authors performed experimental tests using a displacement-type scroll expander and compound parabolic concentrator (CPC) solar collector to improve the thermal efficiency of the system. The results shown that, the proposed system is capable of using waste heat from sources such as the combustion heat of biogases or hydrogen and the exhaust heat from other energy systems, improving its overall efficiency. Sun & Li (2011) proposed a mathematical model to optimize the performance of an ORC heat recovery power plant using R134a as working fluid. Their work analyses variables, such as the working fluid mass flow rate, air cooled condenser fan air mass flow rate, and expander inlet pressure, on the system thermal efficiency and system net power generation. Yamamoto *et al.* (2001) developed a numerical simulation model to estimate ORC system performance under various operating conditions. An experimental apparatus was also developed to validate the numerical results.

The most important factors in the evaluation of an ORC system are the investment costs and the overall efficiency. The annual maintenance costs should be less than 0.5% of the total investment costs. The proven lifetime ought to exceed 80 000 operating hours. Data about the ORC investment costs was not found in the literature.

2.2.5. Stirling Engines

Stirling engines are a technology that is not fully developed yet, and it is not widely used. This technology has good potential because of its high efficiency, fuel flexibility, low emissions, low noise/vibration levels and good performance at partial load (Alanne, Söderholm, Sirén, & Beausoleil-Morrison, 2010). Unlike reciprocating internal combustion engines, Stirling engines rely on an external combustion or other exterior heat-source, thus allowing the use of different primary energy sources including fossil fuels (oil derived or natural gas) and renewable energies (solar or biomass). In these engines, the working fluid operates on a closed regenerative thermodynamic cycle, with cyclic compression and expansion of the working gas at different temperature levels (Kongtragool & Wongwises, 2003; Rogdakis, Antonakos, &

Koronaki, 2012). Since the combustion process takes place outside the engine, the continuous combustion process make Stirling engines a smoothly technology, resulting in lower vibration, noise level and emissions when compared with the reciprocating internal combustion engines. This technology is also characterized to have fewer moving parts compared to other engines. Stirling engines have low wear and long maintenance free operating periods. Stirling cycle engines have been developed as an external combustion engine with regeneration. The cycle resembles in the ideal Carnot cycle. Stirling cycle has the potential of achieving higher overall efficiency than those of the Rankine or Joule Cycles, because it more closely approaches the Carnot cycle.

Nevertheless, there are some limitations for Stirling engine technology. Some components of the engine should be manufactured with special alloys because of the high temperature and pressure operational conditions endured by the system. This increases the production costs which require high investment costs. Moreover, the choice of the "ideal" gas can bring some difficulties associated with its ability to diffuse through materials, which works at high operation pressures. Despite these limitative aspects of Stirling engines, this technology fulfils a number of requirements for decentralized energy conversion applications. Table 2.2 presents the actual energy requirements and the attractive features of the Stirling technology.

Table 2.2 Power plant needs and matching attractive features of Stirling engines

Technological Needs	Stirling Engine Characteristics
Reducing conventional fuels use	Flexible fuel sources
Increasing fossil fuel costs	Low fuel consumption
Use of alternative fuels	Low noise and vibrational levels
Reduction of gas emissions	Clean combustion
Waste heat recovery	High thermal efficiency

A number of Stirling engine developers for micro-CHP applications are available. Stirling engine manufactures that are focused on micro-CHP applications are worldwide dispersed.

Stirling engines have been developed in a wide range of power capacity, from 1 W to 1 MW$_{el}$. Both engine drive types show a great potential for combined heat and power systems. The kinematic Stirling units are able to produce 1.1 to 500 kW$_{el}$ of electrical capacity, while free piston Stirling engines can be found in the range between 1 and 25 kW$_{el}$. This makes free piston Stirling engines an attractive technology suitable for small- and micro-scale applications. There are some commercially available cogeneration systems, based on Stirling engines, in development. The company *WhisperTech®* (New Zealand) developed an alpha kinematic engine called WhisperGen™ with a capacity of up to 1.2 kW of electrical power and 7.5-14.5 kW of heat. It is a four-cylinder unit with the option to interface with the electrical grid. WhisperGen™ provides

a low electrical efficiency of 12% but an total efficiency of 80%, leading to smooth and vibration free operation (WhisperTech, 2012).

Microgen™ unit, developed by BG Group from a US (Sunpower) design, contains a supplementary burner that enables it to meet the full heating requirements for larger homes. MicroGen™ is a cogeneration unit for residential and small-office use. The unit is based on free piston Stirling engine and it is fuelled by natural gas. This unit is able to produce 1.1 kW of electricity and a thermal output range of 15-36 kW_{th}. However, when the demand is low, the unit has the capacity of modulating down to 5 kW_{th}. According to BG Group, the MicroGen™ unit can reduce CO_2 emissions in 25% (Baxi, 2012).

Cleanergy® is a leading engine manufacturer in the Stirling technology field. It offers two variants of small power plants: one for biogas and one for solar power, the Solo Stirling model. The units are of open source configuration and have the maximum electrical capacity of 9kW. The combined heat and power unit for biogas also generates 26 kW of thermal power. Cleanergy's Stirling units have a very long lifetime and high efficiency. In 2009, Cleanergy® moved the production of Stirling engines from Germany to the newly refurbished company in Sweden in order to scale-up the production (Cleanenergy, 2012).

The Enatec® consortium in the Netherlands and Rinnai in Japan both use Infinia Stirling generator technology in their residential CHP systems. Their free-piston Stirling generators are designed to deliver energy in a way that is virtually silent, long-lasting, economical, environmentally-friendly and exceptionally low-maintenance. Infinia Corporation® recently launched a new system, the PowerDish™, which uses a parabolic concentrator dish to concentrate the sun's energy onto the hot end of a free-piston Stirling engine. This concentrated solar energy creates a temperature differential across the engine, causing the expansion and the contraction of the working gas which leads to the piston motion and the alternator generates electricity (Infinia Corporation, 2012). Inspirit® has been developing a micro-CHP unit based on a kinematic Stirling engine design. The beta configuration Stirling engine uses helium as its working gas and utilises an external heat source, to provide energy. The micro-CHP unit is capable of simultaneous generation of 15kW thermal and 3 kW electrical output, exporting this electricity back to the utility grid. The appliance offers a total efficiency of up to 92%, comparing to an electrical efficiency of 16% and a thermal efficiency of 76% (Inspirit, 2012).

Stirling BioPower®, previously called STM Power, is a North American company which designs and manufactures Stirling engines. The company developed the PowerUnit™ which uses a Stirling engine to create a prime mover designed for renewable energy and distributed generation applications. The system was designed to operate on natural gas, propane, alcohol and renewable energy such as biomass or hot air as heat source. PowerUnit™ is able to reach a net electrical efficiency of 27-28% and, used in cogeneration mode, the total efficiency can achieve the 75-80% (Stirling BioPower, 2012). Sigma Elektroteknisk (in Norway) developed a Stirling engine, PCP 1-130, to be used in co-generating

applications. The beta-type Stirling uses helium as the working fluid, producing 1.5 kW of electrical power and 9 kW of thermal power with a total efficiency of 95%.

Table 2.3 presents the specifications of several commercial cogeneration units based on Stirling engine technology. The cogeneration units are compared in terms of electrical and thermal output; electrical and thermal efficiency, fuel, working gas, size and engine configuration.

In the literature, there are some interesting works concerning the optimization of Stirling engines for several applications. Some of those studies are numerical and others are experimental. Wu, Chen, Wu and Sun (1998) analysed the optimal performance of a Stirling engine. In their Study, the influence of heat transfer and regeneration time on the Stirling engine cycle performance was discussed. Formosa & Despesse (2010) developed an analytical thermodynamic model to study free-piston Stirling engine's architecture. The model integrated the analysis of the regenerator efficiency and conduction losses, the pressure drops and the heat exchangers effectiveness. The model was validated using the whole range of the experimental data available from the General Motor GPU-3 Stirling engine prototype. The influence of the technological and operating parameters on Stirling engine performance was investigated. The results from the simplified model and the data from the experiment showed a reasonable correlation.

Table 2.3 Cogeneration units based on Stirling engine technology and their specifications

Specifications	Whispergen	Baxi Ecogen	Sunmachine	SM5A	Solo 161
Electr. Power [kW]	1.0	1.0	3.0	8.1	9.0
Therm. Power [kW]	7.0	6.0	10.5	24.9	26.0
Electr. Efficiency [%]	12	13.5	20.0	21.1	25.0
Therm. Efficiency [%]	84.3	81.1	70.0	64.8	72.2
Fuel	NG	NG, Biogas	Wood Pallet	Biogas	NG, LPG, biogas, biomass
Weight [Kg]	137	110	410	900	460
Working fluid	Nitrogen	-	Nitrogen	Helium	Helium, Hydrogen
Engine Type	Alpha	LFP[1]	Alpha	Beta	Alpha
Noise [dBA]	-	45	-	-	-

[1]Linear Free Piston (LFP)

Kaushik & Kumar (2000) studied effects of irreversibility of the regenerator and heat transfer process in heat/sink sources. Ust, Sahin & Kodal (2007) introduced a new thermo-economic performance analysis based on an objective function defined as the power output per unit total cost. Boucher, Lanzetta & Nika (2007) reported a theoretical study of the dynamic behaviour of a dual free-piston Stirling engine coupled with an asynchronous linear alternator. The objective was the evaluation of the thermo-mechanical

conditions for a stable operation of the engine. Kongtragool and Wongwises (2006) investigated the effect of regenerator effectiveness and dead volume on the engine network; and the heat input into the engine efficiency by using a theoretical investigation on the thermodynamic analysis of a Stirling engine.

Nepveu and his co-authors presented a global thermal model of the energy conversion of the 10 kW$_{el}$ Eurodish dish/Stirling unit, using optical measurements to calculate the losses by parabola reflectivity. The authors also performed a thermodynamic analysis of a SOLO Stirling 161 engine. The model was divided in 32 control-volumes and equations of ideal gas, mass and energy conservation are written for each control-volume. The differential equation system was then solved, iteratively by using a MatLab programming environment (Nepveu, Ferriere & Bataille, 2009). Rogdakis et al. (2012) studied a Solo Stirling Engine V161 cogeneration module via a thermodynamic analysis. Calculations were conducted using different operational conditions concerning the heat load of the engine and the produced electrical power. The authors achieved good results in terms of electrical and thermal efficiencies as well as a positive primary energy saving. Asnaghi and his co-authors (2012) also performed a numerical simulation and thermodynamic analysis of SOLO 161 Solar Stirling engine. He and his co-authors considered several imperfect working conditions, pistons' dead volumes, and work losses in the simulation process. According to their studies, regenerator effectiveness, heater and cooler temperatures, working gas, phase difference, average engine pressure, and dead volumes are parameters that affect Stirling engine performance, which was estimated for different input considerations. Also, the results indicated that the increase in the heater and cooler temperature difference and the decrease in the dead volumes will lead to an increase in thermal efficiency.

Cheng & Yang (2012) developed a theoretical analysis of the effects of the geometrical parameters on the shaft work of the Stirling engines. The optimal combination of the phase angle and the swept volume ratio was studied and the maximization of the shaft work of the engine was obtained under different specified conditions. Effects of the mechanism effectiveness, the dead volume ratio, and the temperature ratio on the maximum shaft work of the engine as well as the optimal combination of the phase angle and the swept volume ration were also evaluated. Puech and Tishkova, (2011) performed a thermodynamic analysis of a Stirling engine conducting an investigation about the influence of regenerator dead volume variations. The results showed that the dead volume amplifies the imperfect regeneration effect. Zarinchang and Yarmahmoudi (2008) performed a very interesting study in order to optimize the thermal components in a 20 kW$_{el}$ Stirling engine. The main objective of their study was re-designing the heat exchangers by using two programs, the STRENG and the OPTIMUM. The authors presented an evaluation to the geometrical parameters effect in the Von-Mises stress, engine efficiency and power output. A sensitivity analysis to the geometrical parameters of each heat exchanger was presented in order to determine the best configuration of the thermal components in order to improve the engine performance. The authors concluded that the analysis of the relationships between the geometric characteristics of the

heat exchangers gives important insights of their relevance in the engine performance. Moreover, significant improvements in terms of engine efficiency can be achieved (Zarinchang & Yarmahmoudi, 2008, 2009). Ahmadi and co-authors (2013) presented the optimization of a solar-powered high temperature differential Stirling engine considering multiple criteria. A thermal model was developed so that the output power and thermal efficiency of the solar Stirling system with finite rate of heat transfer, regenerative heat loss, conductive thermal bridging loss, finite regeneration process time and imperfect performance of the dish collector could be obtained. The problem was formulated as a multi-objective problem applying evolutionary algorithms (MOEAs) based on the NSGA-II algorithm. The solar absorber temperature and the highest and lowest temperatures of the working fluid were considered as decision variables (Mohammad H. Ahmadi, Sayyaadi, Mohammadi, & Barranco-Jimenez, 2013). The system under study is presented at Figure 2.5.
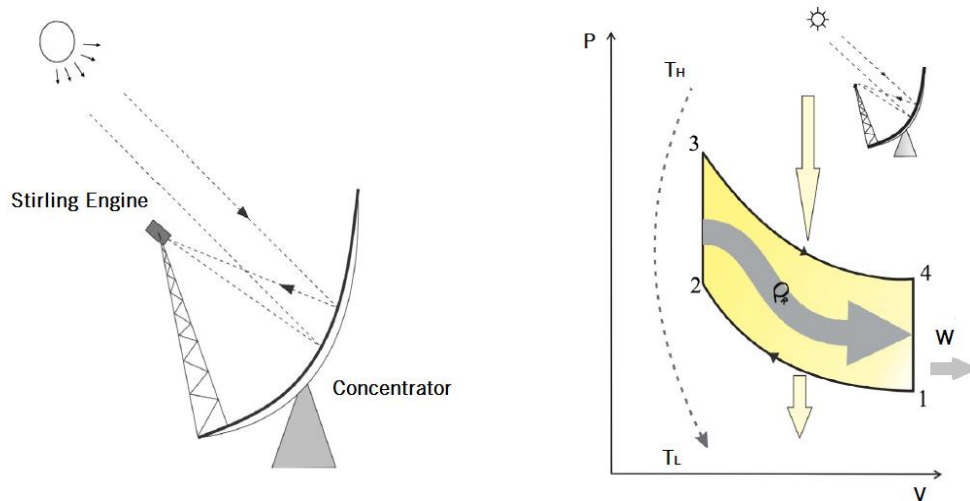
Figure 2.5 PV diagram of an isothermal solar Stirling engine cycle. Adapted from (Ahmadi et al., 2013).

The study showed that in the multi-objective optimization of the solar-dish Stirling engine, if a great weight factor is considered for the thermal efficiency, absorber temperature and temperature ratio of the engine should be considered at a lower value in comparison to the case in which a lower weight factor is considered for the thermal efficiency.

2.2.6. Comparison between the Technologies

For micro-CHP applications, spark ignition engines are used when the exhaust heat as well as the heat from the oil and engine cooling is recovered using heat exchangers. Reciprocating engines are produced and commercialized in large scale by a variety of companies worldwide. One of the most sold systems is the Dachs model by Senertec® Company. Different models are available which generates 5.0 or 5.5 kW of electricity and 14 kW of thermal energy. It achieves 25% and 80% of electrical and total efficiency, respectively. An interesting unit for single-family house applications is the Honda's Ecowill unit, which

delivers 1 kW of electricity. Fuel Cells, which convert the chemical energy into electrical energy, are under development by several companies. Leading examples include the Plug Power PEM (Polymer Exchange Membrane) unit with a production of 4.6 kW of electricity, plus 7 kW of heat and the Sulzer Hexis SOFC (Solid Oxide Fuel Cell) 1 kW_{el} unit with integral gas burner to provide flexible thermal output. The main disadvantages of this technology are that the heat cannot be extracted at well-defined points in the system, investment costs are extremely high and reliability issues are still a problematic.

The most used Rankine engine is the steam engine in which water is boiled by an external heat source, expands and exerts pressure on a piston or turbine rotor and hence does useful work. Some of these systems use an organic fluid and operates at temperatures and pressures much closer to conventional heating and refrigeration purposes. An example of these units is the *Energetix Genlec* system, based on the Inergia prototype developed by the Battelle Institute in the USA. This system is able to produce 1 kW of electricity and 10 kW of heat. Although having rather low electrical efficiency, it is well matched to many domestic applications and appears to offer relatively low manufacturing costs and good service life characteristics. In 2011, this system was in laboratory tests phase (Energetix Group Web Site, 2012).

Micro gas turbines are also used as prime movers for cogeneration applications, but not at the micro-scale level due to the fact that these systems are only available for higher power outputs (30kW_e). In Table 2.4, the different technologies are compared considering the electrical and overall efficiencies, the stage of the technology development, fuel versatility, and investment costs for each technology and the specific power.

Table 2.4 Comparison of different cogeneration technologies

Technology	η_{el} (%)	$\eta_{overall}$ (%)	Energy Source	Stage of Technology	Investment Costs (€/kW_{el})	Specific Power (W/kg)
Micro-Turbines	28-30		NG, Propane, Gas, Diesel	Mature Technology	1 000 – 1 700	30-47[1]
ICEs	20-30	> 85	Liquid fuel NG	Commercially available	2 100[2] – 4 500	10 - 18
Stirling Engines	11-35	> 85	Any type of fuel, Solar radiation	Some models are already commercially available	2 000[3] – 10 000	7.3 - 9.1 [4]
Fuel Cells	24-39	80-85	Hydrogen hydrocarbon	In R&D and test prototypes	>30 000	-
ORCs	10-20	70-85	Any type of Fuel	In R&D	-	-

[1] Capstone Models; [2] For a 15 kW_e unit; [3] Solo 161 not currently available; [4] not including Solo 161

Considering the data from Table 2.4, it can be said that Stirling engines offer a high variety of fuels with which it is possible to operate, allowing in particular the use of bio fuels or solar energy. Stirling engines have a great potential to achieve high overall efficiencies despite the moderate electrical efficiency. Also, the Stirling engines have good performance at partial load. The reciprocating engines are the technology with higher maturity, which represents a great advantage with respect to their diffusion in the market. Reciprocating engines have similar values for electrical efficiency when compared with the Stirling engines, but theoretically require more periodic maintenance representing a cost increase. In addition, reciprocating engines have high noise levels and pollutant emissions.

Fuel Cells and Rankine engines are still under development with some pilot plants being currently tested. The major potential of these two technologies lies in the highest electrical efficiency and the almost zero pollutant emissions. However, and due to fact that both are emerging technologies, their capital costs are considerable. As a result, their competitiveness remains unclear until they could be distributed in the market.

The performance of several CHP units based on Micro Gas Turbine, Stirling engine, ORC and ICE technologies is graphically compared in Figure 2.6. The electric and thermal efficiency is presented as a function of electrical power, considering data from CHP units varying in the range of few kW to 100 kW.
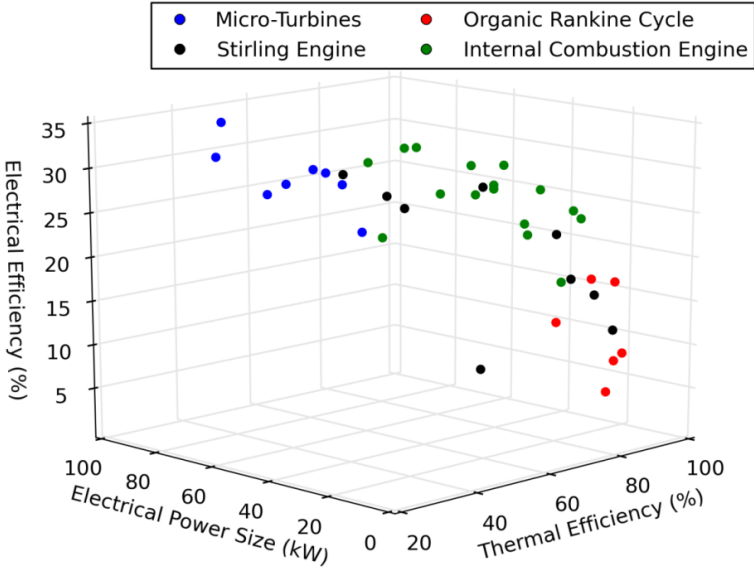
Figure 2.6 Comparison of electric and thermal efficiency as a function of electrical power for different technologies.

Comparing the technologies, it may be said that the ORC and the SE are the technologies that present higher values for the thermal efficiency and MGT and ICE are the technologies which models can achieve a higher electrical efficiency. Accordingly to these data, it can be said that some technologies are more suitable for some size of applications than others, taking into account the heat or the electricity demands. The CHP tecnhologies seem suitable to be applied for heating of residential buildings (mainly systems up

to 5-10 kW$_{el}$). Bigger buildings requires CHP units with an electric power size lower than 100 kW$_{el}$ (Bianchi, De Pascale, & Spina, 2012).

2.3. Optimization Methods

Optimization refers to a field of applied mathematics and computer science concerned with the minimization or maximization of a certain function, possibly under constraints. The birth of the optimization can be perhaps traced back to an astronomy problem solved by the young Gauss in the 1850's. It matured later with advances in physics and mechanics, where phenomena were described as the result of the minimization of a certain ''energy'' function. Optimization has evolved towards the study and application of algorithms to solve mathematical problems with higher or lower complexity (Bejan, Tsatsaronis, & Moran, 1996).

Optimization is an important tool in decision science and in the analysis of physical systems. To make use of this tool, the first step is to identify some objective, a quantitative measure of the performance of the system under study. This objective can represent profit, time, energy, or any quantity or a combination of quantities that can be represented by a single value. This objective (i.e. objective function, $f(x)$) depends on certain characteristics of the system, called variables or unknowns, which optimal values optimize the objective function (Nocedal & Wright, 1999). The process of identifying objective, variables, and constraints for a given problem is a very important step in the design of an appropriate model. If the model is too simplistic, it does not give useful insights into the practical problem. If it is too complex, it may be too difficult to solve (S. S. Rao, 2009). Most of the scientific problems involve equations that relate the changes in some key variables to each other. Modelling a physical phenomenon comprises reasonable assumptions and approximations, always taking into account the relevant physical laws and the dependency degree between the variables. The model should reflect the essential features of the physical problem it represents.

Once the model is formulated, an optimization algorithm can be used to find its solution, usually with the help of computer software or a simulation platform. There is no universal optimization algorithm; a particular algorithm should be applied to a particular optimization problem. Problems can be classified according to the nature of the objective function and constraints (linear or nonlinear), the number of variables, the smoothness of the functions (differentiable or non-differentiable), and so on (Rodríguez-Toral, Morton, & Mitchell, 2000).

The optimization problems can be divided into continuous and discrete types depending on the nature of the objective function. Discrete problems usually have a finite number of variables, each of which assumes exactly one value at an optimal solution. In continuous problems, the optimal values are functions of some parameter, and a solution to the problem requires the specification of this function over

a set of parameters. The continuous optimization problems have a non-linear nature and are characterized by the presence of explicit and implicit constraints on both control variable and objective function. Continuous optimization problems are normally easier to solve because the smoothness of the functions makes it possible to use objective and constraint information at a particular point x value of the decision variable to deduce information about the function's behaviour at all points close to solution. In discrete problems, by contrast, the behaviour of the objective and constraints may change significantly as we move from one feasible point to another.

On the basis of the number of objective functions describing the performance of the system, the objective to find the optimal solution is called single-objective optimization when an optimization problem describing an optimization problem involves only one objective function. When the optimization problem involves more than one objective function, it is known as multi-objective optimization problems, which use multiple decision-making criteria.

Optimization problems can also be characterized as unconstrained and constrained problems. Unconstrained optimization problems arise even in some problems with natural constraints on the variables, as they do not influence the solution and do not interfere with algorithm procedure. Other situation regards to the problems that arise as a reformulation of constrained optimization problems, in which the constraints are replaced by penalty techniques added to objective function. Constrained optimization problems arise from models in which constraints play an essential role, for example in imposing physical or economic constraints in a design problem. These constraints may be simple bounds, more general linear constraints, or nonlinear inequalities that represent complex relationships among the variables.

Many algorithms for nonlinear optimization problems seek only a local solution, a point at which the objective function is smaller than at all other feasible nearby points. They do not always find the global solution, which is the point with lowest function value among all feasible points. Global solutions are needed in some applications, but for many problems they are difficult to recognize and even more difficult to locate (Nocedal & Wright, 1999).

Optimization algorithms are iterative. They start with an initial feasible point (a set of values for the decision variables) and generate a sequence of improved estimates (called "iterates") until they terminate, hopefully at a solution. The strategy used to move from one iterate to the next distinguishes one algorithm from another. Most strategies make use of the values of the objective function, the constraint functions, and possibly the first and second derivatives of these functions. Some algorithms accumulate information gathered at previous iterations, while others use only local information obtained at the current point. Good algorithms should possess: robustness, efficiency and accuracy. A robust algorithm is able to solve well a wide variety of problems in their class and does not require excessive computer time or storage; an

efficient and accurate algorithm is able to identify a solution with precision, without being too much sensitive to errors in the data when implemented on a computer.

Nevertheless, compromises between convergence rate and computational effort, and between robustness and speed must be considered when applying these numerical approaches in solving engineering problems. A rapidly convergent method for a large unconstrained non-linear problem may require too much computer effort. On the other hand, a robust method may also be the slowest (Thomas, David, & Leon, 2001a).

There is a great variety of optimization methods and/or algorithms. Its choice and application depends on the problem that is intended to solve: constrained or unconstrained; linear or non-linear; global or local optimization problems. In the literature, there are gradient-based as well as derivative-free optimization methods that converge to solutions of problems.

Most algorithms require the user to supply a starting point, denote by x_1. The user with knowledge about the application and the data set may be in a good position to choose x_1 to be a reasonable estimate of the solution. Otherwise, the algorithm must choose the starting point, either by a systematic approach or in some arbitrary manner. Optimization algorithms generate a sequence of iterates that terminate when either no more progress can be made or when it seems that a solution point has been approximated with sufficient accuracy. In deciding how to move from one iterate to the next, the algorithms use information about the function. They use this information to find a new iterate with a lower function value than. Many constrained optimization algorithms can be adapted to the unconstrained case, often via the use of a penalty method. However, search steps taken by the unconstrained method may be unacceptable for the constrained problem, leading to a lack of convergence. Nevertheless, most problems in engineering are somehow constrained (Williamson & Shmoys, 2010).

2.3.1. Optimization Methods for Multidimensional Problems

Derivative-free as well as gradient-based optimization methods are used to solve problems with several decision variables and its application depends on the problem formulation and if the functions are differentiable or not. Direct Search methods attempt to solve optimization problems when the functions are not differentiable and when the explicit information about its gradient is unavailable or untrustworthy. According to Kolda, Lewis, & Torczon (2003), interest in direct search methods was revived after its application in parallel computing. Since then, it was proved that direct search methods continue to be an effective option, and sometimes the only option, for several varieties of difficult optimization problems and that it is possible to provide rigorous guarantees of convergence of most of them.

The Nelder–Mead simplex algorithm (or the method of the polyhedron in R) is one of the most widely cited of the direct search methods. This method does not calculate derivatives, using only the information of the

objective function whose expression is not differentiable. The simplex is composed by *n+1* vertices. The simplex is usually represented by $S_k = \langle X_1, X_2, X_n, X_{n+1} \rangle$, where the vertices are represented by crescent order (i.e. $f(X_1) \le f(X_2)$), where the X_1 is the better vertex of the simplex and X_{n+1}, is the worst. For each iteration, auxiliary points are defined and those points are candidate vertices of a new simplex that will be accepted or rejected by comparing only the values of function with their value. The first step of the algorithm is to calculate the centroid of the simplex defined by the better n vertices of the simplex. After that, a new vertex is calculated according to equation (2.3):

$$X_{new} = X_{n+1} + \delta\left(\overline{X} - X_{n+1}\right) \tag{2.3}$$

where δ begins with the value 2 when the first auxiliary point is calculated. Four scenarios are possible: if its function value is good ($f(X_1) \le f(X_{new}) \le f(X_n)$), the reflected vertex is accepted and the worst one is removed from the simplex; it its function value is very good ($f(X_{new}) < f(X_1)$), the simplex is expanded (X_{exp}); if the reflected vertex is weak ($f(X_n) < f(X_{new}) < f(X_{n+1})$), the simplex is contracted(X_{contr}); finally, if the reflected point is very weak ($f(X_{new}) > f(X_{n+1})$), the simplex is contracted to the interior of the polyhedron (X_{contr_int}).If none of the four conditions is found out, the polyhedron is shrunk. This means that each vertex is replaced by the midpoint of the segment joining the vertex to its collinear one. To calculate the simplex for the next iteration, it is necessary to order the simplex to check the stopping criterion. Figure 2.7 presents the design of each type of algorithm vertices.

2.7-a

2.7-b

2.7-c

2.7-d
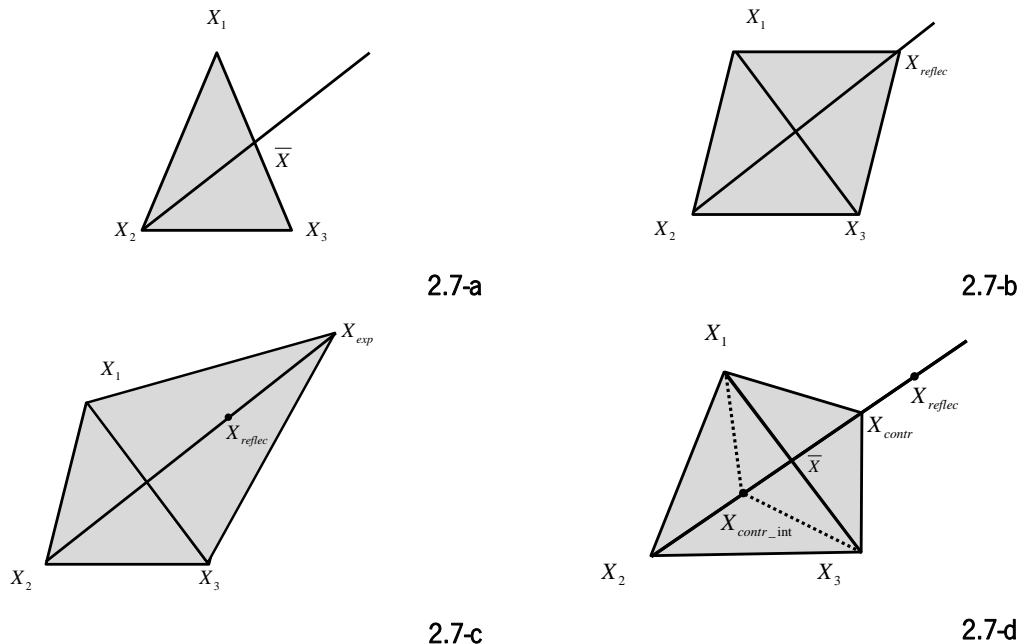
Figure 2.7-a Calculation of the simplex centroid for the Nelder–Mead simplex algorithm. **2.7-b** Calculation of the reflected vertex for the Nelder–Mead simplex algorithm. **2.7-c** Calculation of an expanded vertex for the Nelder–Mead simplex algorithm. **2.7-d** Calculation of a contracted vertex for the Nelder–Mead simplex algorithm.

Gradient methods use the information from the objective function and they can only be applied to problems that are differentiable. In general, these methods reach the convergence easily when compared to the search methods and generate a succession of approximations to the solution $(x^{(j)})$ according to the equation(2.4):

$$x^{(j+1)} = x^{(j)} + \sigma^{(j)} d^{(j)} \qquad (2.4)$$

where $d^{(j)}$ is the search direction (a vector) and $\sigma^{(j)}$ is the step length (a scalar). The iterative equation to calculate the search direction is different for each method. Gradient based methods include the safeguarded Newton method and the Quasi-Newton method, both using the information of the objective function and the derivatives (gradient and/or Hessian matrix) and can only be applied to problems whose functions are differentiable.

2.3.2. Constrained Optimization Methods

Algorithms about minimizing (maximizing) functions subject to constraints on the variables are usually based on the formulation described by equation (2.5):

$$\min f(x) \qquad subject\ to \begin{cases} c_i(x) = 0 \\ c_i(x) \geq 0 \end{cases} \qquad (2.5)$$

where $f(x)$ is the objective function and c_i are the constraints, both real-valued functions on a subset of $\mathbb{R}^n$. Finding a solution in constrained optimization problems can be much harder than in unconstrained ones, since the feasible domain might exclude many of the local minima and it may be comparatively easy to pick the global minimum from those that remain. However, constraints can also make things more difficult (Thomas, David, & Leon, 2001c). If the constrained problem has only equality constraints, the method of Lagrange multipliers is usually used to convert it into an unconstrained problem whose number of variables is equal to the original variables number plus the number of equality constraints. Alternatively, if the equality constraints are all linear, they can be solved for some of the variables in terms of the others, leading to an unconstrained problem in a lower number of variables (S. S. Rao, 2009).

For problems with inequality constraints, it can be characterized in terms of the Karush–Kuhn–Tucker conditions (KKT conditions), in which simple problems may be solvable.

If the objective function and all of the constraints are linear, then the problem is a linear programming problem. This can be solved by the simplex method, which usually works in polynomial time in the problem size but is not guaranteed to, or by interior point methods which are guaranteed to work in polynomial time (Thomas, David, & Leon, 2001b). If all the hard constraints are linear but the objective function is quadratic, the problem is a quadratic programming problem.

Penalty methods correspond to a class of algorithms for solving constrained optimization problems. A penalty method substitutes a constrained optimization problem by a series of unconstrained problems whose solutions converge to a proximal solution of the original constrained problem. The subsequent unconstrained problems are defined by adding a term, called a penalty function, to the objective function that consists of a penalty parameter multiplied by a measure of violation of the constraints. The measure of violation is non-zero when the constraints are violated and is zero in the domain where constraints are not violated. The penalty method can be commonly defined as in equation (2.6).

$$x*(r) = \arg\min_{x \in R^n} \quad \Theta(x, r) \tag{2.6}$$

where $\Theta(x, r) = f(x) + P(x, r)$, $f(x)$ is the initial objective function, $P(x, r)$ is the penalty function that measures the constraint violation.

The application of the penalty functions depends on the constraints typology. Different penalty function may be applied taking into account if the constraints are equality or non-equality constraints. The quadratic penalty function and the penalty function of absolute value correspond to non-exact and exact methods to solve the optimization problem.

Penalty Function of Absolute Value for equality constraints (exact):

$$\min \Theta(x, r) = f(x) + P(x, r)$$
$$P(x, r) = r \sum_{i=1}^{m} |c_i(x)| \tag{2.7}$$

$\Theta(x, r)$ is not differentiable, then the solution can only be calculated by a method that does not use derivatives such as the Nelder-Mead method. Exact penalty methods for the solution of constrained optimization problems are based on the construction of a function whose unconstrained minimizing points are also solution of the constrained problem.

Quadratic Penalty Function for equality constraints (not exact):

$$\min \Theta(x, r) = f(x) + P(x, r)$$
$$P(x, r) = \frac{1}{2} r \sum_{i=1}^{m} (c_i(x))^2 \tag{2.8}$$

where $\Theta(x, r)$ consists of differentiable functions and the solution can be calculated by a method that uses derivatives such as safeguarded Newton method or Quasi-Newton method.

<u>Penalty Function for inequality constraints (exact)</u>

$$\min \Theta(x,r) = f(x) + P(x,r)$$

$$P(x,r) = r \sum_{j=1}^{p} \max(0; h_j(x))$$

(2.9)

$\Theta(x,r)$ is not differentiable at points where $h_j(x) = 0$, then the solution can be calculated by a method that does not use derivatives, such as the Nelder-Mead method (Fernandes, 1997).

The obvious advantage of applying the penalty function approach is obtaining a method that converts constrained problems of any type into unconstrained problems. Another advantage to the penalty function approach is that many constraints in the real optimization problems are "soft", in the sense that they need not be satisfied precisely. The drawback to penalty function methods is that the solution to the unconstrained-penalized problem will not be an exact solution to the original problem (except in the limit cases). The Pattern Search algorithms handle optimization problems with nonlinear, linear, and bound constraints. When these methods are applied to constrained optimization problems, they can be considered as penalty methods and it is required to specify a penalty parameter for the nonlinear constraints as well as a penalty update characteristic of the implemented search method.

Sequential Quadratic Programming (SQP) is a method for solving optimization problems with all kinds of constraints (equality, inequality and simple limits). SQP relies on theoretical foundation and provides powerful algorithmic tools for the solution of optimization problems.

The idea of SQP is to model the constrained nonlinear problem at the current point x_k (k is the iteration number) by a quadratic sub-problem (QP) and to use the solution of this sub-problem to find the new point x_{k+1}. SQP is the application of Newtons' method to the KKT optimality conditions. The QP sub-problems, which have to be solved in each iteration step, should reflect the local properties of the non-linear problem with respect to the current iterate. This is done in such a way that the sequence converges to a local minimum (x^*) of the nonlinear problem as $k \to \infty$. Then, the objective function is approximated by a quadratic function while the constraints are approximated by linear functions.

The Lagrange function $L(x,\lambda)$ is given by the equation (2.10):

$$L(x,\lambda) = f(x) - \lambda^T c(x)$$

(2.10)

where λ^T is the Lagrange multiplier for the k constraints $c(x)$ of the nonlinear problem. The Kuhn-Tucker optimal conditions can be identified by equations (2.11) and (2.12).

$$\nabla_x L(x,\lambda) = \nabla f(x) - \lambda \nabla c(x) = 0$$

(2.11)

$$\nabla_{xx} L(x, \lambda) = \nabla^2 f(X) - \sum \lambda \, \nabla^2 c \, (x) \tag{2.12}$$

As the minimum of the augmented Lagrange function is involved, the SQP method is also known as the projected Lagrangean method and the problem is formulated as in the equation (2.13):

$$\begin{aligned} \min \quad & d\nabla^T f(x_k) + \frac{1}{2} d^T \nabla^2 L \, (x^k, \lambda^k) d \\ s.t. \quad & c(x_k) + \nabla c(x_k)^T d = 0 \end{aligned} \tag{2.13}$$

where d is the search direction. The first-order conditions to solve this quadratic problem are defined using the Lagrangean function associated $L_q(\, d, \eta \,)$ as in equations (2.14) and (2.15):

$$\nabla_d L_q(d, \eta) \equiv \nabla f(x_k) + \nabla^2_{xx} L(x_k, \lambda_k) d - \nabla c(x_k) \eta = 0 \tag{2.14}$$

$$\nabla_\eta L_q(d, \eta) \equiv -c(x_k) - \nabla c(x_k)^T d = 0 \tag{2.15}$$

where η is the vector of multipliers for the quadratic problem. In the matrix form the problem can be solved iteratively by solving the quadratic programming problem through the Newton's method, as shown by the equation (2.16):

$$\begin{pmatrix} \nabla^2_{xx} L(x_k, \lambda_k) & -\nabla c(x_k)^T \\ -\nabla c(x_k)^T & 0 \end{pmatrix} \begin{pmatrix} d \\ \eta \end{pmatrix} = \begin{pmatrix} -\nabla f(x_k) \\ c(x_k) \end{pmatrix} \tag{2.16}$$

where $\nabla^2 L(X, \lambda)$ is the Hessian matrix of the Lagrange function, $\nabla c(x)$ is the gradient matrix of the constraints and the solution $(d, \eta)^T$ is a vector with n elements that defines the search direction, d, and m elements that define η, the vector of multipliers for the quadratic problem.

As this method is valid for a restricted trust region near to ($x*$), the convergence of the method is guaranteed only locally. To ensure the global convergence from any initial approximation and to ensure a downward direction of the algorithm search, it is required to verify the admissibility criterion and to implement a technique of globalization. The admissibility criterions tests if the constrain have decreased sufficiently $\|c(x_k)\|$. The function used to measure the progress of the algorithm is a *merit function*, which combines terms that depend not only of the objective function but also on the constraints, as in equation (2.17):

$$M(x, \lambda) = f(x) - c(x)^T \lambda + \frac{1}{2} \beta_p \|c(x)\|_2^2 \tag{2.17}$$

where β_p is a positive penalty parameter. The convergence of the method depends on the Lagrange multiplier estimates. In addition, a reasonable value for the penalty parameter is very important since it is essential to ensure that the search direction is descendent for the *merit function* and, therefore, that the condition described by the equation (2.18) is verified.

$$\nabla_x M(x_k, \lambda)^T d < 0 \tag{2.18}$$

Note that a major advantage of SQP is that the initial point (or any future iterations points) need not be feasible points (solutions that solve the constraints of the problem).

Recently, engineering problems begun to be solved by applying the genetic algorithms (GA) (Mohammad H. Ahmadi et al., 2013; Valdés, Durán, & Rovira, 2003). While a classical algorithm, at each iteration, generates a single point to approach an optimal solution, a GA generates a population of points and the best point in the population approaches an optimal solution. The GA is a method for solving both constrained and unconstrained optimization problems based on a natural selection process that mimics biological evolution. The algorithm repeatedly modifies a population of individual solutions. At each step, the genetic algorithm randomly selects individuals from the current population and uses them as parents to produce the children for the next generation. Over successive generations, the population "evolves" toward an optimal solution. The population size depends on the nature of the problem, but typically contains several hundreds or thousands of possible solutions. Usually, the population is generated randomly, allowing the entire range of possible solutions (the search space). The solutions may be "seeded" in areas where optimal solutions are likely to be found.

Traditionally, a GA requires a genetic representation of the solution domain and a fitness function to evaluate it. The fitness function is a particular objective function that is used to give merit of a given solution. After each simulation step, the idea is to delete the worst solutions, and breed new ones. Thus, fitness functions indicate how close a certain solution came to meeting the overall specification of the optimization problem. These algorithms are usually applied to find global minima for highly nonlinear problems (R. V. Rao & Patel, 2013).

Evolutionary algorithms (EA) are also applied in energy systems optimization. An EA is a category of evolutionary computation, a generic population-based meta-heuristic optimization algorithm. An EA also uses mechanisms inspired by biological evolution, such as reproduction, mutation, recombination, and selection. Candidate solutions to the optimization problem play the role of individuals in a population, and the fitness function determines the quality of the solutions as in GA algorithms.

2.3.3. Thermo-economic Modelling Approaches

Thermo-economics can be applied to improve the design, thermodynamic and economic aspects of a system and its components. Thermo-economics combines energy and exergy analysis with conventional cost analysis in order to assess and improve the performance of energy systems. The thermo-economic studies in literature can be divided in two different streams: (i) studies focused on the cost flow analysis if the objective is the determination of cost generation and/or cost losses and (ii) studies focused on the optimization of the design, i.e., the selection of the best system operational conditions if the objective is the optimization of power system. The objective of a thermodynamic optimization is to minimize the

thermodynamic inefficiencies within the system, whereas the objective of a thermo-economic optimization of a system is to estimate the cost-optimal structure and the cost-optimal values of the thermodynamic inefficiencies in each component (Bejan et al., 1996).

Coupling exergy and cost streams is not a new idea. In 1932, Keenan was the first researcher pointed out that the value of the steam and the electricity rests in the ''availability'' not only in their energy. Latter, studies focused on desalination processes by exergy analysis, conduced to the idea of exergy costing and its applications to engineering economics, for which they coined the word ''thermo-economics'' (El-Sayed, 1993). Nevertheless, "exergo-economics" is considered as a part of thermo-economics, since the latter have been used in a general sense expressing the interaction between any thermodynamic variables and economics. The main idea behind this methodology was to trace the flow of money, fuel cost and operation and amortized capital cost through a power plant, associating the utility of each stream with its exergy (Tsatsaronis, 1994).

Numerous studies and theoretical approaches in the thermo-economic field have been developed to design and optimize thermal systems since 50s. Bergmann and Schmidt assigned costs to the exergy destruction in each component of a steam power plant and optimized feed water heaters. Szargut used exergy costing method in the analysis of a simple cogeneration plant and introduced ecological cost coefficient by developing an estimated formulation (Szargut, Morris, & Steward, 1988). The use of this coefficient made the determination of cumulative consumption of non-renewable natural resources in a production process possible. Some of these thermo-economic analyses were collected in a book in 1985 by Kotas, which is still seen as one of the major references in exergy analysis and thermo-economics of thermal systems (Kotas, 1985).

During 90s, the studies concerning exergo-economic analysis techniques and applications increased considerably. Spakovsky (1993), (El-Sayed, 1993) and Valero et al. (1994) developed methods that incorporate some key concepts of thermo-economics: sizing constraint through component costing equations, integration of both decomposition and large-scale optimization schemes, distinction of thermodynamic variables (power, mass rate, heat rate, enthalpy, entropy, heat loss, efficiency, heat exchanger effectiveness), adaptation of thermo-economic models to non-linear programming problems and development of a new methodology related to exergy cost analysis.

Lozano and Valero (1993) published another key paper on thermo-economics and presented the basic methodology related to exergy based cost analysis and applications, the theory of exergetic cost and thermodynamic optimization. This theory lies within the context of cost allocation, which provides an important methodology to outline the costing equations.

One of the most interesting works was the CGAM problem, which proposed a standard and common mathematical formulation for all thermo-economic models. The CGAM (Cristhos Frangopoulos, George Tsatsaronis, Antonio Valero and Michael von Spakovsky). CGAM was constructed to assess the optimum

design parameters of a simple CHP apparatus that produces 30 MW of electricity and 14 kg/s of saturated steam. The purpose of this physical model was the standardization of thermo-economic methodologies through the common definitions of physical, thermodynamic and cost models plus the objective function (Valero et al., 1994).

Two main categories of thermo-economic methodologies have been identified: the algebraic methods and the methods based on differential equations. These methodologies rely on the definition of subsystems; all of them are based on optimization of the system by the optimization of the various components of the complex thermal systems. The change in one operating condition of a component influences the other components. The classification of most important theories about thermo-economic methodologies is presented in Figure 2.8.
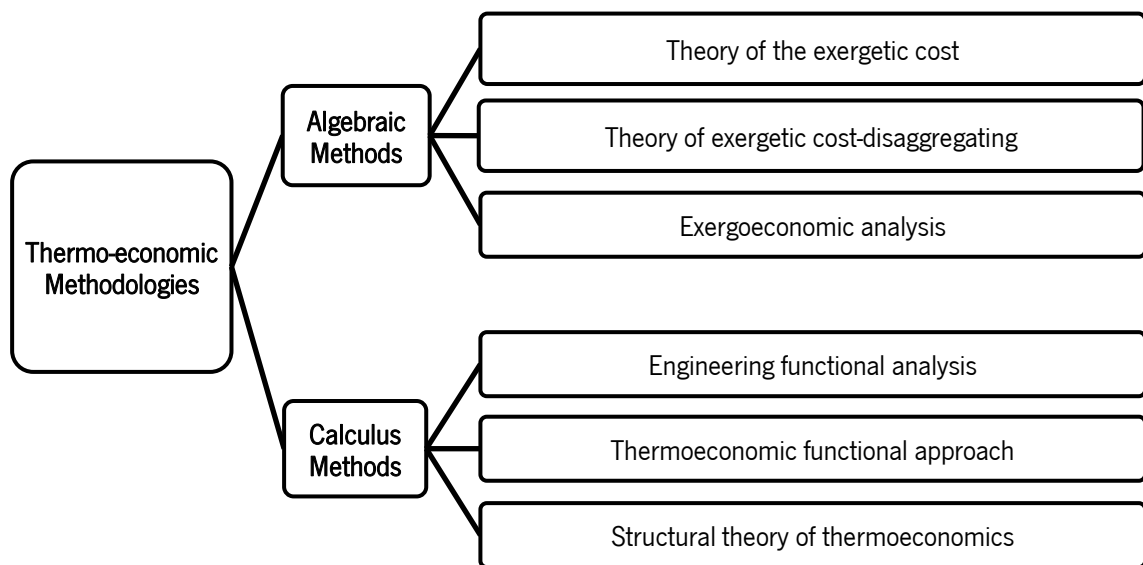
Figure 2.8 Classificaton of thermo-economic methodologies.

The algebraic methods define algebraic cost-balance equations resultant of conventional economic analysis and auxiliary cost equations for each a component or a sub-system of any unit. They are related with the cost formation process of the system in order to investigate the average costs. In algebraic methods, three approaches can be applied: the Theory of Exergetic Cost (TEC) developed by Valero & Lozano (1993), the Theory of Exergetic Costs considering the Disaggregating method (TECD) and the Exergoeconomic Analysis (EEA) proposed by Tsatsaronis & Ho-Park (2002).

The two first approaches use the concept called the exergetic cost. The system is divided into units (a component, or a set of components) and a system of equations can be defined with a cost-balance equation for each unit. A single product and fuel for each component in the system must be defined. Thus, a system of equations can be built with a cost-balance equation for each unit, cost allocation equations for external flows into the system for which costs are externally defined, and losses for which the cost is set equal to zero.

The optimization of EEA is based on an iterative procedure that does not achieve the global optimum of the predefined objective function, but attempts to find a reasonable solution for the overall system design. Two possible alternatives in these methodologies were formulated: average cost and specific cost. The average cost concept is very similar to the application of TEC theory. In the specific cost technique, the cost of the addition of exergy to a material/stream current is determined and charged to the unit that makes use of that exergy. This means that a component will obtain the exergy from a stream at different costs, depending on the components that supplied the exergy to that stream. The division in components of the main plant may be made. If power produced is the main product, cost of all external irreversibility is loaded on the electricity. In opposition, if heat is produced as main one, the steam produced in the plant follows the similar procedure.

Silveira and Tuna (2003) presented a thermo-economic analysis of a cogeneration plant, applied as a rational technique to produce electric power and saturated steam. The aim was to obtain the minimum exergetic production cost, based on the second law of thermodynamics. The variables selected for the optimization were the pressure and the temperature of the steam leaving the boiler, the pressure ratio, turbine exhaust temperature and mass flow in the case of using gas turbines. The equations for calculating the capital costs of the components and products were formulated as a function of these decision variables.

The methodologies based on calculus use differential equations. Cost flows are solved with the optimization algorithms based on the method of Lagrange multipliers and they are used to determine marginal costs. The variation of Lagrange multipliers from iteration to iteration is a consequent difficulty of this methodology when the component thermo-economic isolation is not accomplished. There are three different approaches: Thermo-economic Functional Approach (TFA), Engineering Functional Analysis (EFA) and Structural Theory of Thermo-economics (STT).

TFA optimization is based on the implementation of a nonlinear optimization Lagrangian method. An accurate simulation of the system is necessary to determine the first order derivatives of the objective function. The methods used in EFA approach can be categorized on decomposition methods, modular or Lagrangian approaches.

STT methods were proposed as a standard mathematical formulation for all thermodynamic methodologies employing models that can be expressed by linear equations.

The main characteristic of the cited methods is that they propose a cost balance equation applying the exergetic unit cost to the exergy balance equation according to a specific principle. However, there is a disadvantage of applying those methods to actual systems: too many equations are required to fully define the thermo-economic model (Kim, 2010). Some nonlinear programming techniques for thermo-economic analysis should be used exclusively for a specific type of problem, being inefficient for some complex

models. Bilgen (2000) performed an exergetic and engineering analyses of gas turbine-based cogeneration plants consisting of a turbine, heat recovery steam generator and steam turbine.

The CGAM problem was fully explored for thermo-economic optimization of cogeneration systems based on gas turbines. This model was the basis of the Silva (2000) work, who studied the optimization of CHP applications by adapting the CGAM problem. The same energy output as the original CGAM (30MW of electrical power and 14kg/s of saturated steam at 20 bar) have been considered. After that, Silva and her co-authors performed a thermodynamic study of a cogeneration system based on a gas turbine applied to a local textile factory at the northwest region of Portugal. The model was developed considering a compressor/turbine rated at 5 MW$_{el}$, a boiler (10 bar) and a heat recovery unit for the thermal fluid. The problem was formulated as a non-linear optimization problem with constraints and it was solved with different numerical methods. The methodology was based on the thermodynamic analysis based on the first law of the thermodynamics and the cost constants were tuned for the Portuguese market and the costs updated to the moment according to the inflation rate. In this first approach, the mathematical model was implemented as a FORTRAN program and in MatLab® in order to proceed to its validation. A correlation for the different physical parameters was achieved in order to better define the coefficients of cost equations and the model was implemented considering two optimization criteria: the minimization of the total costs including those related with the thermodynamic inefficiencies of the system operation (Silva, 2003).

Subsequently, this mathematical model was reformulated and adapted to small-scale application where the system was based on the central component of the plant, a micro gas-turbine, working under the *Joule-Brayton* thermodynamic cycle. The system was intended to deliver 125 kW of useful heat and 90 to 100kW of electricity (Ferreira et al., 2011). The thermal-economic model was defined as a non-linear optimization problem for which the objective function was defined as the maximization of the annual worth subjected to the physical and economic constraints. The optimization problem was solved by the Box Method, a search method without the need of analytic derivatives, which was implemented in the MatLab® environment. This method has the advantage of being a direct optimization method similar to the 'Simplex' method, requiring a computation time relatively low in getting the optimal solution(Martins et al., 2011).

Ferreira and her co-authors performed different sensitivity analysis regarding the best method to perform the thermal-economic optimization of the micro-gas turbines for small-scale cogeneration applications. Thus, the purpose was to optimize the main components, for application to medium size buildings, taking into account the specificities of the European market (e.g. high energy prices, support schemes). The authors intended to find the answer to: "What will be the optimal match between compressor pressure ratio, turbine inlet temperature and, internal pre-heater and external heat recovery system effectiveness that will lead to the best economical result?" According to the results, different sensitivity analyses have

been performed in order to understand how the electricity and fuel prices affect all the physical and economic variables (Ferreira, Nunes, Martins, & Teixeira, 2012; Ferreira et al., 2012).

These studies were performed by comparing different optimization methods: derivative free methods such as the Box Method and methods based on the gradient information SQP by using the optimization toolbox of MatLab (Ferreira, Rocha, Teixeira, Nunes, & Martins, 2012). Those studies performed by Ferreira *et al.* were based on energy balance equations, applying the first law of thermodynamics.

Lately, in 2013, the authors applied optimization methods by implementing exergy-based energy equations to the micro-gas turbine system (Ferreira et al., 2013; Ferreira, Teixeira, Nunes, Martins, & Teixeira, 2013).

Recently, several authors have proposed approximate methods, including heuristic approaches and artificial neural networks, to solve these problems instead of using "traditional" optimization methods, such as linear-programming or quadratic programming. Heuristic methods can be seen as simple procedures that provide satisfactory, but not necessarily optimal, solutions to complex problems. Meta-heuristics are generalizations of heuristics in the sense that they can be applied to a wide set of problems, needing few modifications to be adapted to a specific case. In some cases, the complexity of the problems to solve is so high that even heuristic and meta-heuristic methods requires large runtimes to obtain accurate solutions. In these cases parallel processing becomes an interesting way to obtain good solutions in reduced runtimes (Gendreau & Potvin, 2010).

The most used way to classify meta-heuristic algorithms is based on trajectory methods versus population-based methods. Trajectory meta-heuristics methods use a single solution during the search step and the outcome is also a single optimized solution. Most of them are extensions of simple iterative improvement procedures that include techniques that enable the algorithm to escape from local optima.

Also, meta-heuristics based or population methods are also applied. Population-based methods use a population of solutions which evolve during a given number of iterations, also returning a population of solutions when the stop condition is achieved. The main population-based meta-heuristics include: d. The main population-based meta-heuristics include: genetic algorithms (GA) and evolutionary algorithms (EA), scatter search, particle swarm optimization (PSO), differential evolution, etc (Baños et al., 2011).

Valdés et al. (2003) presented a study concerning the thermo-economic optimization of combined cycle gas turbine power plants using a genetic algorithm. Authors proposed two different objective functions: the minimization of the cost of production per unit of output and the maximization of the annual cash flow. Comparing the results, authors concluded that it is possible to find an optimum for every design parameter and this optimum depends on the selected optimization strategy.

Most computational optimization methods have focused on solving single-objective problems, including constraints in some cases. Nevertheless, there is simultaneous optimization of several objective functions. Multi-objective approaches are often divided into two main categories: aggregate weight functions and

Pareto-based optimization methods. Aggregating functions consist of combining all the objectives to optimize in a single mathematical function, where the relative importance of each objective is adjusted according to relative weights, whereas, Pareto-based multi-objective optimization establishes relationships among solutions according to the Pareto-dominance concept.

Multi-objective optimization has also been carried out in thermo-economic analysis. The importance of multi-criteria optimization in design and optimization of thermal systems has been discussed extensively (Lazzaretto & Toffolo, 2004). Multi-objective optimization of energy systems involves very complicated processes. The new optimization methods are based in genetic algorithms (crossover, mutation and selection) and artificial intelligence techniques. Recently, the most suitable technique is using a particular class of search algorithm, known as Multi-Objective Evolutionary Algorithms (MOEAs), which have been proven to be able to overcome the difficulties faced by classical or gradient-based method (S. S. Rao, 2009).

Basu (2010) applied differential evolution, an improved version of the genetic algorithm and evolutionary programming to solve to solve the combined heat and power economic dispatch problem. The proposed algorithm test results are compared with those obtained from particle swarm optimization and evolutionary programming and proved to be a very efficient algorithm.

Mathematical optimization, exergoeconomic or not, of real thermal systems correspond to complex problems due to the nonlinear characteristics and because mass, energy and exergy balance equations should be considered as restrictions (Vieira, Donatelli, & Cruz, 2004).

Erdil (2005) analyzed and optimized the exergy output rate and exergy efficiency performance of an irreversible Carnot cycle cogeneration plant with heat resistance, heat leakage and internal irreversibility. Ahmadi & Dincer (2011) report a comprehensive thermodynamic and exergo-economic modeling of a Gas Turbine (GT) power plant, aiming to validate the thermodynamic model through a multi-objective optimization. The authors reported that the combustion chamber is the component with the highest irreversibility rate. Kaushik, Reddy, & Tyagi (2011) presented the second-law approach for the thermodynamic analysis of the reheat combined Brayton/Rankine power cycle.

Depending on the purpose, studies on combined heat and power production in literature can be grouped in two groups. The aim of study can be the quantification the monetary flow rate through components in the plant if the purpose is the allocation and determination of the production costs and/or cost of losses of the plant. Differently, if the objective is the optimization of a power system, the study is focused on the selection of the best conditions for operating the system. The latter approach usually uses energy balances from the first law of the thermodynamics, being more a techno-economic assessment of the power plants (Alanne et al., 2010; Ferreira et al., 2012). Table 2.5 presents some works on the thermo-economic analysis and optimization of CHP systems.

Table 2.5 Thermo-economic analysis and optimization methodologies applied on CHP systems

Author	Thermo-economic methodology	System
(El-Sayed, 1993)	Decomposition Strategy	Gas Turbine
(Frangopoulos, 1993)	Thermo-economic Functional Approach	Steam cycle cogeneration/ CGAM Problem
(Von Spakovsky, 1993)	Engineering Functional Analysis	Combined Cycle Cogeneration
(Lozano & Valero, 1993)	TEC & method of Lagrange multipliers	CHP system with boiler, turbine-alternator and pump
(Tsatsaronis, 1994)	Specific Exergetic Cost Analysis Method	Simple Gas Turbine Cogeneration
(Valero et al., 1994)	Nonlinear Optimization Algorithms	CGAM Problem
(Manolas, Frangopoulus, Gialamas, & Tsahalis, 1997)	Thermo-economic Functional Approach and Genetic Algorithm	Industrial Cogeneration System
(Rodríguez-Toral et al., 2000)	Sequential Quadratic Programming.	Combined Cycle Cogeneration
(Valdés et al., 2003)	Thermo-economic Functional Approach and Genetic Algorithm	Combined cycle gas turbine plant
(Silveira & Tuna, 2003)	Exergoeconomic Analysis and Optimization	Combined Cycle Cogeneration
(Marechal, Palazzi, Godat & Favrat, 2004)	Multi-Objective Optimizer (MOO)	Thermo-economic optimization of fuel cells
(A. Silva, Teixeira, & Teixeira, 2003)	Nonlinear Optimization Algorithms	Gas Turbine
(Vieira et al., 2004)	Structural Theory of Thermo-economics	CGAM Problem
(Bonnet, Alaphilippe, & Stouffs, 2005)	Exergoeconomic Analysis	Micro-cogeneration
(Kong, Wang & Huang, 2005)	Linear programming model	CCHP system with gas turbine generator, chiller and a heat recovery boiler
(Keppo & Savola, 2007)	Mixed Integer Linear Programming (MILP)	3 small Biofuel Fired CHP Plants
(Sanaye & Ardali, 2009)	Thermodynamic Analysis	Micro-turbines
(P. Ahmadi & Dincer, 2011)	Genetic algorithm (NSGA-II)	Gas Turbine power plant
(Ferreira et al., 2011)	Box Method	Micro-gas turbines
(Ferreira et al., 2012)	SQP Method	Micro-gas turbines
(Ferreira et al., 2013)	Pattern Search Algorithm	Micro-gas turbines
(Rao & Patel, 2013)	Teaching-learning-based optimization (TLBO)	Heat Exchangers
(Ahamadi, Sayyaadi & Hosseinzade, 2013)	MOEAs, NSGA-II	Solar Stirling engine cycle

Optimization is the discipline concerned with finding inputs of a function that minimize or maximize its value which may be subjected to constraints. Computational optimization can be defined as the process of designing, implementing and testing algorithms for solving a vast diversity of optimization problems. Computational optimization includes the scientific domains of mathematics to formulate the model, operations research to model the system, computer science for algorithmic design and analysis, and software engineering to implement the model.

According to the carefully analysis of the literature, it seems that different methods to a given system yields different values for the variables in the models. The resemblance between the methodologies depends on the assumptions made in the formulations of cost-balance equations. Besides, the chosen level of aggregation that specifies the sub-systems affects the cost structure of combined heat and power systems. The number of assumed parameters is crucial in achieving the costs. Some of these methodologies are difficult to implement, once the thermodynamic restrictions make the optimization problem difficult to be solved.

Moreover, assessing the flow streams cost in a complex system allows understanding the process of cost formation from the input sources to the final products. These analyses can solve problems related to complex energy systems such as combined heat and power production.

Ahmadi, M. H., Sayyaadi, H., Dehghani, S., & Hosseinzade, H. (2013). Designing a solar powered Stirling heat engine based on multiple criteria: Maximized thermal efficiency and power. *Energy Conversion and Management*, *75*, 282–291. doi:10.1016/j.enconman.2013.06.025

Ahmadi, M. H., Sayyaadi, H., Mohammadi, A. H., & Barranco-Jimenez, M. a. (2013). Thermo-economic multi-objective optimization of solar dish-Stirling engine by implementing evolutionary algorithm. *Energy Conversion and Management*, *73*, 370–380. doi:10.1016/j.enconman.2013.05.031

Ahmadi, P., & Dincer, I. (2011). Thermodynamic and exergoenvironmental analyses, and multi-objective optimization of a gas turbine power plant. *Applied Thermal Engineering*, *31*(14-15), 2529–2540. doi:10.1016/j.applthermaleng.2011.04.018

Alanne, K., Söderholm, N., Sirén, K., & Beausoleil-Morrison, I. (2010). Techno-economic assessment and optimization of Stirling engine micro-cogeneration systems in residential buildings. *Energy Conversion and Management*, *51*(12), 2635–2646. doi:10.1016/j.enconman.2010.05.029

Asnaghi, A., Ladjevardi, S. M., Saleh Izadkhast, P., & Kashani, a. H. (2012). Thermodynamics Performance Analysis of Solar Stirling Engines. *ISRN Renewable Energy*, *2012*, 1–14. doi:10.5402/2012/321923

Baños, R., Manzano-Agugliaro, F., Montoya, F. G., Gil, C., Alcayde, a., & Gómez, J. (2011). Optimization methods applied to renewable and sustainable energy: A review. *Renewable and Sustainable Energy Reviews*, *15*(4), 1753–1766. doi:10.1016/j.rser.2010.12.008

Basu, M. (2010). Combined Heat and Power Economic Dispatch by Using Differential Evolution. *Electric Power Components and Systems*, *38*(8), 996–1004. doi:10.1080/15325000903571574

Baxi. (2012). Baxi Group and De Dietrich Remeha Group official Web Site. Retrieved February 07, 2012, from http://www.bdrthermea.com/home.html

Bejan, A., Tsatsaronis, G., & Moran, M. (1996). *Thermal Design and Optimization* (Wiley.). New York: Wiley.

Bianchi, M., De Pascale, A., & Spina, P. R. (2012). Guidelines for residential micro-CHP systems design. *Applied Energy*, *97*, 673–685. doi:10.1016/j.apenergy.2011.11.023

Bilgen, E. (2000). Exergetic and engineering analyses of gas turbine based cogeneration systems. *Energy*, *25*(12), 1215–1229. doi:10.1016/S0360-5442(00)00041-4

Bonnet, S., Alaphilippe, M., & Stouffs, P. (2005). Energy, exergy and cost analysis of a micro-cogeneration system based on an Ericsson engine. *International Journal of Thermal Sciences*, *44*(12), 1161–1168. doi:10.1016/j.ijthermalsci.2005.09.005

Boucher, J., Lanzetta, F., & Nika, P. (2007). Optimization of a dual free piston Stirling engine. *Applied Thermal Engineering*, *27*(4), 802–811. doi:10.1016/j.applthermaleng.2006.10.021

Capstone Turbine Corporation. (2012). *Copyright 2013 Capstone Turbine Corporation*. Retrieved October 07, 2011, from http://www.capstoneturbine.com/

Cells2000, F. (2005). The Leading Independent Fuel Cells Resources WebPage. *Fuel Cells Technology Update*. Retrieved June 29, 2013, from http://www.fuelcells.org/

Cheng, C.-H., & Yang, H.-S. (2012). Optimization of geometrical parameters for Stirling engines based on theoretical analysis. *Applied Energy*, *92*, 395–405. doi:10.1016/j.apenergy.2011.11.046

Cleanenergy. (2012). Cleanenergy Web Site. Retrieved January 12, 2012, from http://www.cleanergy.com

De Paepe, M., D'Herdt, P., & Mertens, D. (2006). Micro-CHP systems for residential applications. *Energy Conversion and Management*, *47*(18-19), 3435–3446. doi:10.1016/j.enconman.2005.12.024

Dentice d'Accadia, M., Sasso, M., Sibilio, S., & Vanoli, L. (2003). Micro-combined heat and power in residential and light commercial applications. *Applied Thermal Engineering*, *23*(10), 1247–1259. doi:10.1016/S1359-4311(03)00030-9

Dong, L., Liu, H., & Riffat, S. (2009). Development of small-scale and micro-scale biomass-fuelled CHP systems – A literature review. *Applied Thermal Engineering*, *29*(11-12), 2119–2126. doi:10.1016/j.applthermaleng.2008.12.004

El-Sayed, Y. M. (1993). A decomposition strategy for the thermoeconomic optimization of a given system configuration. *Energy*, 41–47.

Energetix Group Web Site. (2012). Retrieved February 07, 2012, from http://www.energetixgroup.com

Erdil, A. (2005). Exergy optimization for an irreversible combined cogeneration cycle. *Journal of the Energy Institute*, *78*(1), 27–31. doi:10.1179/174602205X39588

Fernandes, E. M. G. P. (1997). *Computação numérica*. (E. M. G. P. Fernandes, Ed.) (2ª Edição., Vol. 546, p. 414). Braga: University of Minho.

Ferreira, A. C. M., Nunes, M. L., Leão, C. P., Teixeira, S. F. C., Silva, Â. M., Martins, L. A. S. B., & Teixeira, J. C. (2011). Thermo-Economic Optimization of CHP Systems: from large to small scale applications. *International Journal of Engineering and Industrial Management*, *3*, 175–192.

Ferreira, A. C. M., Nunes, M. L., Teixeira, S. F. C. F., Leão, C. P., Silva, Â. M., Teixeira, J. C. F., & Martins, L. A. S. B. (2012). An economic perspective on the optimisation of a small-scale cogeneration system for the Portuguese scenario. *Energy*, *45*(1), 436–444. doi:10.1016/j.energy.2012.05.054

Ferreira, A. C. M., Rocha, A. M. A. C., Teixeira, S. F. C. F., Nunes, M. L., & Martins, L. A. S. B. (2012). On Solving the Profit Maximization of Small Cogeneration Systems. *ICCSA 2012 - 12th International Conference on Computational Science and Its Applications - Lecture Notes in Computer Science Journal*, *7335*, 147–158. doi:10.1007/978-3-642-31137-6_11

Ferreira, A. C., Nunes, M. L., Martins, L. B., & Teixeira, S. (2012). Optimization of Small Scale Cogeneration Systems : Comparison of Nonlinear Optimization Algorithms. In H. V. (editors) A. Andrade-Campos, N. Lopes, R.A.F. Valente (Ed.), *YIC 2012 - ECCOMAS Young Investifgators Conference* (pp. 1–10). Aveiro. Retrieved from repositorium.sdum.uminho.pt/handle/1822/27988

Ferreira, A. C., Teixeira, S. F., Teixeira, J. C. F., Nunes, M. L., & Martins, L. B. (2013). Exergy Efficiency Optimization for Gas Turbine Based Cogeneration Systems. In ASME (Ed.), *Volume 6A: Energy* (p. V06AT07A064). San Diego, EUA: ASME. doi:10.1115/IMECE2013-65080

Ferreira, A., Nunes, L., Teixeira, S., Silva, A., Martins, L., & Teixeira, J. (2013). Tecno-Economic and Exergy Analysis of a Small-Scale CHP Unit Based on a Micro-gas Turbine. In *MICROGEN 3 - International Conference on Microgeneration and Related Technologies*. Naples.

Formosa, F., & Despesse, G. (2010). Analytical model for Stirling cycle machine design. *Energy Conversion and Management*, *51*(10), 1855–1863. doi:10.1016/j.enconman.2010.02.010

Frangopoulos, C. A. (1993). Application of the Thermoeconomic Functional Approach to the CGAM Problem. *Energy*, *19*(3), 323–342.

Gendreau, M., & Potvin, J.-Y. (Eds.). (2010). *Handbook of Metaheuristics* (Vol. 146). Boston, MA: Springer US. doi:10.1007/978-1-4419-1665-5

Gullì, F. (2006). Small distributed generation versus centralised supply: a social cost–benefit analysis in the residential and service sectors. *Energy Policy*, *34*(7), 804–832. doi:10.1016/j.enpol.2004.08.008

Infinia Corporation. (2012). Infinia Corporation Web Site. Retrieved January 12, 2012, from http://www.infiniacorp.com

Inspirit. (2012). Inspirit Web Site. Retrieved January 31, 2012, from http://www.inspiritenergy.com/producttechnology.html

Kaikko, J., & Backman, J. (2007). Technical and economic performance analysis for a microturbine in combined heat and power generation. *Energy*, *32*(4), 378–387. doi:10.1016/j.energy.2006.06.013

Kaushik, S. ., & Kumar, S. (2000). Finite time thermodynamic analysis of endoreversible Stirling heat engine with regenerative losses. *Energy*, *25*(10), 989–1003. doi:10.1016/S0360-5442(00)00023-2

Kaushik, S. C., Reddy, V. S., & Tyagi, S. K. (2011). Energy and exergy analyses of thermal power plants: A review. *Renewable and Sustainable Energy Reviews*, *15*(4), 1857–1872. doi:10.1016/j.rser.2010.12.007

Keppo, I., & Savola, T. (2007). Economic appraisal of small biofuel fired CHP plants. *Energy Conversion and Management*, *48*(4), 1212–1221. doi:10.1016/j.enconman.2006.10.010

Kim, D. J. (2010). A new thermoeconomic methodology for energy systems. *Energy*, *35*(1), 410–422. doi:10.1016/j.energy.2009.10.008

Kolda, T. G., Lewis, R. M., & Torczon, V. (2003). Optimization by Direct Search: New Perspectives on Some Classical and Modern Methods. *SIAM Review*, *45*(3), 385–482. doi:10.1137/S003614450242889

Kongtragool, B., & Wongwises, S. (2003). A review of Solar-power Stirling engines and low temperature differential Stirling engines. *Renewable and Sustainable Energy Reviews*, *7*(2), 131–154. doi:10.1016/S1364-0321(02)00053-9

Kongtragool, B., & Wongwises, S. (2006). Thermodynamic analysis of a Stirling engine including dead volumes of hot space, cold space and regenerator. *Renewable Energy*, *31*(3), 345–359. doi:10.1016/j.renene.2005.03.012

Kotas, T. J. (1985). Exergy Analysis of Simple processes. In *The Exergy Method of Thermal Plant Analysis* (pp. 99–150). Anchor Brendon Ldt.

Kuhn, V., Klemeš, J., & Bulatov, I. (2008). MicroCHP: Overview of selected technologies, products and field test results. *Applied Thermal Engineering*, *28*(16), 2039–2048. doi:10.1016/j.applthermaleng.2008.02.003

Lazzaretto, a., & Toffolo, a. (2004). Energy, economy and environment as objectives in multi-criterion optimization of thermal systems design. *Energy*, *29*(8), 1139–1157. doi:10.1016/j.energy.2004.02.022

Lozano, M. A., & Valero, A. (1993). Theory of the exergetic cost. *Energy*, *18*(9), 939–960.

Manolas, D. A., Frangopoulus, C. A., Gialamas, T. P., & Tsahalis, D. T. (1997). Operation Optimization of an Industrial Cogeneration System by a Genetic Algorithm. *Energy Conversion & Management*, *38*(15), 1625–1636.

Martins, L. B., Ferreira, A. C. M., Nunes, M. L., Leão, C. P., Teixeira, S. F. C. F., Marques, F., & Teixeira, J. C. F. (2011). Optimal Design of Micro-Turbine Cogeneration Systems for the Portuguese Buildings Sector. In ASME (Ed.), *Volume 4: Energy Systems Analysis, Thermodynamics and Sustainability; Combustion Science and Engineering; Nanoengineering for Energy, Parts A and B* (pp. 179–186). Denver: ASME. doi:10.1115/IMECE2011-64470

McDonald, C. F. (2003). Recuperator considerations for future higher efficiency microturbines. *Applied Thermal Engineering*, *23*(12), 1463–1487. doi:10.1016/S1359-4311(03)00083-8

Nepveu, F., Ferriere, A., & Bataille, F. (2009). Thermal model of a dish/Stirling systems. *Solar Energy*, *83*(1), 81–89. doi:10.1016/j.solener.2008.07.008

Nocedal, J., & Wright, S. J. (1999). *Numerical Optimization*. (P. Glynn & S. M. Robinson, Eds.) (p. 651). Springer.

Onovwiona, H. I., Ismet Ugursal, V., & Fung, A. S. (2007). Modeling of internal combustion engine based cogeneration systems for residential applications. *Applied Thermal Engineering*, *27*(5-6), 848–861. doi:10.1016/j.applthermaleng.2006.09.014

Onovwiona, H. I., & Ugursal, V. I. (2006). Residential cogeneration systems: review of the current technology. *Renewable and Sustainable Energy Reviews*, *10*(5), 389–431. doi:10.1016/j.rser.2004.07.005

Pehnt, M., Praetorius, B., Schumacher, K., Berlin, D. I. W., Fischer, C., Schneider, L., ... Voß, J. (2004). *Micro CHP – a sustainable innovation?* (p. 32).

Perry, M. L., & Fuller, T. F. (2002). A Historical Perspective of Fuel Cell Technology in the 20th Century. *Journal of The Electrochemical Society*, *149*(7), S59. doi:10.1149/1.1488651

Puech, P., & Tishkova, V. (2011). Thermodynamic analysis of a Stirling engine including regenerator dead volume. *Renewable Energy*, *36*(2), 872–878. doi:10.1016/j.renene.2010.07.013

Rao, R. V., & Patel, V. (2013). Multi-objective optimization of heat exchangers using a modified teaching-learning-based optimization algorithm. *Applied Mathematical Modelling*, *37*(3), 1147–1162. doi:10.1016/j.apm.2012.03.043

Rao, S. S. (2009). *Engineering Optimization* (Fourth Edi., p. 830). Hoboken, NJ, USA: John Wiley & Sons, Inc. doi:10.1002/9780470549124

Rodríguez-Toral, M. A., Morton, W., & Mitchell, D. R. (2000). Using new packages for modelling, equation oriented simulation and optimization of a cogeneration plant. *Computers & Chemical Engineering*, *24*, 2667–2685.

Rogdakis, E. D., Antonakos, G. D., & Koronaki, I. P. (2012). Thermodynamic analysis and experimental investigation of a Solo V161 Stirling cogeneration unit. *Energy*, *45*(1), 503–511. doi:10.1016/j.energy.2012.03.012

Saitoh, T., Yamada, N., & Wakashima, S. (2007). Solar Rankine Cycle System Using Scroll Expander. *Journal of Environment and Engineering*, *2*(4), 708–719. doi:10.1299/jee.2.708

Sanaye, S., & Ardali, M. R. (2009). Estimating the power and number of microturbines in small-scale combined heat and power systems. *Applied Energy*, *86*(6), 895–903. doi:10.1016/j.apenergy.2008.11.015

Silva, Â. M. (2003). *Optimização Numérica Termo-económica de um Sistema de Cogeração*. Universidade do Minho.

Silva, A., Teixeira, J. C. F., & Teixeira, S. F. C. F. (2003). A Numerical Thermoeconomic Study of a Cogeneration Plant. In N. Houbak, B. Elmegaard, B. Qvale, & M. Moran (Eds.), *Ecos 2003 - 16th International Conference on Efficiency, Cost, Optimization, Simulation and Enviromental Impact of Energy Systems* (p. 9). Copenhagen.

Silveira, J. L., & Tuna, C. E. (2003). Thermoeconomic analysis method for optimization of combined heat and power systems. Part I. *Progress in Energy and Combustion Science*, *29*(6), 479–485. doi:10.1016/S0360-1285(03)00041-8

Stirling BioPower. (2012). Stirling BioPower Web Site. Retrieved January 31, 2012, from http://www.stirlingbiopower.com

Sun, J., & Li, W. (2011). Operation optimization of an organic rankine cycle (ORC) heat recovery power plant. *Applied Thermal Engineering*, *31*(11-12), 2032–2041. doi:10.1016/j.applthermaleng.2011.03.012

Szargut, J., Morris, D. R., & Steward, F. R. (1988). *Exergy analysis of thermal, chemical and metallurgical processes*. Hemisphere Publishing Corporation.

Thomas, E., David, H., & Leon, L. (2001a). Basic Concepts of Optimization. In L. Leon (Ed.), *Optimization of Chemical Processes* (2nd Edotio., pp. 113–151). New York: McGraw Hill Higher Education.

Thomas, E., David, H., & Leon, L. (2001b). Linear Programming and Applications. In L. Leon (Ed.), *Optimization of Chemical Processes* (2nd Editio., pp. 223–263). New York: McGraw Hill Higher Education.

Thomas, E., David, H., & Leon, L. (2001c). Non-linear Programming with constraints. In T. Casson (Ed.), *Optimization of Chemical Processes* (2nd Editio., pp. 284–329). New York: McGraw Hill Higher Education.

Tsatsaronis, G. (1994). Application of Thermo-economics to the Design and Synthesis of Energy Plants. *Energy, Energy System Analysis and Optimizationnalysis and Optimization*, 13.

Ust, Y., Sahin, B., & Kodal, A. (2007). Optimization of a dual cycle cogeneration system based on a new exergetic performance criterion. *Applied Energy*, *84*(11), 1079–1091. doi:10.1016/j.apenergy.2007.04.004

Valdés, M., Durán, M. D., & Rovira, A. (2003). Thermoeconomic optimization of combined cycle gas turbine power plants using genetic algorithms. *Applied Thermal Engineering*, *23*(17), 2169–2182. doi:10.1016/S1359-4311(03)00203-5

Valero, A., Lozano, M. A., Serra, L., Tsatsaronis, G., Pisa, J., Frangopoulus, C., & Spakovsky, M. R. (1994). CGAM Problem: Definition and Conventional Solution. *Energy*, *19*(3), 279–286.

Vieira, L. S., Donatelli, J. L., & Cruz, M. E. (2004). Integration of an iterative methodology for exergoeconomic improvement of thermal systems with a process simulator. *Energy Conversion and Management*, *45*(15-16), 2495–2523. doi:10.1016/j.enconman.2003.11.007

Von Spakovsky, M. R. (1993). Application of Engineering Functional Analysis to the Analysis and Optimization of the CGAM Problem. *Energy*, *I*(3), 343–364.

WhisperTech. (2012). WhisperGen CHP System from WhisperTech Company Web Site.

Williamson, D. P., & Shmoys, D. B. (2010). *The Design of Approximation Algorithms*. (D. Williamson & D. Shmoys, Eds.) (p. 500). Cambridge University Press.

Wu, F., Chen, L., Wu, C., & Sun, F. (1998). Optimum performance of irreversible stirling engine with imperfect regeneration. *Energy Conversion and Management*, *39*(8), 727–732. doi:10.1016/S0196-8904(97)10036-X

Yamamoto, T., Furuhata, T., Arai, N., & Mori, K. (2001). Design and testing of the Organic Rankine Cycle. *Energy*, *26*(3), 239–251. doi:10.1016/S0360-5442(00)00063-3

Yun, K. T., Cho, H., Luck, R., & Mago, P. J. (2013). Modeling of reciprocating internal combustion engines for power generation and heat recovery. *Applied Energy*, *102*, 327–335. doi:10.1016/j.apenergy.2012.07.020

Zarinchang, J., & Yarmahmoudi, A. (2008). Optimization of Stirling Engine Heat Exchangers. In WSEAS (Ed.), *World Scientific and Engineering Academy and Society (WSEAS)* (pp. 143–150). Santander, Cantabria.

Zarinchang, J., & Yarmahmoudi, A. (2009). Optimization of Thermal Components in a Stirling Engine. In *WSEAS Transactions on Heat and Mass Transfer* (Vol. 4, pp. 1–10).

This page was intentionally left in blank

3

Energy Consumption Profiles |

3.1   Energy Policy Framework

3.2.   Portuguese Energy Scenario

3.3.   Thermal Load Methodology

3.1. Energy Policy Framework

Portugal has a low level of electricity consumption per capita when compared with the EU's average. However, the electricity consumption has greatly increased during the last two decades and mainly in the building sector. According to Eurostat data, Portugal (in 2007) was one of the EU countries with the highest energy dependence, importing 82% of the total primary energy, when compared to the EU-27 average of about 53% (Eurostat, 2009). Energy demand has been increasing slightly faster than the rate of economic growth and consequently, the energy intensity is 4% higher than it was in 1991, and it is 10% above the EU 15-average.

Thus, the Portuguese energy scenario is characterized by a huge import of primary fossil sources that justifies the high-energy dependence. In fact, the energy costs of the imported fuels have been subject to a significant growth and, together with the external factors, particularly those which cause variations of energy price and exchange rates in the international markets, lead to the research and development of cleaner and more efficient alternatives of energy production and conversion.

Concerning the final energy consumption, a considerable structural change has been reported in the last 15 years The Portuguese electricity demand has grown considerably in the last decade, at an average annual growth rate of 4.4%. Electricity consumption has increased particularly fast in residential, services and commercial sectors (International Energy Agency - IEA, 2012). Natural gas was introduced in 1996 and its share has been continuously increasing while industrial fuel oil decreased and wind energy capacity dramatically augmented.

Nowadays, Portugal's economy is dominated by the services sector (63%), while the industrial sector accounts for about 30% and it is decreasing. The commercial, public and residential sectors offer an interesting potential for cogeneration applications. Small and medium size buildings (e.g. hotels, company buildings, hospitals or residential condominiums) are the most suitable for the installation of small- and micro-cogeneration power plants.

The micro-cogeneration market in Portugal has the potential for 6 000 units distributed across these sectors. Specifically in the residential sector, there is an estimated potential of around 500 MW$_{el}$, for systems with less than 150kW$_{el}$. In addition, Portugal is the fourth country of the European Union with higher electricity prices without taxes for households, which creates a favourable scenario for micro-CHP implementation (Monteiro, Moreira, & Ferreira, 2009).

Since the 80s, the energy sector suffered profound changes as the production and distribution of electricity was opened to the private initiative. The figure of the independent electricity producer was created by the historical Decree-Law 88/90 (1988) and the Decree-Law 99/91 established the general principles of the legal regimes for the activities of production, transmission and distribution of electric energy. Also this decree-law defined the principles of the organization and functioning of the National Electric System.

The subsequent Decree-Laws 183/95, 184/95, 185/95, and 187/95 of 27th July redefined the above three and introduced the independent regulation, through the creation of the Portuguese Energy Services Regulatory Authority (ERSE).

The Directive 96/92/CE of the European Parliament and the Council resulted in widespread changes to the legal organizational of the electric sector. The National Electric System (NES) has been subject to many alterations. Based on the above- mentioned legal instruments, specific regulations were produced, and revised in September 2001, of which special mention should be made to the Tariff Code, the Commercial Relations Code, the Dispatch Code and the Access to the public grid and to the Inter-connections Code.

In 2002, the entity ''producer–consumer'' was created by the Decree-Law 68/2002 allowing the power production in low tension, where at least 50% of the produced electrical energy must be self-consumed and the maximum power which can be delivered to the power utility is 150 kW$_{el}$.

In 2004, the European Union launched the Directive on the promotion of cogeneration based on a useful heat demand in the internal energy market (DIRECTIVE 2004/8/EC, 2004). The directive aims the promotion of high-efficiency systems led by heat demand. This Directive states that the whole generated electricity is to be considered as produced from cogeneration when a 75% overall annual efficiency is obtained, if the overall efficiency is below this value, the electricity amount from cogeneration can be calculated considering the power–heat ratio of the power plant.

This directive also establishes a framework for the promotion of high-efficiency cogeneration based on useful heat demand and Primary Energy Saving (PES). PES is considered as the evaluation criteria for the installation of cogeneration systems. For small-scale systems, a PES of at least 10% is required, so that the system can be classified as a high efficient, whereas in the case of micro-scale systems, it is only required a positive value of PES. Thus, PES allows the estimation of the fuel input savings that are possible to achieve by a cogeneration unit when compared with the conventional separate production of heat and power.

In 2007, the European Council emphasised the need to increase energy efficiency in the EU member states and defined the objective of saving 20% of the primary energy consumption by 2020. The projections depicted a primary energy consumption of 1.842 Mtoe in 2020. Plus, on 23 April 2009, the Decision N° 406/2009/EC of the European Parliament and of the Council requested the effort of member states to reduce their greenhouse gas emissions to meet the Community's greenhouse gas emission reduction commitments up to 2020.

After that, and regarding the cogeneration directive, the European commission established harmonized efficiency reference values for the separate production of electricity and heat, by taking into account factors such as the fuel type and year of construction. The guidelines recommend that correction factors should be applied for electricity production should be applied by taking into account the local climate and the avoided grid losses. The reference values for the separate production of heat should not be related to the year of construction neither heat grid losses because heat is always used near the site of production (Decision 2011/877/EU, 2011).

The increased use of cogeneration constitutes an important part of the package of measures needed to comply with the Kyoto Protocol to the United Nations Framework Convention on Climate Change, and of any policy package to meet further commitments.

In 2010, the Portuguese Decree-Law 23/2010 established the guidelines for high-efficiency cogeneration based on useful heat demand, which is considered a priority due to its potential primary energy savings and consequently reducing CO_2 emissions. This Decree-Law also established the remuneration scheme for the cogeneration production (Decrew-Law n.° 23/2010, 2010).

In the specific Portuguese scenario, the government has been promoting energy efficiency policies, trying to reduce the greenhouse gas emissions. The cogeneration has been benefiting from this political orientation, namely via feed-in-tariffs (FIT), and presently represents approximately 13% of the total National electricity production. According to the Energy Services Regulatory Authority (ERSE), between January 2008 and May 2011, the average FIT was 108 €/MWh$_{el}$ for large-scale CHP systems (ERSE, 2011). Nevertheless, the FIT is calculated monthly via a rather complex formula that involves, among other factors, oil market prices. The FIT for these large systems varies depending on the hour of the day, but it is always higher than the buy-back electricity price. A recent law guarantees a fixed FIT at any time

of the day or night, for micro-cogeneration systems with a grid power connection not exceeding 3.7 kW$_{el}$ in the case of single dwellings, or 11 kW$_{el}$ in the case of apartment blocks. For renewable micro-cogeneration systems (e.g. using biogas) the FIT is 20 €/MWh$_{el}$ during the first 8 years after commissioning, followed by 168 €/ MWh$_{el}$ from 9-15 years. In the specific case of non-renewable cogeneration, the corresponding FITs are 160 and 96 €/MWh$_{el}$ (or market value if above). Considering the Portuguese scenario, it is expected that this fixed hourly FITs will be soon extended to small-scale cogeneration systems up to 250 kW$_{el}$.

The European Energy Performance of Buildings Directive (EPBD) and its 2000 recast obliges all member states to ensure that, for new buildings with a floor area over 1000 m^2, the economic feasibility of alternative systems, such as decentralized energy supply systems based on CHP or renewable energy, is considered at the design stage (DIRECTIVE 2010/31/EU, 2010). The Directive also outlines that buildings should become energy producers and, that by 2020 all new buildings should have nearly to zero energy requirements.

It is expected that the rising costs of fossil resources and the future economic incentives associated with this legislation, will lead to a strong growth of CHP systems in the building sector.

In 2012, the Energy Efficiency Directive (EED – 2012/27/EU) was adopted, repealing the Energy Services Directive (ESD – 2006/32/EC), as well as, the Cogeneration Directive (2004/8/EC). This directive has to be transposed by all Member States by the beginning of June 2014. The Directive establishes a common framework of measures for the promotion of energy efficiency within the EU in order to ensure the achievement of the 20 % headline target on energy efficiency in 2020, and to pave the way for further energy efficiency improvements beyond that date. According to the directive paragraph 35: "*High-efficiency cogeneration and district heating and cooling has significant potential for saving primary energy, which is largely untapped in the Union*". Member States should carry out a comprehensive assessment of the potential for high-efficiency cogeneration and district heating and cooling. These assessments should be updated, at the request of the Commission, to provide investors with information concerning national development plans and contribute to a stable and supportive investment environment". Among the key measurements, the Directive states that EU countries are requested to draw up a roadmap to make the entire buildings sector more energy efficient by 2050 (commercial, public and private households included). Energy audits and management plans are required for large companies, with cost-benefit analyses for the deployment of combined heat and power generation (CHP) and public procurement.

The Annex I of the EED Directive defines general principles for the calculation of electricity produced by cogeneration. According to the EED Directive, for large systems, the calculated values used of electricity shall be determined on the basis of the actual operation of the unit under normal conditions of use and, in the case of the micro-cogeneration units, the calculation may be based on certified values.

Electricity production from cogeneration shall be considered equal to total annual electricity production of the unit measured at the outlet mains of the generator, in cogeneration units where the prime mover is back pressure steam turbine, gas turbine with heat recovery, ICE, micro-turbines, Stirling engines and Fuel Cells with an annual overall efficiency set by Member States at a level of at least 75% (Directive 2012/27/EU, 2012).

3.2. Portuguese Energy Scenario

The current national energy scenario is characterized by a strong external dependency, with an energy sector heavily reliant on fossil energy sources (oil, natural gas and coal). The transportation and electricity production sectors share the main responsibility for this negative energy picture.

3.2.1. Energy production

According to Eurostat data, Portugal, in 2007, was one of the EU countries with the highest energy dependence, importing in that year 82% of the total primary energy consumed, when compared to the EU-27 average of about 53% (Eurostat, 2009). Energy demand has been increasing slightly faster than the rate of economic growth and, consequently, the energy intensity of the economy is 4% higher than it was in 1991, and it is 10% above the EU 15-average (EUROSTAT, 2009).

Thus, the Portuguese energy scenario is characterized by a huge import of primary fossil sources that justifies the high-energy dependence. In fact, the energy costs of imported fuel have been suffering a significant growth, together with the external factors that cause variations of exchange rates in the international markets, as well as, the energy price variations. Figure 3.1 shows the evolution of energy dependency between 2005 and 2011.
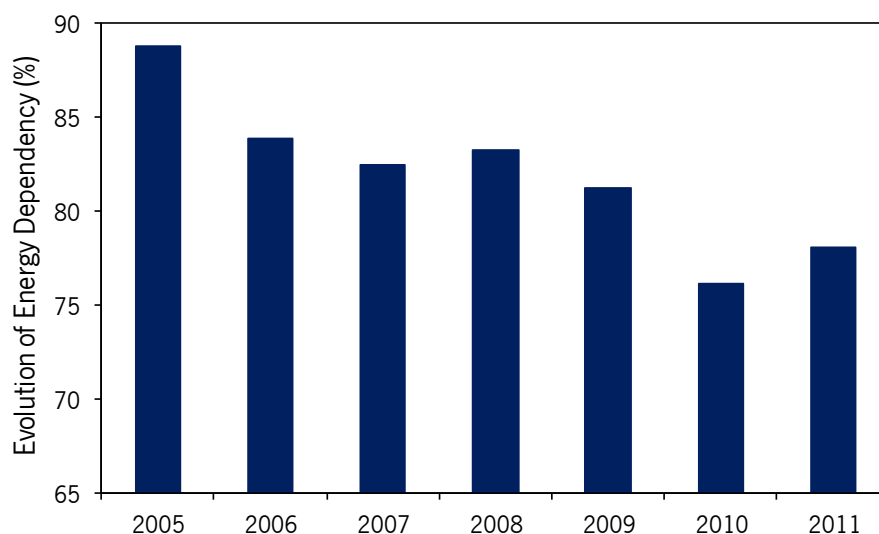
Figure 3.1 Evolution of energy dependency in Portugal between 2008 and 2011. Adapted from (DGEG, 2013).

The scarcity of fossil resources leads to a high dependence on foreign energy. The highest value of energy dependence, during the last decade, was registered in 2005 due to low production of hydro plants due to the dry climatic conditions over the year. In 2011 it was also registered a growth of energy dependency due to increased consumption of coal in electricity production to offset the reduction in hydric production Accordingly to Directorate-General for Energy and Geology (DGEG), in 2012, the Portuguese energy bill resulted in net imports of 7.1 billion euros, which represents an increase of 4.2% when compared with the previous year. The trade in of energy products increased due to the exportations, which was positive for the economic balance. The most negative aspect was the increase of oil price. Actually, the imports of crude and refined oil increased almost 6.3% in value, to 9.2 billion euros, while the quantity suffered a reduction in 1.6%. The electricity imported in 2012 grew almost 75% and the amount of electricity purchased from Spain risen more than 86% to 8 297 GWh.

Portugal has significantly shifted its electricity production system by introducing Natural Gas (NG) power plants, wind energy and a few new hydroelectric power plants. Electricity production from NG has increased from zero to near to 12.3 TWh between 1996 and 2006 and wind energy capacity dramatically augmented from 253 MW in 2003 to 4630 MW in 2013.

Figure 3.2 presents the non-renewable power capacity from different primary energy sources for the period between the years 2008 and 2012. In 2012, the total installed power capacity was 9.4 GW, which represented a decrease of almost 6.4% when compared with the year 2011 and can be explained by the closure of the old fuel oil units. The NG power stations represent the main capacity share with a small slice corresponding to the cogeneration units. Note that 19% of the 4.97 GW of power generated by using NG is produced in cogeneration power stations.

†include includes fuel oil, refinery gas, diesel, propane and industrial waste
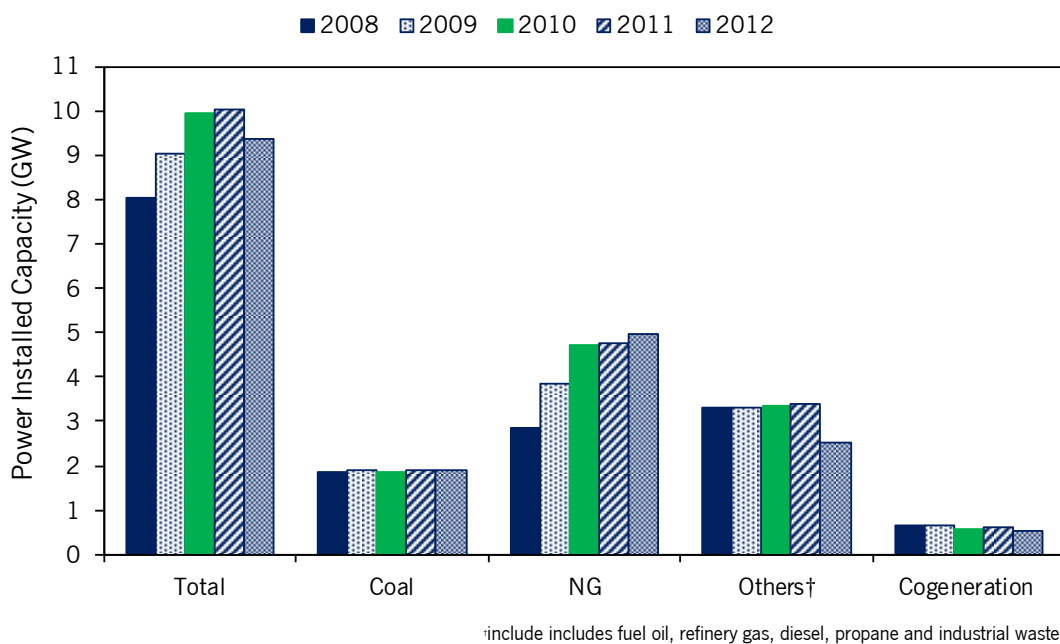
Figure 3.2 Non-renewable power capacities in Portugal between 2008 and 2012. Adapted from (DGEG, 2013).

The urgent need to balance supply and demand, as well as, the growing concern with environmental issues and reduction of external energy dependency, justifies the increased interest in the exploitation of Renewable Energy Sources (RES) and other more efficient strategies in terms of economic and social or environmental dimensions. The electricity sector represented a clear example of this RES trend with European and Portuguese policies focused on strategies promoting renewable resources and energy efficiency (DGEG, 2010a). The total electric capacity for all types of renewable energy sources has doubled from 1995 to 2009 and has reached 9.2 GW, by March 2010.

Figure 3.3 presents the evolution of renewable power capacity from different primary energy sources for the period between the years 2008 and 2012. Data shows that, in the last four years, the increase in the installed capacity using renewable energy sources was mainly due to new wind energy units. Portugal is one of the European Union countries with the highest usable potential for hydropower. Nevertheless, there is an exploitable potential that remains unexplored, despite being a clear priority and one of the commitments in the national energy policy (Krajačić, Duić, & Carvalho, 2011). For instance, in 2012, the hydroelectric and wind power represented 91% of the total renewable energy power capacity. Biogas and geothermal energies are residual contributors in the renewable energy sector.
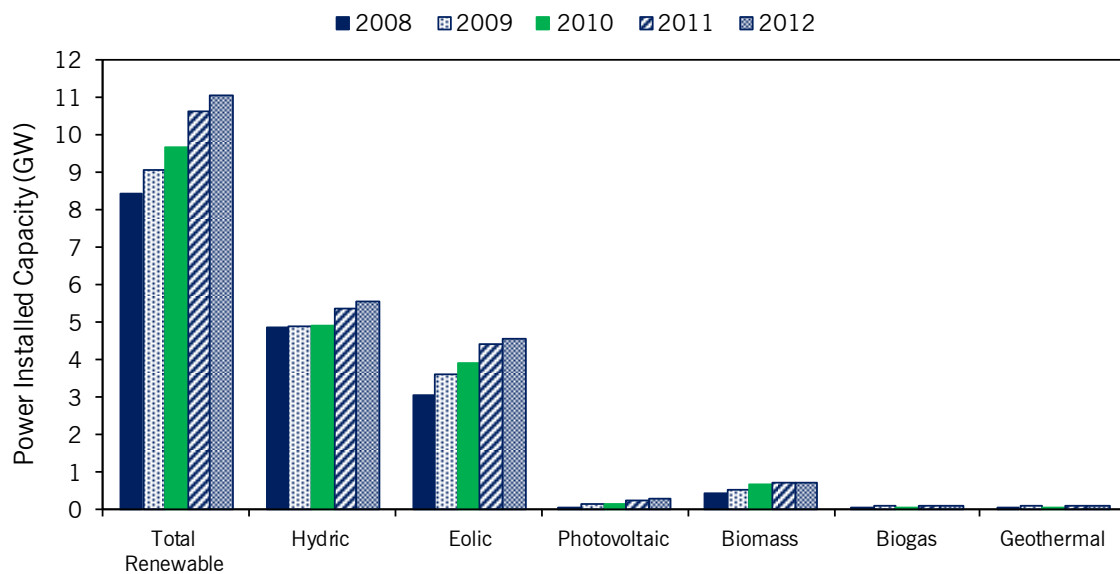
Figure 3.3 Renewable power capacities in Portugal between 2008 and 2012. Adapted from (DGEG, 2013).

Almost 65% of the electricity produced from biomass comes from systems which operate in cogeneration mode. In fact, biomass cogeneration is a prime example of how renewables and cogeneration can be combined. There is a double low-carbon benefit because of the use of renewable energy sources and, secondly, because these technologies when operating in cogeneration mode also enjoy the economic benefits of energy efficiency.

Among the policies used to promote RES, feed-in tariffs are a solution used by Portugal and many other countries. These price guarantees are valid for several years and their costs are supported by electricity consumers. The justification for this support mechanism is that free market would constrain RES use as they are still economically less attractive than the traditional technologies. Among renewable energy technologies, the exception to this rule is hydro power, which has been playing a major role in Portugal since the 50's and is mostly operating outside the feed-in-tariff schemes.

Among the remainder renewable energy sources, the most prominent is wind power. The first wind farm was built in 1992 and the growth of installed power was exponential until the end of 2011, when it already totalled 4081 MW. According to the Portuguese Renewable Action Plan, this number will reach 5300 MW in 2020 (DGEG, 2010).

There are several types of biomass production, and they can be divided in a first type where the origin of biomass is the forest or agriculture (dedicated production), and a second type where biomass results from the processing of primary biomass, including residues, waste and sub-products (Daminabo, 2009). In some cases, the power plant may generate, besides the electricity, an amount of heat that is useful for industrial purposes.

Currently Portugal has 462 MW of biomass installed power, among which 348 MW exist in cogeneration mode, mainly in the paper industry (INEGI, 2012).

Thus, the Portuguese electricity generating system presents a diversified structure including a different set of renewable and non-renewable technologies. The role of the RES has been increasing over the years strongly supported by the government objectives of reducing energy importations and reducing CO_2 emissions. The special regime for producers includes the production from other renewable sources, waste and the cogeneration. These producers have priority access to the grid system and benefit from the established feed-in-tariffs for the licence period (Krajačić et al., 2011). The future of the electricity power systems is strongly constrained by international environmental agreements, namely, in the aftermath of the Kyoto protocol, several EU Directives such as the RES, EED and EPDB Directives.

3.2.2. Energy Consumption

Concerning the energy consumption, a considerable change in habits in the last 15 years has been reported. Final energy consumption has increased slowly since 1994, reaching its highest value in 2005. After that, the level remained relatively steady, being affected by financial and economic crises since 2009. The decrease in energy consumption was the sharpest in the industry sector, which was one the activity sectors also affected by the economic recession. Nevertheless, in 2011, the share of final energy consumption of the main economic activity sectors was 33.7% in industry, 35.8% in transport, 16.6% residential, 11.3% in services and 2.6% in agriculture and fisheries. Yet, Portugal's total energy

consumption per capita is lower that the EU average. The most consumed final energy resources are oil products, electricity, NG, biomass and other renewables in this order (IEA, 2011).

Electricity consumption has increased particularly fast in households and in the services sector, by 37.8% and 38.3% respectively since 2000 (IEA, 2011). Figure 3.4 presents the evolution of production and consumption of electricity between the years 2000 and 2012.
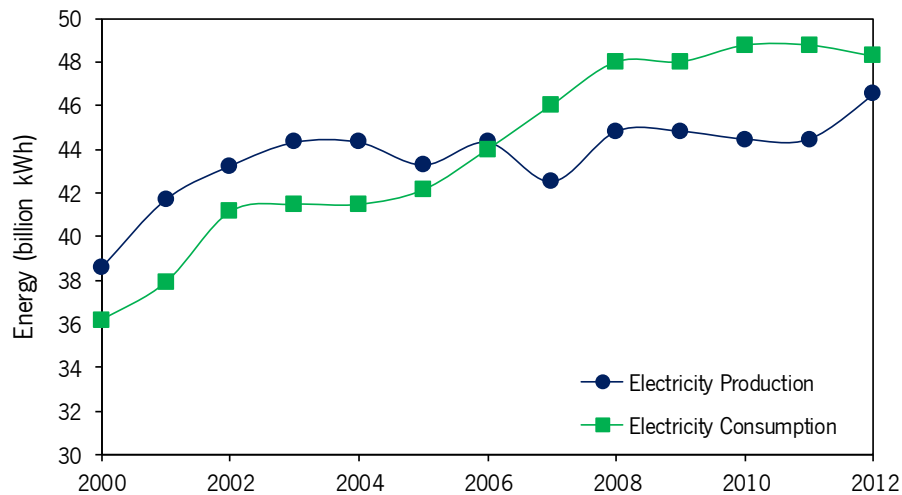
Figure 3.4 Production and consumption of electricity in Portugal.

In 2006, 76% of electricity consumption was focused in urban areas when cities comprised less than half of the total population. With the foreseen growth of urbanization, it becomes imperative to study the dynamics of cities and their impact on energy use (International Energy Agency - IEA, 2012).

Buildings consume a great amount of final energy. Domestic energy consumption can be defined as the amount of energy that is spent on the different appliances (heating, lightening, hot water, electrical equipment, etc.). The amount of energy used per dwelling varies, depending on the standard of living, climate of the country and the building characteristics. Although significant improvements in energy efficiency have been achieved in household appliances, the electricity consumption in households has been increasing during the past years. Some of the reasons for such increase in the residential sector are associated to a higher level of basic comfort and level of amenities and also to the widespread utilization of relatively new types of loads whose penetration and use has experienced a very significant growth in recent years. According to DGEG data, a Portuguese citizen consumes, in average, 20% less electricity than the average citizen of the European Union.

Matching supply with the buildings energy requirements is a very demandable task. There are two policies that address energy conversion and consumption in buildings: regulatory instruments and incentive schemes. The main regulatory instrument is the building energy code, which is a set of minimum energy performance requirements. The purpose of the energy code is to ensure that a building's energy performance is considered during the design stage of a building project (building energy codes are

mandatory in the European Union and often voluntary in other countries). Incentive schemes are complementary policies to regulatory instruments used to help increase the attractiveness of energy efficiency investments. They include all policy instruments that relate to fiscal, financial and other economic incentives to deliver energy efficiency improvements and disincentives to energy waste. Their objective is to motivate consumers to pursue investments they would not have ordinarily considered.

In this sense, different alternatives are being studied in order to supress the net energy needs of the buildings, mainly because of the targets established by the EU, which aim at self-sustainability and nearly zero energy buildings by 2020. Cogeneration systems have a great potential in this field, because these technologies are able to produce electricity and heat on a more efficient way and using renewable energy sources.

3.2.3. Cogeneration Share in energy generation

The first cogeneration units were introduced in our country during the 40's (in industry) with the installation of backpressure turbines, but it was only in the 90's that CHP had a significant growth in terms of installed capacity and produced energy. Figure 3.5 shows the percentage of electricity generation from cogeneration technologies in Portugal and in EU27 by 2011. The contributions from cogeneration power plants have been increasing during the last decade, with the exception of the year 2009.

In 2010, cogeneration contributed approximately with 12.7% of total national electricity production. The share of distributed generation (of which cogeneration accounts for over 80%) has increased steadily since the early 90s.

††1997-2002 non-available data
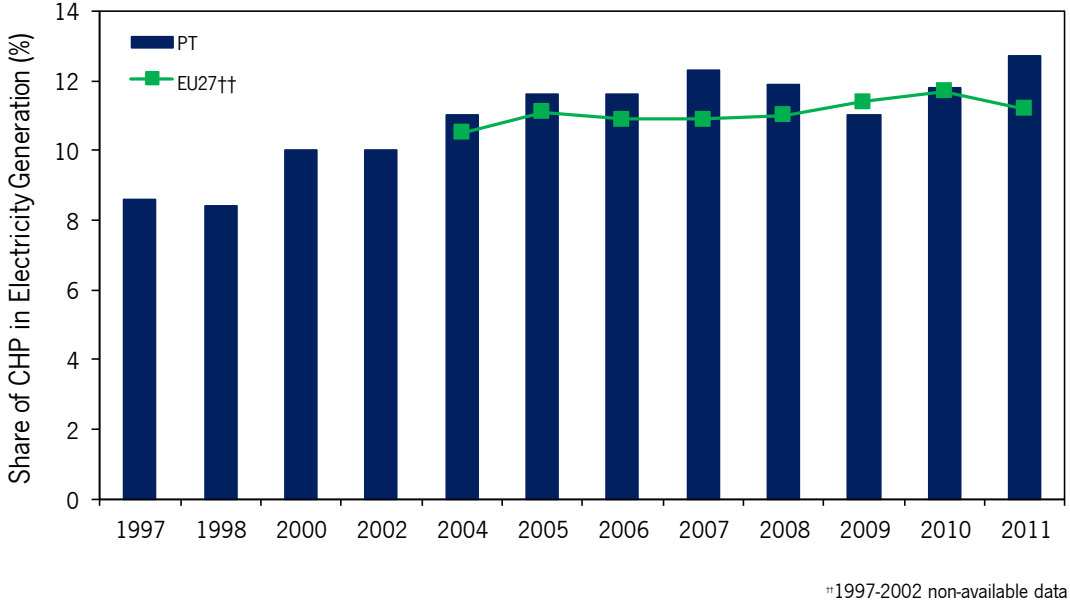
Figure 3.5 Evolution of cogeneration share in the total production of electricity in Portugal and in EU27. Adapted from (Eurostat, 2011).

The share of heat production supplied by CHP for the EU member states is presented ate Figure 3.6. The share of heat production supplied by CHP has been estimated by analysing fuel that was used by final consumers (excluding energy industries, non-fuel uses and transport). Eurostat does collect data on derived heat from district heating. These two data sets have been combined and assumptions used for boiler efficiency and other uses. The countries with a high market penetration are Finland (37.5%), Denmark (32.0%), Sweden (29.4%), Bulgaria (26.7%) and Portugal (22.5%). These data reveal that the share of heat generation by cogeneration is above the EU27 average.
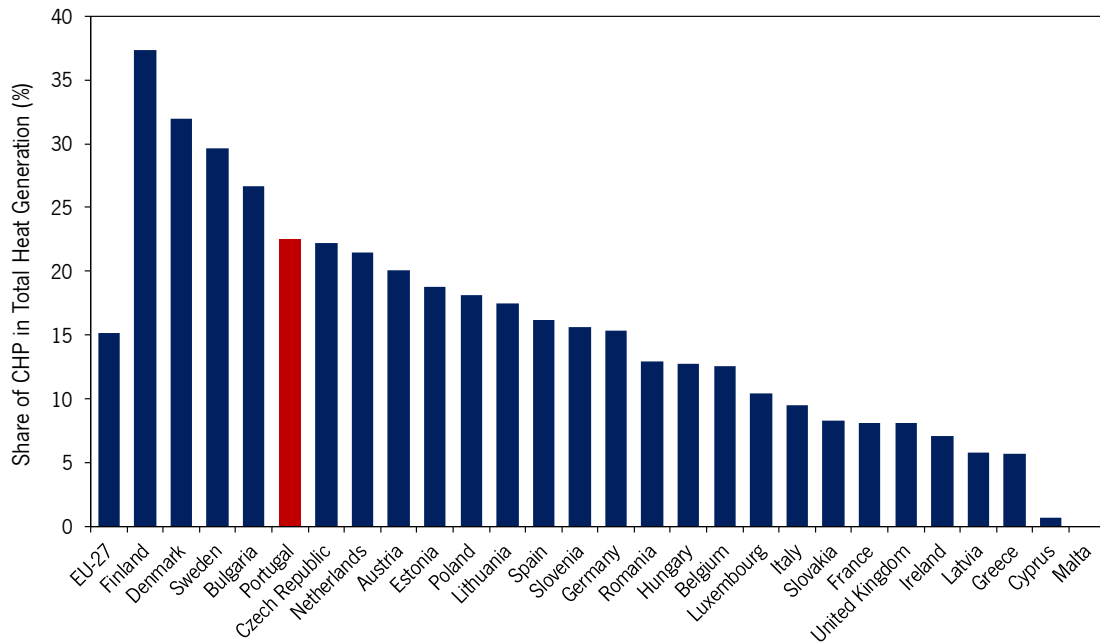
Figure 3.6 Share of cogeneration in total heat production in EU-27. Data was adapted from (European Environment Agency, 2012)

The already installed cogeneration puts Portugal in a comfortable position with regard to this technology, just behind the countries that make use of large-scale networks of heat distribution.

Figure 3.7 shows the evolution of cumulative cogeneration installed capacity until 2010. A marked increase can be observed from the early 90's, particularly after 1993. The backpressure steam turbines were the most used technology in Portugal until 1990. In the 90's, the increase of power cogeneration was mainly associated with the installation of combustion engines running with fuel oil and more recently with natural gas.

The implemented remuneration schemes over the time created an impetus for improving efficiency through the adoption of the principle of proportionality to define the surplus in the selling price of the produced electricity, according to the avoided costs to the national generation, where environmental costs are included. It is thus possible to establish an intrinsic relationship between the development of cogeneration and a framework of remuneration for the selling price of electricity.

A fact worthy of note is the installations using more than 50% of renewable fuels (including biomass), represent almost 24% of the total installed cogeneration units (DGEG, 2010b).
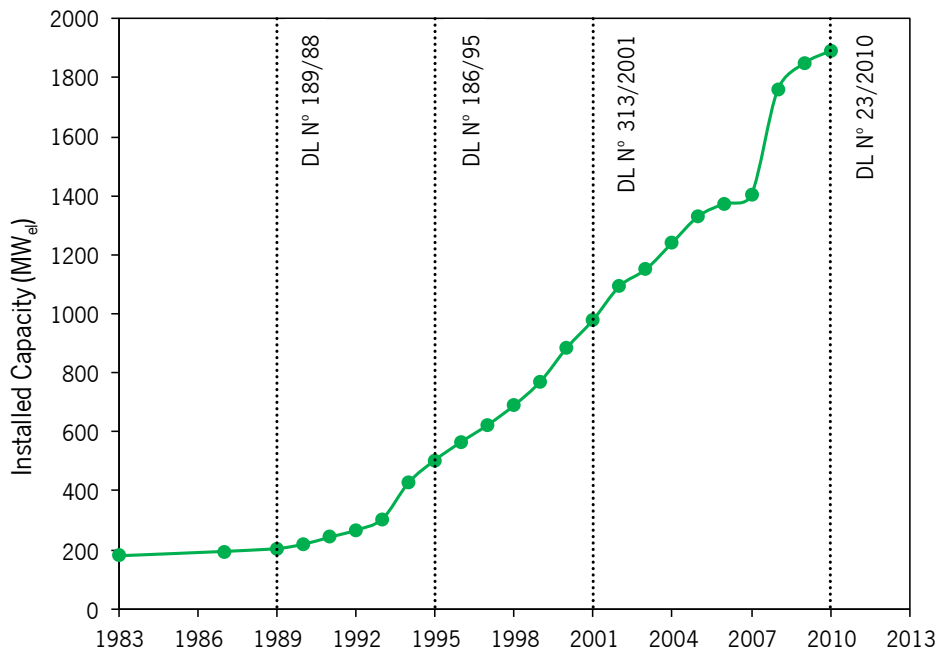
Figure 3.7 Evolution of total cumulative installed capacity of cogeneration in Portugal and legislation publication.

There is a recognized potential market for additional cogeneration units. For example, the buildings sector has an estimated market of around 500 MW$_{el}$ for cogeneration systems of less than 150 kW$_{el}$ in size. With this installed capacity, the CO_2 emissions could be reduced by 290,000 tonnes per year. Applications for small- and micro-cogeneration in Portugal include shopping centres, hotels and small industrial sites single or multifamily dwellings.

The potential for new, small-scale and micro-cogeneration installations in Portugal is very considerable. According to the Research Centre for Energy, Transport and Environmental Economics, the micro-cogeneration market has the potential for 6000 units for the building sector (Monteiro et al., 2009).

These systems should allow a number of energy policy goals to be achieved, including the reduction in greenhouse gas emissions, improved energy safety, investment reduction in the electrical transmission and distribution network and potentially reduced energy costs to consumers (Ferreira, Martins, Nunes, & Teixeira, 2011).

The plant evaluation must be based in two principles: a harmonised methodology for calculating the energy inputs required by the conventional separate production of electricity and heat, and a methodology for determining the efficiency of the cogeneration process. Conventional reference values of efficiency must be taken into account if cogeneration units and conventional separate production are to be compared. These reference values must consider the same fuel category and reflect the local climatic characteristics. The feasibility of micro-cogeneration systems in comparison with the alternative options for

residential energy supply depends on their capacity to satisfy the energy demands. It is very important to know the energy consumption profile for the correct sizing of the Cogeneration units, and to fulfil the policy requirements (Alanne, Söderholm, Sirén, & Beausoleil-Morrison, 2010). Thus, it is of utmost importance to define a methodology able to disclose the thermal energy needs of a dwelling.

3.3. Thermal Load Methodology

According to the European guidelines (Directive 2004/8/EC), high-efficient cogeneration shall operate based on the useful heat demand of the building, and provide a PES of at least 10%, compared with the references for separate production of heat and electricity. The cogeneration systems used for the heating of residential buildings are usually interconnected with the energy grid, as the surplus or even all the produced electricity can be sold to the external electric network. A simplified layout of the cogeneration-integrated system is presented in Figure 3.8.
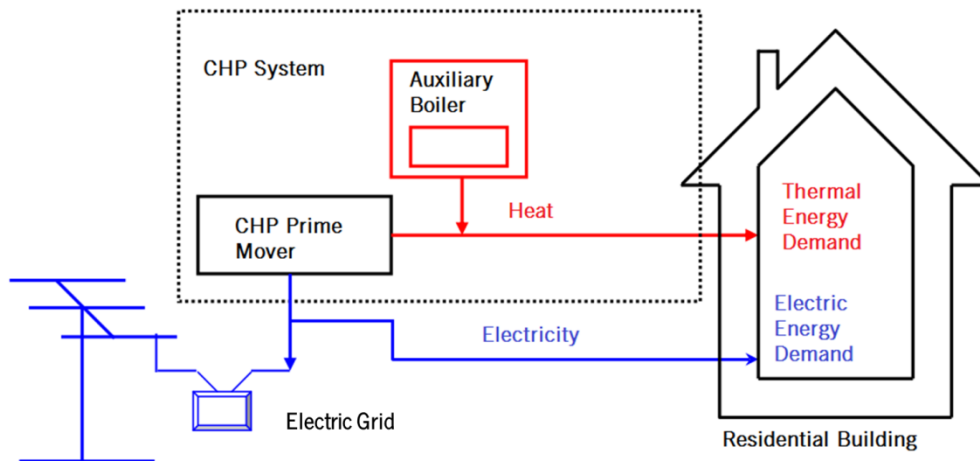
Figure 3.8 Layout of the cogeneration system for a residential building. Adapted from (Maghanki, Ghobadian, Najafi, & Galogah, 2013).

The evaluation of dwelling energy demands (i.e. hot water, electricity demand for space heating) is required. The thermal demand, considered as the sum of space and hot-water heating, is evaluated by the legislation for the energy certification of buildings. Thus, it is of utmost importance to match the thermal capacity of the cogeneration system to the total thermal load of the building.

A simplified methodology was defined to estimate the annual Thermal Power Duration Curve (TPDC) of a building that includes both the heating and the domestic hot water needs. Both thermal loads were calculated according to the Portuguese regulation for the thermal behaviour of buildings (Regulation of the Thermal Performance of Buildings RCCTE, 2006) that complies with the energy performance of buildings

directive EPBD. The TPDC is obtained from the sum of the hourly heating load plus the hourly hot water needs.

3.3.1. Heating Demand

In order to determine the hourly heating load, the starting point was to define the building specific Winter Heating Demand (WHD) per unit of floor area (kWh/m²). This reference parameter, easily calculated following the RCCTE, expresses the amount of useful energy required to keep the building at a reference temperature of 20 ºC (293 K) during the heating season. The yearly overall thermal energy demand for heating a building, for a specific building envelop, mainly depends on the following two aspects: (i) building geometry and (ii) climatic zone (Bianchi, De Pascale, & Spina, 2012).

This heating demand depends on the building Form Factor (FF) and on the Heating Degree Days (HDD₂₀) of the local climate. FF corresponds to the building envelope area ((i.e. the sum of the areas in contact with the outside atmosphere A_{ext}, and the areas in contact with non-heated spaces A_{int}) divided by inside volume, V. The term FF can be calculated according to equation (3.1).

$$FF = \frac{A_{outside} + \sum (\chi A_{inside})_i}{V}$$

(3.1)

where the variable χ can be defined by the expression in equation (3.2).

$$\chi = \frac{T_{inside} - T_a}{T_{inside} - T_{ref}}$$

(3.2)

where T_{inside} is the inside air temperature at the reference temperature during the heating season, T_a is the temperature at the non-heated local and T_{ref} is the outside ambient temperature. The Heating Degree Days depends on the location (local climate). Table 3.1 presents the identification of the winter climatic zones, the corresponding number of heating degree-days and the heating season duration for the Portuguese district counties.

The WHD can be calculated considering the characteristics of the building and the surrounding climatic conditions as shown in equations (3.3) to (3.6).

$$WDH = 4.5 + 0.0395\ HDD_{20} \quad for\ FF \leq 0.5$$

(3.3)

$$WDH = 4.5 + (0.021 + 0.037\ FF)\ HDD_{20} \quad for\ 0.5 < FF \leq 1;$$

(3.4)

$$WHD = [4.5 + (0.021 + 0.037\ FF)\ HDD_{20}]\ (1.2 - 0.2\ FF) \quad for\ 1 < FF \leq 1.5;$$

(3.5)
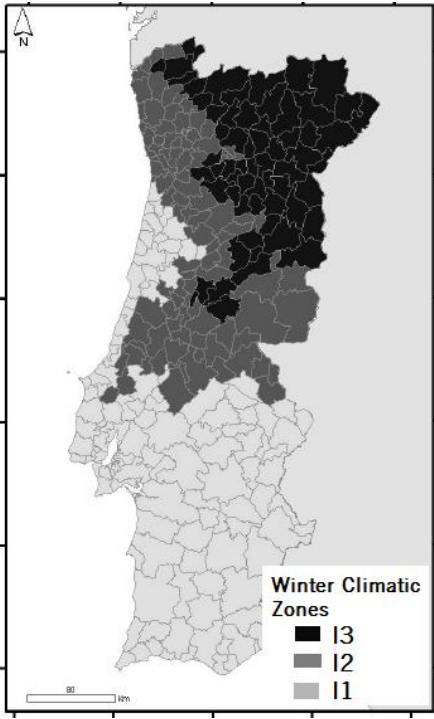
$$WHD = 4.05 + 0.068\ 85\ HDD_{20} \quad for\ FF > 1.5$$

(3.6)

It was assumed a hypothetical dwelling classified as energy class B minus (i.e. the reference class of the RCCTE) located in the city of Porto, North of Portugal. For this case, FF was considered to be 1.0, and the value of HDD₂₀ is 1610 ºC.*days*, for a heating season with the duration of 6.7 months (see Table 3.1).

Thus, the specific winter heating demand can, thereby, be obtained from equation (3.7).

$$WHD = 4.5 + (0.021 + 0.037\,FF)\,HDD_{20} \qquad \left[kWh/m^2\ per\ winter \right] \tag{3.7}$$

Table 3.1 Identification of winter climatic zones and respective reference climatic data

Portuguese County	Winter climatic zone	Heating Degree Days (°C.*days*)	Heating season duration (*months*)	Distribution of Winter Climatic Zones in Portuguese Territory
Aveiro	I1	1390	6	
Braga	I2	1800	7	
Bragança	I3	2850	8	
Beja	I1	1290	5.7	
Castelo Branco	I2	1650	6.7	
Coimbra	I1	1460	6	
Évora	I1	1390	5.7	
Faro	I1	1060	4.3	
Guarda	I3	2500	8	
Leiria	I2	1610	6	
Lisboa	I1	1190	5.3	
Portalegre	I2	1740	6.7	
Porto	I2	1610	6.7	
Santarém	I1	1440	5.7	
Setubal	I1	1190	5.3	
Viana do Castelo	I2	1760	6.3	
Vila Real	I3	2660	7	
Viseu	I2	1940	7.3	

From the WHD, a global heat loss coefficient was calculated in W/(m².°C) and the hourly heat demand of the building was then computed, based on the difference between the inside reference temperature (kept constant) and the hourly outside temperatures for the local climate (for each month, the average day was used) and the total floor area (assumed to be 150 m² per dwelling). The climate data was obtained from the database of the Soltherm software (LNEG, 2012).

3.3.2. Domestic hot water needs

Considering an occupation of 4 persons and that the Domestic Hot Water (DHW) needs are 40 L per person, per day at 333 K (60 °C), the daily domestic hot water needs were calculated. The specific daily hot water consumption, ($Cons_{dhw}$) (in L.m².*day*), was computed by taking into consideration the ratio between the water needs per person per day and the occupancy of the building (i.e. area divided by the

number of residents). Finaly, the thermal requirements for domestic hot water, (Q_{dhw}) can be calculated by equation(3.8).

$$Q_{dhw} = Cons_{dhw} \cdot (4.187 / 3600) \cdot \Delta T \qquad \left[kWh \cdot m^{-2} \cdot day^{-1} \right] \qquad (3.8)$$

where ΔT is temperature increase from the grid water temperature up to the required value, 333 K. The temperature increase required for hot water, if not calculated, can be assumed as the reference value of 318 K (45 °C). This value considers that water coming from the public water supply is available at an average temperature of 288 K (15 °C) and must be heated to a temperature of 333 K (60 °C). The number of days of consumption depends on the conventional DHW period of the building use, which in the case of residential buildings corresponds to 365 days/year. The hourly energy demand was then obtained by assuming the distribution presented in Figure 3.9.
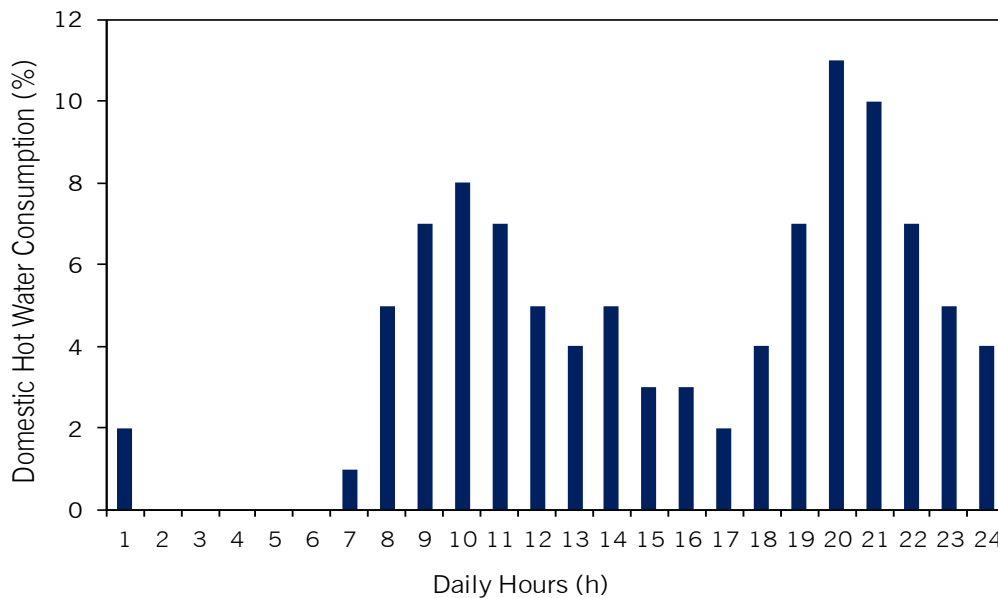
Figure 3.9 Assumed daily domestic hot water load distribution.

This non-dimensional daily distribution of the domestic hot water consumption is assumed to be representative of a typical day for a residential domestic user. Considering the thermal requirements for each month, the hourly water consumption and the dwelling area, the hot water annual thermal load can be estimated.

3.3.3. Thermal power duration curve

The total thermal load of the building, on an hourly basis, was calculated by adding the hourly values of heating and hot water loads (Martins et al., 2011). Figure 3.10 presents the total annual thermal power duration and the hot water thermal load duration curves for the reference dwelling.

The annual curves were obtained by sorting the hourly values from maximum to minimum. According to the implemented methodology, the peak thermal demand is about 7 kW$_{th}$. This result is within the expected values, considering that, for individual dwellings, the decentralized energy systems available in the market are characterized by a thermal power in the range of 2-35 kW$_{th}$ (Konrad, Obé, & Frey, 2009).
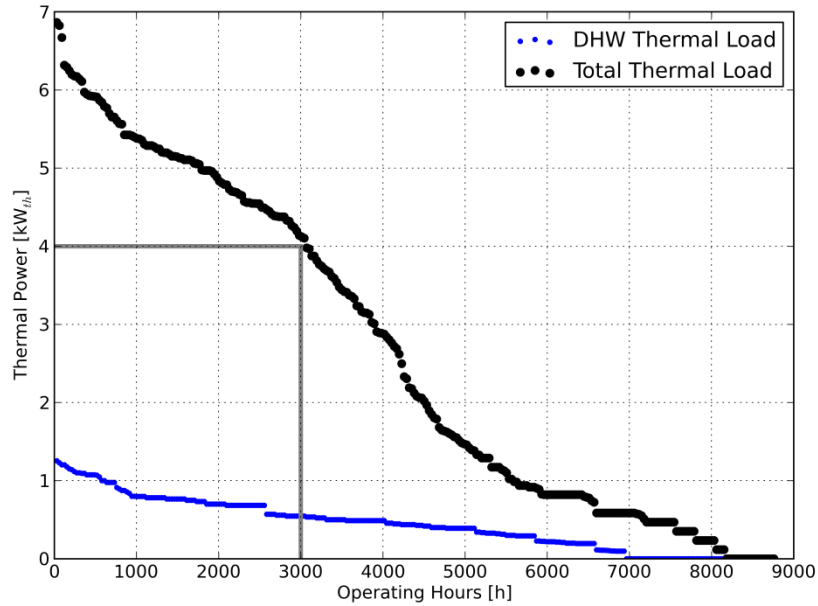
Figure 3.10 Annual power thermal power duration curve and hot water thermal load duration curve for the reference dwelling.

Figure 3.11 presents the evolution of the annual thermal energy production with the corresponding number of annual working hours matching the TPDC of Figure 3.10. The maximum output is 12.5 MWh$_{th}$ for a corresponding 3000 hours of operation, and a CHP system with a thermal capacity of 4.1 kW$_{th}$.
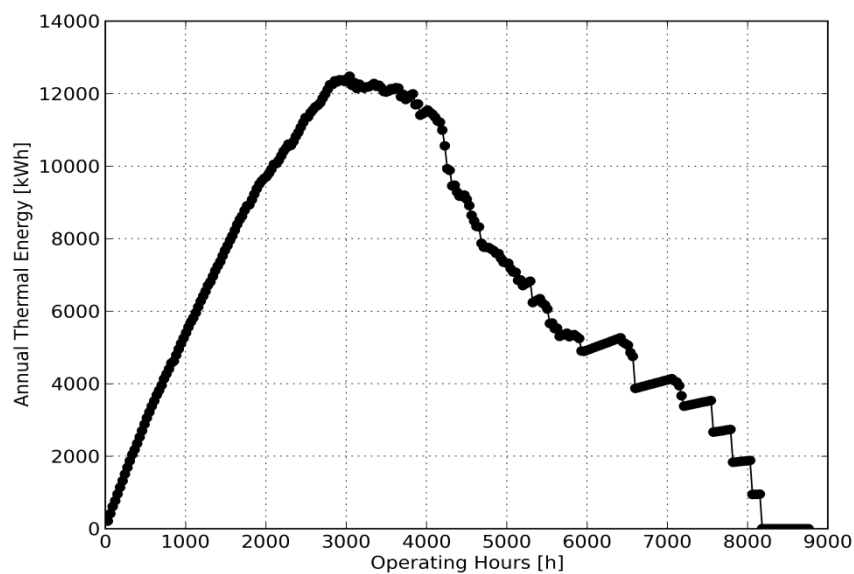
Figure 3.11 Thermal energy output as function of yearly operating hours at nominal capacity matching the TPDC.

Alanne, K., Söderholm, N., Sirén, K., & Beausoleil-Morrison, I. (2010). Techno-economic assessment and optimization of Stirling engine micro-cogeneration systems in residential buildings. *Energy Conversion and Management*, *51*(12), 2635–2646. doi:10.1016/j.enconman.2010.05.029

Bianchi, M., De Pascale, A., & Spina, P. R. (2012). Guidelines for residential micro-CHP systems design. *Applied Energy*, *97*, 673–685. doi:10.1016/j.apenergy.2011.11.023

Daminabo, F. F. O. (2009). *A Novel 2kWe Biomass-Organic Rankine Cycle Micro Cogeneration System*. University of Nottingham.

Decision(2011/877/EU). (2011). Establishing Harmonized efficiency reference values for separate production of electricity and heat in application of Directive 2004/8/EC of the Parliament and of the Council and repealing Commision Decision 2007/74/EC. Official Journal of the European Union.

Decrew-Law n.º 23/2010. (2010). Diário da República 1.ª série — N.º 59 — 25 de Março de 2010*(in portuguese)*..

DGEG. (2010a). *A factura energética portuguesa 2009* (p. 12) *(in portuguese)*..

DGEG. (2010b). *Estudo do Potencial de Cogeração de elevada eficiência em Portugal (in portuguese)*.

DIRECTIVE 2004/8/EC - Directive on the promotion of cogeneration based on a useful heat demand in the internal energy market. (2004). *European parliament and the council of the european union* (pp. 1–11).

DIRECTIVE 2010/31/EU. (2010). *DIRECTIVE 2010/31/EU OF THE EUROPEAN PARLIAMENT AND OF THE COUNCIL on the energy performance of buildings (recast)* (pp. 13–35).

Directive 2012/27/EU. (2012). *Energy Efficiency Directive 2012/27/EU of the European Parliament and of the Council* (pp. 1–56). Retrieved from http://ec.europa.eu/energy/efficiency/eed/eed_en.htm

European Environment Agency. (2012). Combined heat and power (CHP). *Share of combined heat and power in gross electricity production in 2009*. Retrieved November 25, 2011, from http://www.eea.europa.eu/data-and-maps/indicators/combined-heat-and-power-chp-1/combined-heat-and-power-chp-2

Eurostat, E. C. (2009). *Panorama of energy - Energy statistics to support EU policies and solutions* (p. 150). European Commision. doi:10.2785/26846

Eurostat, E. C. (2011). Combined heat and power generation. *Combined heat and power generation Statistics*. Retrieved September 12, 2012, from http://epp.eurostat.ec.europa.eu/portal/page/portal/product_details/dataset?p_product_code=TSDCC350

Ferreira, A. C. M., Martins, L. A. S. B., Nunes, M. L., & Teixeira, S. F. C. F. (2011). Development of a Cost-benefit Model for Micro CHP Systems. In *ICOPEV '2011- 1st International Conference on Project Economic Evaluation* (pp. 1–7). Guimarães. Retrieved from http://repositorium.sdum.uminho.pt/handle/1822/27990

IEA. (2011). Statistics International Energy Agency. *Final Consumption by Sector*. Retrieved January 04, 2012, from http://www.iea.org/stats/graphresults.asp?COUNTRY_CODE=PT

INEGI. (2012). Energias Endógenas de Portugal. *Base de Dados de fontes de energias renováveis*. Retrieved October 12, 2013, from http://e2p.inegi.up.pt/

International Energy Agency - IEA. (2012). International Energy Agency - Statistics of Electricity Consumption. *IEA*. Retrieved from http://www.iea.org

Konrad, C., Obé, E., & Frey, H. (2009). Distributed generation potential in the German residential sector. *Cogeneration & On-Site Power Reviews*, 59–65. Retrieved from http://www.cospp.com/articles/article_display.cfm?ARTICLE_ID=361546&p=122

Krajačić, G., Duić, N., & Carvalho, M. D. G. (2011). How to achieve a 100% RES electricity supply for Portugal? *Applied Energy*, *88*(2), 508–517. doi:10.1016/j.apenergy.2010.09.006

LNEG. (2012). SolTerm Manual. LNEG Laboratório Nacional de Energia e Geologia. IP.

Maghanki, M. M., Ghobadian, B., Najafi, G., & Galogah, R. J. (2013). Micro combined heat and power (MCHP) technologies and applications. *Renewable and Sustainable Energy Reviews*, *28*, 510–524. doi:10.1016/j.rser.2013.07.053

Martins, L. B., Ferreira, A. C. M., Nunes, M. L., Leão, C. P., Teixeira, S. F. C. F., Marques, F., & Teixeira, J. C. F. (2011). Optimal Design of Micro-Turbine Cogeneration Systems for the Portuguese Buildings Sector. In ASME (Ed.), *Volume 4: Energy Systems Analysis, Thermodynamics and Sustainability; Combustion Science and Engineering; Nanoengineering for Energy, Parts A and B* (pp. 179–186). Denver: ASME. doi:10.1115/IMECE2011-64470

Monteiro, E., Moreira, N. A., & Ferreira, S. (2009). Planning of micro-combined heat and power systems in the Portuguese scenario. *Applied Energy*, *86*(3), 290–298. doi:10.1016/j.apenergy.2008.04.010

Regulation of the Thermal Performance of Buildings RCCTE, D. L. 80/2006. Regulation of the Thermal Performance of Buildings RCCTE (2006) *(in portuguese)*..

The Portuguese Energy Services Regulatory Authority (ERSE), . (2011). The Portuguese Energy Services Regulatory Authority ERSE. *Informação sobre Produção em Regime Especial (PRE)*. Retrieved July 31, 2011, from http://www.erse.pt/pt/electricidade/ *(in portuguese)*.

This page was intentionally left in blank

This page was intentionally left in blank

4

Characterization and Modelling of the Stirling System

Since the presentation of the patent by Robert Stirling in 1816, Stirling engines have been developed for different purposes and applications. This versatility is due to the fact that the heat source in Stirling engines is external and thus can accept a wide variety of fuels. Another good point is that the combustion process can occur in steady state and therefore is easier to control. Stirling engines are very flexible and its most outstanding feature is related to their capacity to work at low temperatures. In this chapter, a full characterization of the technology will be provided.

4.1. Stirling Engine Design and Configurations

A Stirling engine is a device that converts heat into mechanical energy by alternately compressing and expanding a fixed quantity of a certain gas between a hot and a cold sink. The original idea of Robert Stirling was to develop of a special heat exchanger, called "economiser", to improve the fuel efficiency of a variety of industrial processes. In 1816 he incorporated this "economiser" in an air engine, thus creating what we call today a Stirling engine. His patent described in detail the use of that "economiser", explaining the cyclic heating and cooling of the internal gas by means of an external heat source and heat sink, and the characteristic phase difference between the displacer and expansion pistons. His intension

was to develop an alternative for steam engines because, in those days, they were not safe due to the risk of explosion of their boilers. However, the need to operate a Stirling engine at high temperatures to obtain a reasonable efficiency, revealed the engine's limitations.

Consequently and also because of material constraints and their incapacity to deliver the required energy, Stirling engines were overcome by steam engines even with the risk of explosion.

Later on, only smaller engines of the Stirling/hot air type were produced in reasonable number for applications where a low to medium power was required, for instance, rising water. Furthermore, in the early 20th century, this technology gained an exciting interest as the core component of micro-combined heat and power units. The very first known application dates to the 30's, when the Philips, motivated to expand their equipment sales, decided to offer a low-power portable generator for users living in locations where the electricity was not available. At the time, Stirling engine seemed to be the best choice as prime mover due to its ability to run on a variety of heat sources (e.g. lamp oil).

Since then, this company has invested millions of dollars and has created a very strong position in Stirling engine technology. Their developments have led to smooth and quiet-running demonstration engines with good efficiency.

During the 80s and early 90s, Professor Senft of the University of Wisconsin came up with the low temperature differential Stirling engine. The first produced prototypes have no direct connection between the flywheel and the displacer, as the changing pressure inside the main chamber is the responsible for the displacer movement.

Several experimental Stirling engines have been manufactured from the same general principles for vehicle applications, biomedical devices (e.g. blood pumps), electricity or hydraulic power generation or even in submarines. With a few notable exceptions of independent individuals who have done a very good work, most of the development on Stirling engines has been done by teams of engineers funded by the large companies, such as, Infinia Corporation, BAXI or Whispergen (Knowles, 1997).

The Stirling engine consists of an engine piston (small tightly sealed piston that moves out when the gas inside the engine expands), the exchanger piston (a larger piston that moves easily between the heated and cooled sections of the engine) and three heat exchangers: a heater, a regenerator and a cooler. The engine piston converts the pressure variation of the working gas into mechanical power, whereas the exchanger piston is used to move the working gas between the hot and cold sources. Considering the forms of cylinder coupling, these engines can be classified in three arrangements: alpha, beta and gamma.

The alpha configuration has two mechanically linked pistons (expansion and compression pistons, both working as gas exchangers) in separate cylinders, connected in series by the heater, the regenerator and the cooler. In some cases, the hot expansion cylinder is surrounded by the high temperature heat exchanger and the cold compression cylinder is surrounded by the cooler. The two-cylinder Stirling engine

is characterized by four different phases: expansion, pre-cooling transfer, compression, and pre-heating transfer. The complete cycle of an alpha Stirling engine is presented in Figure 4.1.

Expansion: The gas is heated, expands and pushes the hot piston. The expansion continues in the cold cylinder, which is 90° behind the hot piston in its cycle, extracting more work from the hot gas.
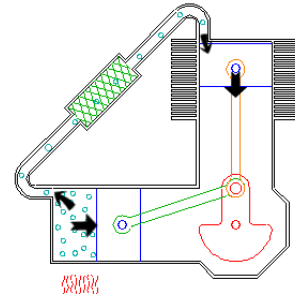
Pre-Cooling Transfer: About 2/3 of the working fluid is still located in the hot cylinder. Flywheel momentum carries the crankshaft the next 90°, transferring the main part of the gas to the cold cylinder. The working gas is pre-cooled while crossing the regenerator.
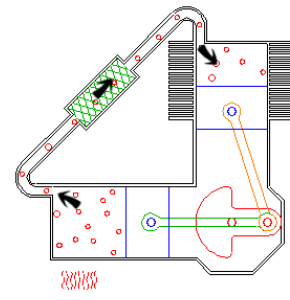
Compression: Almost all the gas is now in the cold cylinder and cooling starts. The cold piston, powered by flywheel momentum (or other piston pairs on the same shaft) moves up and compresses the gas.
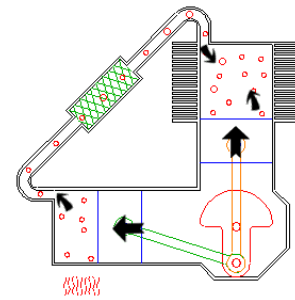
Pre-Heating Transfer: The contracted gas reaches its minimum volume, and it will be transferred back to the hot cylinder to complete the cycle in the hot cylinder where it will be heated once more.
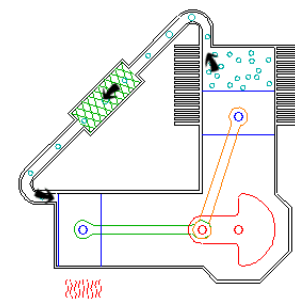
Figure 4.1 Phases of a complete alpha type Stirling cycle. Adapted from Keveney (2009) website animation.

The Beta configuration corresponds to the classic Stirling engine, having a power/compression piston arranged within a single cylinder with a displacer/expansion piston, both connected to the same shaft in a rather complex manner. The existence of a displacer aims to move the working gas between the expansion and the compression spaces at constant volume. When the gas is transferred to the hot space, it suffers expansion and the power piston is pushed, whereas when it passes to the cold end, the gas is compressed. The complete cycle of a beta Stirling engine is presented in Figure 4.2.

Expansion	Transfer	Compression	Transfer

Power piston has compressed the gas, the displacer piston starts to move down, while the gas is heated and expands, driving the power piston outward.

The displacer piston moves up, transferring the gas from the hot to the cold space.

The power piston moves up with energy from the flywheel, compressing the gas in the cold cylinder. This takes less energy, since the pressure is lower when the gas is cold.

The displacer piston moves down transferring the gas from the cold to the hot space.

Figure 4.2 Phases of a complete beta type Stirling cycle. Adapted from Keveney (2009) website animation.

Gamma engines use a displacer-piston arrangement, quite similar to a beta Stirling (see Figure 4.3). The main difference between these two configurations is that, in the Gamma engine, the power piston is mounted in a separate cylinder alongside the displacer-piston cylinder and the working gas can flow freely between them (Onovwiona & Ugursal, 2006).
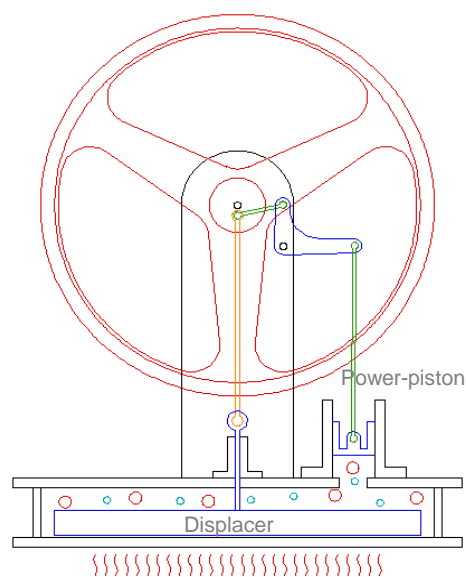
Figure 4.3 Schematic representation of gamma type Stirling cycle. Adapted from Keveney (2009) website animation.

This configuration produces a lower compression ratio, but allows an easier mechanical linkage between the pistons and a convenient separation between the heat exchangers, located at the ends of the displacer cylinder, and the work space associated to the power piston (Timoumi, Tlili, & Ben Nasrallah, 2008a). In addition, this configuration presents higher dead volumes and lower specific power and efficiency.

Comparing the three configurations, it can be said that the alpha engine is the simplest one, suitable for large power requirements, whereas the Beta engine generates higher pressures. The Gamma engine is usually used when the benefit from having power piston in separate cylinders overcomes the low specific power (Asnaghi, Ladjevardi, Saleh Izadkhast, & Kashani, 2012).

Another type of Stirling engine is the so called free-piston. In free piston-displacer Stirling engines, the reciprocating elements are driven by the pressure variations in the spaces surrounding them. As the linear alternator is tightly attached, the mechanical friction is minimized and, as a result, the leakage of the working gas is substantial reduced. So, the free piston engine does not require large maintenance costs, allowing a continuous power operation and revealing a great potential for high efficiency (Boucher, Lanzetta, & Nika, 2007). This concept was firstly idealized by William Beale, who realized that these engines could be properly used to generate power, and heat.

According to Formosa et al. (2011), the free piston Stirling engine uses the working gas like a spring, in order to give adequate movements to the piston and displacer. A double free piston Stirling engine (DFPSE) acts as a vibrating generator in which gas is compressed and expanded by an oscillating system of masses and gas springs.

Considering the operation mode, Stirling engines can be classified as single and double action. The term single action and double action in Stirling engine technology, is used to describe the mode of operation of a particular engine. In single action engines, the working fluid is only in contact with one side of the piston. The first engine conceived by Robert Stirling in 1815 was single action. The double action engine uses both sides of the piston to move the fluid from one space to another. Whereas, the double action engine arrangement is more complex because it requires a duct to connect the working spaces with the regenerator. Stirling engines using the double action principle require a multi-cylinder arrangement, since a minimum of three pistons is necessary in order to obtain the appropriate difference between the expansion and compression processes. The first double action engine was developed by Babcock in 1885.

There is another form of Stirling engines classification: forms of piston coupling. This classification category can be divided into rigid coupling, gas coupling and liquid coupling. The rigid coupling implies a physic mechanism, e.g. a slider crank drive or a rhombic drive for the engine operation: the slider cranks were widely used in double action engines due to its reliability and simple manufacture; the rhombic drive was developed mainly for single cylinder Stirling engines by Philips in the 50s (Thombare & Verma,

2008). In fact, the need of bigger systems leads to the need to seal off the cylinder space from the crankcase. An insight of the Stirling engine classification is presented in Figure 4.4.
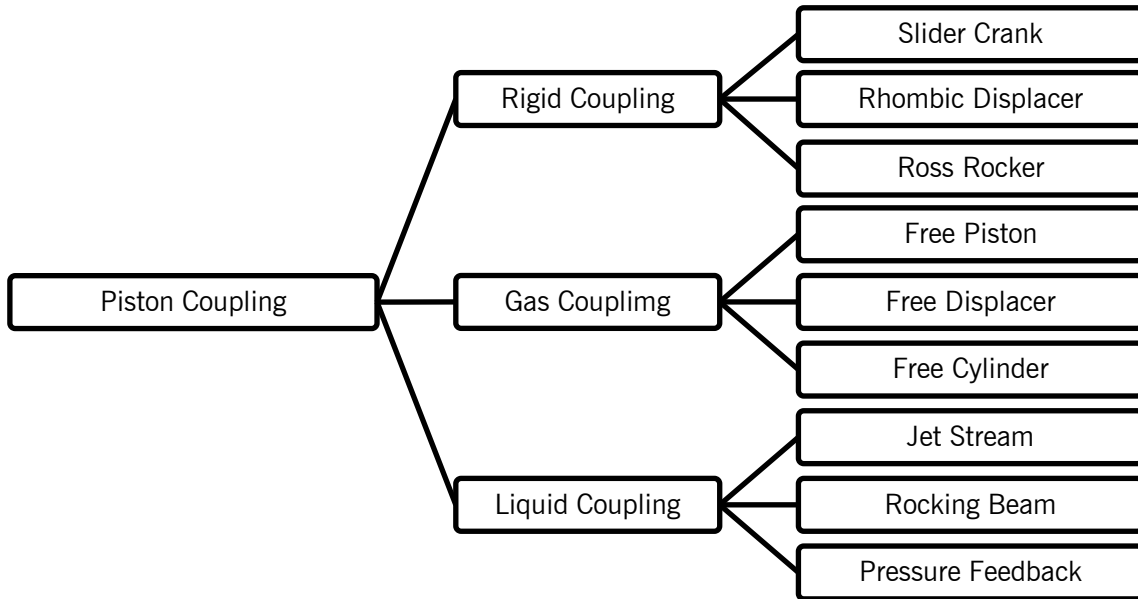
Figure 4.4 Stirling engines classification based on piston coupling.

4.2. Thermodynamic Cycle

The Stirling engine works in a closed thermodynamic cycle and contains a fixed mass of a working gas. The ideal Stirling cycle combines four thermodynamic distinct processes: two constant-temperature processes and two constant-volume processes. The working gas is alternately heated and cooled as it is cyclic compressed and expanded. Figure 4.5-a represents the pressure/volume diagram of the ideal Stirling engine. The first process of the ideal Stirling engine cycle is the reversible isothermal compression. During this stage work (W_{1-2}) is done on the working fluid (i.e. negative work), while an equal amount of heat ($Q_{1-2}=W_{1-2}$) is rejected by the system to the cooling source (equation (4.1), valid for an ideal gas). As the working fluid is compressed, the pressure increases from P_1 to P_2,(equation(4.2)). The temperature is maintained constant due to heat flow from the compression space to its vicinity. There is a decrease in entropy but the internal energy does not change.

$$Q_{1-2} = W_{1-2} = P_1 \cdot V_1 \cdot \ln(1/r_v) \tag{4.1}$$

$$P_2 = \frac{P_1 V_1}{V_2}; \quad T_1 = T_2 = T_{\min} \tag{4.2}$$

W_{1-2} is the compression work, P and V are the pressure and the volume at points 1 and 2 of the PV diagram of the ideal cycle in Figure 4.5-a, and r_v is the volume compression ratio, defined to be $r_v = \left(V_1 \middle/ V_2 \right)$. Note that the heat and work done during this processes are negative.

At the second step, a constant-volume process occurs with heat addiction (Q_{23}) because the working fluid is transferred from the compression to the expansion space through the regenerator. There is a gradual increase in temperature of the working fluid as heat is being received from the regenerator matrix. The passage of working fluid through the regenerator also causes an increase in pressure (equation (4.3)). No work is done (W_{23}=0) as the process is isochoric and there is an increase in the entropy and internal energy of the working fluid.

$$P_3 = \frac{P_2 T_3}{T_2}; \quad V_3 = V_2 \tag{4.3}$$

The terms P and T are the pressure and the temperature at the points 2 and 3 of the pressure/volume diagram of the ideal Stirling engine cycle in Figure 4.5-a. The heat transferred to the working fluid is equal to the increase in internal energy as in equation (4.4):

$$Q_{2-3} = \int_{T_2}^{T_3} c_v . dT = c_v \cdot (T_3 - T_2) \tag{4.4}$$

where T is the temperature at the points 2 and 3 of the pressure/volume diagram of the ideal Stirling engine cycle in Figure 4.5-a and c_v is the specific heat capacity of the working fluid.

At the third stage, the working fluid suffers an isothermal expansion, as heat is added (Q_{34}) to the system from the external source. Positive work is done by the working fluid (W_{34}) on the piston with the same magnitude of the supplied heat (equation (4.5)). The internal energy remains constant, but the entropy of the working fluid rises. As the expansion process proceeds, the pressure decreases (equation (4.6)):

$$Q_{3-4} = W_{3-4} = P_3 \cdot V_3 \cdot \ln r_v \tag{4.5}$$

$$P_4 = \frac{P_3 V_3}{V_4}; \quad T_4 = T_3 = T_{max} \tag{4.6}$$

where P, T and V are the pressures, the temperatures and the volumes, respectively, at the points 3 and 4 of the PV diagram of the ideal cycle in Figure 4.5-a. Here, the volume ratio is defined to be $r_v = \left(V_4 \big/ V_3 \right)$.

In the final evolution, the working gas flows through the regenerator, while heat (Q_{41}) is rejected to the regenerator matrix, decreasing the gas temperature. No work is done (W_{41}=0) during this isochoric process and the internal energy and entropy of the working fluid decreases. The pressure of the working fluid during can be evaluated according to equation (4.7) and the heat rejection according to equation (4.8):

$$P_1 = \frac{P_4 T_4}{T_1}; \quad V_1 = V_4 \tag{4.7}$$

where P, T and V are the pressure, the temperature and the volume, respectively, at the points 4 and 1 of the PV diagram of the ideal cycle in Figure 4.5-a.

$$Q_{4-1} = \int_{T4}^{T_1} c_v.dT = c_v \cdot (T_1 - T_4)$$ (4.8)

In the ideal Stirling cycle, it is assumed that the total heat rejected during process 4→1 is absorbed by the regenerator and then released to the working fluid during the process 2→3, corresponding to a thermodynamically reversible cycle. These assumptions imply that the heat exchangers are required to be perfect (i.e. an infinite heat transfer coefficient between the component walls and the working gas and perfect regeneration). Then, the efficiency can be calculated by equation (4.9).

$$\eta = 1 - \frac{T_1}{T_3} = 1 - \frac{T_{min}}{T_{max}}$$ (4.9)

that corresponds to the Carnot efficiency of an engine working between a hot source and a cold sink with constant temperatures T_{max} and T_{min}, respectively. It should be noted that this theoretically best possible efficiency is also achievable even if the regenerative processes are non-isochoric, as will be seen in section 6.2.1 with a sinusoidal engine. The relevant conditions are the reversible isothermal processes and a perfect regeneration.

However, in real cycles, there are no perfect regenerators and, one of the causes for inefficiency of the real Stirling cycle is friction to the flow of the working gas when passing through the regenerator. Figure 4.5-b represents the PV diagram of the real Stirling cycle with a sinusoidal piston motion.

4.5-a
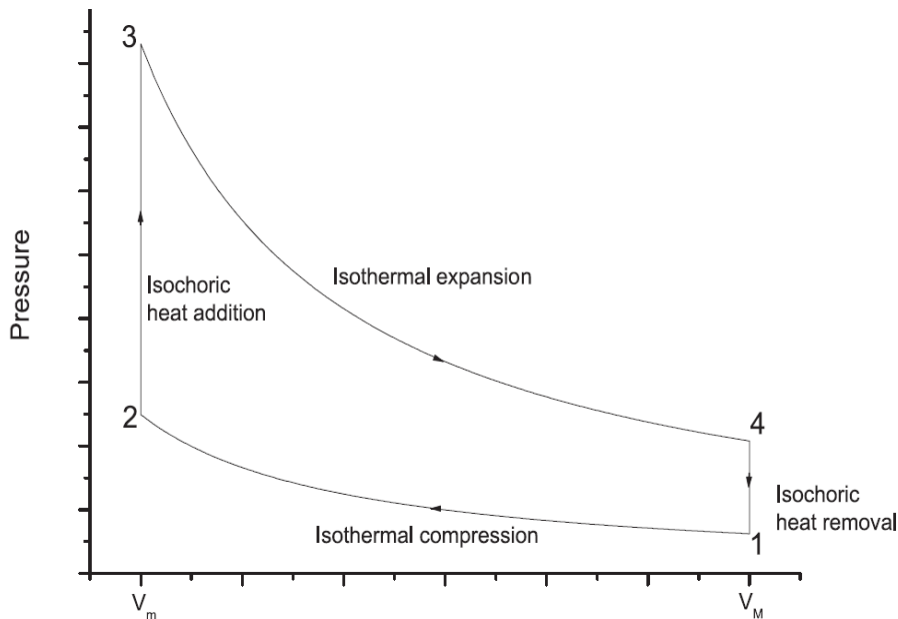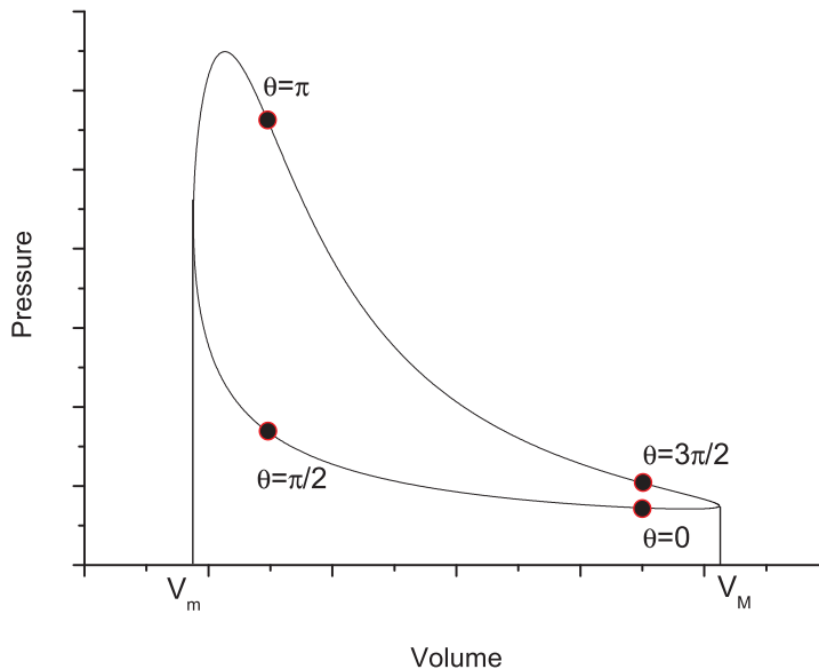
Figure 4.5-a PV diagram of the ideal Stirling engine cycle. 4.5-b PV diagram of a real Stirling engine cycle with a sinusoidal piston motion. Adapted from (Puech & Tishkova, 2011).

One of the major causes of Stirling cycle inefficiency is the fact that not all the gas in the engine participates in the compression/expansion processes, since there is a certain amount of gas that remains in the heater, regenerator, cooler and connecting passages. In the ideal analysis, there is a decrease in specific power as dead volumes increase. In practice, the loss of efficiency happens because the pumping losses increase with the dead volumes. This "dead volume" is defined as the total void volume in a Stirling engine.

Many authors have studied the effect of heat losses, irreversibilities and several design parameters on the thermodynamic performance of Stirling engines. Timoumi and co-workers (2008b) presented a study where a numerical simulation was developed using the experimental data from the General Motor (GPU-3) Stirling engine. The model was used to determine the influence of geometrical and physical parameters in the engine performance. Puech & Tishkova (2011) performed a theoretical analysis of the thermodynamic cycle of a Stirling engine with linear and sinusoidal variations of the volume. The authors concluded that the dead volume strongly amplifies the imperfect regeneration effect and, therefore, the cycle thermal efficiency. Kongtragool & Wongwises (2006) also studied the effects of dead volume and regenerator effectiveness on Stirling thermal efficiency and concluded that the dead volume leads to a reduction of engine network and thermal efficiency.

The nature and the pressure of the working gas influence the power performance of the Stirling engine. Gases, such as helium and hydrogen, which allow a rapid heat transfer without a change of phase, are typically used in high-performance Stirling engines. Hydrogen is thermodynamically a better choice; it has

a higher thermal diffusivity and a lower viscosity and therefore lower friction losses than helium. On other hand, helium has fewer material compatibility problems and it is safer to work with. Also, air can be used as the working fluid but with a prejudice on performance. The influence of the gas properties will be further discussed in this chapter.

The Stirling engine is currently an exciting choice as the core component of micro combined heat and power units, being considered more efficient and safer than other technologies. Presently, these engines are able to achieve an electrical efficiency of about 30% and a total efficiency of 85-98% operating in cogeneration mode (based on Low Heating Value, LHV). Stirling engines also have good capability to operate under partial-load conditions. In theory, the Stirling engine is the most efficient technology for converting heat into mechanical work, with its thermal efficiency limited by the Carnot cycle (ideal engine) efficiency, already defined in equation (4.9).

4.3. Stirling Engine Components

The elements of Stirling engine include two volumes at different temperatures connected to each other through a regenerative heat exchanger and auxiliary heat exchangers (heater and cooler). The heat transfer requirements of the engine implicate that these volumes change periodically. An insight of the engine base, heater, regenerator and cooler operation is characterized in this section.

4.3.1. Engine Base

A basic Stirling engine has a cylinder with two pistons in opposed positions and a regenerator. The spaces between the regenerator and the respective pistons correspond to the expansion and the compression spaces (Asnaghi et al., 2012). The piston rods are connected to the crankshaft by connecting rods, the dry-running pistons in the high pressure chambers are sealed against the oil-lubricated crankcase by piston seals. The expansion space must be maintained at a high temperature whereas the compression volume must be maintained at a low temperature while the regenerator is responsible for the pre-cooling and pre-heating of the gas. Consequently, the heat exchangers are relevant components in a Stirling engine. The mechanical friction is due to the contact between different parts that compose the engine: piston rings, bearings, rubbing seals and other moving parts. Control systems are required to regulate the power output and speed of a Stirling engine. For engines which operate at constant speed, connected to fixed frequency electric power generators, its constancy is maintained by varying a load condition. The power of Stirling engines can be controlled by changing the operational parameters, such as the temperature, pressure, phase angle, dead volume and speed (Cheng & Yang, 2012). These latter are key parameters in the Stirling engine performance. The power output of the engine is directly proportional to

the mean cycle pressure of the working gas. Thus, if the pressure level is changed, then the engine power output can be adjusted. Also, dead volume has an impact in the engine output.

Ideally, dead volumes should be zero but in real engines can represent almost 50% of the total engine internal gas volume (Thombare & Verma, 2008). An increase in the dead volume results in a loss of power output but not necessarily a decrease in efficiency. In fact, the effects of dead volume depend on its location in the engine. For instance, Puech & Tishkova (2011) have shown that the efficiency reduction is amplified by the increase of the regenerator dead volume.

4.3.2. Heater

The heater is responsible for the heat transfer from the heat source to the operating fluid. This type of heat exchangers is not easy to design because of the distinct operation conditions inside and outside the exchanger. The outer surface of the heater is subjected to high temperature and low constant pressure flow, while the inner surface is at high pressure and high temperature turbulent flow. The heat source type and the ratio between the internal and external diameter are two other parameters that affect the choice of best heat exchanger to use. The most used configuration for heat exchangers are smooth pipes in a parallel arrangement (Figure 4.6). These heat exchangers are used when the pressure/temperature gradient between the fluids is high. In terms of materials, the pipes are usually made of stainless steel, nickel alloys, aluminium or titanium, all good conductors of heat.
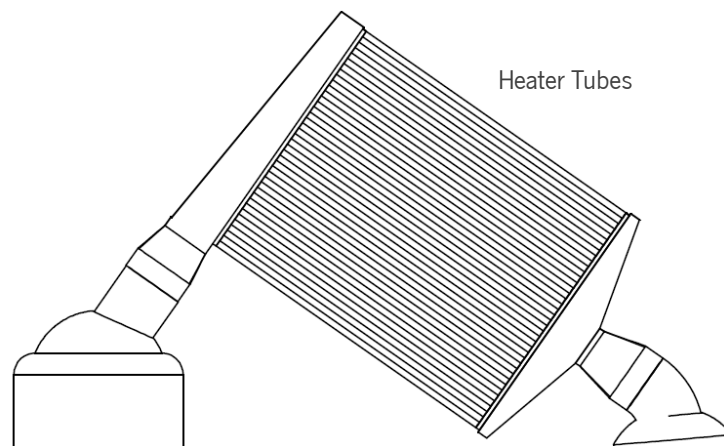
Figure 4.6 Schematics of heater parallel tubes arrangement.

The heat transfer phenomena in this component include the convective heat transfer from the external heating source/medium to the walls of the heat exchangers (e.g. tubes or fins) followed by conduction from the outer to the inner surface of the walls, and by convective heat transfer from the inner wall to the working fluid. The heat source is a crucial aspect in designing the heater. The outer surface of the heat-exchanger pipes will experience, in most of cases, a high temperature low-pressure steady flow boundary conditions or no flow in the case of a solar concentrator, whereas the inner surface experiences an

unsteady flow at high pressure and temperature. As a result, the heat transfer coefficients will be different inside and outside. Usually, the outside coefficient poses no problem, as fins can be easily added or it tends to infinity with a solar concentrator, but inside fins are not commonly used due to friction problems. Thus, the most crucial parameters are the inside convective heat transfer coefficient and the friction factor. These two parameters of heat exchanger can be assessed and the optimum dimensions of a proposed design can be accomplished for given thermodynamic specifications. The rate at which the heat flux is transferred to the working gas depends upon well-gas temperature difference, the mass flow rate and the specific heat of the gas. The working gas is highly pressurized and moves with high velocity, promoting the heat transfer process. So, in manufacturing these heat exchangers, alloys that can endure very high temperatures should be used. A reasonable thermal conductivity is also required to obtain a small temperature difference between the outer and inner wall surfaces.

4.3.3. Cooler

In a Stirling engine, the cooler absorbs heat from the working gas adjacent to compression space and rejects the heat to a coolant. Stirling engines may be water-cooled (common) or air-cooled (less common) similarly to IC engines. As the coolant temperature increases, there is a considerable drop in thermal efficiency, so it is desirable to have coolant temperature low as possible. The internal flow conditions are comparable to those of the heater but at lower temperatures. Almost all engine designers have adopted water-cooling and the outer cooler tubes experience the same flow conditions as in a conventional engine. The engine parameters should be optimised to minimize losses and to obtain high thermal efficiency for all the engine components, mainly the heat exchangers. While the main target of the engine is to produce sufficient power to run an application, there are conditions which pose critical constraints on the design. The temperature difference between the heater and the cooler is one of those parameters (Ercan Ataer & Karabulut, 2005). For the cooler analysis, the total heat transfer coefficient includes the heat transfer coefficient of the outside water film. Considering their operational conditions, coolers are usually designed as a set of smooth pipes (as presented in Figure 4.7), or finned tubes.
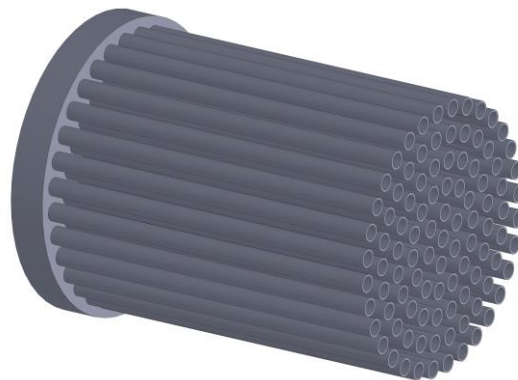
Figure 4.7 Bundle of parallel smooth tubes for a cooler.

The main limitation on cooler performance is usually related with the poor heat transfer between the inner surface of the cooler tubes and the working gas, with a consequently high value for the mean temperature of the gas in the cooler (Zarinchang & Yarmahmoudi, 2008). Nevertheless, inside-tube fins are not common, due to the increased friction.

4.3.4. Regenerator

Regenerator is a special heat exchanger, usually containing a finely matrix of metal wires, which is able to absorb and release heat from and back to the working gas (Knowles, 1997). After the expansion process of the thermodynamic cycle, when the heat supplied to the working gas by an external source is converted into useful work, the hot expanded gas is pre-cooled in the regenerator while moving from the expansion to the compression space. This energy is internally stored in the regenerator. After the compression-cooling process, the working gas flows back to the expansion space through the regenerator and the previously stored heat is transferred back to the working gas. This process is called regeneration and the efficiency of it dramatically influences the efficiency of the Stirling cycle (Thombare & Verma, 2008).

An ideal regeneration would only be possible if the heat transfer coefficient or the area of heat transfer and the heat capacity of the regenerator matrix were infinite or in the case heat transfer capacity of fluid would be zero. However, in real practical conditions, the temperatures of the working gas entering the regenerator fluctuates because of the thermodynamic properties of the gas (e.g. density), its velocity and pressure (Zarinchang & Yarmahmoudi, 2008), and do not reach at the exit, the temperatures required for the isothermal expansion and compression processes (points 3 and 1 in Figure 4.5-a).

As previously referred by Knowles (1997), the regenerator is the heart of the Stirling engine because it is responsible for critical temperature changes in the working fluid.

Less heat internally transferred by the regenerator, in the pre-cooling and pre-heating processes, will correspond to increases in the external hot source and cold source energies, thus leading to a significant reduction in the cycle thermal efficiency. The regenerator thermal quality is thus defined as the ratio between the real heat transferred from the matrix to the working gas and the ideal equivalent amount from the hot to the cold-source temperature change of the gas (A. C. M. Ferreira et al., 2013; He, Sanders, & Berkeley, n.d.).

To improve heat transfer coefficient and to establish the minimum temperature difference between matrix and the fluid, it is necessary to expose the maximum surface area of matrix. The regenerator also increases the pumping losses due to gas flow friction through the pipes, and contributes to the dead volume. Thus, a commitment between the geometrical characteristics of the regenerator matrix is required (Thombare & Verma, 2008; Zarinchang & Yarmahmoudi, 2009):

- For maximum heat capacity: a large, solid matrix;
- For minimum flow losses: a small, highly porous matrix;

- For minimum dead space: a small, dense matrix;
- For maximum heat transfer: a large, finely divided matrix;
- For minimum contamination: a matrix with no obstruction.

According to Thombare & Verma, (2008) the choice of the materials for the regenerator matrix highly influences the performance of the engine. The efficiency and power output of the engine are a function of engine speed for metallic and ceramic regenerator materials. Due to lower permeation rate of ceramics when compared to metals, it is found that efficiency and power output of the engine with ceramic-coated materials is higher than the metallic regenerator. Several materials and configurations may be used for the regenerator matrix, such as steels wool, steel felt, wire mesh, fine pipes, spring mesh, foils or packed annulus. As shown in Figure 4.8-a, a typical regenerator is cylindrical in overall shape and includes axial passage(s) containing a matrix (Figure 4.8-b). This latter is an open, thermally conductive structure with many flow paths and large surface area for high heat transfer to and from the working fluid.
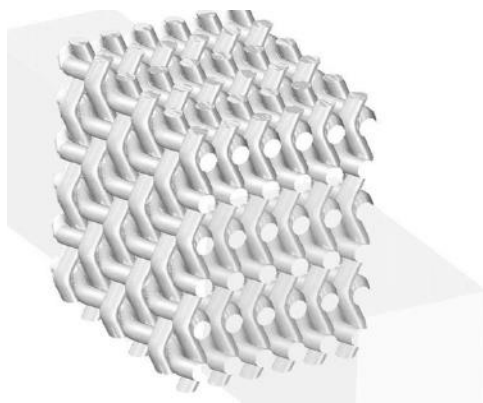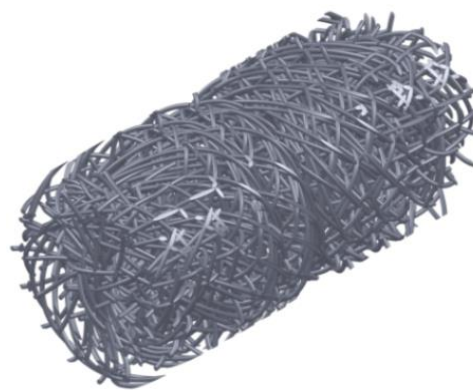
| 4.8-a | 4.8-b |

Figure 4.8-a Wired matrix of a Stirling regenerator with an oriented arrangement. **4.8-b** Ultra-fine wired matrix of a Stirling regenerator with chaotic arrangement.

The regenerator matrix is usually made up of an ultra-fine wire mesh arranged in a grid or chaotically as shown by Figure 4.9. The porosity of the matrix is important since it will have a direct impact on the performance of the regenerator, and can be determined by its geometry, namely, wire diameter and the void volume. Any changes in the porosity will also change the regenerator effectiveness and the pressure drop (Tlili, Timoumi, & Nasrallah, 2008).

Figure 4.9 Microscope views of the matrix of three different regenerator matrices. Adapted from (Jiří, 2009).

Regarding the heat exchangers, the most important in its design them it is their ability to supply or reject the required amount of heat to or from the working gas inside the engine. In this aspect, one crucial factor is the heat transfer area, which outlines the amount of heat energy to be permuted. Therefore, in order to achieve a high effectiveness for the heater and the cooler, larger transfer areas are needed (Tlili et al., 2008).

4.4. Working Fluids

During the 19th century, most Stirling engines used air as working fluid. Nevertheless, helium and hydrogen are much better gases for Stirling engines. The selection of a specific working fluid is based on the following fluid properties: thermal conductivity, specific heat capacity, density, and dynamic viscosity. The working gas should have a high thermal conductivity (Figure 4.10) to improve the efficacy of the heat exchangers, and a low density and viscosity.
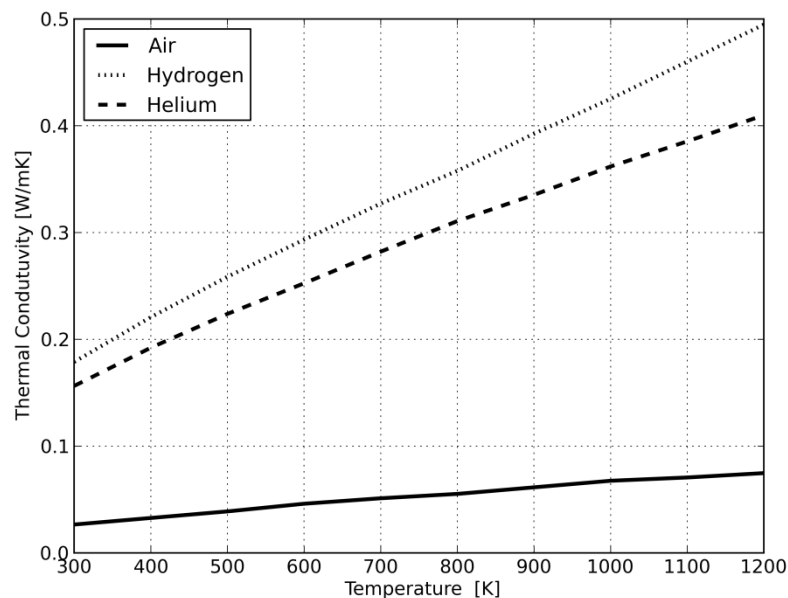
Figure 4.10 Thermal conductivity as a function of temperature for three working fluids: air, helium and hydrogen.

Lower dynamic viscosity and density are more related with the fluid friction, reducing the pumping losses and improving engine specific power and efficiency. The evolution of viscosity with the temperature is

---

shown in Figure 4.11, for three gases. Working fluids with high specific heat capacity leads to a larger increase in pressure or volume for a given amount of heat.
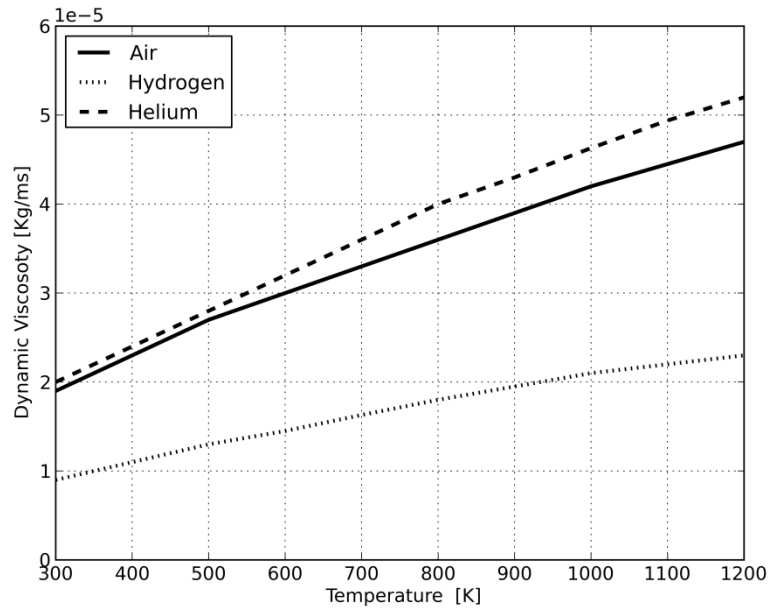
Figure 4.11 Dynamic viscosity as a function of temperature for three working fluids: air, helium and hydrogen.

The working fluid selection must be made based on the best combination of the parameters, which establish a relation between the heat transfer and the frictional drag in a flowing stream. The combined relevant property for heat transfer is the thermal diffusivity (thermal conductivity divided by volumetric heat capacity, $\rho \cdot c_p$ (J/(m³·K)), as shown by equation (4.10):

$$\alpha = \frac{k}{\rho c_p} \ (m^2 / s) \tag{4.10}$$

Where k is the thermal conductivity (W/(m·K)), ρ is the density (kg/m³) and c_p is the specific heat capacity (kJ/(kg·K)).

The thermal diffusivity evolution with the temperature for air, helium and hydrogen, at atmospheric pressure, is shown in Figure 4.12. Hydrogen has a lower dynamic viscosity when compared with the Helium. Helium is inert, has a thermal conductivity similar to the hydrogen but it has a volumetric thermal capacity even smaller than hydrogen, resulting in a better thermal diffusivity. Overall, hydrogen´s low viscosity and high thermal diffusivity make it the top compromise in terms of efficiency and specific power, mainly because the engine can run at higher speeds. Engine specific power is roughly proportional to the engine speed and mean pressure. However, due to its behaviour at high temperature, leaks through the solid metal of the heater may occur as well as metal embrittlement. These drawbacks are due to its high diffusion rate associated with this low molecular weight. As a consequence, engines using helium are more popular. The characteristic properties of the three working gases are presented at Table 4.1.
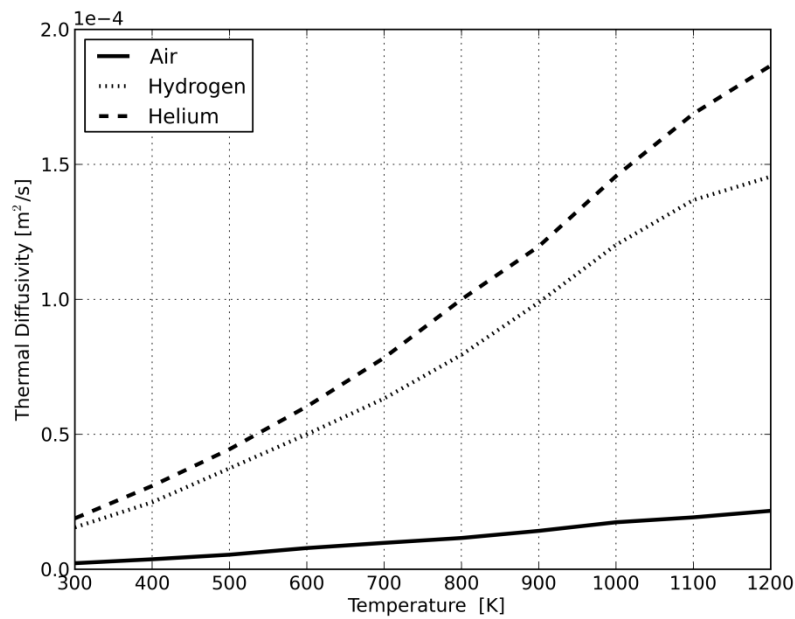
Figure 4.12 Thermal diffusivity as a function of temperature for three working fluids: air, helium and hydrogen.

Nitrogen can also be used as working gas, with minimum sealing and supply problems (lower costs) but leading to an engine with much lower specific power and efficiency (increased capital and operating costs). Furthermore, when air is used, the temperatures of internal components are limited due to the presence of oxygen which contributes to the degradation of materials, apart from safety issues and the reduction of engine efficiency.

Table 4.1 Properties of selected working fluid

Gas	Gas Constant, R (kJ/kgK)	Specific Heat, c_p (kJ/kgK)	Specific Heat Ration, γ
Hydrogen	4.122	14.20	1.41
Helium	2.079	5.19	1.67
Air	0.2870	1.004	1.4

It is well known that hydrogen and helium are the working fluids for which the performance of Stirling engines is better due to the fact that both have greater thermal diffusivity and lower dynamic viscosity than the air/nitrogen. Most technically advanced Stirling engines use helium as the working gas. Also, the cost, the safety during operation and the reliability cannot be neglected when choosing the working fluid.

4.5. Stirling Engine Analysis

4.5.1. Ideal Isothermal Analysis

The analysis of operation of Stirling cycle was first done by Gustav Schmidt of the German Polytechnic Institute of Prague published. In 1871, he published an analysis in which he obtained closed-form solutions of the equations for the special case of sinusoidal volume variations of the working spaces of a Stirling cycle. This analysis is still considered as a classic analysis and includes an isothermal compression, expansion and regeneration. Schmidt's analysis of Stirling engines includes several assumptions:

- All processes are reversible.
- The regeneration process is perfect.
- The working fluid is considered as an ideal gas, $PV=mRT$.
- The mass of the gas is constant.
- Steady state conditions are assumed and there are no flow or pressure losses
- Temperature is the same and constant in the heater and expansion space.
- Temperature is the same and constant in the cooler and compression space.

In the ideal isothermal analysis, the fact that the gas in the expansion space and the heater is at the constant upper source temperature and the gas in the compression space and the cooler is at the constant lower sink temperature, allows to deduce a simple expression for the working gas pressure as a function of the volume variations. The assumption of isothermal working spaces implies that all heat exchangers, heater, cooler and the regenerator are perfectly effective. The engine is considered as a set of five connected components (see Figure 4.13), consisting of a compression variable space *(c)*, a cooler *(k)*, regenerator *(r)*, heater *(h)* and an variable expansion space *(e)*. Each engine component represents an entity endowed with its respective volume *(V)*, temperature *(T)*, absolute pressure *(P)* and mass *(m)*.
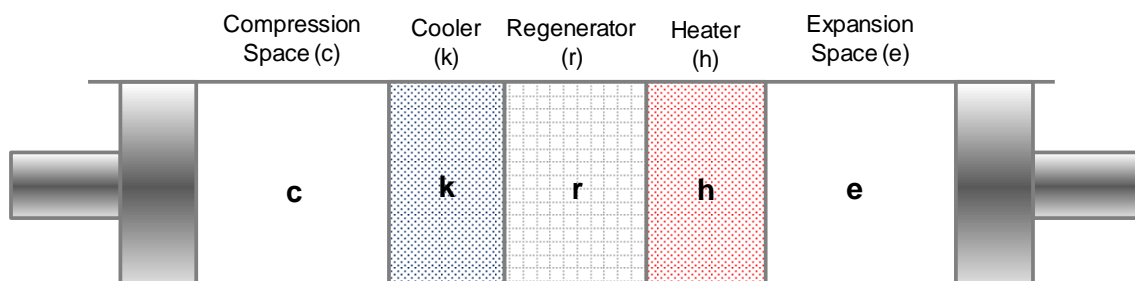
Figure 4.13 Simplified Stirling model configuration.

The temperature of the working fluid within the heat exchangers volumes V_k and V_h are, respectively, T_k and T_h and the temperature within the regenerator can be described by a linear function between T_k and T_h.

The total mass of the working gas in the engine is constant and can be taken as the sum of the gas contained in each component $m_{total} = \sum m_c + m_k + m_r + m_h + m_e$. If the mass expressions are calculated considering the ideal gas law, the mass of gas can be expressed as in equation (4.11).

$$m_{total} = \frac{P}{R}\left(\frac{V_c}{T_k} + \frac{V_k}{T_k} + \frac{V_r}{T_r} + \frac{V_h}{T_h} + \frac{V_e}{T_h}\right) \qquad (4.11)$$

where R is the gas constant, V_c and V_e are the compression and expansion volumes, respectively. As it is assumed that the temperature varies linearly (see Figure 4.14) between T_k and T_h, the mean effective temperature at the regenerator (T_r) is given by the equation (4.12).

$$Tr = \frac{T_h - T_k}{\ln\left(T_h / T_k\right)} \qquad (4.12)$$
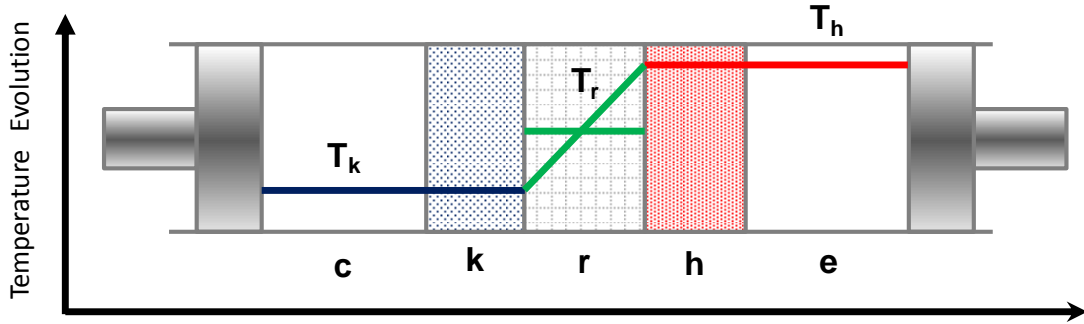
Figure 4.14 Schematic diagram of temperature distribution in the ideal isothermal analysis.

Thus, the pressure can be obtained as a function of the expansion and compression volumes, according to equation (4.13) as these are the only variables along the cycle.

$$P = \frac{m_{total}.R}{\dfrac{V_c}{T_k} + \dfrac{V_k}{T_k} + \dfrac{V_r \ln(T_h - T_k)}{T_h - T_k} + \dfrac{V_h}{T_h} + \dfrac{V_e}{T_h}} \qquad (4.13)$$

The volume evolutions of the compression and expansion spaces (V_c and V_e) are sinusoidal and can be given by equation (4.14) and equation (4.15), respectively:

$$V_c = V_{d,c} + V_{sw,c}\left(1 + \cos(\theta)\right)/2 \qquad (4.14)$$

$$V_e = V_{d,e} + V_{sw,e}\left(1 + \cos(\theta + \omega)\right)/2 \qquad (4.15)$$

where V_d and V_{sw} correspond to the dead and the swept volumes (respectively) for both compression and expansion spaces; θ represents the cycle crank angle, varying between 0 and 2π (point of maximum volume of compression cylinder), and ω is the advance phase angle of the expansion cylinder. So,

substituting equation (4.14) and equation (4.15) into equation (4.13), the pressure as a function of θ can be calculated as in equation (4.16).

$$P(\theta) = \frac{m_{total}.R}{\left(s + \left(\dfrac{V_{sw,e}\cos\omega}{2T_h} + \dfrac{V_{sw,c}}{2T_k} \right) \cdot \cos\theta - \left(\dfrac{V_{sw,e}\sin\omega}{2T_h} \right) \cdot \sin\theta \right)} \tag{4.16}$$

where s is defined by equation (4.17).

$$s = \frac{V_{sw,c}}{2T_k} + \frac{V_{d,c}}{T_k} + \frac{V_k}{T_k} + \frac{V_r\ln(T_h - T_k)}{T_h - T_k} + \frac{V_h}{T_h} + \frac{V_{d,e}}{T_h} + \frac{V_{sw,e}}{2T_h} \tag{4.17}$$

In order to simplify the pressure expression, trigonometric substitutions in a right-angled triangle were introduced as shown from equation (4.18) to (4.21), accordingly to the description in Figure 4.15.
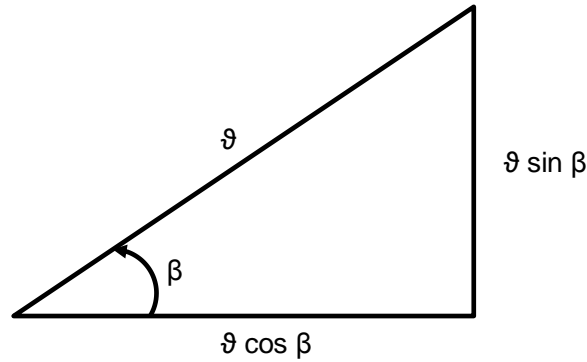
Figure 4.15 Schematics of trigonometric substitutions in the right-angled triangle for Schmidt analysis.

$$\vartheta\sin\beta = \frac{V_{sw,e}\cdot\sin\omega}{2T_h} \tag{4.18}$$

$$\vartheta\cos\beta = \frac{V_{sw,e}\cdot\cos\omega}{2T_h} + \frac{V_{sw,c}}{2T_k} \tag{4.19}$$

$$\beta = \tan^{-1}\left(\frac{\dfrac{V_{sw,e}\cdot\sin\omega}{T_h}}{\dfrac{V_{sw,e}\cdot\cos\omega}{T_h} + \dfrac{V_{sw,c}}{T_k}} \right) \tag{4.20}$$

$$\vartheta = \frac{1}{2}\left(\left(\frac{V_{sw,e}}{T_h} \right)^2 + 2\frac{V_{sw,e}}{T_h}\frac{V_{sw,c}}{T_k}\cdot\cos\omega + \left(\frac{V_{sw,c}}{T_k} \right)^2 \right)^{1/2} \tag{4.21}$$

Therefore, replacing the variables in the pressure expression results in a more compact equation (4.22).

$$P = \frac{m_{total}\cdot R}{s\cdot\left(1 + \dfrac{\vartheta}{s}\cdot\cos(\theta + \beta) \right)} \tag{4.22}$$

The total work done by the engine can be considered as the sum of the works done by the compression and expansion pistons over a complete cycle ($W = W_e + W_c$). The expansion and compression work can be defined as in equations (4.23) and (4.24), respectively:

$$W_e = \int_0^{2\pi} \left(P \frac{dV_e}{d\theta} \right) d\theta \qquad (4.23)$$

$$W_c = \int_0^{2\pi} \left(P \frac{dV_c}{d\theta} \right) d\theta \qquad (4.24)$$

After solving these integrals one can obtain, as presented by equation (4.25):

$$W = P_{mean} \cdot \pi \left(V_{sw,e} . \sin\left(\beta - \omega\right) \cdot \left(\sqrt{1-b^2} - 1 \right) / b + V_{sw,c} . \sin\beta \cdot \left(\sqrt{1-b^2} - 1 \right) / b \right) \qquad (4.25)$$

where $b = \vartheta / s$ and P_{mean}, the mean pressure along the cycle is given by equation

$$P_{mean} = \frac{m_{total} \cdot R}{\left(s \cdot \sqrt{1-b^2} \right)} \qquad (4.26)$$

Thus, for a certain engine geometry and mass of gas, the Schmidt analysis permits the calculation of the mean pressure and of W, the total useful work per cycle.

On evaluating the heat transfer over a complete cycle, it can be easily concluded that $W_e = Q_e$ and $W_c = Q_c$. For the ideal regenerator, $Q_r = 0$ because it is considered that all the heat exchange between the regenerator matrix and the working gas is internal. The thermal efficiency of the isothermal Stirling cycle will then be the total work divided by the heat transferred to the expansion space and despite the absence of isochoric evolutions, it os possible to demonstrate that is equal to the Carnot efficiency. The Schmidt analysis for Beta and Gama configuration is also presented in Annex I.

Obviously, the isothermal analysis leads to an analysis where neither the heater nor the cooler contributed to any net heat transfer over the cycle. The ideal cycle only considers that all the heat transfer occurred across the boundaries of the isothermal working spaces. Nevertheless, in real engines the working spaces will approach the adiabatic condition which implies that the net heat transferred over the cycle must be provided by the heat exchangers.

4.5.2. Ideal Adiabatic Analysis

In opposition to the isothermal analysis, the compression and expansion spaces are considered adiabatic and, thus, their temperatures (T_c and T_e) are not constant, varying over the compression and expansion phases, as shown by the temperature distribution diagram of Figure 4.16.
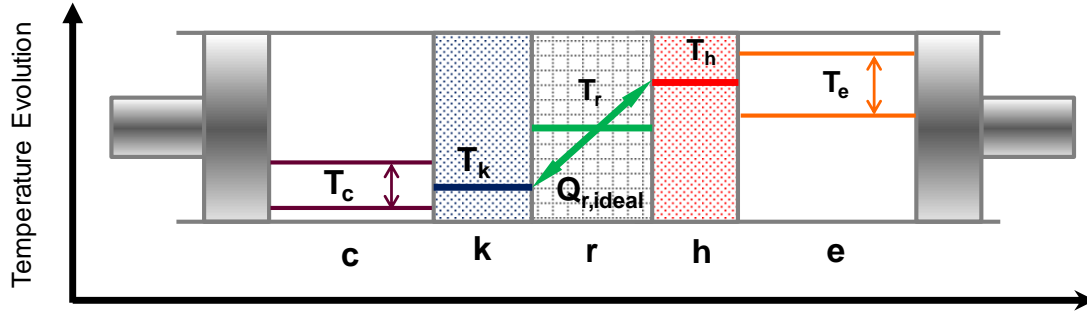
Figure 4.16 Schematic diagram of temperature distribution in the ideal adiabatic analysis.

In this analysis, the model is treated as a "quasi steady-flow" system. A set of ordinary differential equations is iteratively solved, considering an initial-value problem in which the initial values of all the variables are arbitrated and the equations are integrated from that initial state over a complete cycle. The final state of the cycle is then used as a new initial-value for a new cycle and several iterations are made until cycle convergence is obtained. The resulting equations are linked by applying the mass and energy equations across five components (c,k,r,h and e) that form the entire system. Enthalpy is transported by means of mass flow and temperature entering and/or exiting at each component. There is no gas leakage, the total mass of gas in the system is constant ($m_{total} = \sum m_c + m_k + m_r + m_h + m_e$) and there is no pressure drop. Work is done by varying the volumes of the working spaces V_c and V_e, and heat (Q_k and Q_h) is only transferred between the external environment and the working gas in the cooler (k) and heater (h), respectively. Also, $Q_{r,ideal}$ is the reversely heat transferred between the regenerator matrix and the working gas.

Each component of the Stirling engine is considered as a single cell (i.e. thermodynamic equilibrium with uniform properties) where a working fluid mass flow suffers compression and expansion. A generalized cell of working spaces is presented in Figure 4.17.
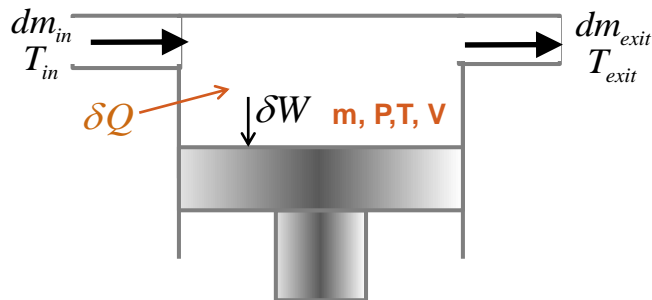
Figure 4.17 Representation of a generalized cell engine for a differential cycle movement, $d\theta$.

The energy equation for the working gas in a generalized cell becomes as in equation (4.27):

$$\delta Q + (c_p T_{in} dm_{in} - c_p T_{exit} dm_{exit}) = \delta W + c_v d(mT) \qquad (4.27)$$

where c_p and c_v are the specific heat capacities of the gas at constant pressure and constant volume, respectively, δQ is the thermal energy transferred into a cell of the working space and δW is the mechanical work done on the environment (positive when expanding). The adiabatic analysis also assume a linear temperature profile in the regenerator, being the effective temperature, T_r, equal to the log mean temperature of T_h and T_k. For this analysis, it is reasonable to assume the ideal gas law ($PV = mRT$) as equation of state. So, deriving the mass equation ($dm_c + dm_k + dm_r + dm_h + dm_e = 0$), the mass equation for the three heat exchangers can be calculated as in equation (4.28) since the respective temperatures and volumes are constant. The derivative operator is denoted by d, thus for example dm corresponds to the mass derivative $dm/d\theta$, where is θ is the cycle angle (engine crankshaft angle).

$$\frac{dm}{m} = \frac{dP}{P} \Leftrightarrow dm = \frac{dP}{P} m \Leftrightarrow dm = \frac{dP \cdot V}{RT} \qquad (4.28)$$

Regarding the compression and the expansion spaces, both are adiabatic, meaning that $dQ_c = dQ_e = 0$ and the work done is $dW = pdV$ for both spaces. Therefore, the mass equation for the compression can be reduced to the form presented by equation (4.29), always considering the ideal gas law and relationships.

$$dm_c = \frac{PdV_c + \dfrac{V_c dP}{\gamma}}{RT_{c/k}} \qquad (4.29)$$

where γ is heat capacity ratio of the working fluid. A similar expression can be achieved for the expansion space, equation (4.30).

$$dm_e = \frac{PdV_e + \dfrac{V_e dP}{\gamma}}{RT_{h/e}} \qquad (4.30)$$

From the differential equation of state, it is possible to obtain dT_c and dT_e as presented by equation (4.31) and equation (4.32).

$$dT_c = T_c \left(\frac{dP}{P} + \frac{dV_c}{V_c} + \frac{dm_c}{m_c} \right) \qquad (4.31)$$

$$dT_e = T_e \left(\frac{dP}{P} + \frac{dV_e}{V_e} + \frac{dm_e}{m_e} \right) \qquad (4.32)$$

Applying the energy equation to the heat exchangers and substituting for the equation of state, the energy transferred at each heat exchanger can be calculated, considering the temperature and mass flow at the boundary between the compression space and the cooler ($T_{c/k}$), the boundary temperature between the cooler and the regenerator ($T_{k/r}$ and $dm_{c/k}$), the temperature and the mass flow at the boundary between the regenerator and the heater ($T_{r/h}$ and $dm_{r/h}$) and the temperature and mass flow at the boundary

between the heater and the expansion space ($T_{h/e}$ and $dm_{h/e}$). The energies transferred in the cooler, regenerator and heater are calculated by equations (4.33), (4.34) and (4.35), respectively. Figure 4.18 represents the heat transfer process between the compression space and the cooler.
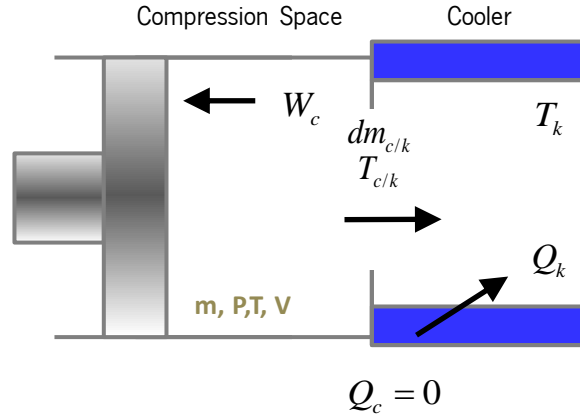
Figure 4.18 Representation of heat transfer between the compression space and cooler.

Thus the enthalpies flowing across the interfaces/boundaries depend on the respective adjacent upstream cell temperatures and mass flows.

$$dQ_k = \frac{V_k \cdot dP \cdot c_v}{R} - c_p \left(T_{c/k} \cdot m_{c/k} - T_{k/r} \cdot m_{k/r} \right) \tag{4.33}$$

$$dQ_r = \frac{V_r \cdot dP \cdot c_v}{R} - c_p \left(T_{k/r} \cdot m_{k/r} - T_{r/h} \cdot m_{r/h} \right) \tag{4.34}$$

$$dQ_h = \frac{V_h \cdot dP \cdot c_v}{R} - c_p \left(T_{r/h} \cdot m_{r/h} - T_{h/e} \cdot m_{h/e} \right) \tag{4.35}$$

The total work corresponds to the sum of the work done in the compression and expansion spaces given, respectively, by equation (4.36) and equation (4.37).

$$dW_c = PdV_c \tag{4.36}$$

$$dW_e = PdV_e \tag{4.37}$$

The independent differential equations here presented are solved simultaneously for the seven unknown variables: $T_c, T_e, Q_k, Q_r, Q_h, W_c, W_e$. The objective is to find the unknown function $Y(\theta)$ which satisfies both the differential equations and the initial conditions. The system of equations is solved numerically using the classical fourth-order Runge–Kutta method, cycle after cycle until convergence conditions are reached. The vector Y denotes the seven unknown functions and the corresponding set of differential equations is expressed as in equation (4.38).

$$\frac{dY}{d\theta} = F(\theta, Y) \tag{4.38}$$

A numerical solution to this problem is accomplished by computing the values of the derivatives at θ_i ₀ and proceeding in small increments of θ to a new point $\theta_{i+1} = \theta_i + \Delta\theta$. Therefore, there are 22 variables and 7 derivatives in the equation set, to be solved over a complete cycle.

4.5.3. Non-Ideal Analysis

The so called Non-Ideal analysis corresponds to a third modelling approach, where non-perfect heat transfer and flow-friction effects are taken in the engine performance evolution. This corresponds to a more realistic analysis, which permits a parametric sensitivity analysis as required for the design optimization of this kind of systems. Heat is transferred from the external heat source to the working gas in the heater, cyclically stored and recovered in the regenerator, and then rejected by the working gas in the cooler. In the non-ideal analysis, the regenerator heat capacity is diminished, and leads to an increase in both the hot source and cold sink heats. Also, the fluid friction associated with the flow through the heat exchangers result in a pressure drop. This pressure drop (also referred as "pumping losses") corresponds to the work required to move the working gas through the heat exchangers, thus reducing the net power output of the engine.

Evaluating the heat transfer in the regenerator, cooler and heater

The non-ideal effects of the regeneration are mainly due to the convective thermal resistance between the gas and the regenerator surface, and can be modeled by using the Number of Transfer Units (NTU). NTU value is defined as a function of the heat exchanger size. This includes the actual contact area ($A_{w,i}$), as well as the actual mass flow of gas being transferred. The NTU method is used to calculate the rate of heat transfer in heat exchangers, as presented by equation (4.39):

$$NTU = \frac{h.A_{w,i}}{\dot{m}.c_p} \tag{4.39}$$

where h is the convective heat transfer coefficient. The heat transfer coefficient can be calculated by relating the heat transfer to fluid friction by using standard non-dimensional parameters. The Prandtl number, Pr, is a property of the of the fluid and the Reynolds number, Re, is a property of flow. For the range of working gases used in Stirling engines, in the range between 300 and 1000 K, the Prandtl number is approximately constant, at around a value of 0.7. The Nusselt number relates the heat transfer coefficient, the length of the heater pipe and the thermal conductivity of the working fluid, k. Considering the heat transfer in a pipe, the Nusselt number is written as in equation (4.40):

$$Nu = \frac{h \cdot D}{k} \tag{4.40}$$

The correlations between Nusselt, Reynolds and Prandtl numbers were taken as in equation (4.41):

$$Nu = f(\mathrm{Pr}, \mathrm{Re}) \tag{4.41}$$

In the analysis of a heat exchanger, the NTU is assessed in terms of fluid properties. NTU is defined in terms of a Stanton number (St) as presented in equation (4.42).

$$NTU = \mathrm{St} \cdot \left(\frac{A_w}{A} \right) \cdot \frac{1}{2} \tag{4.42}$$

where A_w refers to the effective or "wetted" heat transfer area of the heat exchanger and A is the free flow area through the matrix. The factor 2 is due to the fact that St is defined for heat transfer from a gas stream to a wall, whereas in the cyclic process of the regenerator, heat is also transferred from the matrix to the gas flow. Stanton number for heat transfer, St, is a dimensionless parameter relating heat transfer coefficient to heat capacity of the fluid stream per unit cross-sectional area per unit time as in equation (4.43):

$$\mathrm{St} = \frac{h}{\rho u c_p} = \frac{A}{A_w} \left(\frac{T_{exit} - T_{in}}{T_{wall} - T} \right) \tag{4.43}$$

where h is the convective heat transfer coefficient, ρ is the gas density, u is the velocity and c_p is the specific heat capacity of the gas.

In the "loading" process, the hot working gas is pre-cooled, while flowing through the regenerator from the heater to the cooler, transferring heat to the regenerator matrix. Then, in the reverse process, the heat that was previously stored in the matrix is "discharged" and pre-heats the cold gas that flows into the heater and expansion space.

The regenerator effectiveness can be defined as the ratio between the real amount of heat exchanged between the matrix and the working fluid and the maximum amount of heat transferred in the regenerator of the adiabatic model (Ferreira, 2010). The analysis of the effectiveness of the regenerator is made by the temperatures of the fluid, see Figure 4.19.
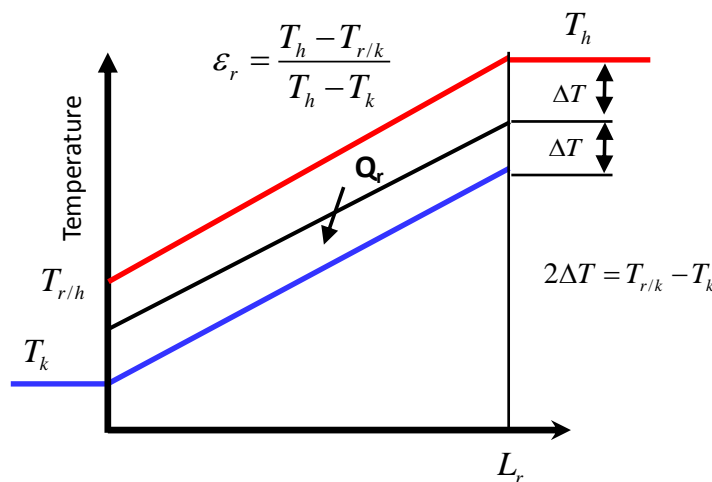
Figure 4.19 Temperature profile of the working fluid across regenerator.

Accordingly, the regenerator effectiveness can be calculated as presented by equation (4.44).

$$\varepsilon_r = \frac{1}{1 + \dfrac{2\Delta T}{T_h - T_{r/k}}}$$

(4.44)

By the NTU method, the regenerator effectiveness can be obtained by equation (4.45).

$$\varepsilon_r = \frac{NTU}{1 + NTU}$$

(4.45)

Thus, the regenerator heat-transfer reduction, defined as Q_{rloss}, can be calculated as a function of the regenerator effectiveness and the amount of heat transferred by the ideal adiabatic regenerator, $Q_{r,ideal}$, as in equation (4.46).

$$\dot{Q}_{rloss} = (1 - \varepsilon_r) \cdot \dot{Q}_{r,ideal}$$

(4.46)

The effectiveness of the heater and cooler can also be evaluated by means of NTU. The heat exchanger effectiveness for both exchangers can be defined according to equation (4.47), valid if the heat transfer limitations are on the gas side.

$$\varepsilon = 1 - e^{-NTU}$$

(4.47)

The mean effective temperatures in heater (T_h) and cooler (T_k) are, respectively, lower and higher than the corresponding heat exchanger wall temperatures: heater ($T_{wall,h}$) and cooler ($T_{wall,k}$) walls, as shown in Figure 4.20.
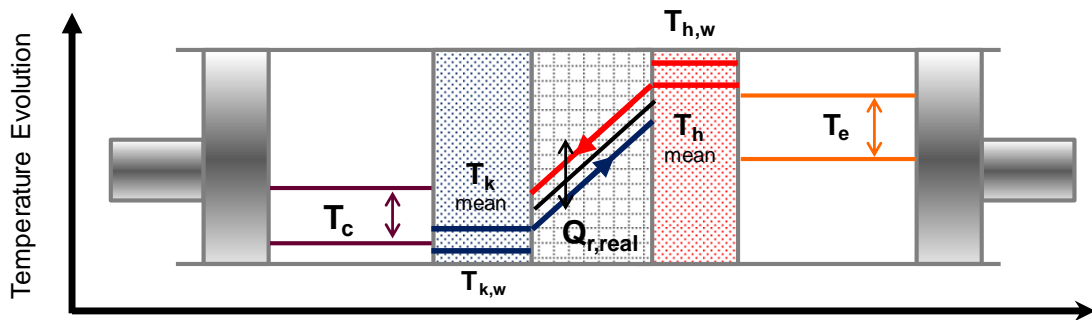
Figure 4.20 Schematic diagram of temperature distribution for the non-ideal analysis.

This implies that the engine is operating between narrower temperature limits than originally specified which effectively reduces the thermodynamic engine efficiency. Thus, the relationship between the total heat transfer and the mean gas/wall temperature difference can be calculated by the basic equation for convective heat transfer, equation (4.48).

$$\dot{Q} = h \cdot A_w \left(T_{wall} - T \right)$$

(4.48)

where T_{wall} is the wall temperature, and T the mean effective gas temperature (heater or cooler). In fact, the temperatures, T_h and T_k, are determined iteratively after the evaluation of Q_h and $Q_{k\,in}$ each accordingly

to the equation (4.49) and the equation (4.50), respectively. The less heat transfer in the regenerator leads to increases in the heats of the hot and cold sources so that, the actual heat for both heat exchangers is determined.

$$\dot{Q}_h = \dot{Q}_{h,ideal} + \dot{Q}_{rloss} \tag{4.49}$$

$$\dot{Q}_k = \dot{Q}_{k,Ideal} + \dot{Q}_{rloss} \tag{4.50}$$

The mass flow rates through the heater and cooler are used to determine the Reynolds number and thus the heat transfer coefficients. Thus, it is possible to evaluate the heater and cooler gas temperatures, according to equations (4.51) and (4.52).

$$T_h = T_{wall,h} - (Q_{h,ideal} + Q_{rloss})\left(\frac{1}{h_{inner,h} \cdot A_{w,h}}\right) \tag{4.51}$$

where $h_{inner,h}$ is the heat transfer coefficient from the gas side because the model only considers the convective heat transfer from inner wall of the heater tubes to the working gas and assumes a constant temperature at the outer surface.

T_k is evaluated by calculating the overall heat transfer coefficient, which includes the convective heat transfer from the cooler tubes to the working fluid, the conductive process through the cooler tubes wall and the convective heat transfer to the coolant (an external mass flow of water). The calculation of the latter is explained in section 4.6.3.

$$T_k = \bar{T}_{water} + (Q_{k,ideal} + Q_{rloss})\left(\frac{1}{h_{inner,k} \cdot A_{w,k}} + \frac{\ln\left(d_{out,k}/d_{inner,k}\right)}{2\pi L_k nt_k k} + \frac{1}{h_{out,k} \cdot A_{water,k}}\right) \tag{4.52}$$

$\bar{T}_{water}$ is the mean temperature of the external water, $d_{out,k}$ is the outer diameter of the cooler tubes, L_k is the length and n_t the number of the cooler tubes; k is the thermal conductivity of the tubes, which was assumed to be equal to 54 W/(mK) (carbon steel) and $A_{water,k}$ corresponds to water flow area at the external side of the heat exchanger.

Evaluating the pumping losses

Fluid friction associated with the flow through the heat exchangers, results in a pressure drop, thus reducing the output power of the engine. At each instant in time (and corresponding cycle angle θ), the pressure drop (ΔP) is taken over the three heat exchangers and then, the value of the corresponding work can be achieved by integration over the complete cycle. The total engine work per cycle, W is given by equation (4.53).

$$W = \int_0^{2\pi} P\left(dV_e + dV_c\right) - \Delta W \tag{4.53}$$

where V_e and V_c are, respectively, the expansion and compression volumes. The first term in the equation represents the ideal adiabatic work done per cycle and the second one represents the pressure drop per cycle. The pressure drop converted to work loss, ΔW, can be calculated by equation (4.54).

$$\Delta W = \int_0^{2\pi} \delta W \cdot d\theta \quad \Leftrightarrow \quad \Delta W = \int_0^{2\pi} \left(\sum_{i=1}^{3} \Delta P_i \frac{dV_e}{d\theta} \right) \cdot d\theta \tag{4.54}$$

where θ is the crank angle. The pressure drop is evaluated by equation (4.55).

$$\Delta P = \frac{-2C_f \cdot \text{Re} \cdot \mu \cdot u \cdot V}{d^2 A} \tag{4.55}$$

where C_f is the friction coefficient, Re is the Reynolds number, μ and u are the gas viscosity and velocity, d is the hydraulic diameter of the small parallel passages and V the void volume. The friction coefficient is the non-dimensional wall shear-stress, defined according to equation (4.56).

$$C_f = \frac{\tau}{0.5 \rho u^2} \tag{4.56}$$

where τ, is the wall shear stress, ρ is the working fluid density and u is velocity. Dimension analysis proves that C_f is a function of Re and the relative roughness of the pipe surface and can be obtained from the Moody diagram. In the case of smooth pipes C_f can be calculated by using the Blasius equations. The Reynolds number represents the ratio of the inertia to viscous forces. The Reynolds number (equation (4.57)) is calculated because the friction factor and the heat transfer coefficient are strongly dependent on the flow regime.

$$\text{Re} = \frac{\rho \cdot u \cdot d}{\mu} \tag{4.57}$$

The dynamic viscosity is a fluid property that influences the internal friction of the fluid. It is independent of pressure but varies with the temperature. Thus, it is important to account the effect of gas temperature changes in the dynamic viscosity.. The Sutherland law defines the dynamic viscosity as a function of temperature (see equation (4.58).

$$\mu = \mu_0 \left(\frac{T_0 + C_{su}}{T + C_{su}} \right) \cdot \sqrt{\left(\frac{T}{T_0} \right)^3} \tag{4.58}$$

where μ_0 is the viscosity value at the reference temperature, T_0 is the reference temperature (assuming the value of 273.15 K) and C_{su} is the Sutherland constant for each working gas.

The algorithm of the non-ideal analysis can be better understood considering the diagram of Figure 4.21, which explains the sequence of the calculus. The solution algorithm requires iterative invoking of the Ideal Adiabatic analysis, each time with new T_h and T_k values, until convergence is attained. After each

simulation run, values of Q_h and Q_k are available and Q_{loss} is determined in terms of the regenerator effectiveness.
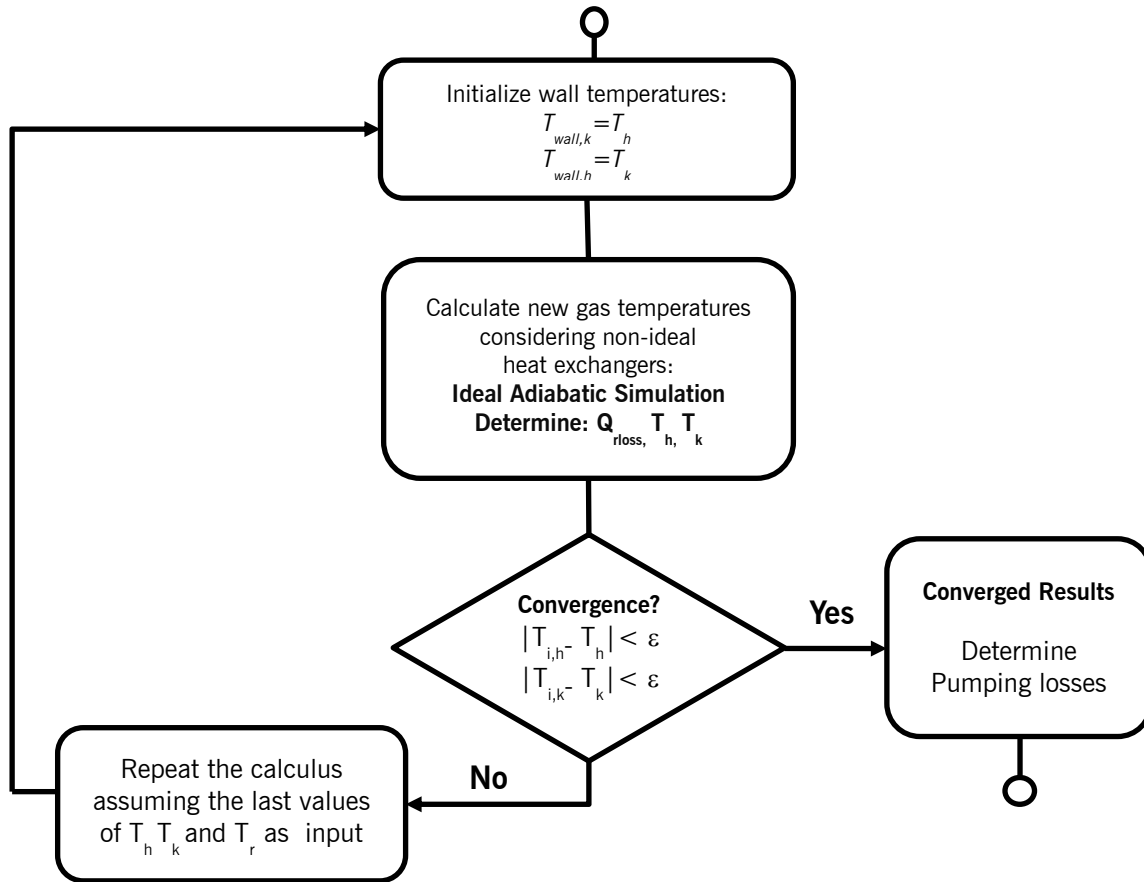
Figure 4.21 Flow diagram of the non-ideal algorithm.

4.6. Heat Exchangers Configuration

In the literature, several configurations are mentioned for the Stirling heat exchangers (Sanz & Fayad, 2008; Scollo, Valdez, & Baron, 2008; Tlili et al., 2008; Zarinchang & Yarmahmoudi, 2008). The most common configurations of heater and cooler are smooth tubes and finned or slotted tubes. Regenerators are usually tubular or annular and, depending on the application, regenerators could have a fine wired mesh or a foil.

The use of a given configuration depends on design requirements, material constraints and, the most important, on improvement of the heat transfer rate. The heat transfer depends on the heat transfer coefficient and the heat transfer area.

4.6.1. Heater: bank of smooth tubes

In this study, solar energy will be considered as the hot source with heat transfer occurring by the incidence of the concentrated radiation on the heat exchanger walls. In this case there is no convection

from the outside and the wall temperature can be considered constant. Thus, agood option for the heater will be a bank of parallel thin tubes. This choice results from the need for a large contact area together with the capacity for a large mass flow of working gas.

In order to calculate the effective heat transfer, it is important to calculate the inside contact wetted area of the heater ($A_{w,h}$) which can be defined by equation (4.59).

$$A_{w,h} = \pi d_{inner,h} nt_h L_h \tag{4.59}$$

where $d_{inner,h}$ is the inner diameter of the heater tubes, nt_h the number of the heater tubes L_h correspond to their length.

4.6.2. Tubular Regenerator

As previously mentioned, the regenerator is a special heat exchanger used in Stirling engines to improve its efficiency. Heat is transferred from the regenerator to the working fluid and it is therefore pre-heated when moving from the compression to the expansion space. At the end of the expansion process the flow is reversed and working fluid is pre-cooled with the heat transferred and stored in the regenerator. Preliminary studies demonstrated that, in a Stirling engine the regenerator can achieve effectiveness's of up to 98 %, which indicates that the working fluid will leave the regenerator close to the temperature of the space it is occupying (A. C. Ferreira, Oliveira, Nunes, Martins, & Teixeira, 2014). The large improvement in engine efficiency by using a regenerator far balances the minor reduction in specific power. In the present work, the choice was a tubular regenerator with a fine-wire mesh matrix, as represented by Figure 4.22.
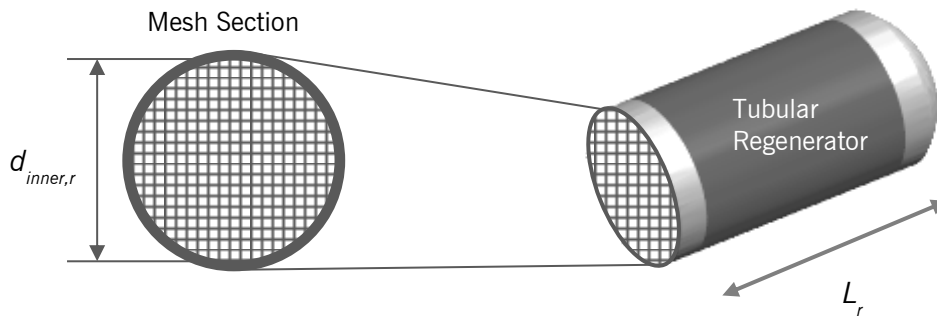
Figure 4.22 Ilustration of geometrical parameters of the regenerator.

The free section regenerator matrix area ($A_{r,matrix}$) is defined as in equation (4.60).

$$A_{matrix,r} = \frac{\pi \cdot d_{inner,r}^2}{4} \tag{4.60}$$

Considering the assumed configuration, the regenerator wetted area ($A_{w,r}$) can be calculated from the ratio of regenerator void volume (V_r) to the hydraulic diameter ($d_{hydraulic,r}$) and adding the tubular wall area ($A_{w0,r}$) as in equation (4.61):

$$A_{w,r} = \frac{4V_r}{d_{hydraulic,r}} + A_{w0,r} \tag{4.61}$$

where the $d_{hydraulic,r}$ accounts for the mesh porosity. Thus, the regenerator wetted area can be calculated according to equation (4.62).

$$A_{w,r} = 4 \cdot \frac{A_{matrix,r}\Phi_{matrix} \cdot L_r}{\left(\dfrac{d_{wire} \cdot \Phi_{matrix}}{1-\Phi_{matrix}}\right)} + \left(\pi \cdot d_{inner,r} \cdot L_r\right) \tag{4.62}$$

4.6.3. Cooler: bank of smooth tubes

The cooler was also considered as a bank of parallel smooth tubes. In order to calculate the effective heat transfer at the cooler one must consider the inner heat transfer from the working fluid and the external heat transfer to the coolant. The contact wetted area of determined by equation (4.63).

$$A_{w,k} = \pi d_{inner,k} nt_k L_k \tag{4.63}$$

Tube banks are commonly-employed design elements in heat exchangers. Tube bundles are a sub-component in shell-and-tube heat exchangers, where the flow resembles cross flow (outside) and longitudinal flow (inside). Figure 4.23 shows the two basic tube-bank patterns. These are referred to as in-line tube banks and misaligned tube banks, respectively. They are characterized by crosswise pitch-to-diameter ratios, S_T/d_{out} and S_L/d_{out}, where d_{out} is the external diameter of the tubes, and S_T and S_L the space between the tubes.
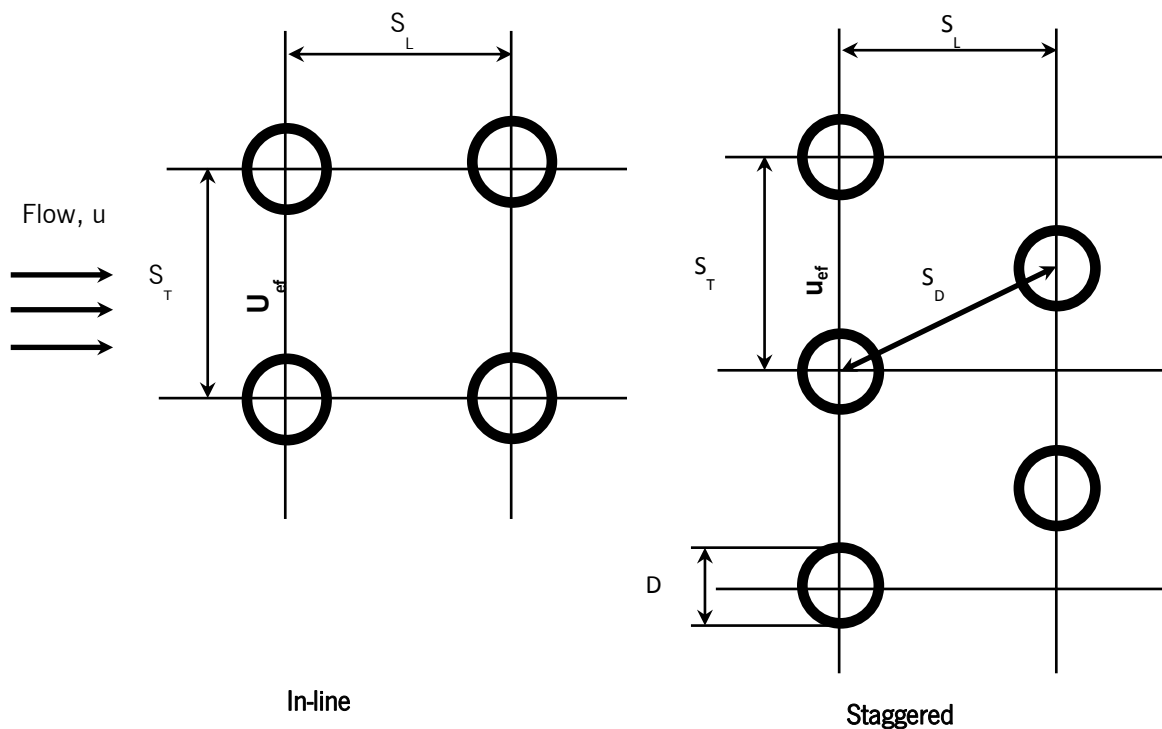
Figure 4.23 Schematic of an in-line and a staggered tube bank illustrating nomenclature.

By defining the ratio between the space of heat exchanger tubes and their external diameter, it is possible to calculate the maximum velocity accordingly to the correlations presented by equation (4.64) if the tubes are aligned or by equation (4.65) in case of a staggered tube bank.

$$u_{ef} = u \frac{S_T}{S_T - d_{out}} \tag{4.64}$$

$$u_{ef} = u \frac{S_T}{2(S_D - d_{out})} \quad if \ S_D < \frac{S_T + d_{out}}{2} \tag{4.65}$$

In this study the $d_{out,k}$ is assumed as a function of the cooler tube internal diameter, with an assumed tube thickness of 1 mm and the cooler shell width. For calculations, it was assumed that S_T/d_{out}=2 and S_L/ d_{out} =2. This means that the tubes alignment will be dependent of the value of the internal diameter on the cooler tubes. Then, the correspondent Reynolds number is calculated and the water heat transfer coefficient ($h_{out,k}$) can be determined through the Nusselt number, given by the equation (4.66).

$$\overline{Nu} = 1.13 c_1 \ \text{Re}_{d_{out},max}^m \ \text{Pr}^{1/3} \tag{4.66}$$

The water flow area at the external side of the heat exchanger ($A_{water,k}$) is calculated by equation

$$A_{water,k} = \pi d_{out,k} nt_k L_k \tag{4.67}$$

Regarding the description of the physical model, this project is focused on the optimization of a system for cogeneration applications based on an alpha Stirling engine (see Figure 4.24) as prime mover, able to produce 1-5 kW of electricity and a larger heat load suitable to supply the residential energy needs.
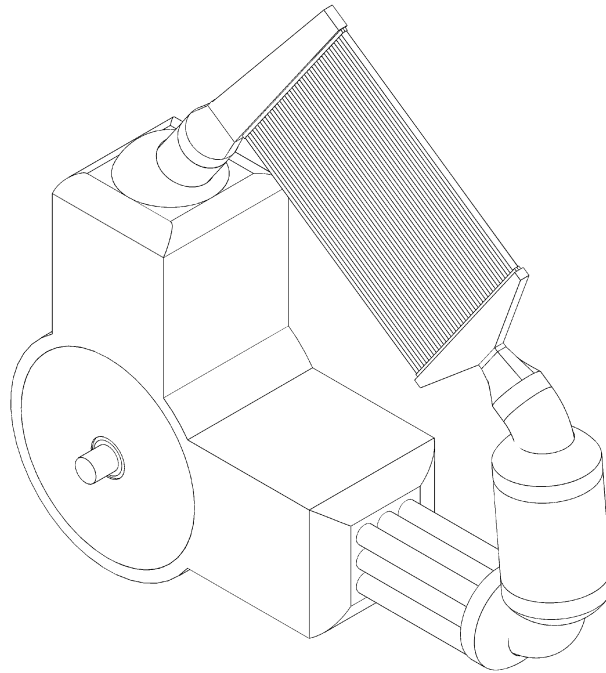
Figure 4.24 Representation of an alpha Stirling Engine.

Stirling engine works between two temperatures T_h and T_c (hot and cold sink, respectively). The value for the hot temperature was assumed considering that the energy source is concentred solar radiation. The cold sink of the engine is refrigerated by a mass flow of water which removes heat from the cooler to produce hot water. It was assumed that the mass flow of water is heated from 288 K to 343 K.

Asnaghi, A., Ladjevardi, S. M., Saleh Izadkhast, P., & Kashani, a. H. (2012). Thermodynamics Performance Analysis of Solar Stirling Engines. *ISRN Renewable Energy*, *2012*, 1–14. doi:10.5402/2012/321923

Boucher, J., Lanzetta, F., & Nika, P. (2007). Optimization of a dual free piston Stirling engine. *Applied Thermal Engineering*, *27*(4), 802–811. doi:10.1016/j.applthermaleng.2006.10.021

Cheng, C.-H., & Yang, H.-S. (2012). Optimization of geometrical parameters for Stirling engines based on theoretical analysis. *Applied Energy*, *92*, 395–405. doi:10.1016/j.apenergy.2011.11.046

Ercan Ataer, Ö., & Karabulut, H. (2005). Thermodynamic analysis of the V-type Stirling-cycle refrigerator. *International Journal of Refrigeration*, *28*(2), 183–189. doi:10.1016/j.ijrefrig.2004.06.004

Ferreira, A. C. M., Costa, J. M., Nunes, M. L., Teixeira, S. F. C. F., Teixeira, J. C. F., & Martins, L. a. S. B. (2013). Tecno-Economical issues in the design of a heat-regenerator for Stirling engines. In *2º Encontro Nacional de Engenharia e Gestão Industrial* (Vol. 45, pp. 1–2). Aveiro.

Ferreira, A. C., Oliveira, R. F., Nunes, M. L., Martins, L. B., & Teixeira, S. F. (2014). Modelling and Cost Estimation of Stirling Engine for CHP Applications. In EUROPMENT (Ed.), *International Conference on Mechanics, Fluid Mechanics, Heat and Mass Transfer* (pp. 1–9). Interlaken, Switzerland: Europment.

Ferreira, C. (2010). *Ante-Projecto de um Motor Stirling*. Master Thesis in Mechanical Engineering, Guimarães, University of Minho.

Formosa, F. (2011). Coupled thermodynamic–dynamic semi-analytical model of free piston Stirling engines. *Energy Conversion and Management*, *52*(5), 2098–2109. doi:10.1016/j.enconman.2010.12.014

He, M., Sanders, S., & Berkeley, C. (n.d.). *Design of a 2.5 kW Low Temperature Stirling Engine for Distributed Solar Thermal Generation* (pp. 1–8). California, EUA.

Jiří, Š. (2009). Stirling engine: Regenerator of Stirling engine. Retrieved February 27, 2014, from http://www.transformacni-technologie.cz/en_stirlinguv-motor.html

Keveney, M. (2009). Animated Engines. *Two Cylinder Stirling Engine*. Retrieved March 21, 2011, from http://www.animatedengines.com/

Knowles, T. R. (1997). *Composite Matrix Regenerator for Stifling Engines*. San Diego, California, USA.

Kongtragool, B., & Wongwises, S. (2006). Thermodynamic analysis of a Stirling engine including dead volumes of hot space, cold space and regenerator. *Renewable Energy*, *31*(3), 345–359. doi:10.1016/j.renene.2005.03.012

Onovwiona, H. I., & Ugursal, V. I. (2006). Residential cogeneration systems: review of the current technology. *Renewable and Sustainable Energy Reviews*, *10*(5), 389–431. doi:10.1016/j.rser.2004.07.005

Puech, P., & Tishkova, V. (2011). Thermodynamic analysis of a Stirling engine including regenerator dead volume. *Renewable Energy*, *36*(2), 872–878. doi:10.1016/j.renene.2010.07.013

Sanz, J., & Fayad, Z. a. (2008). Imaging of atherosclerotic cardiovascular disease. *Nature*, *451*(7181), 953–7. doi:10.1038/nature06803

Scollo, L., Valdez, P., & Baron, J. (2008). Design and construction of a Stirling engine prototype. *International Journal of Hydrogen Energy*, *33*(13), 3506–3510. doi:10.1016/j.ijhydene.2007.12.069

Thombare, D. G., & Verma, S. K. (2008). Technological development in the Stirling cycle engines. *Renewable and Sustainable Energy Reviews*, *12*(1), 1–38. doi:10.1016/j.rser.2006.07.001

Timoumi, Y., Tlili, I., & Ben Nasrallah, S. (2008a). Design and performance optimization of GPU-3 Stirling engines. *Energy*, *33*(7), 1100–1114. doi:10.1016/j.energy.2008.02.005

Timoumi, Y., Tlili, I., & Ben Nasrallah, S. (2008b). Performance optimization of Stirling engines. *Renewable Energy*, *33*(9), 2134–2144. doi:10.1016/j.renene.2007.12.012

Tlili, I., Timoumi, Y., & Nasrallah, S. Ben. (2008). Analysis and design consideration of mean temperature differential Stirling engine for solar application. *Renewable Energy*, *33*(8), 1911–1921. doi:10.1016/j.renene.2007.09.024

Zarinchang, J., & Yarmahmoudi, A. (2008). Optimization of Stirling Engine Heat Exchangers. In WSEAS (Ed.), *World Scientific and Engineering Academy and Society (WSEAS)* (pp. 143–150). Santander, Cantabria.

Zarinchang, J., & Yarmahmoudi, A. (2009). Optimization of Thermal Components in a Stirling Engine. In *WSEAS Transactions on Heat and Mass Transfer* (Vol. 4, pp. 1–10).

5

Development of the Thermal-economic Optimization Model

5.1   Formulation of the Conceptual Model

5.2   Thermal-economic Optimization Model Definition

5.3   Numerical Solution

In this chapter, the thermal-economic formulation is presented, which is based on the definition of a non-linear objective function, subject to physical constraints. The methodology for developing the purchase cost equations are presented and discussed. Also, the decision variables and the optimization constraints are presented and their choice is discussed. Finally, the numerical solution is discussed and presented.

5.1 Formulation of the Conceptual Model

The development of a mathematical model for cogeneration systems evaluation aims the design of an effective way to globally analyse a thermal system from the techno-economical point of view. The development of thermal systems models involves different steps that depend on technical and economic constraints. A cogeneration system sizing depends on the energy requirements. This means that the system components have to be chosen according to the thermal and power demands of the consumer (Pehnt, 2008). The identification of end user consumption necessities has a great importance in the definition of technical characteristics of the cogeneration unit. The definition of energy consumption profiles is determinant in finding out the appropriate relationship between the power production and its consumption. So, for small-scale applications, it is important to define if the system is to satisfy the energy needs of a single and/or multi-family residence; a commercial or an administrative building.

The evaluation of the energy consumptions is very important to minimize electricity demand from the network grid and maximize the efficiency of the cogeneration unit. The main idea in the process is the

design of a system that satisfies the energy requirements by a flexible adaptation to user consumption, also taking into account the tariffs of electrical power (Moreira, Monteiro, & Ferreira, 2007). It is also important to define the type of fuel and the tariff applied. This characteristic is significant in the operational costs of the system. In fact, the variation of fuel and electricity prices may have an important impact in the cash flows from the CHP system operation (Ana C.M. Ferreira et al., 2012). The main steps in the process of a modelling a thermal system for small-scale cogeneration applications are schematically describes in Figure 5.1.
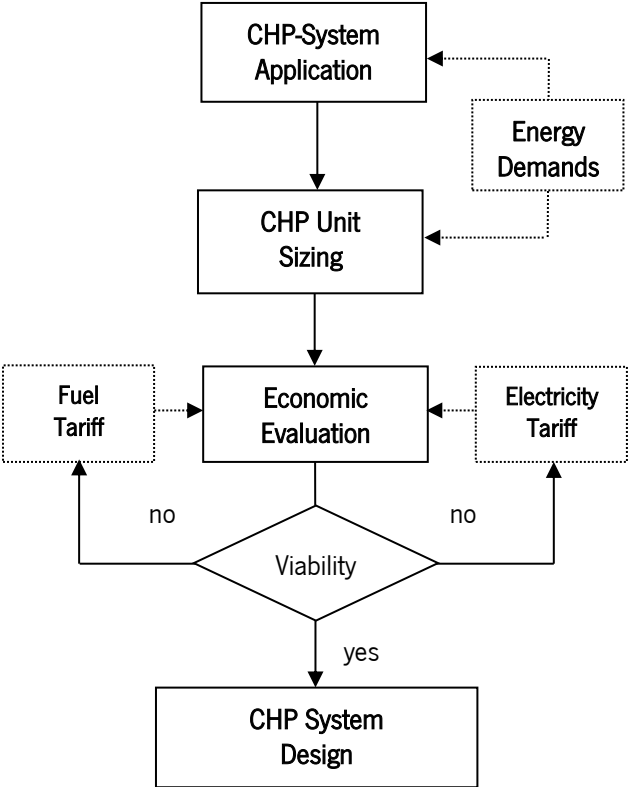
Figure 5.1 Diagram of thermal system modelling for small-scale cogeneration applications.

A cost-benefit analysis can be performed to assess the economic evaluation of thermal systems (Commission, 2008). Estimating the fixed and variable costs for the new system and comparing them to the costs of a reference/conventional system may do the economic evaluation. Regarding the fixed costs, they can be calculated according to the costs on a component level. The variable costs are the hardest to identify since they depend on system operational conditions and performance, thus, a reasonable relationship between the physical variables must be achieved (Jackson, 2007).

In the development of cost-benefit analysis, two types of variables should be considered: the variables that quantify and parameterize the investment and operational costs and revenues of the cogeneration system; and external variables that perform a cost-benefit analysis of social and environmental aspects arising from the use of cogeneration technology (e.g. monetize the carbon emission savings) (Ferreira, Martins,

Nunes, & Teixeira, 2011). The most explicit way to compare costs and benefits in an economic evaluation is to monetize both. Thus, the economic assessment of a cogeneration power plant requires a complete methodology that takes into account all decision relevant variables (internal costs and revenues plus the externalities) able to affect the decision-making process (Ren & Gao, 2010; Soliño, Prada, & Vázquez, 2009).

The evaluation of the economic feasibility of a CHP system can be processed in three main steps: (1) assessment of the technical data; (2) costing methodology; and (3) evaluating the economic viability of the CHP residential system.

The cost methodology allows the user to define the costs in a transparent manner, so that options can be validated and compared in an equitable manner. Cost estimation of the investment associated with the implementation of a particular system has to be made. Firstly, there is the need to gather and validate the cost data. For this, one can collect cost data from literature, technology suppliers and consultants. Secondly, the cost components have to be defined and allocated into investment cost, operation and maintenance costs, revenues and avoided costs. The financial analysis of power plants usually considers the value of electricity produced by the unit, which represents the most valuable income from the systems operation. Moreover, and for any given system, the payback relies on the unit's operating hours and the total electricity produced annually. Obviously, it is not only the system purchase costs that are important to calculate. The installation and the frequency of the maintenance service over the system-working lifetime have to be quantified. Finally, it is necessary to use some parameters, such as, exchange rates, discount and interest rates, in order to enable a fair comparison of different CHP residential systems. These data are used to estimate whether the annual worth of the investment is positive or negative. The process describing the development of the thermal-economic optimization model is presented at Figure 5.2.

Physical and Economic Model Definition	Optimization Problem Development	Implementation of an Optimization Algorithm
Phase 1 System sizing and purchase cost equations definition	**Phase 2** Definition of Objective function & decision variables	**Phase 3** Numerical Optimization using MatLab environment
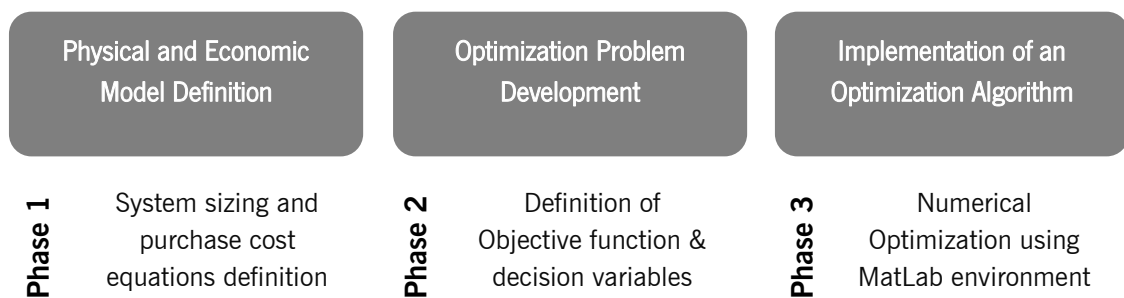
Figure 5.2 Process of the development of the thermal-economic optimization model.

Therefore, the thermal-economic model includes the definition of the physical and economic mathematical model, for which an optimization problem is formulated in order to disclose the best solution for the physical model for the best economic output through the application of an optimization algorithm.

5.2 Thermal-economic Optimization Model Definition

The thermal-economic model includes the definition of the objective-function, the decision variables and the constraints that give significance to the results. In the developed work, a single objective function on an economic basis is presented. The terms of the objective function represent the balance between costs and revenues from the system operation. The equation term that represents the investment cost consists on the sum of the purchase cost equations of each component of the system, which will be describe in more detail.

5.2.1 Definition of the Objective Function

The main objective of the present optimization study is the maximisation of the Annual Worth (AW) of the cogeneration system subjected to economic and thermodynamic non-linear constraints. Therefore, the objective function is defined by the balance between the incomes and the costs of the system operation, as described by equation (5.1).

$$max\ AW$$
$$where\quad AW = \mathrm{Re}\,v_{sell} + C_{avoided} + \mathrm{Re}\,v_{CO_2} + \mathrm{Re}\,v_{res} - C_{inv} - C_m \tag{5.1}$$

The revenues are: the income from selling electricity to the grid (Rev_{sell}), the residual value of the system at its lifetime (Rev_{res}), the avoided cost of heat generation by a conventional boiler ($C_{avoided}$) and the monetization of the carbon emission savings (Rev_{co2}). The considered costs were: the annual system investment cost (C_{inv}) and the maintenance costs involved in the production of electricity and heat using the CHP system (C_m).

The annual income from selling electricity power to the grid was calculated from the electrical power delivered to the grid ($\dot{W}_{el}$) considering the yearly number of system working hours (t) which corresponds to 4000 h, multiplied by the electricity-selling price (p_{sell}), as in equation (5.2) .

$$\mathrm{Re}\,v_{sell} = \dot{W}_{el}\ p_{sell}\ t \tag{5.2}$$

The electricity-selling price was taken as a guaranteed and fixed feed-in-tariff of 0.12 €/kWh. The avoided cost represents the cost of NG that would be consumed by a conventional system (typically a boiler) to produce the same amount of useful thermal energy, Q. This avoided cost can be calculated as in equation (5.3).

$$C_{avoided} = p_{fuel}\ \frac{Q}{\eta_b} \tag{5.3}$$

where, p_{fuel}, is the NG price per energy unit (p_{fuel}=10 €/GJ) on a Low Heating Value (LHV) basis and η_b is the efficiency of a conventional boiler. This value is usually assumed to be 90% (Decision(2011/877/EU), 2011).

Considering that the system under optimization uses a renewable energy source, the carbon dioxide emission factor is null. Nevertheless, it was intended to monetize of the avoided carbon emission from the CHP unit considered. Therefore, the avoided carbon emissions were calculated considering as if a conventional boiler running with NG as the fuel, with an efficiency of 90%, produced the thermal power and if the power was obtained from the grid. The economic benefit from the avoided carbon emissions was calculated by equation (5.4), assuming a constant price (p_{CO_2} =24.0 €/ton Co₂) per ton (Cozijnsen, 2012) and an equivalent CO₂ emission factor (FE_{CO_2}) in the view of the conventional energy production.

$$\mathrm{Re}\, v_{CO_2} = p_{CO_2} \cdot FE_{CO_2} \cdot t \cdot (\dot{W}_{el} + \dot{Q}) \tag{5.4}$$

The residual value of the equipment at the end of its useful lifetime should be considered as revenue. From the economic point of view, the residual value of equipment is usually estimated as a percentage (ψ) of the initial system investment cost, C_{inv}, as in equation (5.5). The ψ was assumed to be 5%.

$$Rev_{res} = \psi \cdot C_{inv} \tag{5.5}$$

The annual system investment cost C_{inv} is calculated according to the annualised capital cost. Annualising the initial investment corresponds to the spreading of the initial cost across the lifetime of a system, while accounting for the time value of the money. The initial capital cost is annualised as if it were being paid off a loan at a particular interest of discount rate over the lifetime of the option. The power production costs are sensitive to changes in the discount rate (i.e. the interest rate used to determine the present value of future cash flows) (Larsson, Fantazzini, Davidsson, Kullander, & Höök, 2014). The Capital Recovery Factor (CRF) is used to determine the equal amounts of n cash transactions for an investment and can be expressed as in equation (5.6).

$$CRF = \frac{i_e(1+i_e)^n}{(1+i_e)^n - 1} \tag{5.6}$$

where i_e is the effective rate of return. The lifetime of the system was defined to be 20 years. According to Öberg, Olsson, & Palsson (2004), the total accumulated operating time for the Stirling engines is about 180000 h, corresponding to $\cong$ 20.5 years. In addition, some caution should be introduced when a new technology is applied to an emergent market, and so, the investment risks are higher than with mature technologies and traditional markets.

For thermal-economic optimisation, the i_e can be approximated as: nominal rate of return (i.e interest rate) minus inflation rate plus owners' risk factor and correction for the method of compounding (Larsson et al., 2014). The i_e herein considered was 7% resulted in a CRF of 0.0944. Thus, the annual system investment cost becomes as in equation (5.7).

$$C_{inv} = \sum_i C_i \cdot CRF \tag{5.7}$$

where C_i is the purchase cost of each component of the CHP system $(C_i \rightarrow C_k; C_h; C_c; C_{eng})$.

For Stirling engines, the normal maintenance intervals are of 5000-8000 h. According to a Swedish study (Öberg et al., 2004), the maintenance service can include the regenerator maintenance and the replacement of some engine components, oil and filters. Thus, the maintenance costs are evaluated as in equation (5.8).

$$C_m = p_m \cdot \dot{W}_{el} \cdot t \tag{5.8}$$

where p_m is the maintenance price per unit of electricity produced. The maintenance costs are estimated to be 0.015 €/kWh$_{el}$ (Öberg et al., 2004). The electrical power ($\dot{W}_{el}$) already includes the efficiency of the electrical generator, herein assumed to be 93%.

5.2.2 Definition of Purchase Cost Equations

The total system investment cost corresponds to the sum of the purchase cost of each component of the system. Thus, four representative purchase cost equations are presented for each one of the heat exchangers (heater, regenerator and cooler) and for the engine bulk. The purchase cost equation of the engine bulk is representative of the remaining components of the Stirling engine.

Methodology

Each purchase cost equation should include terms, which relate the cost of the equipment with the physical parameters that have greatest relevance in the cost estimation. The mathematical expressions that define the cost of each component were based on the methodology developed by Marechal, Palazzi, Godat, & Favrat (2005) and already applied to micro-gas turbines (Ferreira et al., 2012) and to Stirling engine technology (Ferreira, Oliveira, Nunes, Martins, & Teixeira, 2014). The costing methodology also integrates cost coefficients adjusted for this kind of technology and based on real market data. The variables included in the purchase cost equations can be divided in size and quality variables. In terms of methodology, the equations were defined considering that the cost of each component of the system is based on a reference case and includes a cost coefficient, a factor of size, which scales the component, and a temperature quality factor as is represented in equation (5.9).

$$Component\ Cost = C_{ref,i} F_{m,i} F_{T,i} \tag{5.9}$$

The term C_{ref} is the reference cost coefficient that corresponds to a cost per unit of (one or more) physical parameter. The term F_m is the sizing factor that scales the system component from a reference case, as presented in equation (5.10).

$$F_m = F_{ref} \cdot \left(\frac{F_i}{F_{ref}} \right)^b \tag{5.10}$$

where F_{ref} and F_i are the reference and the physical variable value and b the sizing exponent. A sensitivity analysis is required in order to determine the best value for the sizing exponents.

Due to the high temperatures at which certain system components operates, such as, the heater and the regenerator, an additional term can be included into the cost component equation. The temperature factor, F_T, can be defined as in equation (5.11).

$$F_T = \frac{1 + e^{C_i \cdot (T_i - T_{ref})}}{2}$$
(5.11)

where T_{ref} is the reference temperature for the working gas at the component, T_i is the effective temperature of the working gas at the components and C_i is the temperature cost coefficient.

Heat Exchangers Purchase Cost Equations

The purchase cost equations for the heater and the regenerator are presented by equations (5.12) and (5.13), respectively. For both heat exchangers, the equations relate the cost of the exchanger with its effective heat transfer area. An additional correction term must be added in order to include the temperature effect in their cost.

$$C_h = C_{11,h} \cdot A_{ref,wh} \cdot \left(\frac{A_{wh}}{A_{ref,wh}}\right)^{0.5} \cdot \left[\frac{1 + e^{C_{12,h} \cdot (T_h - 725)}}{2}\right]$$
(5.12)

$$C_r = C_{21,r} \cdot A_{ref,wr} \cdot \left(\frac{A_{wr}}{A_{ref,wr}}\right)^{0.6} \cdot \left[\frac{1 + e^{C_{22,r} \cdot (T_r - 600)}}{2}\right]$$
(5.13)

where $C_{11,h}$ and $C_{21,r}$ are the reference cost coefficients [in €/cm²] for heater and regenerator, respectively; $C_{12,h}$ and $C_{22,r}$ are correction constants of the temperature factor for heater and regenerator. Reference values for the heat transfer area and cost coefficients are assumed by considering a reference case from the available market. Working fluid temperatures, pressures and the type of heat source, affect the design of these two special heat exchangers. For instance, a high temperature, low-pressure steady conditions, while, in the internal surface, the fluid flows at high temperature and high pressure, subject to turbulence, characterizes the flow at heater's outer surface. These limitations make these thermal components more expensive due to the materials used in their manufacture. The temperature reference values for heater and regenerator were assumed to be 725 K and 600 K, respectively.

Figure 5.3 and Figure 5.4 presents the heater and regenerator cost estimation considering three different sizing exponents. Considering the obtained curves, it was assumed a size exponent of 0.5 for the heater purchase cost equation and a value of 0.6 for the regenerator.

The regenerator can be considered the heart of the Stirling engine. Thus, the heat transfer is calculated assuming that the regenerator has a fine-wired matrix that improves the heat transfer process by exposing

the maximum surface area of the matrix. In that way, reference values were assumed for the heater and regenerator heat transfer area with similar configuration (Timoumi, Tlili, & Ben Nasrallah, 2008).
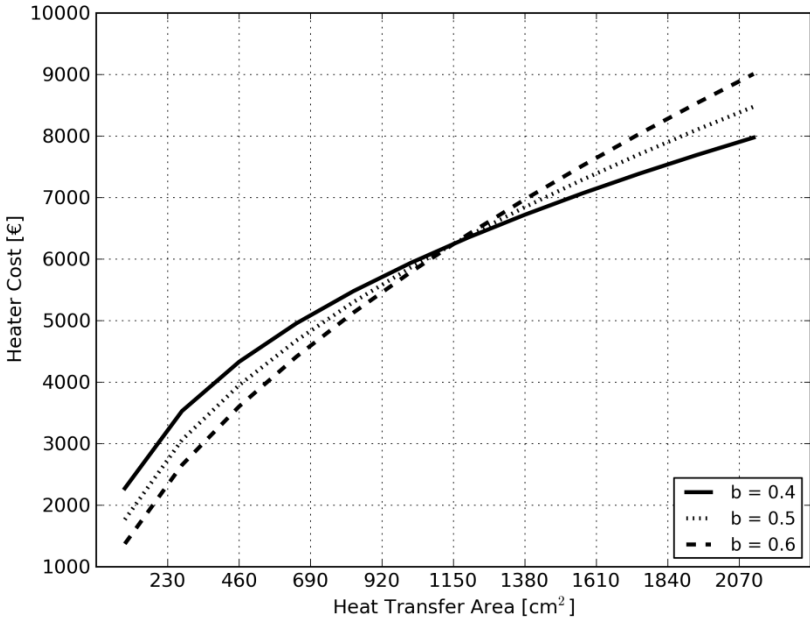
Figure 5.3 Cost estimation of the heater considering different size exponents.
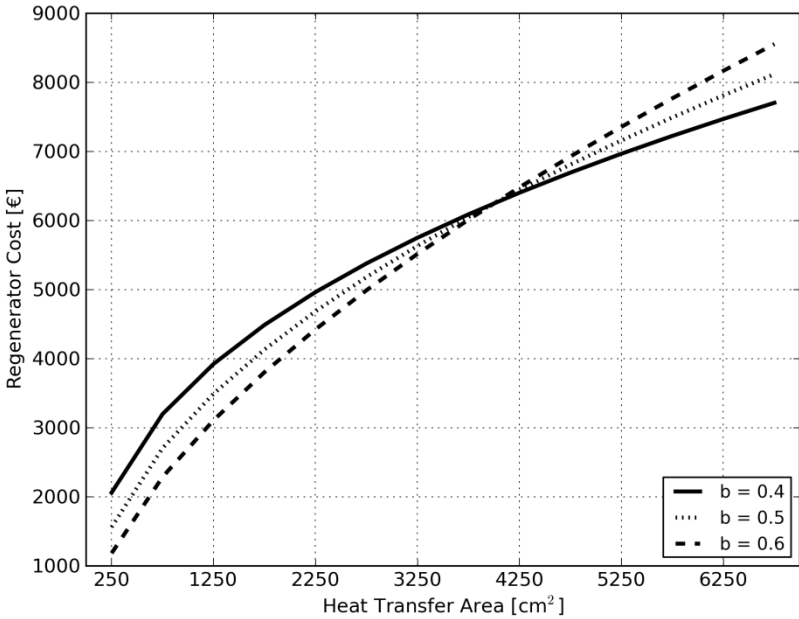
Figure 5.4 Cost estimation of the regenerator considering different size exponents.

The purchase cost equation for the cooler is presented by equation (5.14). For this component, the temperature factor was neglected because despite the gas flow conditions in the cooler are quite similar to the ones at the heater, the working fluid flows at lower temperature values.

$$C_k = C_{31,k} \cdot A_{ref,wk} \cdot \left(\frac{A_{wk}}{A_{ref,wk}} \right)^{0.4} \tag{5.14}$$

where $C_{31,h}$ is the reference cost coefficient [in €/cm²] for cooler cost equation.

The heat transfer area at the cooler purchase cost equation was assumed to be the wetted area of the gas side because the gas convective heat transfer coefficient is relatively higher when compared with the water convective heat transfer coefficient. Figure 5.5 presents the cooler cost estimation considering three different sizing exponents. For the cooler purchase cost, it was assumed a size exponent of 0.4.
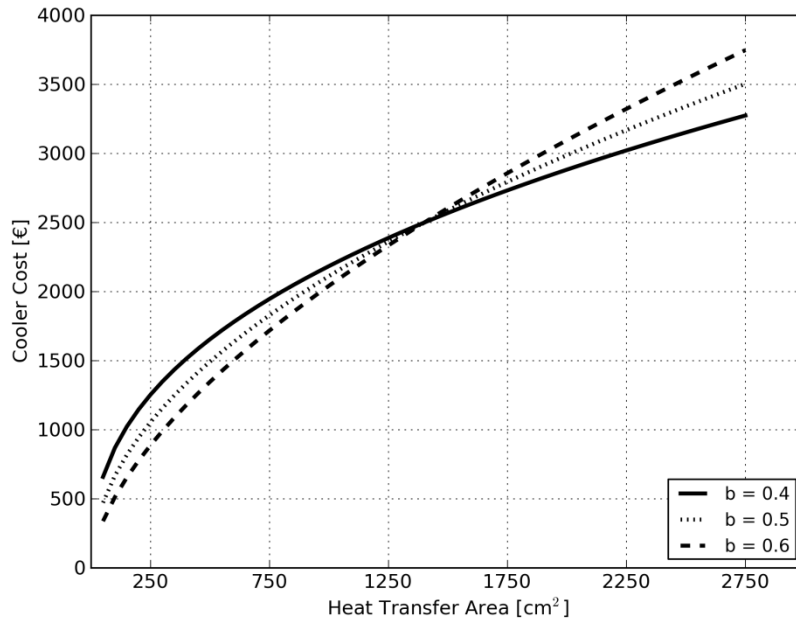
Figure 5.5 Cost estimation of the cooler considering different size exponents.

Engine Bulk Purchase Cost Equation

The power of Stirling engines is affected by changing the operational parameters such as the pressure, phase angle, volume and speed (Tlili, Timoumi, & Nasrallah, 2008). Because of the complexity of system modelling, the engine bulk cost equation was estimated considering two main relevant physical parameters in its cost definition: the cylinders capacity (V_{eng}), a size factor, and the mean operating pressure (P_{mean}), that influences the cost of sealants. The engine bulk cost equation can be defined as in the equation (5.15).

$$C_{eng} = C_{41,eng} \left[V_{ref,eng} \left(\frac{V_{eng}}{V_{ref,eng}} \right)^{b1} \cdot P_{ref,mean} \left(\frac{P_{mean}}{P_{ref,mean}} \right)^{b2} \right] \tag{5.15}$$

where $C_{41,eng}$ is the reference cost coefficient [in €/(cm³.bar)] for engine bulk cost equation.

Engine bulk cost includes the P_{mean} of the system because of the proportionality between the mean pressure and the power output. Higher pressures also mean higher material costs and the need for better sealing solutions.

Considering that the engine cost equation includes two physical parameters, it is of utmost importance to study the impact of each physical parameter as well as the respective sizing exponent in the engine bulk cost estimation. At Figure 5.6-a) the engine cost was estimated considering a constant value for the mean pressure equal of 50 bar; while Figure 5.6-b) presents the engine cost estimation as a function of the mean pressure, varying the sizing exponent and assuming it equal to the reference value for the engine volume, $V_{ref,eng} = 125$ cm³.

5.6-a

5.6-b
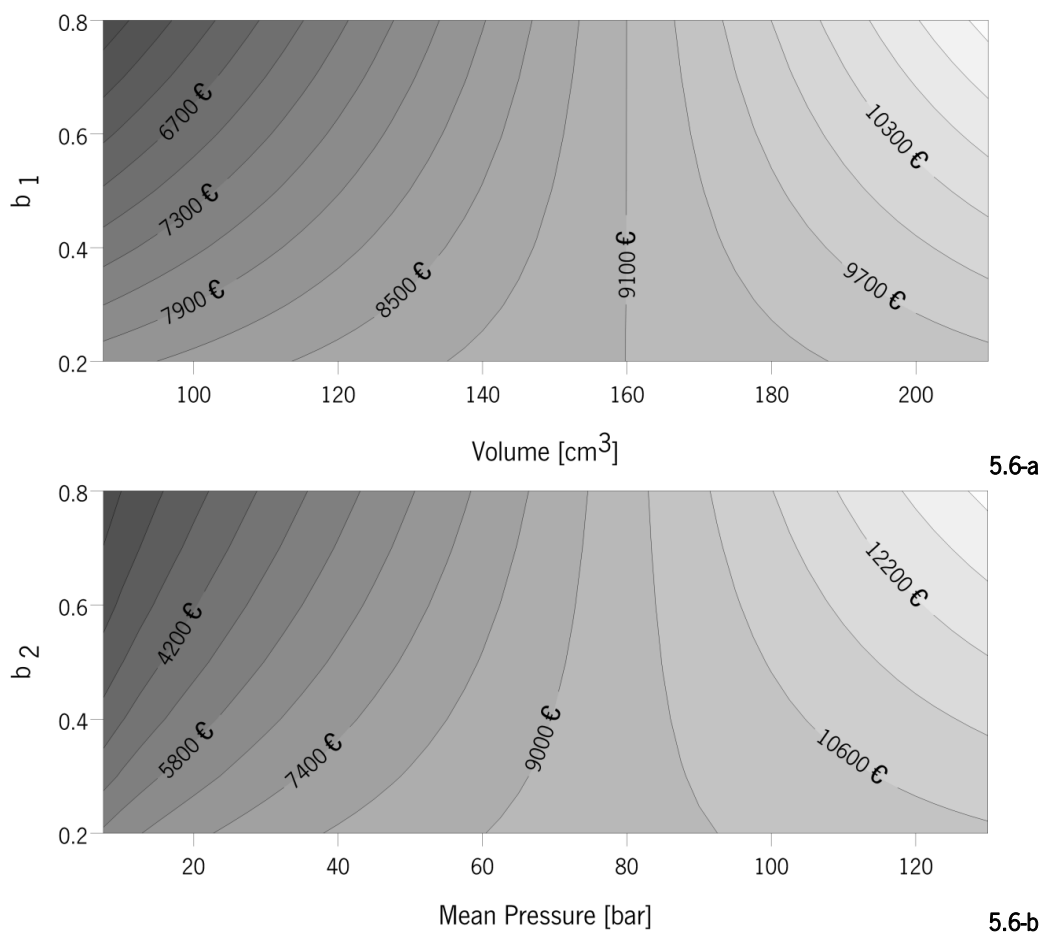
Figure 5.6-a Engine cost estimation as a function of the volume; 5.6-b Engine cost estimation as a function of the mean pressure.

For those assumptions, data show that the engine cost achieves a higher range when varying the mean pressure in relation to the volume. Assuming the reference cost of this Stirling engine component of about 10000€ (25% of the investment cost of the Solo Stirling engine (GmbH, 2007)), the analysis shows that it is acceptable to consider the size exponents for the volume (b_1) and for pressure (b_2) between 0.2 and 0.4.

Nevertheless, the engine cost must be estimated considering the combined effect of these two physical parameters. Figure 5.7 shows the engine cost estimation as a function of the engine volume and the mean pressure, considering different sizing exponents.
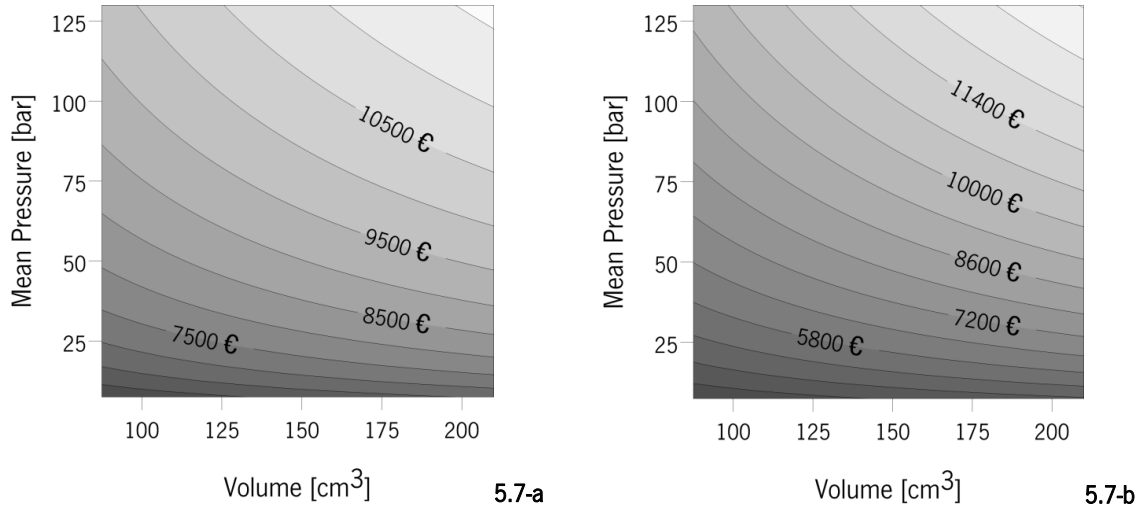
Figure 5.7-a Cost estimation of the engine bulk considering b₁=0.2; b₂=0.2; and 5.7-b Cost estimation of the engine bulk considering b₁=0.4; b₂=0.4.

Based on the analysis, the sizing exponents for the engine purchase cost equation were assumed to be 0.35 for the engine volume (b₁) and 0.2 for the mean pressure (b₂) as presented by equation (5.16)

$$C_{eng} = C_{41,eng} \left[V_{ref,eng} \left(\frac{V_{eng}}{V_{ref,eng}} \right)^{0.35} \cdot P_{ref,mean} \left(\frac{P_{mean}}{P_{ref,mean}} \right)^{0.2} \right] \qquad (5.16)$$

Validation of the Purchase Cost Equations

The cost coefficients, C_{ref}, for each purchase equation was based on the relative weight assumed for each component in the total cost of the equipment. Several combinations for the relative cost of each heat exchanger and the engine bulk were studied and the costs were calculated. Table 5.1 presents the different combinations of the relative component costs that were studied in order define the cost coefficients of the purchase cost equations.

Table 5.1 Different combinations of relative costs weight for the thermal components

	Combination A	Combination B	Combination C	Combination D
Regenerator	0.30	0.30	0.20	0.25
Heater	0.30	0.20	0.30	0.25
Cooler	0.10	0.10	0.10	0.10
Engine Bulk	0.30	0.40	0.40	0.40

Based on those combinations, the cost coefficients of each thermal component were calculated and are presented in Table 5.2. Nevertheless, the relative weight that it is attributed to each component in the final purchase cost of the thermal plant significantly affects the component cost. This coefficient represents the cost per unit of physical parameter: heat transfer area in the case of the heat exchangers and mean pressure and cylinder capacity in the case of the engine bulk purchase cost equation.

Table 5.2 Cost coefficients for different combinations of thermal component relative costs

	Combination A	Combination B	Combination C	Combination D
Regenerator	1.88	1.88	1.25	1.56
Heater	6.64	4.42	6.64	5.53
Cooler	1.79	1.79	1.79	1.79
Engine Bulk	0.31	0.417	0.417	0.417

Based on all the sensitivity analyses performed to the sizing and cost coefficients, Table 5.3 summarizes all the assumed values for cost coefficients, temperature factors and sizing exponents for the purchase cost equations of each component. Note that the regenerator and the heater are the only two components which purchase cost equation includes a temperature factor, due to the temperature values that the working gas experiences.

Table 5.3 Cost coefficients and sizing factors for the purchase cost equations

Component	Sizing Factor	Cost coefficient	Temperature Factor
Heater	b= 0.5	$C_{11,h}$=5.53	$C_{22,h}$=0.001
Regenerator	b=0.6	$C_{21,r}$=1.56	$C_{22,r}$=0.008
Cooler	b=0.4	$C_{31,r}$=1.79	-
Engine Bulk	b1=0.35 b2=0.20	$C_{41,eng}$=0.417	-

The choice of cost coefficients and sizing factors values was based on technical information from commercial systems and sensitivity analysis. The development of a correct methodology to define the cost equations for each component of a thermal power plant is a very demanding process. Manufactures do not provide important information concerning the technical specifications and much less information about production costs. Based on the information presented in the Annex II, the purchase acquisition cost of two commercial models based on Stirling engine technology (the SOLO Stirling 161 ad the 5-ZGM-1 kW) was calculated in order to validate the presented cost equations. These two models were chosen just

because they are the only two models with data required to do the calculations. The purchase cost estimation for both models is presented in Table 5.4 and Table 5.5, respectively.

Table 5.4 Validation of the purchase cost equations for the SOLO Stirling 161 model

Component	Parameter	Parameter Value	Cost (€)
Heater	Wetted Area (cm²)	1200	4481
	Temperature (K)	973	
Regenerator	Wetted Area (cm²)	2000	7347
	Temperature (K)	670*	
Cooler	Wetted Area (cm²)	1500	2570
	Temperature (K)	303	
Engine	Cylinder Capacity (cm³)	160	10000
	Rotational Speed (rpm)	1500	
	Mean pressure (bar)	150	
Total Cost (€)		24398	

Table 5.5 Validation of the purchase cost equations for the ENERLYT 5-ZGM-1 kW model

Component	Parameter	Parameter Value	Cost (€)
Heater	Wetted Area (cm²)	1696*	4810
	Temperature (K)	1073	
Regenerator	Wetted Area (cm²)	1202*	2288
	Temperature (K)	730*	
Cooler	Wetted Area (cm²)	1696*	1404
	Temperature (K)	343	
Engine	Cylinder Capacity (cm³)	328	5602
	Rotational Speed (rpm)	1100	
	Mean pressure (bar)	6.5	
Total Cost (€)		14104	

*values estimated by applying reverse engineering

Results show that calculating the purchase cost of both commercial models by using the developed cost equations, it is obtained a value of 14104€ and 24398€ for 5-ZGM-1 kW and the SOLO Stirling 161, respectively. These values demonstrate a good correlation between the costing methodology here presented and purchase cost documented in the literature. According to the data from Annex I, the

purchase cost correspond to 13000€ and 25000€, respectively. This output leads to the conclusion that, applying the purchase cost equations to different commercial models, the total equipment costs have the same cost magnitude, even without all the technical data.

5.2.3 Definition of Non-linear Constraints

Several inequality constraints were formulated in order to give physical significance to the mathematical model. The definition of these constraints aims bounding some of the variables according to their feasible limits in the system operation. The constraints divide the design space into two domains, the feasible domain where the constraints are satisfied and the respective values have significance in the optimization problem, and the infeasible domain where at least one of the constraints is violated and the variables results is no longer acceptable as optimal solution.

For the optimization problem presented in this work, two main categories of constrains are defined: the thermodynamic and the economic conditions. The first group is defined to impose some relationships between the thermodynamic variables (e.g. temperature evolutions, thermal and power production ratios, etc.) and the second one that bound the relationships between the purchase costs of the different system components.

For a machine that operates as an engine, the available electrical power produced should be always positive. Then, the most basic constraint of this model is to ensure that energy is produced, as in equation (5.17).

$$\dot{W} \geq 0 \tag{5.17}$$

In view of the data from the market, a constraint bounding the heat-to-power ratio, λ, was included into the model. It is well known from the literature that the systems available on the market have an electric power size ranging from 1 kW to 9 kW and a corresponding thermal power output between 5 kW to 25 kW. From the analysis of five commercial models: Solo 161, WhisperGen, Sunmachine, SM5A and Baxi Ecogen, the heat to power ratio was calculated for those commercial systems (see Figure 5.8).
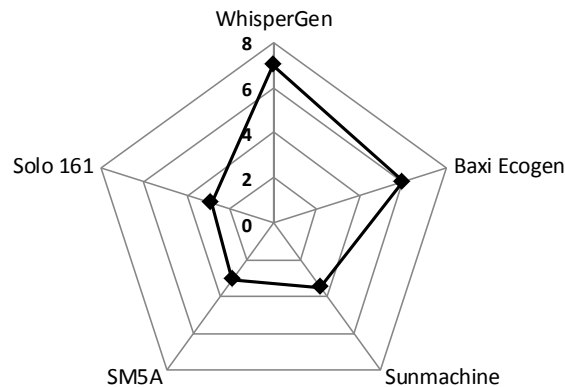
Figure 5.8 Comparison of the heat-to-power ratio of several commercial Stirling systems.

According to this analysis, the heat-to-power ratio was assumed to range between the values of 2.5 to 3.5 as in equation (5.18). In addition, the production of thermal power was also restricted to a maximum value of 10.5 kW

$$2.5 \leq \lambda \leq 3.5 \tag{5.18}$$

Considering the temperature evolution, the temperature of the working gas at the cooler was constrained as shown in equation (5.19). This constraint limits the temperature of the working fluid above 353 K, which corresponds to the cooler wall temperature.

$$\bar{T}_{water} + \left(Q_k + Q_{rloss}\right) \cdot \left(\frac{1}{h_{inner,k} A_{w,k}} + \frac{\ln\left(\dfrac{d_{out,k}}{d_{inner,k}}\right)}{2\pi L \cdot nt_k \cdot k} + \frac{1}{h_{out,k} A_{water,k}} \right) \geq 353 \tag{5.19}$$

where $\bar{T}_{water}$ is the mean temperature of the mass flow of water, where $d_{out,k}$ is the outer diameter of the cooler tubes, L_k is the length and n_t the number of the cooler tubes; k is the thermal conductivity of the tubes, which was assumed to be equal to 54 W/(mK) (carbon steel) and A_{water} corresponds to water flow area at the external side of the heat exchanger.

The temperature of the working gas at the heater was constrained as shown in equation (5.20). This constraint bound the temperature of the working fluid below the minimum acceptable value to the hot source temperature.

$$T_{wall,h} - \left(Q_{h,ideal} + Q_{rloss}\right) \cdot \frac{1}{h_{inner,h} A_{w,h}} \leq T_h \tag{5.20}$$

Regarding the costs of each component, inequality constraints were defined in order to guarantee the relative share in terms of costs for each system component, by assuming a percentage in the total cost of the power plant. The constraints concerning the relative weight of each component in the total investment cost of the system is presented by equations (5.21) to (5.24).

$$C_h > 0.20 \left[\sum_i C_i \right] \tag{5.21}$$

$$C_r > 0.20 \left[\sum_i C_i \right] \tag{5.22}$$

$$C_k > 0.10 \left[\sum_i C_i \right] \tag{5.23}$$

$$C_{eng} < 0.40 \left[\sum_i C_i \right] \tag{5.24}$$

The European Directive 2004/8/EC (DIRECTIVE 2004/8/EC, 2004) aims the promotion of high-efficiency systems led by heat demand and defines the PES value, accordingly to the unit size. For small-scale

systems, a PES of at least 10% is required so that the system can be classified as a system of high efficiency, whereas in the case of micro-scale systems, a positive value of PES is required (DIRECTIVE 2004/8/EC - Directive on the promotion of cogeneration based on a useful heat demand in the internal energy market, 2004). Thus, PES allows estimating the total primary energy savings that are possible to achieve by a cogeneration unit (considering the combined electric and thermal efficiencies) when compared with the conventional power production process. The amount of primary energy provided by cogeneration production (equation (5.25)) must be a positive value in order to the system is classified as a high efficient system.

$$PES > 0 \tag{5.25}$$

The European Communities Commission gives a method to evaluate the harmonized efficiency reference values for separate production of electricity and heat. In particular, the value of the electric reference efficiency is a function of the year of construction of the cogeneration unit, the climatic condition, the electricity used on-site and the avoided grid losses due to decentralized production (Decision(2011/877/EU), 2011).

5.2.4 Definition of Decision Variables

Defining the decision variables is in fact one of the hardest and/or most crucial steps in formulating an optimization problem. Based on the study of the physical model, explicit decision variables were defined in the numerical model. Upper and lower bounds were selected for these decision variables, considering their significance in the model. The decision variables were chosen considering their relevance in the performance of the system on an integrated way. Thus, two types of decision variables were considered in the model: operational and geometrical variables.

The mean pressure is one of the operational parameters that most influences the system output. Considering its variation with the power produced, it was also considered as one the decision variables in the thermal-economic model. The upper and lower limit for this decision variable is presented in equation (5.26).

$$5 \leq P_{mean} \leq 80 \tag{5.26}$$

Several geometrical variables which affect directly the system sizing were also chosen as decision variables: the internal diameter of heater and cooler tubes; the number of tubes for the heater and the cooler; the porosity of regenerator matrix, the wire diameter of the regenerator matrix and the cylinders volumes.

Regarding to heater, the physical model only considers the convective heat transfer from internal wall of the tube to the working gas and assumes a constant temperature at the outer surface of the heater. Thus, the heat transfer coefficient will be significantly affected by the heater inner diameter ($d_{inner,h}$) [in mm], which is used to define the wetted heat transfer area. The heat transfer coefficient is determined by using the well-known Reynolds number in order to relate heat transfer to fluid friction by applying non-

dimensional parameters. The upper and lower limits for the internal diameter of the heater tubes, as decision variable, is presented in equation (5.27).

$$1 \le d_{inner,h} \le 5 \qquad (5.27)$$

The cooler tubes internal flow conditions are quite similar to the heater but at lower temperatures. To reduce the temperature of the working fluid an outside flow of water is used as a cold sink. Thus, heat transfer phenomenon includes the convective heat transfer from working gas inner to the inner wall of the cooler tubes to the, conductive heat transfer through the inner to outer tube wall surface and outside convective heat transfer to the coolant, the water. A preliminary analysis of the cooler showed that the most relevant limitation is the poor heat transfer between the inner surface of the cooler tubes and the working gas. The convective heat transfer coefficient from inner wall to the working fluid is the term that most contribute to the global heat transfer coefficient. Thus, the inner diameter ($d_{inner,k}$) [in mm] of the cooler tubes was selected as a decision variable. The upper and lower limits for both decision variables are presented in equation (5.28)

$$1 \le d_{inner,k} \le 5 \qquad (5.28)$$

The efficacy of the regeneration process is very important in the engine performance because along the thermodynamic cycle, heat transfer losses in the fluid pre-heating and pre-cooling leads to increases in the hot and cold energies and thus to an important decay in engine efficiency (Zarinchang & Yarmahmoudi, 2009). The maximum efficiency of this process would only be achieved if the heat transfer coefficient or the area of heat transfer is infinite. However, the working fluid does not have a null heat transfer capacity neither the regenerator matrix has an infinite heat capacity. To improve the regenerator heat transfer, it is important to establish a commitment between the heat transfer and the fluid friction. Thus, the porosity of the regenerator matrix (Φ) and the wire diameter of the regenerator matrix (d_{wire}) [in mm] were selected as the most relevant variables affecting the system performance.

$$0.3 \le \Phi_{matrix} \le 0.9 \qquad (5.29)$$

$$0.05 \le d_{wire} \le 0.5 \qquad (5.30)$$

The Stirling engine capacity is a very important aspect when sizing the system because the network produced by the engine can be determined as a function of mean effective pressure and the engine volume (V_{eng}) [in cm^3]. The upper and lower limits for this decision variable are presented in equation (5.31).

$$70 \le V_{eng} \le 160 \qquad (5.31)$$

The upper and lower limits for the decision variables were based on the data from the literature, by assuming a feasible range variation.

5.3 Numerical Solution

The search methods may and often do find global optimal solutions, but they are not guaranteed to do so. Nonetheless, these methods are widely used, often finding very good solutions, and can be applied to non-linear, complex problems. A search method usually starts with a feasible solution, exploring all the solutions in the neighbourhood of that point, looking for a better one, and repeats the process if an improved point is found (Thomas, David, & Leon, 2001a). These methods usually use a heuristic procedure that guide the procedure by changing its logic-based search so that the method does not become trapped in a local optimum (Thomas, David, & Leon, 2001b).

Recent developments show that derivative-free methods are highly demanded by researches for solving optimization problems in various practical contexts. Derivative free optimization was developed for solving, in general, small dimensional problems (less than 100 variables) in which the computation of the derivatives are not available (Rao & Patel, 2013). Concerning the complexity of the physical system, the optimization problem was solved using the PS routine in the MatLab® optimisation toolbox.

5.3.1 Optimization Algorithm

Pattern Search (PS) algorithms are derivative free methods for the minimization of smooth functions (Lewis, Shepherd, & Torczon, 2007). This method handles optimization problems with nonlinear, linear, and bound constraints.

At each step, the algorithm generates a set of points, called mesh. These set of points control how the pattern changes over iterations and adjusts the mesh for problems that vary in scale across dimensions. Controlling the initial mesh size, the mesh refining factor, or the mesh contraction factor allows speeding up the method convergence. The mesh is generated by creating a set of vectors based on the pattern by multiplying each direction vector by a scalar that corresponds to the mesh size. The pattern vector that defines a mesh point is called its direction.

The algorithm polls the points in the current mesh by computing their objective function. If the algorithm fails to find a point that improves the objective function, the poll is called unsuccessful, remaining the current point as the best for the next iteration. After polling, the algorithm changes the value of the mesh size (δ), expanding or contracting its size. The mesh expansion depends on the polling step success. The optimization algorithm is briefly presented by the pseudo-code presented below.

The Poll method specifies the pattern the algorithm uses to create the mesh. There are three patterns for each of the classes of direct search algorithms: the generalized pattern search (GPS) algorithm, the generating set search (GSS) algorithm, and the mesh adaptive direct search (MADS) algorithm.

Given δ, ξ and x_1

if $\delta_j \leq \xi$

    then Stop

    compute $min \leftarrow f(x_j)$

    for i^{th} direction vector

        Set $x_j^i \leftarrow x_j + \delta_j p_j^i$

        compute $f(x_j^i)$

        if $f(x_j^i) < min$

            Set $x_{j+1} \leftarrow x_j$;

            Set $\delta_{j+1} \leftarrow \delta_j$;

            $min \leftarrow f(x_j^i)$;

        else

            $\delta_{j+1} \leftarrow \delta_j / 2$;

            $j \leftarrow j + 1$;

The pattern, GPS Positive basis 2N (GPSPositiveBasis2N), consists of a set of 2N vectors, where N is the number of independent variables for the objective function. For example, if the optimization problem has three independent variables, the pattern consists of the following six vectors: [1 0 0] [0 1 0] [0 0 1] [–1 0 0] [0 –1 0] [0 0 –1], as clarified by Figure 5.9.
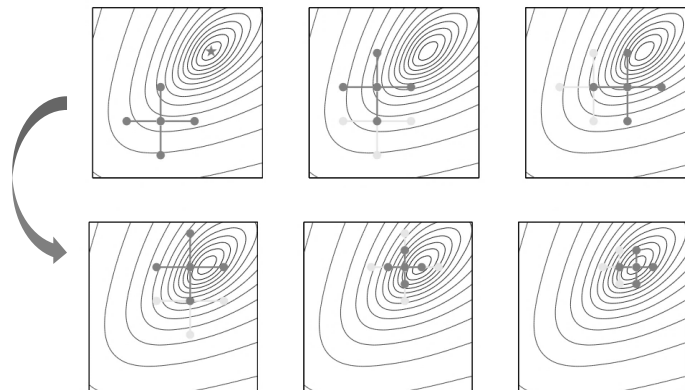
Figure 5.9 Compass of a direct search method. Adapted from (Kolda, Lewis, & Torczon, 2003).

The GSS Positive basis 2N pattern (GSSPositiveBasis2N) is similar to GPS Positive basis 2N, but adjusts the basis vectors to account for linear constraints. GSS Positive basis 2N is more efficient than GPS Positive basis 2N when the current point is near of the constraint boundary. The MADS Positive basis 2N pattern (MADSPositiveBasis2N) consists of 2N randomly generated vectors, where N is the number of independent variables for the objective function. Randomly generating N vectors that form a linearly independent set, and then using this first set do this and the negative of this set gives 2N vectors. This

method requires the definition of an initial point (x_1) and the iterative process is initiated with a "trial step" considering the convergence tolerance (ξ), the length of search step and the initial direction. If the search returns a point that improves the objective function, the algorithm uses that point at the next iteration and omits the polling step. Several algorithms can be used as search methods: GPS, GSS and MAD Positive Basis algorithms, GA algorithms, Nelder-Mead method or Latin hypercube (MathWorks Documentation Center, 2012).

5.3.2 Numerical Simulation

The main objective of this study is to analyse an alpha Stirling engine (non-ideal analysis), by trying to disclose the best operational parameters for the Stirling engine for cogeneration applications. The mathematical model able to describe the physical system, was based on a software-code developed in the MatLab® environment, based on the physical model of Urieli & Berchowitz (2010). The base code was modified, improved and adapted to be part of the thermal-economic model optimization model. When employing the optimization model, several script files were created to define the equations that describe the purchase cost equations. The purchase cost equations depend on physical parameters that also affect the thermodynamic performance of the engine and the solution will be the combination of parameter values that will lead to the best economic output.

To apply this optimization algorithm it was also required to create a configuration script and two others that define the nonlinear constraints as well as the simple bounds of the decision variables (upper and lower bounds). The bounds in the variables guarantee that the optimum solution is within the technical operating capability of the plant. The main routine, Optimization Stirling Engine Analysis (OptSEA), where all the algorithm parameters are called, integrates all the scripts in order to solve the optimization problem, as described by Figure 5.10.
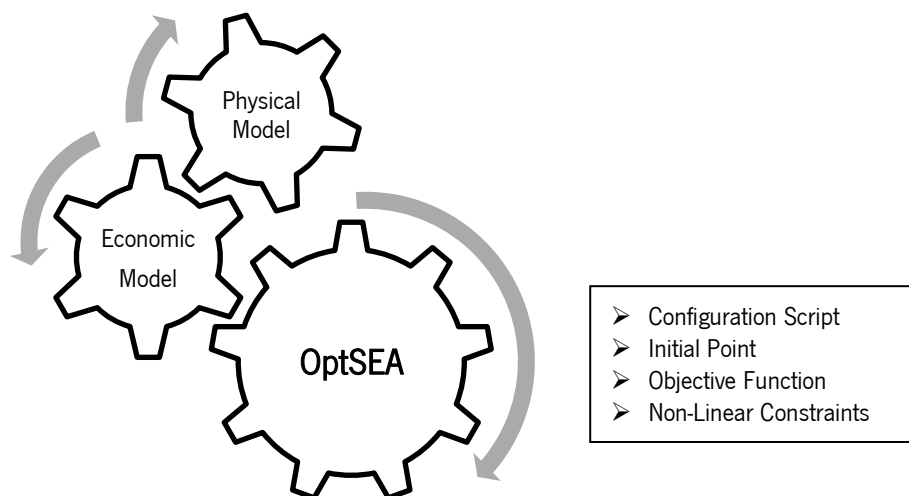
Figure 5.10 Schematics of optimization model structure.

PS method requires a feasible initial point to start the iterative process. The initial point for all the decision variables was assumed to be the: $x_1^T = [\ V_{eng}$ = 125 cm³, P_{mean} =50 bar, $d_{inner,h} = d_{inner,k}$ =3.0 mm, Φ_{matrix} = 0.7 and d_{wire} =0.3 mm. This point was firstly tested in order to verify if any constraint of the model is violated.

Table 5.6 presents the algorithm options used to perform the numerical simulations. Considering the optimization problem under scope, PS algorithm was applied considering the problem as a Non-linear constrained optimization problem. In relation to the poll option, once it controls how the algorithm vote the mesh points at each iteration, the simulations were carried out considering the complete poll 'on' in order to choose the point with the best objective function value by checking all the points in the mesh at each iteration. After few tests to the optimization algorithm, the poll method chosen was the *Positive basis 2N* Generalized Pattern Search algorithm.

Table 5.6 Algorithm options for the numerical simulations

Method Option	Selected Option
Problem Type	Non-linear constrained
Poll Method	GPS Positive basis 2N
Search Method	Nelder-Mead & GA algorithm
Maximum Objective Function Evaluation	8000
Maximum Iterations	200
Convergence Tolerance	1.0E-04
Complete Poll	on

The search method was defined as the *Nelder-Mead* and the GA algorithm from the MatlLab® optimization toolbox. The maximum number of functions evaluation was defined as 8000, taking into account a maximum of 200 iterations. The convergence tolerance was assumed to be 1.0E-04.

Commission, E. (2008). *Guide to Cost Benefit Analysis of Investment Projects* (p. 259).

Cozijnsen, J. (2012). CO2 Prices analysis of the EU CO2 Market. Retrieved January 11, 2013, from http://www.co2prices.eu/

Decision(2011/877/EU). (2011). Establishing Harmonized efficiency reference values for separate production of electricity and heat in application of Directive 2004/8/EC of the Parliament and of the Council and repealing Commision Decision 2007/74/EC. Official Journal of the European Union.

DIRECTIVE 2004/8/EC - Directive on the promotion of cogeneration based on a useful heat demand in the internal energy market. (2004). *European parliament and the council of the european union* (pp. 1–11).

Ferreira, A. C. M., Martins, L. A. S. B., Nunes, M. L., & Teixeira, S. F. C. F. (2011). Development of a Cost-benefit Model for Micro CHP Systems. In *ICOPEV '2011- 1st International Conference on Project Economic Evaluation* (pp. 1–7). Guimarães.

Ferreira, A. C. M., Nunes, M. L., Teixeira, S. F. C. F., Leão, C. P., Silva, Â. M., Teixeira, J. C. F., & Martins, L. A. S. B. (2012). An economic perspective on the optimisation of a small-scale cogeneration system for the Portuguese scenario. *Energy*, *45*(1), 436–444. doi:10.1016/j.energy.2012.05.054

Ferreira, A. C., Oliveira, R. F., Nunes, M. L., Martins, L. B., & Teixeira, S. F. (2014). Modelling and Cost Estimation of Stirling Engine for CHP Applications. In EUROPMENT (Ed.), *International Conference on Mechanics, Fluid Mechanics, Heat and Mass Transfer* (pp. 1–9). Interlaken, Switzerland: Europment.

GmbH, S. S. (2007). ProEcoPolyNet Fact Sheet "SOLO Stirling 161" (Brochure). Stuttgarter, Germany: SOLO Stirling GmbH.

Jackson, J. (2007). Ensuring emergency power for critical municipal services with natural gas-fired combined heat and power (CHP) systems: A cost–benefit analysis of a preemptive strategy. *Energy Policy*, *35*(11), 5931–5937. doi:10.1016/j.enpol.2007.07.012

Kolda, T. G., Lewis, R. M., & Torczon, V. (2003). Optimization by Direct Search: New Perspectives on Some Classical and Modern Methods. *SIAM Review*, *45*(3), 385–482. doi:10.1137/S003614450242889

Larsson, S., Fantazzini, D., Davidsson, S., Kullander, S., & Höök, M. (2014). Reviewing electricity production cost assessments. *Renewable and Sustainable Energy Reviews*, *30*, 170–183. doi:10.1016/j.rser.2013.09.028

Lewis, R. M., Shepherd, A., & Torczon, V. (2007). Implementing Generating Set Search Methods for Linearly Constrained Minimization. *SIAM Journal on Scientific Computing*, *29*(6), 2507–2530. doi:10.1137/050635432

Marechal, F., Palazzi, F., Godat, J., & Favrat, D. (2005). Thermo-Economic Modelling and Optimisation of Fuel Cell Systems. *Fuel Cells*, *5*(1), 5–24. doi:10.1002/fuce.200400055

MathWorks Documentation Center. (2012). Pattern Search Options. *Global Optimization Toolbox*. Retrieved July 06, 2012, from http://www.mathworks.com/help/gads/pattern-search-options.html

Moreira, N. A., Monteiro, E., & Ferreira, S. (2007). Transposition of the EU cogeneration directive: A vision for Portugal. *Energy Policy*, *35*(11), 5747–5753. doi:10.1016/j.enpol.2007.06.015

Öberg, R., Olsson, F., & Palsson, M. (2004). *Demonstration Stirling Engine based Micro-CHP with ultra-low emissions* (p. 51). Nordenskiöldsgatan, Sweden. Retrieved from http://www.sgc.se/en/

Pehnt, M. (2008). Environmental impacts of distributed energy systems—The case of micro cogeneration. *Environmental Science & Policy*, *11*(1), 25–37. doi:10.1016/j.envsci.2007.07.001

Rao, R. V., & Patel, V. (2013). Multi-objective optimization of heat exchangers using a modified teaching-learning-based optimization algorithm. *Applied Mathematical Modelling*, *37*(3), 1147–1162. doi:10.1016/j.apm.2012.03.043

Ren, H., & Gao, W. (2010). Economic and environmental evaluation of micro CHP systems with different operating modes for residential buildings in Japan. *Energy and Buildings*, *42*(6), 853–861. doi:10.1016/j.enbuild.2009.12.007

Soliño, M., Prada, a., & Vázquez, M. X. (2009). Green electricity externalities: Forest biomass in an Atlantic European Region. *Biomass and Bioenergy*, *33*(3), 407–414. doi:10.1016/j.biombioe.2008.08.017

Thomas, E., David, H., & Leon, L. (2001a). Global Optimization for Problems with Continuous and Discrete variables. In M.-H. H. Education (Ed.), *Optimization of Chemical Processes* (2nd Editio., pp. 382–414). New York: Thomas Casson.

Thomas, E., David, H., & Leon, L. (2001b). Non-linear Programming with constraints. In T. Casson (Ed.), *Optimization of Chemical Processes* (2nd Editio., pp. 284–329). New York: McGraw Hill Higher Education.

Timoumi, Y., Tlili, I., & Ben Nasrallah, S. (2008). Performance optimization of Stirling engines. *Renewable Energy*, *33*(9), 2134–2144. doi:10.1016/j.renene.2007.12.012

Tlili, I., Timoumi, Y., & Nasrallah, S. Ben. (2008). Analysis and design consideration of mean temperature differential Stirling engine for solar application. *Renewable Energy*, *33*(8), 1911–1921. doi:10.1016/j.renene.2007.09.024

Urieli, I., & Berchowitz, D. M. (2010). Stirling Engine Simple Analysis. *Ohio University*. Retrieved February 10, 2010, from http://www.ohio.edu/mechanical/stirling/me422.html

Zarinchang, J., & Yarmahmoudi, A. (2009). Optimization of Thermal Components in a Stirling Engine. In *WSEAS Transactions on Heat and Mass Transfer* (Vol. 4, pp. 1–10).

This page was intentionally left in blank

6

Results and Discussion |

6.1   Base-case Scenario for Numerical Simulation

6.2   Thermodynamic Cycle Analysis

6.3   Sensitivity Analysis of the Operational Parameters

6.4   Sensitivity Analysis of the Geometrical Parameters of the Heat Exchangers

6.5   Cost Estimation Analysis

6.6   Thermal-economic Optimization

In this chapter, the numerical results are presented and discussed. These are divided in three main groups. The first group concerns the analysis of the Stirling thermodynamic cycle comparing the results from the isothermal, ideal adiabatic and non-ideal analysis for a base-case scenario, where the geometrical configuration was assumed to be fixed. The second group of results is focused on a sensitivity analysis of the geometrical and operational parameters in the performance assessment of Stirling engine thermal components. The computing code used in these two analyses was modified from the one presented by Urieli & Berchowitz (2010). The third main group of results concerns the numerical evaluation of the thermal-economic performance of the Stirling engine.

6.1 Base-case Scenario for Numerical Simulation

The numerical simulations were carried out considering a base-case scenario for which the first results were obtained. Thus, all the input parameters for the engine's geometric characteristics were assumed to be fixed values according to Table 6.1. It was also necessary to define the cylinders dead and swept volumes, the working gas and the operating input parameters for running the code: engine speed [rpm], heater and cooler temperatures (both constant). The temperatures of the hot and cold source are, respectively, 725 K and 353 K.

Table 6.1 Values of geometrical and operational parameters for the base case scenario

Engine Cylinders	
Engine swept volume, [cm³]	130.0
Engine dead volume, [cm³]	25.0
Drive engine configuration	Sinusoidal
Regenerator	
Internal Diameter ($d_{inner,r}$) [mm]	46.0
Regenerator Length (L_r) [mm]	60.0
Matrix Porosity (Φ_{r_matrix}) [-]	0.7
Wire Matrix Diameter ($d_{wire,r}$) [mm]	0.3
Regenerator Volume (V_r),	69.8
Heater	
Internal Diameter($d_{inner,h}$) [mm]	3.0
Heater Length(L_h) [mm]	150.0
Number of Tubes (nt_h) [-]	80
Heater volume (V_h), [cm³]	84.8
Cooler	
External diameter, ($d_{out,k}$) [mm]	4.0
Internal Diameter($d_{inner,k}$) [mm]	3.0
Heater Length(L_k) [mm]	100.0
Number of Tubes (nt_k)[-]	150
Cooler volume (V_k), [cm³]	106.0
Operational Parameters	
Hot Sink Temperature, [K]	725
Cold Sink Temperature, [K]	353

The engine was considered as an alpha type, assuming a phase advance angle for the expansion space ω of 90° for the expansion cylinder and considering that both compression and expansion cylinders have a dead volume of 25 cm³ and a swept volume of 130 cm³. The numerical simulations were carried out considering different values for the rotational speed (i.e. 1500 and 3000 rpm) and mean operational pressure (i.e. 5 to 80 bar) in order to understand the relevance of those operating parameters in the engine performance.

6.2 Thermodynamic Cycle Analysis

6.2.1 Isothermal analysis

The isothermal analysis, also known as the Schmidt analysis, is still considered as the classic analysis and includes the isothermal compression and expansion, as well as, a perfect regeneration. The isothermal analysis when applied to a Stirling cycle results in a theoretical efficiency equal to the Carnot cycle.

The isothermal analysis is usually used as the approach to assess the theoretical maximum for the Stirling engine performance, although all the heat transfer processes are considered as perfect.

Table 6.2 shows the obtained results for the isothermal analysis. The power values correspond to a rotational velocity of 1500 rpm. According to the results, and despite the engine sinusoidal geometry, an efficiency of 51.3% was obtained for all the described operating conditions. This efficiency equals that of the Carnot cycle for the same hot and cold source temperatures ($\eta_{Carnot} = (1 - (T_c/T_h))$).

The results also show that the work per cycle is proportional to the mean pressure and the engine power is directly proportional to the mean pressure and engine speed. In fact these results were expected because, in an ideal analysis, the engine geometry (swept volume, dead volume, phase angle and form of volume evolutions – sinusoidal or other) defines the work per cycle, for a given mean pressure. All engine operational points can then easily be calculated. The nature of the working gas is irrelevant, as viscosity and thermal properties are not considered (no fluid friction and perfect heat transfer).

Table 6.2 Results from the isothermal analysis for different values of mean pressure

Pressure (bar)	Work (J/cycle)	Q_e (J/cycle)	Q_c (J/cycle)	Power(W)
5	10.48	20.43	9.95	262
30	62.9	122.6	59.7	1572
50	104.8	204.3	99.5	2620
80	167.7	326.9	159.2	4192

Figure 6.1 shows the pressure variation along a cycle obtained for a mean pressure of 30 bar. The origin (crank angle θ of 0°) corresponds to the Bottom Dead Centre (BDC or maximum volume) of the cold piston. According to Figure 6.1, the maximum pressure is obtained at the end of the gas pre-heating phase, while the minimum pressure occurs in the reverse process, when the working gas is pre-cooled and the volume is at a maximum, after the gas has been expanded.
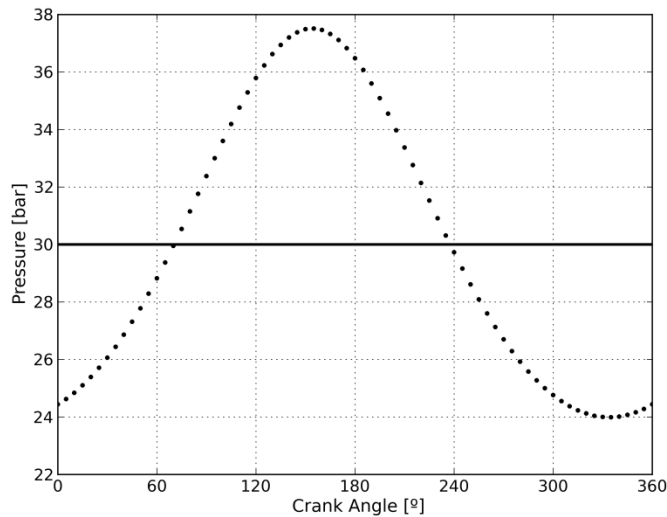
Figure 6.1 Gas pressure evolution along a complete cycle for a mean operating pressure of 30 bar.

Figure 6.2 shows the pressure versus total volume diagram (PV). This simulation was carried out considering a mean pressure of 30 bar. In the isothermal model, the compression and expansion spaces are maintained at the respective cold source and hot source temperatures during the cycle. External heat is only transferred from the working gas and to the working gas during the compression and expansion processes. The closed area defined by the cycle on the P-V diagram represents the net positive cycle work.
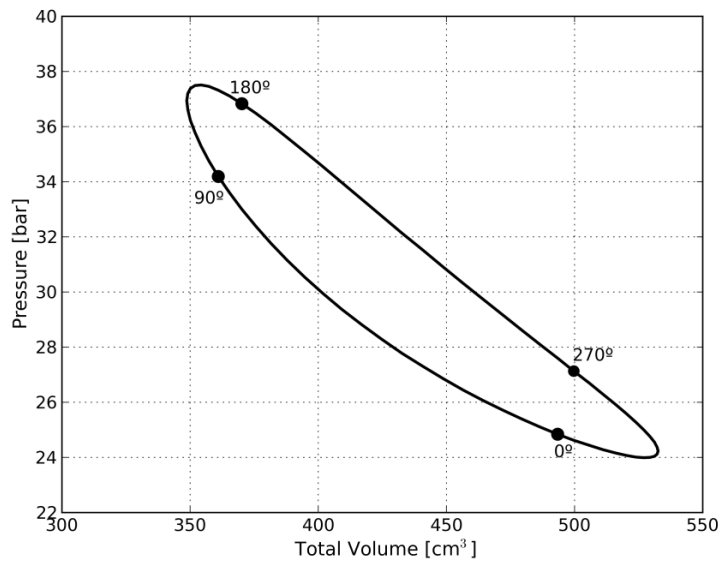
Figure 6.2 Pressure versus total volume diagram for the isothermal analysis at p_{mean} = 30 bar (reference θ points also included).

6.2.2 Ideal adiabatic analysis

In the Ideal Adiabatic Analysis, the working gas temperature in the heat-exchangers remains equal to the cold and hot source temperatures (perfect heat-exchanger). However, as the compression and expansion spaces are considered adiabatic, the respective temperatures will fluctuate during the cycle evolution. The

results indicate that the average gas temperature in the expansion space is lower than the hot source temperature and the opposite happens in the compression space, by comparison to the cold source temperature, see Figure 6.3. As a consequence of this lower temperature difference, the cycle thermal efficiency is reduced to 43.0%, when compared with the previous isothermal or Carnot efficiency of 51.3%. Table 6.3 presents the values of the thermal powers transferred in the heat exchangers and the engine output power considering engine speeds of 1500 and 3000 rpm for pressures of 5, 30, 50 and 80 bar.

Table 6.3 Results from the ideal adiabatic analysis considering different values of mean pressure and rotational speed

Rotational Speed [rpm]	1500				3000			
Mean Pressure [bar]	5	30	50	80	5	30	50	80
Heater Thermal Power $\dot{Q}_h$ [W]	570	3420	5700	9120	1140	6840	11400	18240
Cooler Thermal Power $\dot{Q}_k$ [W]	325	1949	3249	5198	650	3899	6498	10397
Net Power [W]	245	1471	2451	3922	490	2941	4902	7850

Regarding the results, the values of engine power are slightly lower, when comparing them with those obtained for the isothermal analysis (for the same mean pressure and rotational speed). For higher rotational speed values, the heat transferred in the heater is higher. In Figure 6.3 it is presented the temperature variation along a complete thermodynamic cycle.
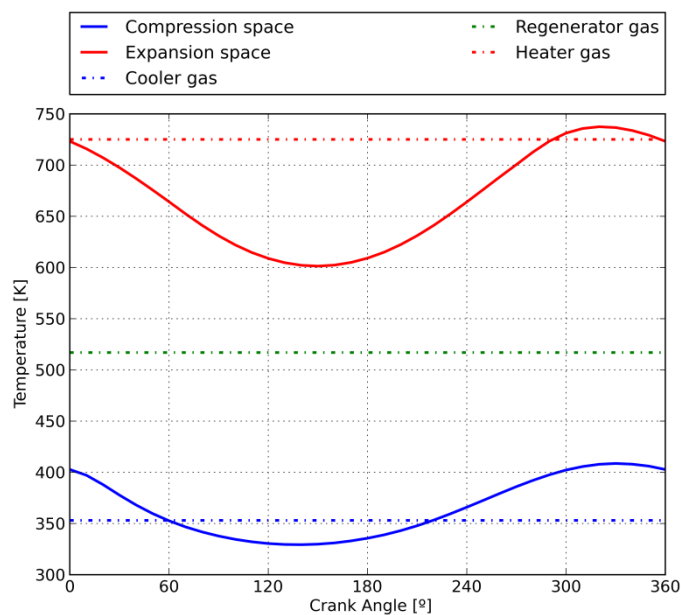
Figure 6.3 Temperature evolution in the heat exchangers, expansion and compression spaces.

The data shows that in the compression space T_c varies between 329.4 K and 408.7 K, while in the expansion space T_e changes from 601.4 K to 737.5 K.

For the same operational conditions, all the thermal energy fluxes and net total work output were analyzed along the ideal adiabatic cycle. These results are presented in Figure 6.4. A significant aspect is the amount of heat transferred in the regenerator. The maximum heat transferred to and from the regenerator matrix is much higher than the net energies transferred in the heater or in the cooler. This reveals the importance of this Stirling engine component. The energy rejected by the gas to the regenerator matrix, roughly in the first half of the cycle, is equal to the energy absorbed by the gas in the second half. Thus, globally, the heat transfer to the regenerator during a complete cycle is zero. The maximum total work reached over a complete cycle is 471.2 J for a mean pressure of 30 bar. As with the isothermal model, the network output per cycle is proportional to the mean pressure, and the mechanical power output is proportional to the mean pressure and rotational velocity.
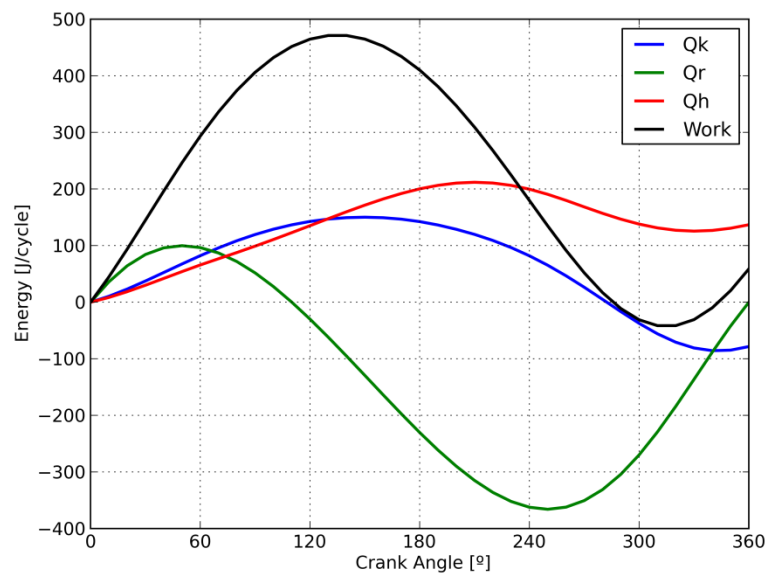
Figure 6.4 Energy variation diagram for a p_{mean} = 30 bar.

The compression and expansion work evolutions are presented in Figure 6.5. The expansion work (W_e) suffers a different process from the heat supplied in the heater (Q_h). Nevertheless, at the end of the cycle they reach the same value of 137 J/cycle (compare Q_h at Figure 6.4 with W_e at Figure 6.5). Similarly, the same behaviour is verified for the compression work (W_c) and for the heat rejected in the cooler (Q_k), reaching the same, 78 J/cycle. A perfect regenerator acts like a perfect insulator: the energy balance from the hot components (heater and expansion space) is isolated from the energy balance of the cold components (cooler and compression space).
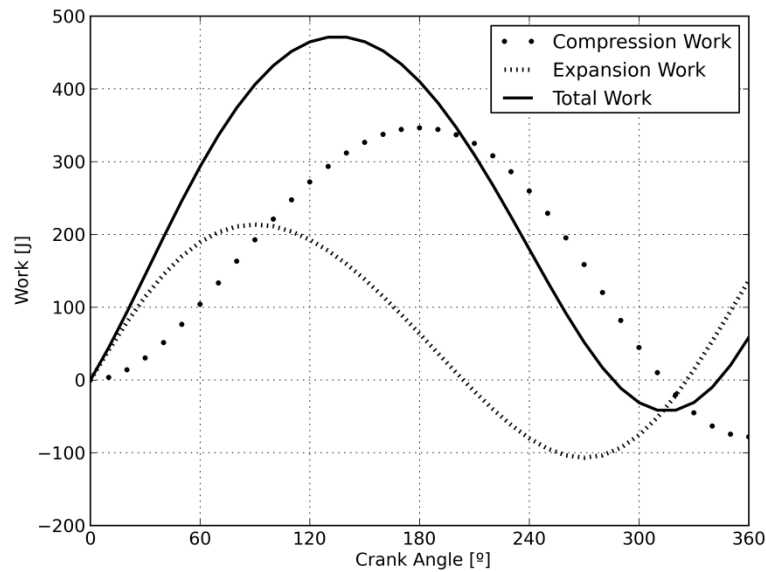
Figure 6.5 Compression and expansion work variation for a p_{mean} = 30 bar.

Figure 6.6 shows, separately, the pressure-volume diagrams for the compression cylinder (P-V$_c$), the expansion cylinder (P-V$_e$) and the total system volume (P-V$_{tot}$). The pressure rises during the compression phase followed by the gas pre-heating phase, where it gets to its maximum value. The minimum pressure occurs in the reverse process, when the working gas is pre-cooled and the volume is at maximum, after the gas has been expanded. The regenerator pre-heating and pre-cooling phases are not exactly isochoric due to the sinusoidal volume variations of the two pistons.
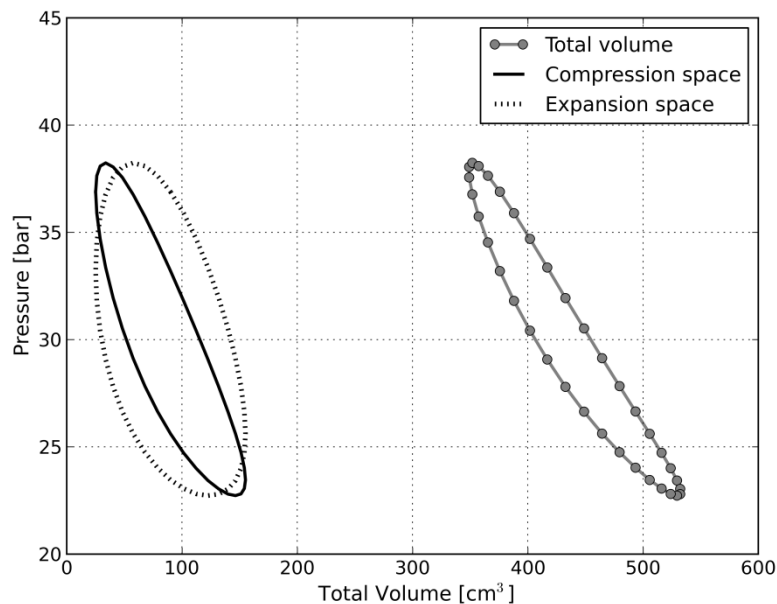
Figure 6.6 Pressure versus space volume diagrams for ideal adiabatic analysis at p_{mean} = 30 bar.

Comparing the isothermal and the ideal adiabatic analysis, the results are not so significantly distinct. For both analyses, the engine power is directly proportional to the mean pressure and engine speed and the

temperature of the heater and cooler are equal to the expansion and compression spaces, respectively. In the adiabatic analysis, the heat exchangers are considered ideal and they do not affect the engine efficiency. Thus, for a more conclusive analysis about the performance of Stirling engines, the quality of the heat exchangers should be taken into account, since they influence the engine efficiency.

6.2.3   Non-ideal analysis

In real engines, in addition to the hot source and cold source temperatures, the main factors that affect and reduce engine efficiency are heat-transfer limitations and pumping losses. Thus, in the optimal design of Stirling engines, the three heat-exchangers characteristics are crucial, namely the compromise between their thermal effectiveness and the pumping losses. These losses are due to the pressure gradient required to move the working fluid through the three heat exchangers (mainly the flow through the regenerator). All these effects were considered in the non-ideal analysis, and several simulations were carried out considering air, helium and hydrogen as working fluids. Table 6.4 presents the results corresponding to simulations performed at 1500 rpm and with mean cycle gas pressures of 30 and 80 bar.

Regarding the results in Table 6.4, the values of engine efficiency are much lower, especially with air, when comparing them with those obtained for the ideal adiabatic analysis. Heat exchangers effectiveness is an important parameter that influences the cycle thermal efficiency. In the adiabatic analysis, the heat exchangers are considered ideal and do not interfere with the efficiency of the engine (regenerator effectiveness equal to 100%). In the non-ideal analysis, the effectiveness of the heat exchangers has an impact in the efficiency of the engine.

The regenerator effectiveness for the non-ideal is higher when helium and hydrogen are used, by comparison with air. Purely in heat transfer terms, helium is slightly better than hydrogen. However, hydrogen's low viscosity and high thermal conductivity also contributes to a good performance.

Concerning engine performance, by comparing the three tested working gases, results show that the hydrogen is the best choice because it always results in the highest engine efficiency and power output. Nevertheless, for the same operational conditions, there is no significant difference in engine efficiency between helium and hydrogen. The difference is already noticeable in the case of the power output (relatively lower when helium is used), and may be explained by the higher volume-specific heat capacity ($\rho.C_p$) of hydrogen. The results with air are downright worse: the effectiveness of the three heat exchangers, the efficiency of the engine and the power output, all are significantly lower than with H_2 or He. . As to the influence of the mean operation pressure (proportional to the mass of working gas in the system), it is easily observed that the power output increases almost linearly with the mean pressure, while the efficiency deteriorates, mainly because of heat transfer limitations (reduction in the effectiveness of all heat-exchangers).

Table 6.4 Results from the non-ideal analysis considering a rotational speed of 1500 rpm

Mean Pressure [bar]	30			80		
Working Fluid	Air	He	H$_2$	Air	He	H$_2$
Real Hot source heat, Q$_h$ [J]	210.2	164.2	176.2	598.4	465.6	512.8
Real Cold source heat, Q$_k$ [J]	164.2	113.2	120.8	500.8	346.2	379.0
Work [J]	45.3	51.1	55.6	96.1	119.6	134.5
Power [W]	1133.7	1277.6	1390.4	2403.6	2990.6	3363.0
Work Losses [W]	12.33	3.37	1.56	26.4	6.38	2.98
Engine Thermal Efficiency [%]	21.82	31.1	31.6	16.25	25.7	26.2
Regenerator Effectiveness [%]	84.4	92.5	92.2	78.5	89.2	88.8
Heater Effectiveness [%]	39.8	57.4	56.6	32.4	48.3	47.6
Cooler Effectiveness [%]	28.9	43.0	41.9	23.8	36.0	34.9

Table 6.5 presents the results corresponding to simulations performed at 3000 rpm, again with. Simulations were run assuming a mean cycle gas pressures of 30 and 80 bar.

Results show that at higher rotational velocities, the hydrogen is the best choice because it achieves the best thermal efficiency when compare with the other two working gases. Also, when H$_2$ is the working gas, the results shows that the system is able to produce much power at the same operation mean pressures. The non-ideal results disclosed that the work losses are very low. Also, for He and H$_2$, work losses are even lower than the results obtained for the air. The working gas used should have a low heat capacity, so that a given amount of transferred heat leads to an increase in pressure. Regarding this issue, He would be the best choice because of its low heat capacity. Nevertheless, hydrogen's low viscosity and high thermal conductivity make it a powerful working gas, mainly because the engine have a higher power production at faster rotational speeds.

Comparing the two tested cases, 1500 and 3000 rpm, the effects are similar to those of the mean pressure: the power output rises nearly proportionally to the increase in rotational speed but the efficiency tends to decrease, mainly due to the rise in pumping losses but also to a reduction in the effectiveness of the heat-transfer processes. At 3000 rpm of speed, the numerical simulations, using helium as the working fluid, show again slightly better values in terms of effectiveness for the three heat exchangers, than with hydrogen.

Mean Pressure [bar]	30			80		
Working Fluid	Air	He	H_2	Air	He	H_2
Real Hot source heat, Q_h [J]	221.0	171.5	187.5	608.2	484.6	543.8
Real Cold source heat, Q_k [J]	181.1	124.6	135.4	533.6	382.6	424.1
Work [J]	36.6	46.4	51.9	68.3	101.2	119.7
Power [W]	1830.8	2318.1	2597.3	3413.7	5060.8	5985.2
Work Losses [W]	84.2	21.0	9.76	183.3	42.2	19.79
Engine Thermal Efficiency [%]	16.7	27.0	27.7	11.3	20.8	22.0
Regenerator Effectiveness [%]	80.4	90.33	89.9	73.4	86.3	85.7
Heater Effectiveness [%]	34.5	50.6	50.2	27.8	42.3	41.6
Cooler Effectiveness [%]	25.2	38.5	36.8	20.7	31.5	30.6

The gas temperature evolutions, in the expansion and compression spaces and in the heat exchangers, were also calculated for the non-ideal analysis. An example is shown in Figure 6.7, with air as working gas, at 3000 rpm and a mean pressure of 30 bar. The working gas temperatures in the compression and expansion spaces fluctuate along the cycle, while the mean effective temperature for the working gas within the heater and the cooler is now different from the hot source and cold sink temperatures, due to the non-perfect heat-transfer. Thus, for the adiabatic analysis, the values of the mean effective temperatures were calculated. Results show that mean effective temperatures in heater and cooler are, respectively, lower and higher than the corresponding heat exchanger wall temperatures (661.3 K and 443.4 K, correspondingly). It was also found that temperature at the expansion space could exceed the hot gas temperature and that the temperature at the compression space could be less than the cold fluid mean temperature, which could be explained by the adiabatic compression and expansion processes in the adjacent cylinders.

Due to the non-perfect heat-transfer, the average temperature of the working gas in the heater is lower than that of the wall. The same is verified in the cold side of the engine, where the mean temperature of the working fluid is higher than the wall temperature of the cooler.
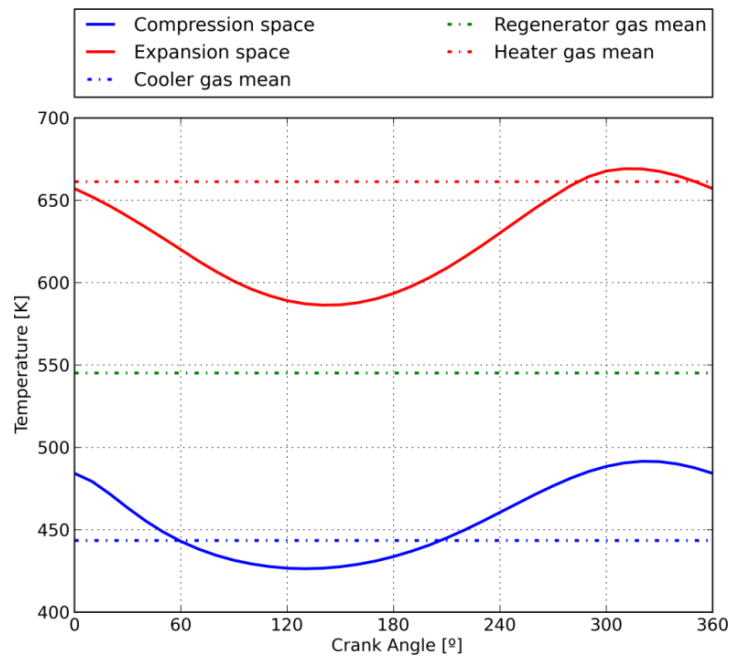
Figure 6.7 Temperature evolution in the heat exchangers, expansion and compression spaces for the non-ideal analysis (3000 rpm, air as working gas and mean pressure 30 bar).

Table 6.6 compares the mean gas temperatures in the heater, regenerator and cooler for the three working gases for a Stirling engine running at 3000 rpm and a mean pressure of 30 bar.

Results show that the hydrogen is the working gas that has the highest temperature difference between the hot and the cold heat exchangers. This result may be explained by the higher heat transfer capacity of the hydrogen when compared to those of helium or air. Accordingly, the power output suffers a reduction of 14.4% when changing from hydrogen to helium and 30.4% to air (based on data from Table 6.5). Furthermore, this reduction in power reaches greater values for higher mean operating pressures. The mean gas temperature of the working fluids in the regenerator it is very similar for the three gases and for all tested conditions.

Table 6.6 Comparison of mean gas temperatures at the three heat exchangers for Air, He and H_2 (3000 rpm and a mean pressure of 30 bar)

Working Fluid	Air	He	H_2
Heater	661.3	681.4	689.6
Regenerator	545.3	537.3	535.7
Cooler	443.4	415.1	406.7

Figure 6.8 presents the pressure drop evolutions, due to flow friction, along the three heat exchangers as a function of the crank angle θ. The results were obtained with the non-ideal engine simulation at 3000

rpm and 30 bar of mean pressure, for which the pressure drop, with the three working gases, is compared. It can be observed that air is the working gas which suffers higher friction when it flows through the heat exchangers while hydrogen is the one that shows the lowest pressure drops.

According to calculations, the work loss due to pressure drop for hydrogen is 9.76 W whereas for air the value is 84.2 W, which is a low value when compared with the total power produced (2597.3 W for hydrogen and 1830.8 W for air). There is a relationship between the work losses, the rotational speed and the mean pressure.
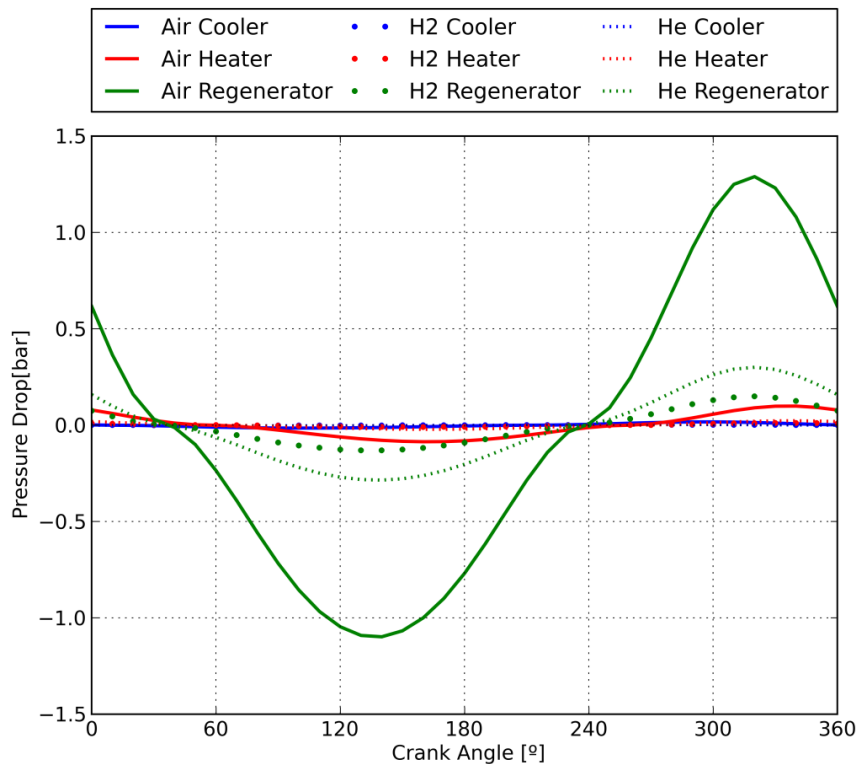
Figure 6.8 Pressure drop across the heat exchangers as a function of the crank angle θ, considering different working fluids: air, helium and hydrogen.

The evolution of work loss should be approximately quadratic with the mean pressure and a cubic evolution with rotational speed. The rise in engine frequency increases the mass flux through the regenerator, as well as, the pressure magnitude. An increase of the total mass of gas in the engine leads to a rise in the mass flow, gas velocity and function pressure. Therefore, an increase in the total mass of gas in the engine leads to more energy loss by pressure drop.

For the same gas, the variables that influence the pressure drop are the engine speed and the mean pressure (mass of gas in the system). To better evaluate the evolution of the pumping losses, they were calculated for 1500 and 3000 rpm and for different values of mean pressure, in a range between 5 and 80 bar. The results for those conditions are presented in Figure 6.9.
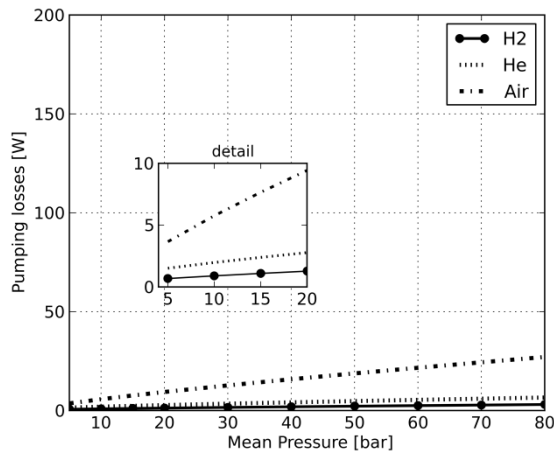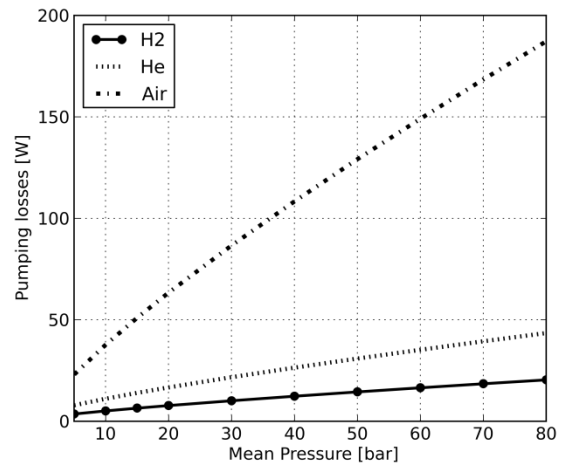
Figure 6.9 Pumping losses as a function of the mean pressure at 1500 rpm; **6.9-b** Work loss as a function of the mean pressure at 3000 rpm.

Mechanical losses should be taken into account because they affect the efficiency of the engine: on one hand, friction within kinematic linkages joints for the piston and displacer; on the other hand, the moving parts of the engine can lead to bigger friction forces.

Air is the working fluid where the power loss is higher, being its value significantly higher when compared with the helium and hydrogen. Also, for higher mean pressures, the variation of work is higher for air as the working gas. Results show that the rotation speed of the engine influences the magnitude of the work loss. For instance, at 1500 rpm and 5 bar of mean pressure, the work loss due to pressure drop for hydrogen is 0.68 W and 3.7 W for air, whereas, at 3000 rpm and 5 bar, the value is 3.6 W for hydrogen and 23.1 W for air. In fact, low-speed engines allow reducing viscous losses.

Making a comparison between the three gases, it is possible to conclude that hydrogen is slightly better than helium, mainly when the Stirling engine operates at high rotational speeds and pressures. The fact may be explained through their thermo-physic properties. In fact, the thermal diffusivity of helium is higher than that of hydrogen, which improves heat transfer, although the density and viscosity are also higher. Hydrogen has better results in terms of power, efficiencies and lower pressure drop. Moreover, low-pressure engines must operate at a higher speed to achieve reasonable specific powers, while high-pressure engines may operate at lower speeds. The use of air should be precluded in high specific-power engines, which require an important load of working gas (i.e. mean pressure) and high rotational velocities.

Figure 6.10 shows the pressure versus total space volume (P-V) for the non-ideal analysis, comparing the three gases under study. Comparing the three curves, it is verified that the non-ideal heat exchangers caused a deviation at the P-V diagram. The deviation is more noticeable for the air, than for hydrogen or helium, for which it is reached a higher pressure value during the thermodynamic cycle. The area

represented in the P-V diagram indicates the work that is done by the engine. From the graphical representation, it seems there is no significant difference in the area of each curve. Although, comparing the results obtained from Table 6.5 there is a significant reduction of the power and efficiency obtained of the air in relation to the helium and hydrogen: 1830.8 W of power and 16.7% of engine efficiency for air, whereas it was obtained a 2318.1 W of power produced and 27.0% of engine efficiency for helium and 2597.3 W of power produced and 27.7% of engine efficiency for hydrogen.
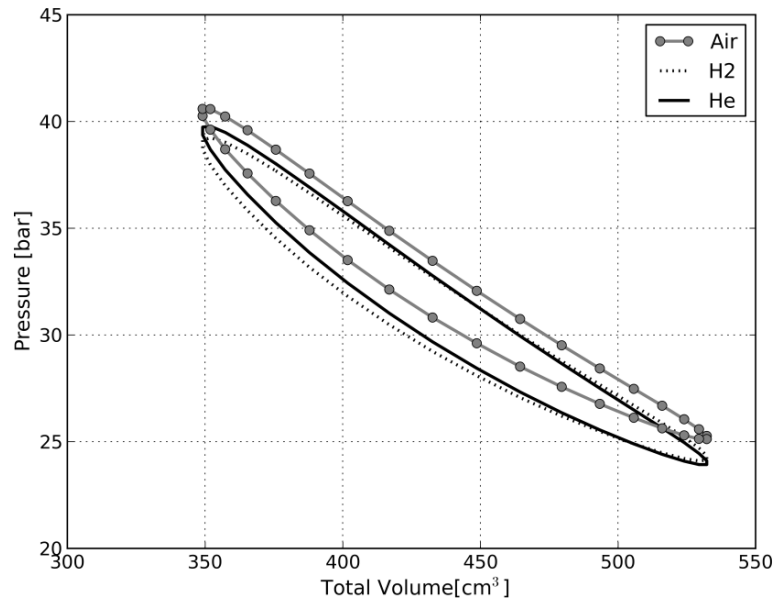
Figure 6.10 Pressure versus space volume diagrams for the non-ideal analysis at p_{mean} = 30 bar.

If the results from the non-ideal analysis are compared with the results from the ideal adiabatic, it is also verified a deviation (compare it with P-Vtot diagram at Figure 6.6), where the working gas experiences a higher pressure variation along the complete cycle.

6.3 Sensitivity Analysis of the Operational Parameters

The performance of the Stirling engine is affected by the operational parameters, which relevance should be studied. These operational parameters include the mean cycle pressure, rotational speed, dead and swept volumes ratio, working fluid type and heat source and sink temperatures. Note that all the results in this subsection concerns numerical simulations performed for the non-ideal analysis (i.e. accounting for the non-perfect regeneration and the pumping losses).

6.3.1 Mean pressure and rotational speed effect

The mean operating pressure is one of the operational parameters that most affects the Stirling engine specific power and efficiency. Engines operating at higher mean pressures represent larger costs in terms of materials (e.g. sealants). Figure 6.11 presents the variation of the engine efficiency as a function of the

mean pressure for two different rotational speeds (1500 and 3000 rpm) and with the three working gases.
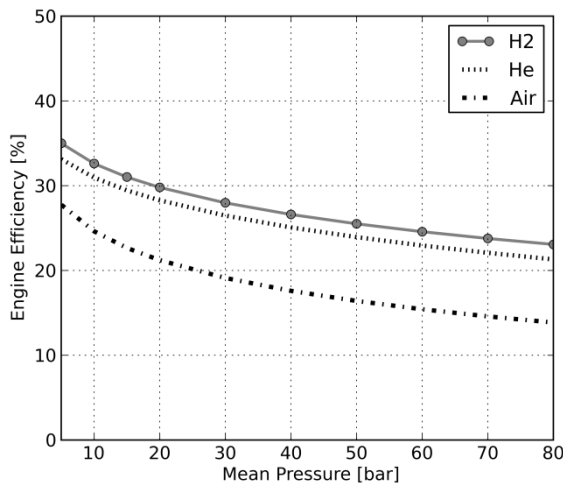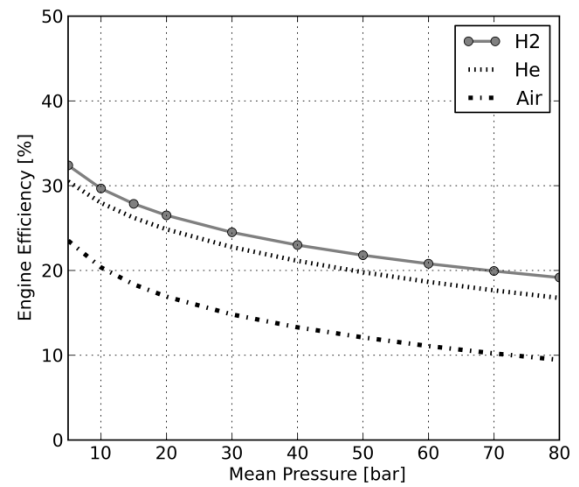
6.11-a   6.11-b

Figure 6.11-a Engine efficiency as a function of the mean pressure at 1500 rpm; **6.11-b** Engine efficiency as a function of the mean pressure at 3000 rpm.

According to the data, the engine efficiency decreases with the increase in mean pressure and when the engine runs at higher rotational speeds, for the three working fluids. Also, and as expected after the results of section 6.2.3, it is clearly shown here that the efficiency is much better when the working fluid is either hydrogen or helium by comparison to the case with air. For instance, with a mean pressure of 30 bar and 1500 rpm, there is a reduction of 31.7% in engine efficiency when changing from hydrogen to air, and of 27.8% in relation to helium. This means that in terms of engine efficiency, the best choice for the working fluid is hydrogen, closely followed by helium.

The heat exchangers effectiveness is an important parameter to understand the trends in the efficiency results. Figure 6.12 presents the heat exchanger effectiveness results considering helium, hydrogen and air at two different mean pressures of 5 and 30 bar. Both graphs correspond to simulations performed at 1500 rpm. The regenerator is the heat exchanger with higher effectiveness, above 90% in the cases of helium and hydrogen. This means that the ratio between the actual amount of heat transferred from the regenerator matrix to the working fluid and the maximum amount of heat transferred in the regenerator of the adiabatic model is near to one.

Results also show that the heat exchangers effectiveness is slightly higher for helium when compared with hydrogen. Purely in heat transfer terms, helium is slightly better than hydrogen. The effectiveness of the heat exchangers considering air as working gas is much lower than the other two working fluids, which is probably due to the low thermal diffusivity of the air. It is important to mention that the effectiveness of the heat exchangers was based on the NTU method explained in chapter 4, and included the determination of the Stanton number, which relates the heat transfer coefficient to heat capacity of the fluid stream per unit

cross-sectional area. Thus, the influence of geometrical parameters in the heat exchangers effectiveness must also be evaluated.

6.12-a   6.12-b
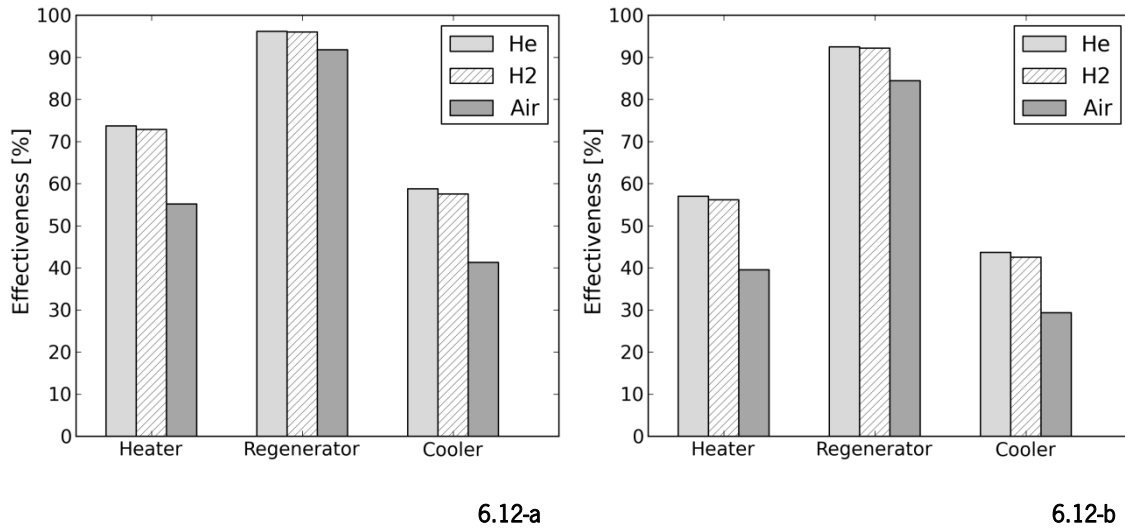
Figure 6.12 Effectiveness of the heat exchangers considering helium, hydrogen and air as working fluids: **6.12-a** at 5 bar of mean pressure; **6.12-b** at 30 bar of mean pressure.

Comparing the results for 5 and 30 bar, it is shown that the heat exchangers effectiveness decreases for higher values of mean pressure. This decrease is higher for the cooler and heater when compared with that of the regenerator. Obviously, the efficiency of the engine depends on several aspects, but it was already proved by numerous authors that the engine performance worsens when the heat-transfer capacity of the regenerator declines and is very sensitive to it (Timoumi, Tlili, & Ben Nasrallah, 2008; Tlili, Timoumi, & Nasrallah, 2008; Zarinchang & Yarmahmoudi, 2008, 2009). This was also explained in chapter 4, where the heat-transfer reduction Q_{rloss} was defined in terms of the regenerator effectiveness and represents extra heat that must be provided by the hot heat exchanger.

Figure 6.13 presents the the regenerator heat-transfer reduction Q_{rloss} (in J/cycle) as a function of the mean operating pressure for hydrogen, air and helium at the rotational speeds of 1500 and 3000 rpm. The results show that the heat-transfer reduction increases when the engine operates at higher values of mean pressure and velocity. The air is the working fluid for which the value of Q_{rloss} achieves a higher value: 259.1 J/cycle for 1500 rpm and 270.8 J/cycle for 3000 rpm. The working gas for which the regenerator enthalpy reduction is lower is the helium. This may be explained by the thermal properties of the working fluids. In fact, helium is inert and has a thermal conductivity near the hydrogen but it also has a volumetric thermal capacity even smaller than hydrogen, thus, presents the highest thermal diffusivity. So, the heater must provide a lower extra amount of heat when a Stirling engine operates with helium.
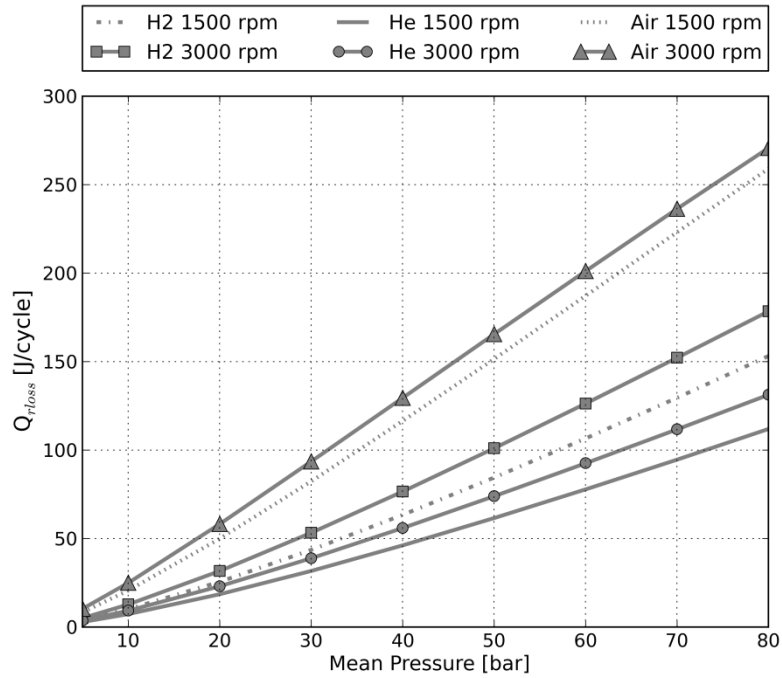
Figure 6.13 Variation of the regenerator heat-transfer reduction as a function of mean pressure for the three working gases.

6.3.2 Regenerator housing thermal conductance losses

The housing thermal conductance losses ($Q_{r,hlss}$) in the regenerator also affect engine efficiency. This aspect is influenced by the regenerator housing material. To reduce losses by conductivity alongside the regenerator and to the exterior, a material with high heat capacity and low conductivity must be chosen. Stainless steel and ordinary steel are the most suitable materials to be used for the regenerator housing. The evaluation of the engine performance taking into account the housing thermal conductance is presented at Table 6.7. The values were obtained for a numerical simulation at 30 bar of mean pressure and 1500 rpm of rotational speed. Results show that the engine efficiency decreases if the thermal housing conductance losses in the regenerator are taken into account.

Table 6.7 Evaluation of engine performance taking into account the regenerator housing thermal conductance

Working Fluid	Air		He		H_2	
Engine Output	Efficiency [%]	Power [W]	Efficiency [%]	Power [W]	Efficiency [%]	Power [W]
Not Including $Q_{r,hlss}$	21.8	1134	31.1	1278	31.6	1390
Stainless Steel	21.5	1146	30.6	1280	31.1	1391
Steel	20.9	1144	29.5	1277	30.0	1389
Carbon Steel	20.7	1143	29.2	1277	29.7	1388

Considering the tested materials for the regenerator housing (i.e. common steel, stainless and carbon steel) it is shown that: the lower the thermal conductivity of the material, the smaller conductance losses, which also results in better engine's efficiency.

6.3.3 Heat source temperature effect

As previously stated, there are numerous Stirling engine systems using different types of energy sources (e.g. GN, biogas, biomass or solar energy). Depending on the system, one of the most relevant parameters affecting the power and efficiency is the temperature of the hot heat source. According to Ahmadi, Sayyaadi, Dehghani, & Hosseinzade (2013), for solar- temperature Stirling engine, the thermal limit of the operation of the Stirling engine depends on working temperatures on the heater and cooler sides. According to them, the Stirling engines powered by solar-concentrator panels operate with heater and cooler temperatures varying between of 923 and 338 K, respectively.

Within the scoop of this project, a Stirling engine for CHP applications and wit a solar concentrator panel as the hot renewable energy source, a sensitivity analysis was carried out to evaluate the influence of the hot source temperature in the Stirling engine efficiency.

Figure 6.14 presents the variation of the engine efficiency as a function of the temperature of the heat source at 1500 and 3000 rpm for helium and hydrogen as working fluids. The cold sink temperature was kept at 353 K.

The results show that the engine efficiency rises with the increase of the temperature of the heat source but decreases with the increase of the mean pressure. According to the results, the engine efficiency is relatively lower when the engine operates at higher values of rotational speed. Comparing the results of hydrogen and helium, the engine efficiency is slightly higher when hydrogen is the working gas.
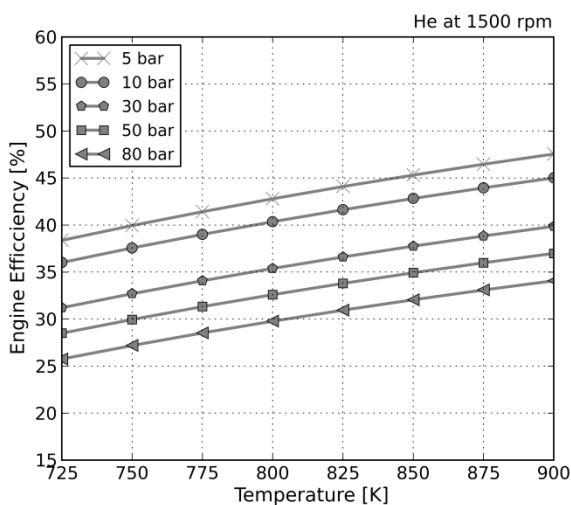
6.14-a
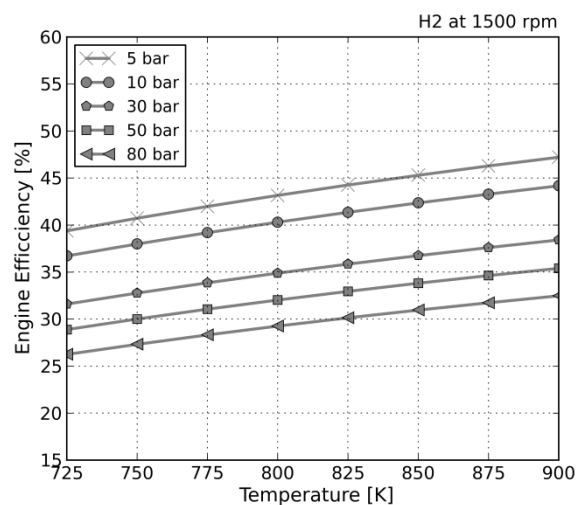
6.14-b
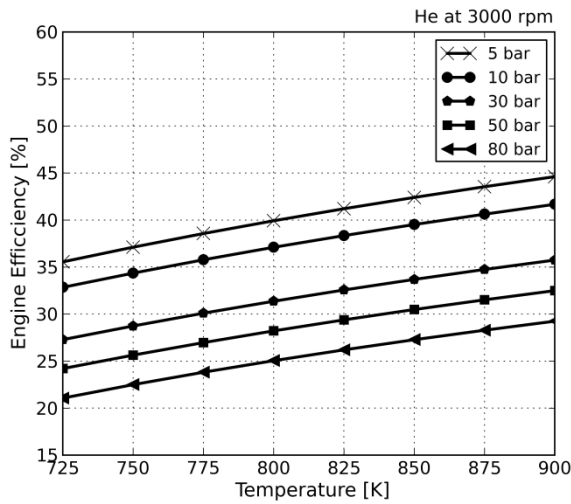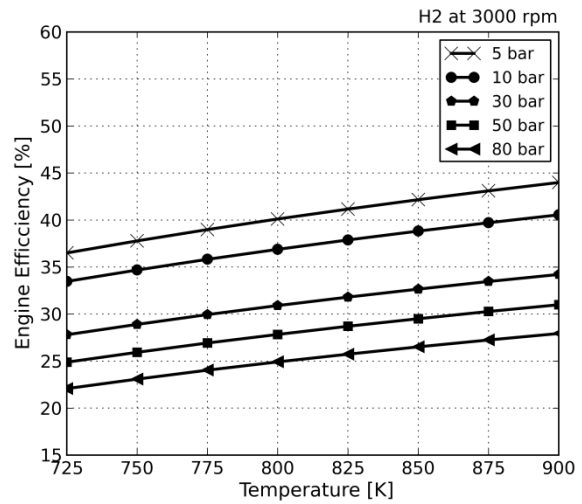
<div align="center">6.14-c   6.14-d</div>

Figure 6.14 Variation of the engine efficiency as a function of the hot source temperature: **6.14-a** for helium at 1500 rpm; **6.14-b** for hydrogen at 1500 rpm; **6.14-c** for helium at 3000 rpm; **6.14-d** for hydrogen at 3000 rpm.

Furthermore, the engine running with hydrogen is able to produce higher values of power when compared with helium. Despite the results for air are not shown graphically, it was verified that the thermal efficiency is much lower compared to hydrogen and helium.

The increase of the heat source temperature also affects the power produced by the engine. The numerical simulations allowed to conclude that, for a range of 175 degrees of temperature (i.e. 725-900 K), the increase in power production is 25.8% for helium (5 bar, 1500 rpm), whereas, for hydrogen, it corresponds to an increase of 23.4%, (5 bar, 1500 rpm). This means that an increase in the heat source temperature as a relatively higher influence in the engine power production when helium is used. The heat source temperature also affects the effectiveness of the heat exchangers. According to the results, for the same temperature increase, the higher variation in terms of effectiveness is registered for the heater, as presented in Table 6.8. The effect of the heat source temperature at the regenerator and cooler is residual (an increase equal or below 1%). The increase of heat exchanger effectiveness is also strengthened by the increase in mean operating pressure.

Table 6.8 Variation of heat exchangers effectiveness with hot source temperature increase (725 to 900 K)

	5 bar, 1500 rpm		80 bar, 1500 rpm	
Heat Exchanger	He	H_2	He	H_2
Heater	+2.45%	+3.50%	+5.03%	+5.07%
Regenerator	+0.31%	+0.33%	+0.83%	+0.88%
Cooler	+0.78%	+0.90%	+0.96%	+1.13%

An increase in heater temperature will increase thermal efficiency and total input heat (i.e. the total heat that is transferred from the hot source).

6.3.4 Relationship for engine power, swept volumes and dead volumes

The un-swept volumes, also called dead volumes, in a Stirling engine should be kept theoretically near to zero, but in practice there is a percentage of the total engine internal gas volume that is accounted as dead volume. Some of these extra inside spaces are due to the components connection and other useful volumes inside the engine cylinders. Accordingly to Thombare and Verma (2008) the increase in dead volume results in a loss of power but not necessarily a reduction in efficiency. Its effect on the engine efficiency depends on the location of the dead volume. Considering the fixed configuration presented at sub-section 6.1, all the heat exchangers have a fixed void volume, which corresponds to 84.8 cm^3 for the heater, 69.8 cm^3 for the regenerator and 106.0 cm^3 for the cooler. Also, for that configuration, the total dead volume of 2X25 cm^3 represented almost 20% of the swept volume of the two cylinders, each of them with a swept volume of 130 cm^3.

To investigate the influence of swept and dead volumes several groups of simulations were carried out. In the first one the influence of the swept volume in engine performance was analysed. Notice that the simulations were carried out considering a mean pressure of 30 bar for different rotational speeds, using helium as working fluid and maintaining the size of the heat exchangers. Figure 6.15 illustrates the variation of the power as a function of the swept volume.
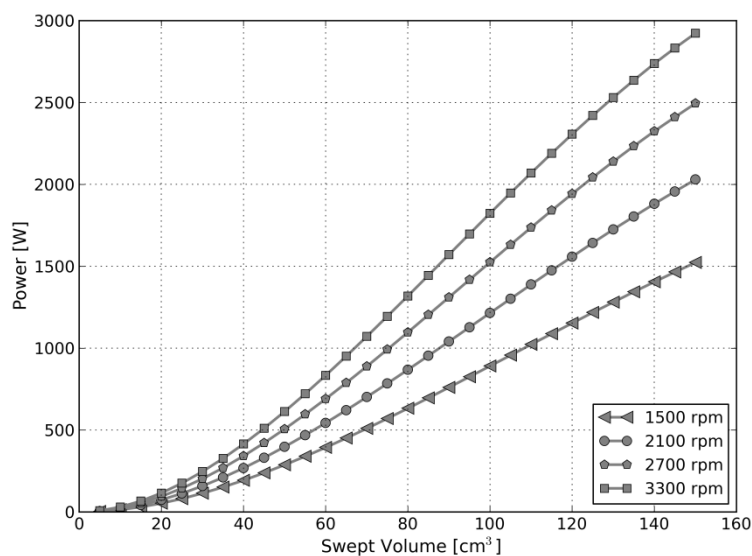
Figure 6.15 Variation of the engine power with the swept volume for different rotational speeds (P_{mean}=30 bar, He).

The results show that the power output rises with the increase in the swept volume of the cylinders. Again, it is also noticeable that the power increases with the increase in rotational speed. The efficiency of the engine was also calculated for the different swept volumes and rotational speeds values as depicted in

Figure 6.16. It is shown that the engine efficiency rises when the swept volume increases until an optimal value. Also and again, higher values of efficiency are obtained for lower values of rotational speed. These remarks imply that, at several values of rotational speed, there exists an optimal value of swept volume for which maximum engine efficiency is obtained. From all these analysis, it may be said that net cycle power is direct function of the engine speed, the pressure of the working fluid and the size of the engine, which is expressed in terms of swept volume.
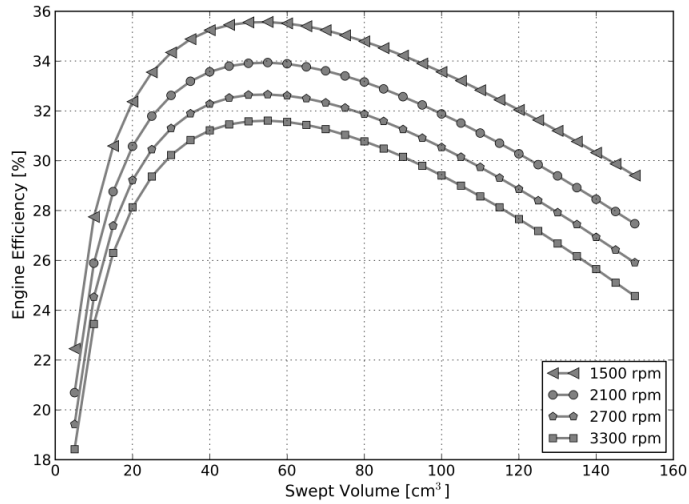
Figure 6.16 Variation of the engine efficiency with the swept volume for different rotational speeds (P_{mean}=30 bar, He).

It is also important to understand the relationship between the variation of dead volume and the performance of the engine (i.e. engine efficiency). A simulation was carried out considering a fixed swept volume of 130 cm³ per cylinder and varying the dead volume. The values of the power output and engine efficiency were calculated as a function of the dead volume and the results are presented in Figures 6.17a and 6.17-b.
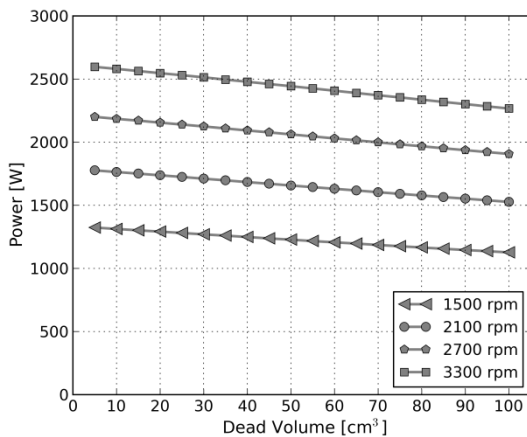
6.17-a
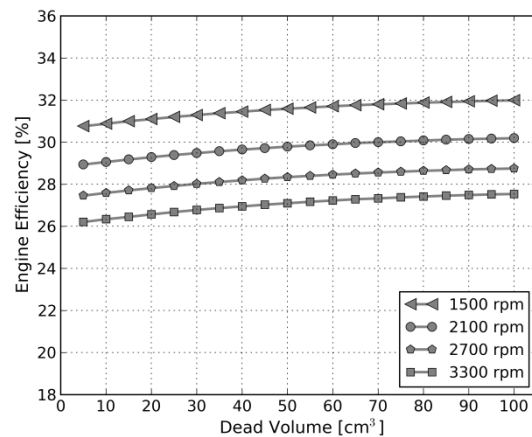
6.17-b

Figure 6.17-a Power output and; **6.17-b** Engine efficiency variation with the dead volume for different rotatinal speeds (P_{mean}=30 bar, He).

It was also verified that the power output of the engine slightly decreases for higher dead volumes in the engine cylinders. The engine efficiency presents a slightly increase with the growth of dead volume. However, from a certain value of dead volume, it appears that the engine efficiency stabilizes and there is no variation. Asnaghi, Ladjevardi, Saleh Izadkhast and Kashani (2012) in their studies concluded that a real Stirling engine must have some unavoidable dead volume. In normal Stirling engine design practice, the total dead volume (i.e. the total dead volumes from the cylinders, connections and heat exchangers) is approximately 58% of the total volume. According to Wu, Chen, Wu and Sun (1998) a certain amount of dead volume is required to allow sufficient heat transfer surfaces. So, it is important to estimate the relationship between the swept and dead volumes and how it affects the power production and the efficiency of Stirling engines. Since it has been decided to adopt the alpha-type configuration, the compression swept volume ($V_{sw,c}$) should be equal to the expansion swept volume ($V_{sw,e}$). Nevertheless, the direct effects of the swept /dead volume ratio (V_{sw}/V_d) should be detailed in terms of the engine performance. Thus, the power produced by the engine is evaluated considering the variation of the swept /dead volume ratio.

Figure 6.18 presents the relationship between the power production and the swept/dead volume ratio. Results show that the amount of power production does not have a significant variation when a V_{sw}/V_d ratio is above the 6. For swept/dead volume ratios below of 4, the power production decreases sharply. Results also indicate that the power production is proportional to the engine rotational speed.
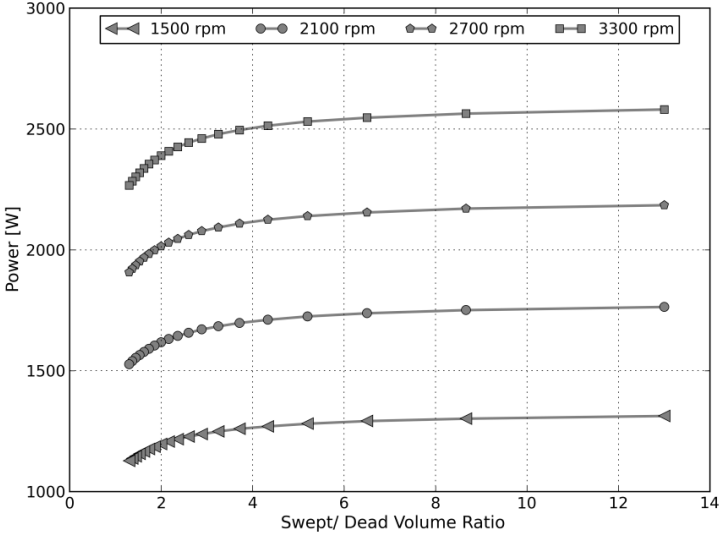
Figure 6.18 Power output as a function of the swept/dead volume ratio for different frequencies (P_{mean}=30 bar, He).

In conclusion, it is observed that an increase in dead volume has a reduced effect in the thermal efficiency but reduces the engine specific power. In contrast, an increase in swept volume while keeping the heat-exchangers size, significantly affects the engine thermal efficiency.

6.4 Sensitivity Analysis of the Geometrical Parameters of Heat exchangers

The Stirling engine performance depends on geometrical and operational characteristics of the engine and its thermal components. Thus, this sub-section presents a sensitivity analysis to the geometrical parameters of the heat exchangers (i.e. cooler, heater and regenerator), where the aim is to analyse the influence of the internal diameter of the tubes, the heat exchanger length, the number of tubes (i.e. for the cooler and heater); and the porosity and the diameter of the regenerator matrix wire in the performance and efficiency of the Stirling engine. To investigate the influence of these parameters on the engine performance, they were studied individually and, at each simulation, the others were kept unchanged and equal to the base case scenario of table 6.1. All the results in this sub-section are referent to simulations performed for a mean pressure of 30 bar and a rotational speed of 3000 rpm. He was the working gas used to perform the sensitivity analysis.

6.4.1 Heater geometric parameters

As previous described in chapter 4, the physical model only considers the convective heat transfer from the internal wall of the heater tubes to the working gas, and assumes a constant temperature at the outer surface of the heater. Changing the geometrical parameters affects the heat transfer between the tubes wall and the gas because the convective heat transfer coefficient will change, as flow conditions are altered, and because the heat transfer area will change too. Thus, the heat transfer may be significantly affected by the heater tubes inner diameter, the heater length and the number of tubes, which are used to define the contact heat transfer area. The values of these variables for the base case scenario were 3 mm, 150 mm and 80, respectively, see table 6.1.

Figure 6.19-a shows the engine efficiency and the heater effectiveness variations with the number of heater tubes. Results show that the engine efficiency slightly increases with the number of the heater tubes, namely from 23.6% to 28.1% with a six-fold increase in the number of tubes from 20 to 120. The heater effectiveness also increases with the number of tubes, with a variation of 15.9%. This variation is probably due to the increase of the heat transfer area with the increment of tubes in the heater. Nevertheless, it was also verified that the convective heat transfer coefficient decreases due to lower flow velocities.

The power ouput was also calculated, as presented in Figure 6.19-b. Results show that the power production increases with the number of the heater tubes until a certain value. This value corresponds to a power of 2345 W, which was obtained for a number of heater tubes between 60 and 65. This means that, for a heater configuration with a set of smooth tubes 150 mm in length and 3 mm inner diameter, the optimum number of tubes corresponds to 60-65 tubes to achieve the maximum power output and an engine efficiency of 26.6 - 26.8%, respectively. Increasing the number of the tubes also reduces the fluid

frictional work in the heater. Nevertheless, of some point, the increase in the void volume of the heat exchanger overlaps the benefits obtained from a lower friction and better heat transfer when rising the number of heater tubes.
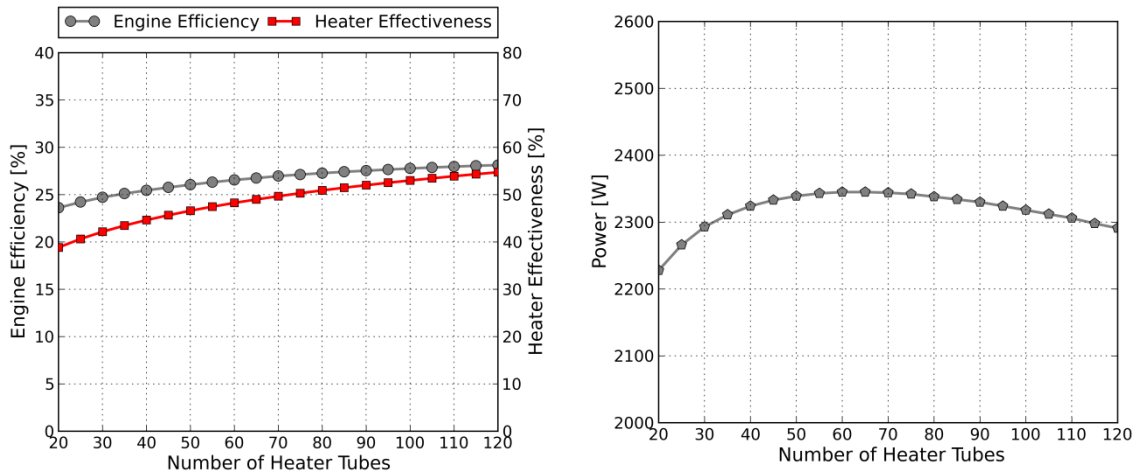
6.19-a

6.19-b

Figure 6.19-a Engine efficiency, heater effectiveness and **6.19-b** Power ouput as a function of the number of heater tubes.

The heat transfer coefficient and the friction are two parameters of prime importance for the internal heater surfaces. When analysing the convective heat transfer coefficient and the pumping losses at Figure 6.20-a and Figure 6.20-b, it was verified that these two parameters decrease with the rise in number of tubes. From the analysis, it was found out that the heat transfer, and hence the overall performance, is slowly improved by increasing the number of tubes. A reasonable evaluation of benefits of increasing the number of tubes in terms of efficiency and the reduction in power ouput must be taken into account.
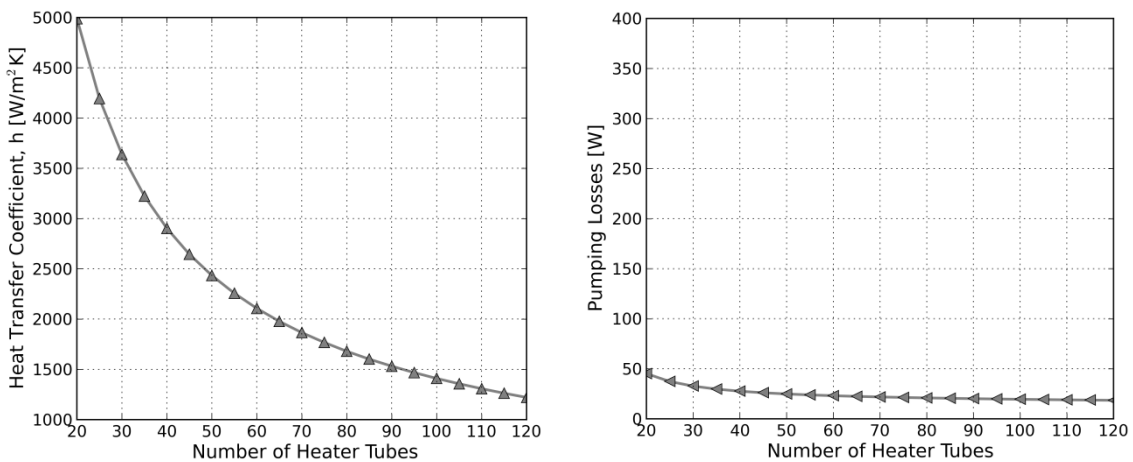
6.20-a

6.20-b

Figure 6.20-a Heat transfer coefficient and **6.20-b** Pumping losses variation for different number of heater tubes.

The internal diameter of the heater tubes is also an important parameter that affects the pressure drop. A variation between 1.0 mm and 8.0 mm has been studied and the results of engine efficiency and heater effectiveness are presented in Figure 6.21-a. They show that the increase of the internal diameter leads to a strong decrease in the heater effectiveness (from 80.0% to 29.0%). This outcome is probably due to a reduction of the convective heat transfer coefficient. Regarding the engine efficiency, the maximum value is achieved for an internal diameter of 4.0 mm. Nevertheless, the power output (Figure 6.21-b) reaches the highest value at lower diameters (i.e. maximum power of 2560 W for an internal diameter of 1.5 mm).
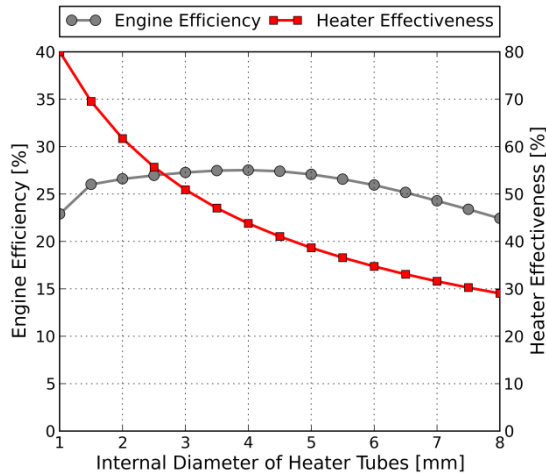
6.21-a
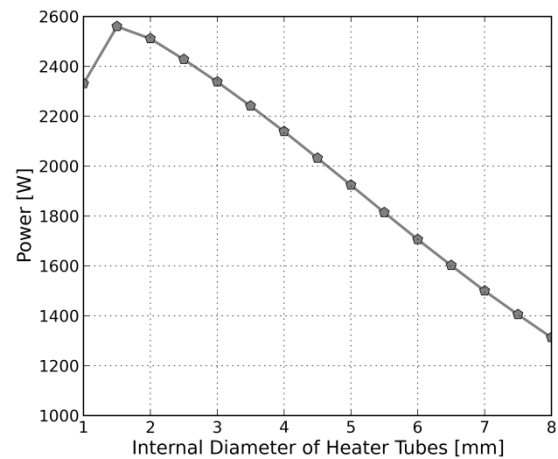
6.21-b

Figure 6.21-a Engine efficiency, heater effectiveness and **6.21-b** Power output as a function of the internal diameter of the heater tubes.

Increasing the internal diameter also reduces the friction between the gas and the heater walls, which results in lower pumping losses, as depicted in Figure 6.24. This outcome is in agreement with the analysis of Zarinchang and Yarmahmoudi (2008) who claimed that an increase in tube diameter produces large reductions in pressure drop due to the reduction of fluid friction.
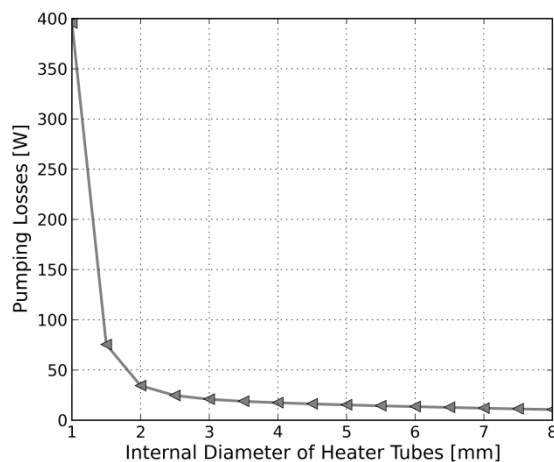
Figure 6.22 Pumping losses variation as a function of the internal diameter of the heater tubes.

The length of the heat exchanger tubes is also an important parameter to investigate. The simulations have been performed by considering tube lengths in the range of 20 mm to 200 mm. Figure 6.23-a and Figure 6.23-b present the results for the engine efficiency and heater effectiveness and power output.
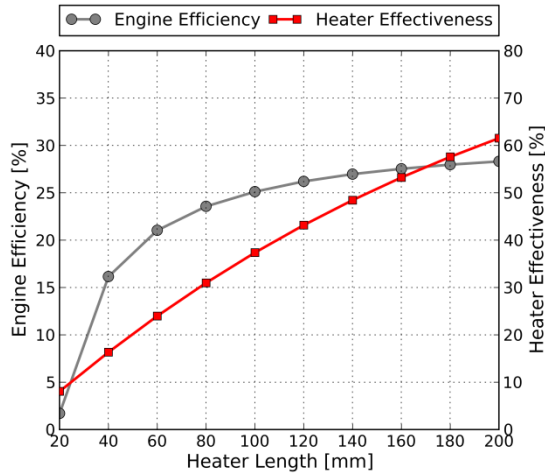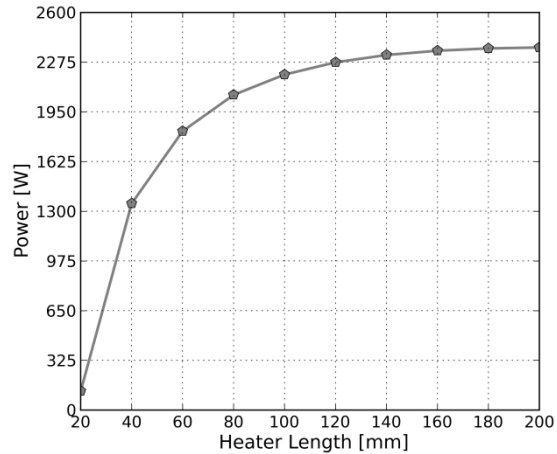
6.23-a   6.23-b

Figure 6.23-a Engine efficiency, heater effectiveness and **6.23-b** Power output as a function of the heater tubes length.

The results show that the heater effectiveness rises almost linearly with the increase of the heater length and is easily explained by the corresponding increase in the heat transfer area. The engine efficiency also improves, but its value shows no relevant variation for heater tubes above 140 mm of length. According to the data from the Figure 6.23-b, it is verified that the power increases continuously with the heater length (but again with no relevant improvement above 140 mm) and this can be explained by the implicit increase in the effectiveness of heat transfer process versus smaller increases in void volume and pumping losses. To improve the engine performance, a certain combination of input geometrical parameters is required. Analysing the results, probably the best combination of parameters relies on heater tubes with a diameter of 4.0 mm, with a length above 100 mm. In terms of number of tubes, if the maximization of the power output is one of the required improvements, the number of tubes should not be more than 80 (considering the commitment between the engine efficiency increase and the no relevant power output reduction).

6.4.2   Regenerator geometric parameters

The efficacy of the regeneration process is very important in the engine performance because, along the thermodynamic cycle, heat transfer reductions in the fluid pre-heating and pre-cooling processes leads to increases in the hot and cold energies and thus to an important decay in engine efficiency. The maximum

efficiency of this process would only be achieved if the heat transfer coefficient or the area of heat transfer and matrix capacity is infinite. However, the working gas does not have a null heat transfer capacity neither the regenerator matrix has an infinite heat capacity. To improve the regenerator heat transfer, it is of utmost importance to establish a commitment between heat transfer and fluid friction.

In that way, the regenerator geometry and the variations in matrix wire diameter and porosity are studied in order to understand their influence in engine and regenerator performance. Figure 6.24 presents the results of the engine efficiency and regenerator effectiveness for different regenerator lengths.
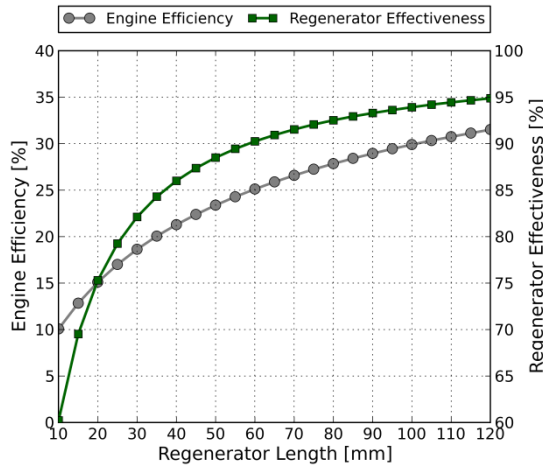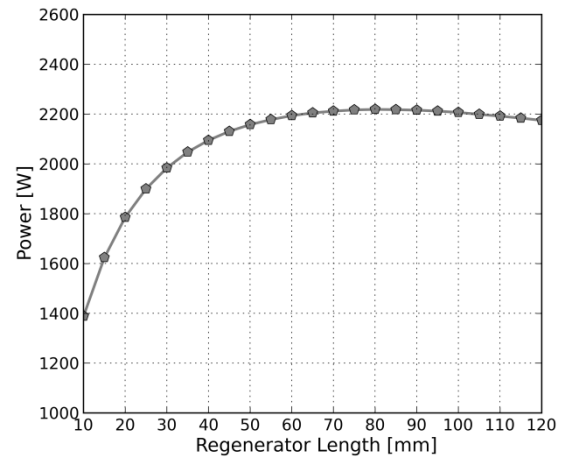
6.24-a   6.24-b

Figure 6.24-a Engine efficiency, regenerator effectiveness and **6.24-b** Power output as a function of the regenerator length.

Results for the engine efficiency and the regenerator effectiveness show a similar trend. According to the results, both rise with the increase of regenerator length. Regarding the power ouput, it is observed that there is no significant variation from 70 mm of length onwards. The additional dead volume and the increase in the pressure losses lead to a maximum power for a length of 80 mm. However, for small regenerator lengths (i.e., below 30 mm), the power, as well as, the efficiency quickly decreases, as presented in Figure 6.24-b.

Figure 6.25-a presents the engine efficiency and the regenerator effectiveness as a function of the internal diameter. It is noteworthy that the thickness of the regenerator wall was kept constant for calculations. Results show that both the engine efficiency and the regenerator effectiveness increase with the internal diameter of the regenerator. The maximum power produced is obtained for an internal diameter of 60 mm. One of the major drawbacks of the regenerator is the great value of fluid friction, and one of the ways to reduce it is to increase the diameter of the regenerator, which was confirmed (a reduction of 396 to 20 W for the pumping losses). Nevertheless, for real conditions, increasing the diameters also leads to the increase in conduction losses. Comparing the results from the internal diameter and the regenerator

length, it is observed that variations in length produce larger changes in engine efficiency and regenerator effectiveness.
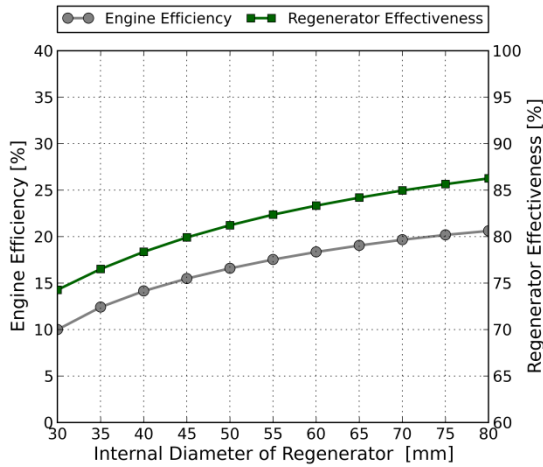

6.25-a   6.25-b

Figure 6.25-a Engine efficiency, regenerator effectiveness and **6.25-b** Power output as a function of the internal diameter of the regenerator.

Thus, for the regenerator optimization, considering the length as a decision variable is probably more reasonably than the regenerator diameter. The porosity of the regenerator is also an important parameter for engine performance. It affects the hydraulic diameter, dead volume, velocity of the gas, regenerator heat transfer surface and regenerator effectiveness; and thus, affects the losses (Timoumi et al., 2008; Tlili et al., 2008).

Figures 6.26-a an 6.26-b present the performance results for several combinations of matrix porosities and matrix wire diameters.
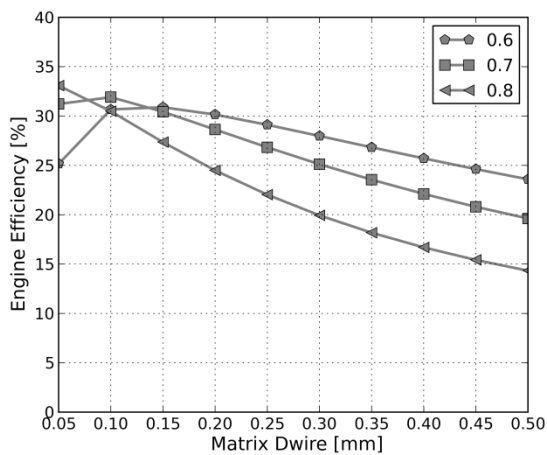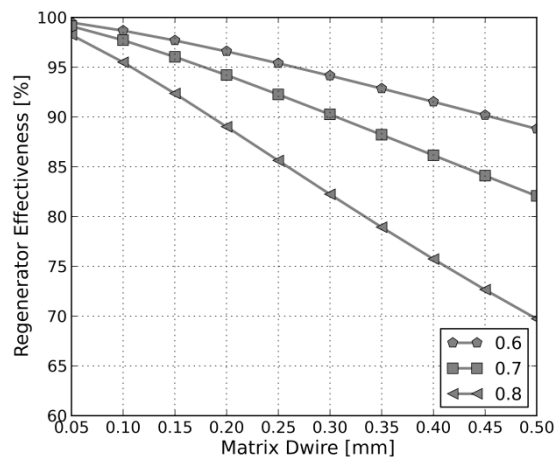
6.26-a   6.26-b

Figure 6.26-a Engine efficiency and **6.26-b** Regenerator effectiveness for different combinations of matrix wire diameter and porosities (0.6, 0.7 and 0.8).

The results indicate that any changes in the porosity leads to great variations in the regenerator effectiveness and pressure drops, which eventually affects the engine efficiency. It was expected that if the wetted surface area is large, the resulting porosity should be low, providing to the working gas the largest contacting surface to achieve the highest rate of heat transfer. Still, for wire diameters bellow 0.1 mm, results show that the highest engine efficiency is obtained for a matrix porosity of 0.7. For bigger values of wire diameter, the engine efficiency is higher when the porosity is lower (i.e. equal to 0.6). The regenerator effectiveness decreases with the rise of the wire diameter and with the matrix porosity as shown by (Figure 6.26-b).

Figure 6.27 presents the power outputs for the same combinations of matrix porosities and wire diameters. The power outputs have a similar trend to the engine efficiency evolutions: for lower wire diameters (0.1 mm) the power output is maximum when a porosity of 0.7 is assumed; for wire diameters above 0.2 mm, the power output is higher if the regenerator matrix has a porosity of 0.6.
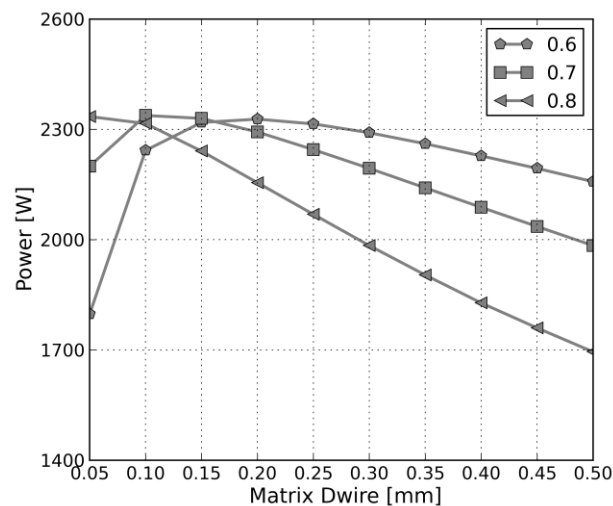
Figure 6.27 Power outputs for different combinations of matrix wire diameters and porosities (0.6, 0.7 and 0.8).

Figure 6.28 presents the pumping losses for the previously combinations of mesh wire diameters and porosities. Results show that for lower values of mesh porosity, the friction factor is higher and so do the pumping losses. Hence, it can be said that for lower diameters (between 0.05 and 0.1 mm) , the pumping losses experiences a sudden and sharp drop, for intance, for a porosity of 0.7, between 0.05 and 0.1 mm, the pumping losses increase by 182 W. The lowest pumping losses are obtained with the curve for the porosity of 0.8.

It may be said that in order to obtain a higher porosity, and thus a lower pressure drop, the meshes should be made from wire with very small diameters and should be coarse.
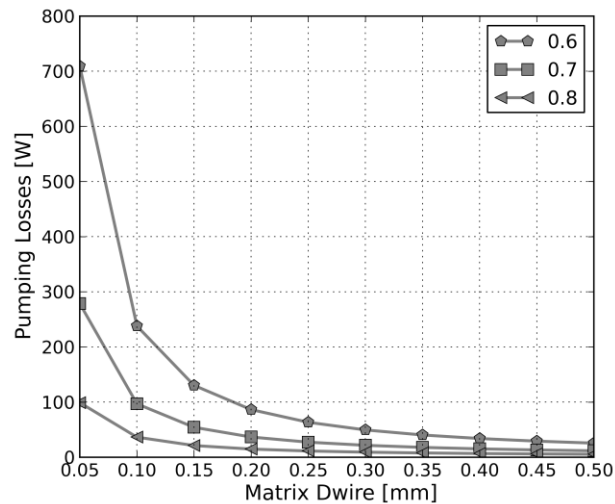
Figure 6.28 Pumping losses variation for different combinations of mesh-wire diameters and regenerator porosities (0.6, 0.7 and 0.8).

From the analyses of regenerator parameters, there is a range of combinations that benefit both engine and power efficiency. The best matrix should compromise between high effectiveness and low-pressure drop in order to obtain minimal losses in the regenerator. In conclusion, the best engine performance is obtained for lower wire mesh diameters (0.1 mm) combined with a mesh porosity of 0.7. For larger wire diameters a lower porosity (0.6) gives better results.

6.4.3 Cooler geometric parameters

The internal flow conditions in the cooler tubes are quite similar to the heater but at lower temperatures and pressures. To reduce the temperature of the working fluid an outside flow of water is used as a cold sink. Thus, heat transfer phenomenon includes the convective heat transfer from inner working gas to the inner wall of the cooler tubes, the conductive heat transfer through the tube wall and the outside convective heat transfer to the coolant, the water. Figure 6.29-a shows the engine efficiency and the cooler effectiveness evolutions as a function of the number of the cooler tubes. Results show that the engine efficiency increases with the number of the cooler tubes, showing an improvement of 16.8% in the tested range (40 to 160 tubes). The results from the cooler effectiveness show that the increase of the number of cooler tubes does not affect it significantly, only a variation of 8.0% in the cooler effectiveness is observed. The power production presents a great increase with the rise of the tubes number. These results may be explained by the counterbalance between the gains in heat transfer (i.e. increase of the heat transfer area) and the reduced pumping losses.
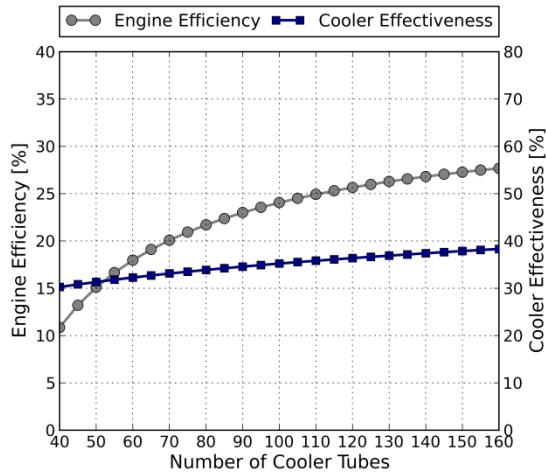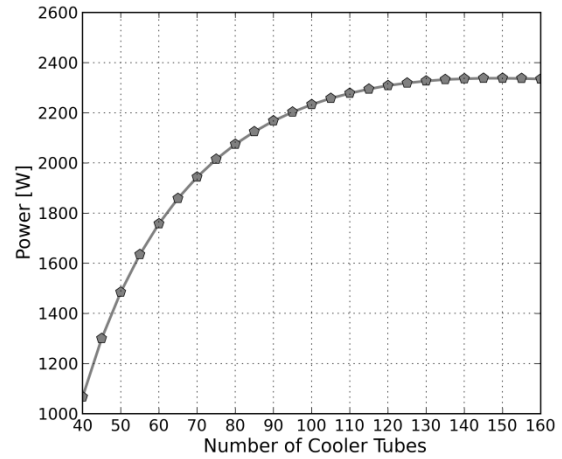
6.29-a   6.29-b

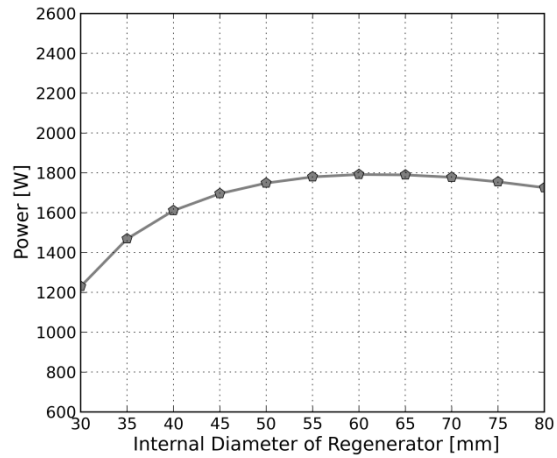**Figure 6.29-a**. Engine efficiency, cooler effectiveness and **6.30-b** Power output as a function of the number of the cooler tubes.

Figure 6.30-a presents the engine efficiency and the cooler effectiveness for different values of the internal diameter of the cooler tubes. The cooler effectiveness, similarly to the heater results, decreases with the rise in internal diameter. Also, the engine efficiency reaches its maximum value for an internal diameter of 4.0 mm. It is also noted that increasing the internal diameter leads to a reduction in the power output (see Figure 6.30-b).
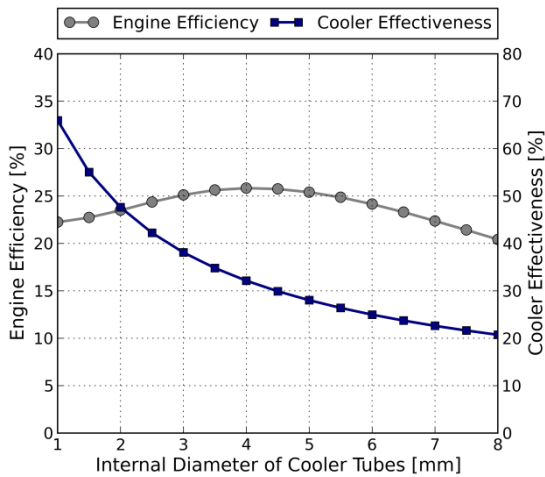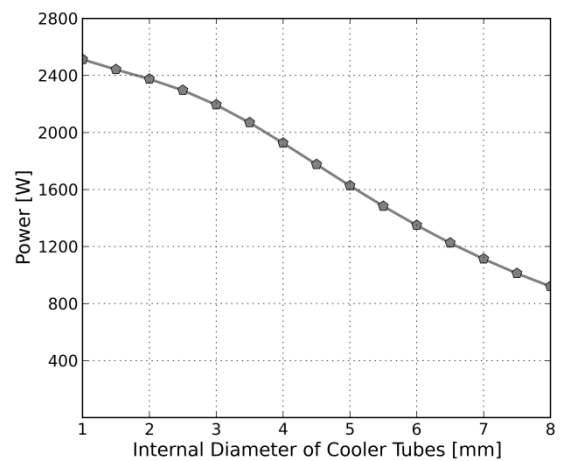
6.30-a   6.30-b

Figure 6.30-a Engine efficiency, cooler effectiveness and **6.30-b** Power output as a function of the internal diameter of the cooler tubes.

Figure 6.31-a presents the engine efficiency and the cooler effectiveness for different values of the cooler tubes length. A range between 40 mm and 240 mm was considered to study the length influence in the Stirling efficiency. It is observed that the engine efficiency and the cooler effectiveness increase with cooler

length, probably due to the gains in heat transfer with the increase of the contact area. Nevertheless and accordingtly to Figure 6.31-b, for lengths larger than 120 mm (where the maximum power is achieved, 2244 W), the power output starts to decrease.
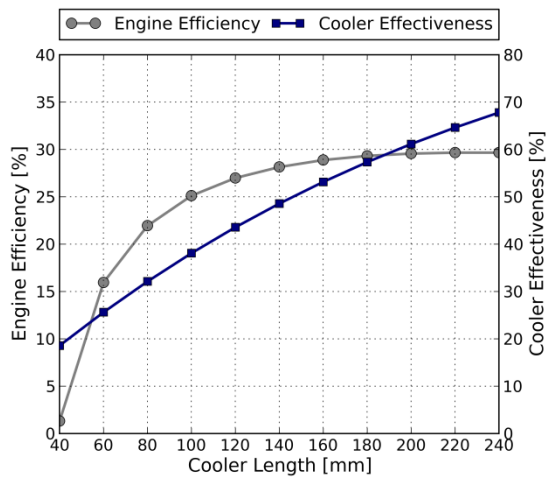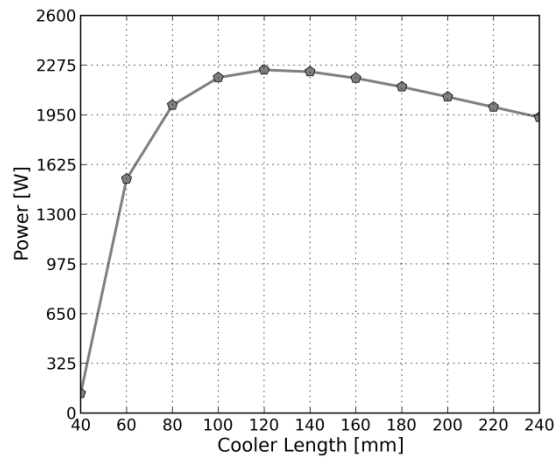
6.31-a   6.31-b

Figure 6.31-a Engine efficiency, cooler effectiveness and **6.31-b** Power production as a function of the cooler tubes length.

From the results analysis, it can be concluded that the performance of the cooler can be improved increasing the internal diameter to 4.0 mm and raising its length in 20 mm (i.e. a cooler with 120 mm of length). Regarding the number of cooler tubes, it seems that 150 tubes is a reasonable value.

6.4.4 Thermodynamic optimization

The study of each geometric parameter of the Stirling engine thermal components gives an insight into the relations of those parameters in the engine performance. Therefore, this knowledge can be used to produce significant improvement to the general performance of a particular engine. Also, the individual analysis of the geometric parameters gives solid bases to decide which are the most relevant to choose as decision variables for the thermo-economic optimization.

Regarding this, a comparison of the engine performance results between the base-case presented at Table 6.1 and the optimized configuration resulting from the analysis is now performed. Table 6.9 resumes the enhanced geometric parameters compared to the values initially considered, whereas Table 6.10 presents the comparison of performance results for both configurations. The trend for each parameter regarding the thermodynamic optimization is also indicated.

The results were obtained considering the He as the working gas, a mean pressure of 30 bar and a rotational speed of 3000 rpm.

Table 6.9 Comparison between geometrical parameters for the base-case and enhanced configuration

	Base case configuration	Enhanced-case configuration	Variation
Regenerator			
External Diameter ($d_{out,r}$) [mm]	56.0	66.0	↗
Internal Diameter ($d_{inner,r}$) [mm]	46.0	56.0	↗
Regenerator Length (L_r) [mm]	60.0	60.0	=
Matrix Porosity (Φ_{matrix}) [-]	0.7	0.7	=
Wire Matrix Diameter ($d_{wire,r}$) [mm]	0.3	0.1	↙
Heater			
Internal Diameter($d_{inner,h}$) [mm]	3.0	4.0	↗
Heater Length(L_h) [mm]	150.0	150	=
Number of Tubes (nt_h)[-]	80	80	=
Cooler			
Internal Diameter($d_{inner,k}$) [mm]	3.0	4.0	↗
Heater Length(L_k) [mm]	100.0	120	↗
Number of Tubes (nt_k)[-]	150	140	↙

Results suggest that the combination of new values for the geometric parameters turns into a higher thermal efficiency of the engine, which corresponds to a relative increase of 45.9%, an increase from 27.0% to 39.4%. Nevertheless, this large increase in the thermal engine efficiency also translates into a reduction in power output, as well as, an increase in total pumping losses. Also, it should be noted the important increase in the regenerator effectiveness.

Table 6.10 Performance results for the base-case and enhanced configuration (He, 3000 rpm, 30 bar)

	Base-case Configuration	Enhanced-case Configuration	Variation
Engine Thermal Efficiency, %	27.0	39.4	↗
Power, W	2318	1801	↙
Work Losses, W	21.0	50.2	↗
Heater Effectiveness, %	50.6	44.1	↙
Regenerator Effectiveness, %	90.3	98.1	↗
Cooler Effectiveness, %	38.5	35.7	↙

6.5 Cost Estimation Analysis

6.5.1 Total costs and revenues

Considering the base-case configuration, the annual worth of a system with those characteristics can be estimated. Results of the annual worth, costs and revenues are presented in Table 6.11. Without optimizing the system, the configuration base discloses a negative annual worth of 779 €/year (i.e. economic loss). The most relevant term is the annualized capital cots from purchasing the cogeneration unit. Regarding the revenues, the income from selling electricity to the grid and the avoided cost for the heat generation are the most profitable terms from system operation. This outcome characterizes a system able to produce 1.25 kW of electrical power and 2.20 kW of thermal power.

Table 6.11 Annual costs and incomes of the thermal plant for the base-case configuration

Annual Costs and Revenues, €/year	
Capital Investment Cost, C_{inv}	(1881)
Maintenance Costs, C_m	(75)
Revenue from equipment residual value, Rev_{res}	94
Revenue from selling electricity to the grid, Rev_{sell}	602
Revenue from CES bonification, Rev_{ces}	129
Avoided cost from separate heat generation, $C_{avoided}$	352
Annual worth of the CHP system, AW	-779

The capital investment cost of the Stirling engine is now presented in Table 6.12 and detailed for each system component. The results were obtained for a simulation assuming a mean pressure of 30 bar and 3000 rpm.

Table 6.12 Cost estimation of the Stirling engine

System Component	Cost [€]
Heater	5597
Regenerator	7203
Cooler	2510
Engine bulk	4616
Total capital cost of Stirling engine	19926

According to the results, the total cost of the equipment is 19926€. Considering the cost of each system component, the heater, the regenerator, the cooler and the engine represent, respectively, 28.1%, 36.1%, 12.6% and 23.2% of the total cost, as shown by Figure 6.32. Thus, the heater and the engine bulk are the most costly components. Regenerator represents an important cost in the system and it weight in the total cost of the equipment rises if better materials are used in its manufacture.
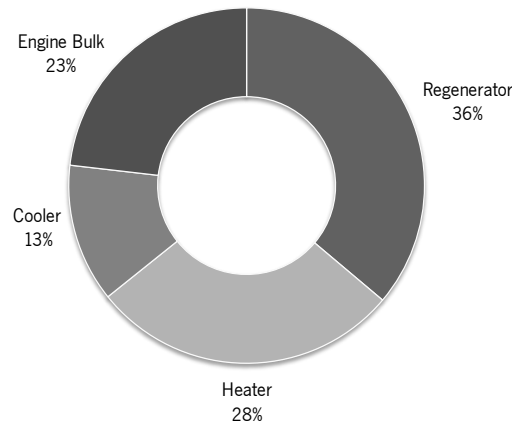
Figure 6.32 Results of relative cost of each component of the Stirling engine.

6.5.2 Sensibility analysis of the purchase cost parameters

The cost equations presented in this work allow the combined variation of size and performance aspects. Therefore, varying the operational and the geometric characteristics of the Stirling engine and optimizing the costs of the system, seems to be the best commitment in optimizing these thermal plants. To investigate the influence of these parameters on the engine performance, they were studied individually and, at each simulation, the others were kept unchanged. All the results in this sub-section are referent to simulations performed at 30 bar of mean pressure and a rotational speed of 3000 rpm.

Heater Cost
Figures 6.33 to 6.35 present the heater cost variation and the engine efficiency as a function of the number and the internal diameter of the cooler tubes, and the cooler length. Considering the heater purchase cost equation definition, the increase in the heat transfer area leads to the increase of heater cost. Nevertheless, some geometrical parameters have a greater influence on the heat transfer are than others. The internal diameter and the heater length are the two geometrical parameter that most affect the heater cost. Results show that there is an optimal value for the internal diameter of the heater tubes for which the engine efficiency is maximum. The Stirling engine efficiency is maximum (i.e. 25.8%) when the internal diameter of the pipes is 4 mm. For this geometrical input, the heater cost corresponds to 7032 €.
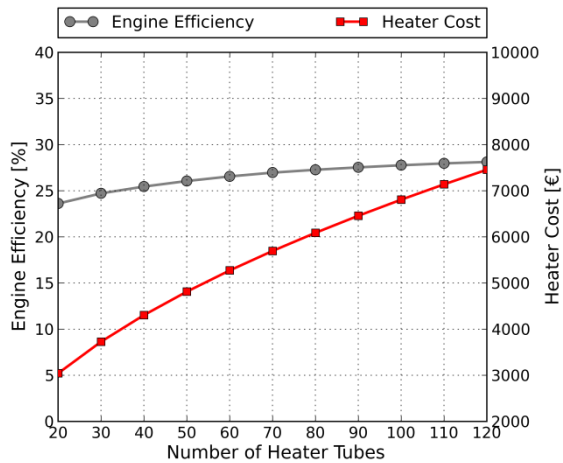
Figure 6.33 Stirling engine efficiency and heater cost as a function of the number of the heater tubes.
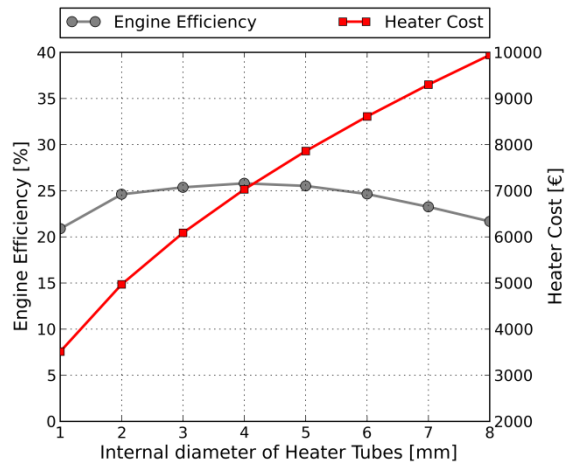
Figure 6.34 Stirling engine efficiency and heater cost as a function of the internal diameter of the heater tubes.
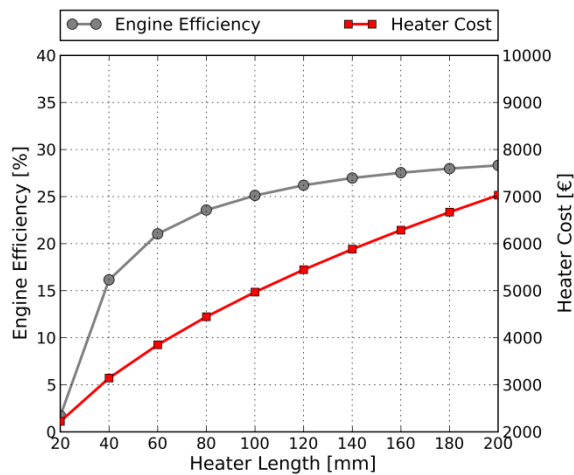
Figure 6.35 Stirling engine efficiency and heater cost as a function of heater length.

According to the results from Figure 6.35, it can be said that for the tube length above 120 mm the increase in engine efficiency is not sufficiently relevant against the rising costs of the thermal component.

Heater Cost

Figure 6.36 shows the relationship between the regenerator cost and the engine efficiency considering different values for the porosity of the regenerator matrix. Results show that the Stirling engine efficiency is maximum (i.e. 28.9%) when the matrix porosity ranges between 0.48 and 0.52. For this range, the regenerator cost is estimated to be 6 800 €. Figure 6.37 shows the regenerator cost and the engine efficiency variation considering different values for the matrix wire diameter, assuming a porosity of 0.7. According to the results, the regenerator cost decreases exponentially with the increase of the matrix wire diameter.
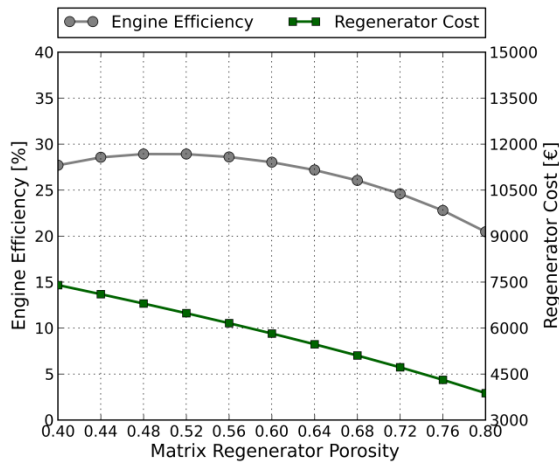
Figure 6.36 Stirling engine efficiency and regenerator cost as a function of porosity of the regenerator matrix.
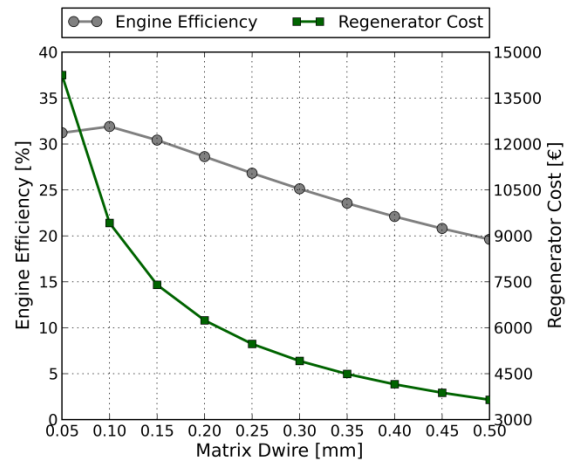
Figure 6.37 Stirling engine efficiency and regenerator cost as a function of matrix wire diameter.

Figure 6.38 and Figure 6.39 present the regenerator cost and engine efficiency variation for different values of regenerator length and regenerator internal diameter, respectively. The regenerator cost increases with the length and regenerator internal diameter, because the heat transfer area increases.
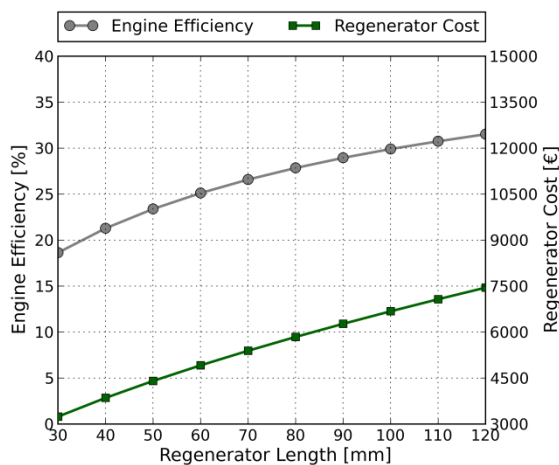
Figure 6.38 Stirling engine efficiency and regenerator cost as a function of regenerator length.
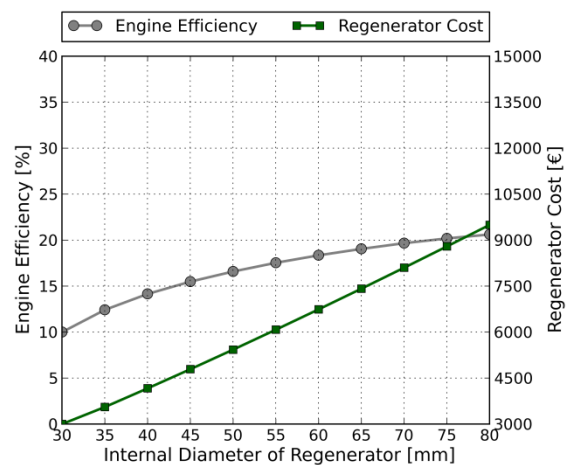
Figure 6.39 Stirling engine efficiency and regenerator cost as a function of internal diameter of regenerator.

The geometrical parameters that most affect the regenerator cost are the matrix wire diameter and the internal diameter of the regenerator. This means that varying these parameters a greater variation is obtained in the regenerator cost.

Cooler Cost

Figures 6.40 to 6.42 present the cooler cost variation and the engine efficiency as a function of each geometrical parameter: number of cooler tubes, internal diameter of cooler tubes and cooler tubes length. The cooler cost increases almost linearly with the increase of the number of tubes, varying between 1474

€ to 2575 €. The cooler cost value is more susceptible to the internal diameter of the tubes than to the length. According to the results, the Stirling engine efficiency is maximum (i.e. 25.8%) when the internal diameter of the tubes is 4 mm, which corresponds to a cooler cost of 2816 €.
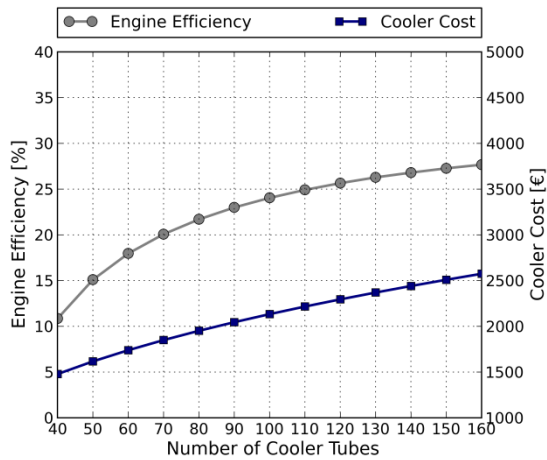
Figure 6.40 Stirling engine efficiency and cooler cost as a function of the number of the cooler tubes.
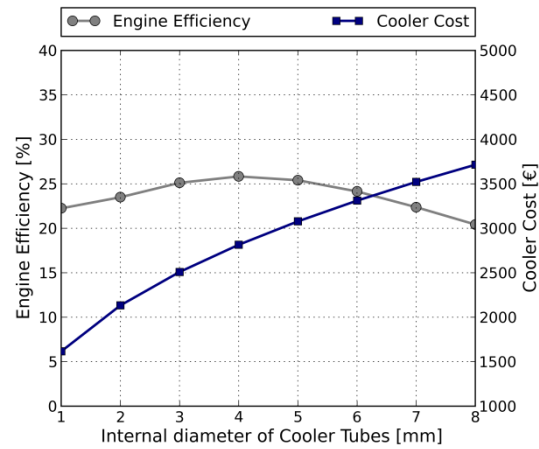
Figure 6.41 Stirling engine efficiency and cooler cost as a function of the internal diameter of the cooler tubes.
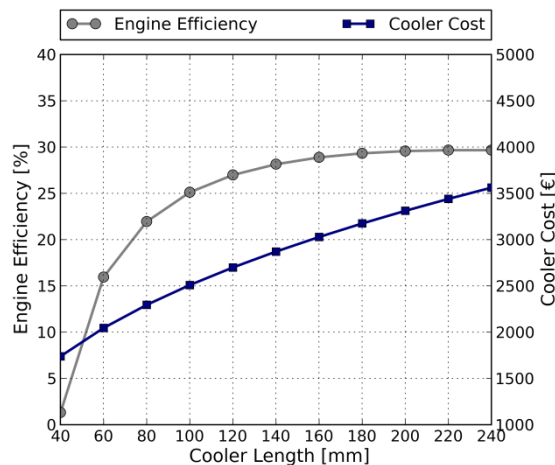
Figure 6.42 Stirling engine efficiency and cooler cost as a function of cooler length.

Engine Bulk Cost

The engine cost depends on the engine volume and mean operational pressure. Figure 6.43 presents the engine bulk cost for different values of mean pressure considering three values of engine volume. Results show that the engine bulk cost increases most significantly with the mean pressure than the engine volume. Systems that operate at higher pressures oblige several design requirements to seal leakage paths of the working gas. Including the mean pressure as one of the key parameters in the engine bulk cost is also justified by the proportionality between the power output and the mean cycle pressure.
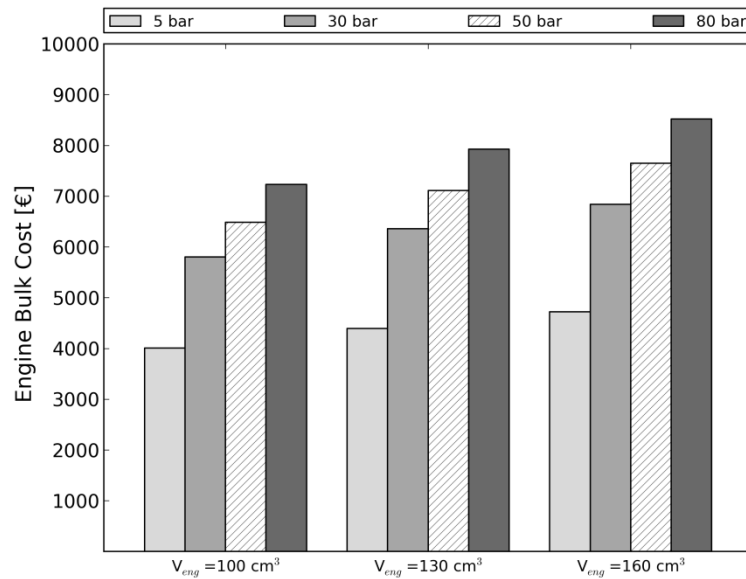
Figure 6.43 Engine cost variation for different values of mean operational pressure at V_{eng} =100 cm³, V_{eng} =130 cm³ and V_{eng} =160 cm³.

Remarks on purchase cost parameters

Obviously, for heater and cooler, the increase of the length, number and internal diameter of the tubes result into the rise of their purchase cost, since the increase of this parameters leads to higher values of the effective heat transfer area, which is the physical parameter used in the definition of the purchase cost equation. However, it seems that for some parameters, there is a certain value from which the gains in engine efficiency no longer compensate the increase in the geometry parameter and cost. For instance, from 160 mm of length, the engine efficiency does not increase significantly that justifies the increase in cooler cost rise. Regarding the regenerator, the matrix wire diameter is the parameter that most affect its cost. The fine wire mesh is commonly obtained in a form of woven screen at variety of wire sizes, weave structures, matrix density and materials, whose complexity affects the manufacturing cost.

All these analyses allow understanding the relationship between an individual parameter and the respective effect in the cost, engine efficiency and performance of the thermal component. Nevertheless, the full thermal-economic optimization of the thermal power plant tests the influence of all these parameters together in the performance and cost output.

6.6 Thermal-economic Optimization

All the sensitivity analysis performed to the physical and the economic model corresponded to an important work in defining the parameters for the thermal-economic optimization. During the process of the thermal-economic model definition, several tests were made in order to delineate the most appropriate model. Those tests include the consideration of different combinations of decision variables, working fluids, numerical methods and respective parameters. The simulations were run considering a rotation

speed of 1500 rpm considering the helium as the working fluids. The value for the other parameters that were not considered as decision variables were assumed constant and equal to the values assumed for the base case configuration.

6.6.1 Results for six decision variable model

The thermal-economic preliminary results are firstly presented considering six decision variables: $P_{mean};V_{eng};d_{inner,h};d_{inner,k};\Phi_{matrix};d_{wire}$. For these simulations, the Nelder-Mead was the search method used to run the PS algorithm.

After convergence was achieved, the optimal values for the objective function, decision variables and others thermodynamic and economic variables were obtained. The optimal solutions were obtained, no constraint was violated, the convergence tolerances were respected and the optimization terminated because the objective function was non-decreasing in feasible directions and the solution was within the value of the function tolerance. Table 6.13 presents the optimal annual costs and revenues from the CHP system operation. Results depicts that for all the optimal solutions it is possible to obtain a positive profit from the system operation.

Table 6.13 Optimal annual costs and incomes of the thermal system considering six decision variables

Annual Costs and Revenues, €/*year*	
Capital Investment Cost, C_{inv}	(1766)
Maintenance Costs, C_m	(168)
Revenue from equipment residual value, Rev_{res}	88
Revenue from selling electricity to the grid, Rev_{sell}	1348
Revenue from CES bonification, Rev_{ces}	408
Avoided cost from separate heat generation, $C_{avoided}$	1573
Annual worth of the CHP system, *AW*	1483

The most predominant costs are the investment costs to acquire the system, whereas, the highest revenue came from the income from the avoided cost of separate heat generation. Arising from the fact that there is no need to have a separate system to produce the total heating demand, the economic benefit from that avoided cost was also accounted, representing a revenue of 1483 €/*year*. Also, the revenues from selling the produced electricity to the grid represent a great economic benefit. Results shows that for a base case scenario considering an electricity FIT of 0.12 €/kWh, it is possible to achieve an annual revenue above 1348 €/*year* if all the electricity generated is sold to the grid.

Stirling engine technology is characterized for long periods without need of maintenance intervention. Considering the results, the maintenance cost represents about 8.7% of the total annual costs of system operation and the annualized investment costs correspond to the highest charge.

Considering the objective function defined for this optimization problem, it may be concluded that applying thermal-economic optimization to the system it is possible to obtain a best economic output and, at same time optimize the physical system, when comparing the objective function value from thermal-economic optimization results with the one obtained from the base-case configuration.

For that optimal solution, Figure 6.44 presents the relative capital cost of each system component. Results show that the most expensive component is the engine bulk, representing 36.2% of the total capital cost, followed by the regenerator (26.0%), the heater (24.5%) and finally the cooler (13.3%). In fact, the regenerator and the heater are the most important heat exchangers of the thermal plant because of the thermal conditions and variations of the working fluid at those components. From the physical optimal solution calculated, the total capital cost of the thermal power plant is of 18714€.
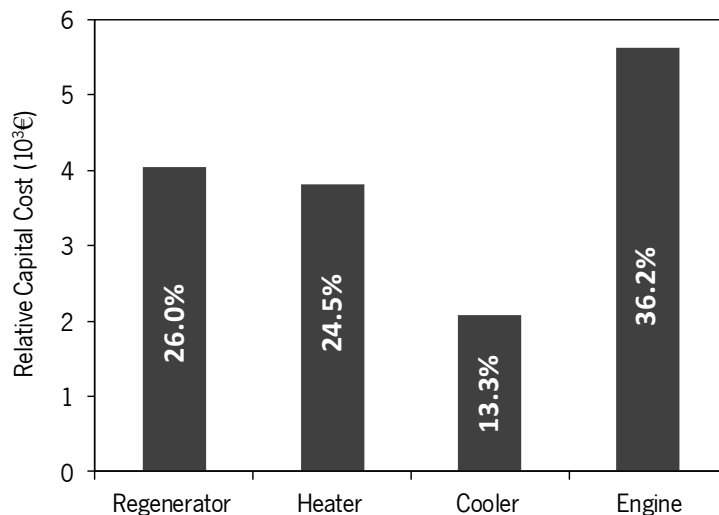
Figure 6.44 Relative capital costs for each thermal plant component.

The optimal values for six the decision values presented in Table 6.14. Therefore, this corresponds to a thermal plant operating at 78.2 bar of mean pressure, considering cylinders with a 128 cm^3 of capacity, a heater with 1.50 mm for the internal diameter of the tubes and 3.0 mm for the cooler tubes. The tubular regenerator should contain a wired matrix with a porosity of 0.7 and the with a wire diameter of 0.297 mm. Considering the results for the He as working fluid, the optimal solution corresponds to a Stirling engine working at higher values of mean pressure. Although the mean operational pressure is one of the physical parameters in the engine bulk purchase cost equation, the increase in the component cost is lower than the gains that are obtained in terms of power produced by the system, that somehow are intended to be maximized.

Table 6.14 Optimum values of the six decision variables

Decision Variables	
P_{mean} , [bar]	78.2
V_{eng} , [cm³]	128.0
$d_{inner,h}$, [mm]	1.50
$d_{inner,k}$, [mm]	3.00
Φ_{matrix} ,[-]	0.70
d_{wire} , [mm]	0.297

Concerning the geometrical parameters, the optimal internal diameter of the heater tubes corresponds to a value of 1.5 mm. Nevertheless, the optimal solution obtained for the internal diameter of cooler tubes reached higher values when compared with the heater diameter tubes. The internal diameter is one of the most important parameters in sizing cooler and heater components, because its variation has a great impact in the heat transfer, affecting not only the heat exchanger effectiveness but also the engine efficiency. Obviously, for tubes with higher diameter, the heat transfer area increase, but also the friction that the fluid suffers during its passage, is influenced. Concerning the regenerator, the two most important parameters are the matrix regenerator porosity and the diameter of the matrix wire. The simulation depicted that the optimal porosity value is of 0.7 and a wire diameter between 0.221 mm and 0.297 mm. The performance criteria for the optimal solutions are presented in Table 6.15. The results disclose that the optimal solution discloses a thermal plant able to produce 2.79 kW electrical power and 9.23 kW of thermal power. These results are within a heat-to-power ratio below 3.5. The results for the thermal power are above the peak thermal demand for individual dwellings, which was estimated to be 6 to 8 kW$_{th}$ for decentralized energy systems (Konrad, Obé, & Frey, 2009). Qualitatively, the optimal solution presented an electrical efficiency of 23.5% and a total efficiency (in cogeneration mode) above 98%. This outcome reveals a great result considering the total efficiency of the system.

Table 6.15 Optimum values of thermal system performance

Performance Criteria	
Thermal Power, [kW]	9.23
Electrical Power, [kW]	2.79
Electrical Efficiency, [%]	23.51
Total Efficiency, [%]	98.38

6.6.2 Analysis to the complexity of the thermal-economic model

Although these results from the thermal-economic model are quite satisfactory, it was decided to increase the degree of complexity of the optimization model, by increasing the number of decision variables.

From the sensitivity analysis performed to the physical model, it was concluded that the temperature of the hot source is one of the most important variables in the system, and so, it should also be regarded as one of the decision variables. The temperature of the heat source has a great influence in the efficiency of the Stirling efficiency. Lower and upper values for this new decision variable were also defined in order to include it in the optimization model ($725 \le T_h \le 900$).

Thus, the heat source temperature was also considered as one of the decision variables: $P_{mean}; V_{eng}; d_{inner,h}; d_{inner,k}; \Phi_{matrix}; d_{wire}; T_h$. Considering this new combination of decision variables, numerical simulations were performed considering a rotation speed of 1500 rpm considering the helium as the working fluids. The Nelder-Mead was the search method used to run the PS algorithm for the numerical simulations. The optimal solution was attained when the objective function was non-decreasing in feasible directions and the solution was within the value of the function tolerance and convergence criteria.

Table 6.16 presents the optimal annual costs and revenues from the CHP system operation for the seven decision variables. Results depicts that for all the optimal solutions it is possible to obtain a positive profit from the system operation. The most predominant costs are the investment costs to acquire the system, whereas, the highest revenue came from the income from the avoided cost of separate heat generation and the revenues from selling the produced electricity to the grid. The investment purchase costs are the most representative costs, representing more than 90% of the economic expenditures. It is important to note, once the energy source is a renewable one, no fuel costs are included in the economic model.

Table 6.16 Optimal annual costs and incomes of the system considering seven decision variables

| Annual Costs and Revenues, €/year	
Capital Investment Cost, C_{inv}	(2016)
Maintenance Costs, C_m	(217)
Revenue from equipment residual value, Rev_{res}	101
Revenue from selling electricity to the grid, Rev_{sell}	1735
Revenue from CES bonification, Rev_{ces}	452
Avoided cost from separate heat generation, $C_{avoided}$	1544
Annual worth of the CHP system, AW	1598

Comparatively to the six decision variable simulation, this combination of decision variables discloses a solution for which it was obtained a higher value of annual worth.

The optimal values for the seven decision values presented in Table 6.17. Despite the solution gives a higher annual profitability, the optimal values for the decision variables are identical from the optimal solution with six decision variables model. Nevertheless, including the hot source temperature as one of the decision variables led to a combination of physical parameters for which, its optimal value is higher than the firstly assumed, 750 K. This is actually expectable because the higher the value of T_h, the greater is the energy that the system can produce. Nevertheless, the heater cost also increases, and so the optimal value of T_h represents the balance between the increase in the available energy and the minimization of heater cost. Thus, this result could also result in the need of a system capable of providing additional heat to the hot heat exchanger, which would lead, for instance, to a solar collector with a higher capacity, and therefore, more expensive, and so, a higher investment. Actually, this is a limitation of the model: the solar collector should also be included in the optimization model.

Table 6.17 Optimum values of the seven decision variables

Decision Variables	
P_{mean} , [bar]	78.22
V_{eng} , [cm³]	128.0
$d_{inner,h}$, [mm]	1.50
$d_{inner,k}$, [mm]	3.00
Φ_{matrix} ,[-]	0.70
d_{wire} , [mm]	0.300
T_h , [K]	808.3

The performance criteria for the optimal solutions are presented in Table 6.18. The results disclose similar values for the electrical and thermal powers when comparing the results with the optimal solution from the six decision variables simulation.

Table 6.18 Optimum values of thermal system performance

Performance Criteria	
Thermal Power, [kW]	9.65
Electrical Power, [kW]	3.61
Electrical Efficiency, [%]	28.72
Total Efficiency, [%]	98.01

The optimal solution, in all presented cases, has an electrical efficiency of 28.7% and a total efficiency (in cogeneration mode) of 98%. This outcome discloses a better result in terms of electrical efficiency when compared with the six decision variables tests.

According to the sensitivity analysis performed to the geometrical parameters of the heat exchangers, the number of the tubes could also be optimized. The number of the tubes affects two aspects: for one hand it affects the pressure drop inside the heat exchanger and the dead volume in the component. Therefore, the number of cooler and heater tubes was also included in the decision variables in order to understand the influence of the commitment between the number and the tubes diameter at the heat exchangers in the system performance. The lower and upper limits for these two variables were defined to be: $50 \leq nt_h \leq 90$ for the number of heater tubes and $80 \leq nt_k \leq 160$ for the number of cooler tubes.

Thus, the number of heater and cooler tubes was introduced in the thermal-economic model as decision variables to perform the numerical simulations: $P_{mean}; V_{eng}; d_{inner,h}; nt_h; nt_k; d_{inner,k}; \Phi_{matrix}; d_{wire}; T_h$.

Table 6.19 presents the optimal annual costs and revenues from the CHP system operation. For a simulation which includes the number of tubes of cooler and heater, the annual worth of the CHP system presents a similar value, once it was obtained an annual profit of 1592 €/years. Comparing the results, the value for the annual worth was obtained considering a decrease of the capital investment costs and an increase on the avoided costs from separate heat generation. This economic output corresponds to a system able to deliver 3 kW$_{el}$ and 10.5 kW$_{th}$ for which it is obtained an electrical efficiency of 23.5% and a total efficiency of 98.5%. The thermal-economic model benefits the power production in order to maximize the economical income from selling the electricity to the grid.

Table 6.19 Optimal annual costs and incomes of the system considering nine decision variables

Annual Costs and Revenues, €/*year*	
Capital Investment Cost, C_{inv}	1878
Maintenance Costs, C_m	180
Revenue from equipment residual value, Rev_{res}	94
Revenue from selling electricity to the grid, Rev_{sell}	1440
Revenue from CES bonification, Rev_{ces}	436
Avoided cost from separate heat generation, $C_{avoided}$	1680
Annual worth of the CHP system, *AW*	1592

The optimal values for the nine decision values presented in Table 6.20. Including the number of heater and cooler tubes affects the optimal value of all the decision variables, resulting on a thermal system operating at slightly lower mean pressures, with higher cylinder capacities. The optimal value for the heat source is of 784 K, which is lower than the optimal value obtained for the simulation with seven decision variables. This means that including the new decision variables affects all the optimal solution. A reasonable explanation for this outcome is that these optimal solutions possibly correspond to local optima and not a global solution. Therefore, other optimization algorithms should be applied and studied. Concerning the optimal results for the heater number of tubes, its value is of 79 tubes, which is quite similar to the number of tubes of base-case configuration. Regarding the number of cooler tubes, the optimal solution presents a reduction of the number of tubes from 150 to 133 tubes. Nevertheless, this reduction of the number of cooler tubes also results into a reduction of the internal diameter of each tube, from 3.0 mm to 2.81 mm. It was also verified an increase in the matrix regenerator porosity (0.7 to 0.77) with a similar value for its wire diameter (0.303 mm).

Table 6.20 Optimum values of the nine decision variables

Decision Variables	
P_{mean} , [bar]	75.1
V_{eng} , [cm³]	131.8
$d_{inner,h}$, [mm]	2.77
$d_{inner,k}$, [mm]	2.81
nt_h ,[-]	79
nt_k ,[-]	133
Φ_{matrix} ,[-]	0.77
d_{wire} , [mm]	0.303
T_h , [K]	784

6.6.3 Comparison of different working fluids

An interesting analysis is to apply the thermal-economic model to the thermal system comparing the optimal solutions systems operating with different working gases. Table 6.21 presents the optimal solution from a system operating with He and H_2.

Results shows that the optimal solution obtained for a system operating with H_2 as working gas provides an higher profit when compared with the optimal solution obtained for He. This outcome is only due to the fact that the investment capital for the system with H2 is lower than the investment cost considering He.

This difference in investment costs is probably due to variations of the optimal values for the decision variables.

Table 6.21 Comparison of optimal costs and incomes of the thermal system working with He and H₂

Annual Costs and Revenues, €/year	He	H₂
Capital Investment Cost, C_{inv}	1878	1829
Maintenance Costs, C_m	180	180
Revenue from equipment residual value, Rev_{res}	94	91
Revenue from selling electricity to the grid, Rev_{sell}	1440	1440
Revenue from CES bonification, Rev_{ces}	436	436
Avoided cost from separate heat generation, $C_{avoided}$	1680	1680
Annual worth of the CHP system, AW	1592	1639

Figure 6.45 presents the relative capital cost of each system component for the optimal solution obtained from both working fluids. The purchase cost obtained for the thermal plant running with He is higher (19892 € than with H₂ (19374 €).

According to the data, the optimal solutions disclose the engine bulk as the most expensive component of the thermal system for both simulations, representing 35% of the total purchase cost of the system. The heater is the second most expensive component, followed by the regenerator and the cooler.
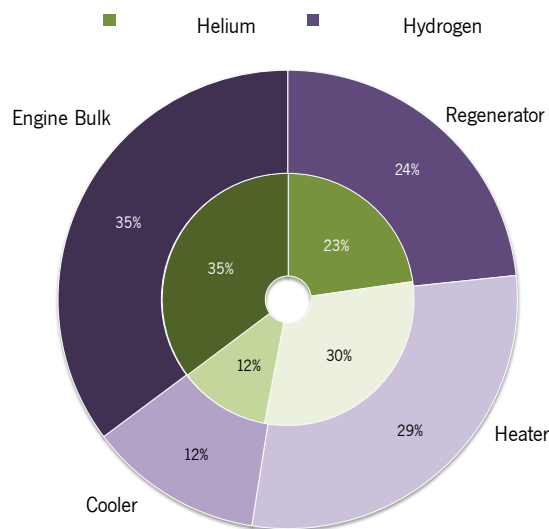
Figure 6.45 Results of relative capital costs for each component, considering He and H₂ as the working fluids.

The small differences in purchase cost of the systems components are due to different results for the decision variables between both cases. Table 6.22 presents the optimum values of the decision variables, by comparing the simulations performed with He and H₂ as working fluids. The results of the decision variables discloses to similar machines with small differences in the operating pressure and cylinder capacities. Geometrically, the commitment between the tubes number at each heat exchanger (i.e. heater

and cooler) and the internal diameter discloses an equivalent heat transfer area for both optimal solutions. Note that both optimal solutions disclose a machine able to deliver, approximately, 3.0 kW$_{th}$ and 10.5 kW$_{el}$. Analysing the results, the main difference between the optimal solutions lies in the temperature of the hot source.

Table 6.22 Optimum values of the decision variables for He and H$_2$

Decision Variables	He	H$_2$
P_{mean} , [bar]	75.06	77.30
V_{eng} , [cm³]	131.8	126.4
$d_{inner,h}$, [mm]	2.77	2.87
$d_{inner,k}$, [mm]	2.81	3.06
nt_h ,[-]	79	78
nt_k ,[-]	133	129
Φ_{matrix} ,[-]	0.77	0.75
d_{wire} , [mm]	0.303	0.306
T_h , [K]	784.1	755.3

Considering the results, the application of the pattern search algorithm with the Nelder-Mead method as the direct search option showed a good performance in obtaining optimal solutions for this complex non-linear constrained optimization problem. Nevertheless, others optimization methods should be tested in order to understand the feasibility of the solutions.

6.6.4 Comparison of different optimization methods

The GA optimization method was also implemented as the search step into the PS algorithm. In order to better compare its results with the optimal solutions from the convergence tolerance criteria was considered to be equal to the Nelder-Mead method. The number of iterations ran by each simulation, the number of objective function evaluations, as well as, the simulation time is presented in Table 6.23.

Table 6.23 Optimization parameters for both the simulations (He)

	PS with Nelder-Mead	PS with GA method
N° of Iterations	3	2
N° of O.F. Evaluations	3246	5034
Simulation Computational Time, h	8.5	10

The data shows that the GA algorithm requires a larger number of objective function evaluations to reach the convergence. The increase in the number of objective function evaluations led to an increase in the computational time to achieve the optimal solutions for both search methods.

Table 6.24 presents the results from two simulations considering the He as the working fluid and the model with nine decision variables, where the optimal solutions for the Nelder-Mead and GA algorithm are compared. The optimal solution from the GA algorithm discloses an optimal solution for which it is obtained a higher profit. The higher profit is obtained because of the lower investment costs obtained for that solution. This outcome implies that the optimal solutions lead to machines with different geometrical and operating conditions.

Table 6.24 Optimal annual costs and incomes comparing different numerical methods (He)

Annual Costs and Revenues, €/$year$	PS with Nelder-Mead	PS with GA method
Capital Investment Cost, C_{inv}	1878	1709
Maintenance Costs, C_m	180	180
Revenue from equipment residual value, Rev_{res}	94	86
Revenue from selling electricity to the grid, Rev_{sell}	1440	1440
Revenue from CES bonification, Rev_{ces}	436	436
Avoided cost from separate heat generation, $C_{avoided}$	1680	1680
Annual worth of the CHP system, AW	1592	1757

Regarding the comparison of the optimization methods, few aspects are important to mention. Due to the complexity of the thermodynamic model, the nature of the constraints (i.e. non-linear), there is no guarantee that it is possible to determine derivatives from the functions, and so, the application of gradient-based methods to this model was discarded. Also, different initial and feasible points were tested in order to understand if the solution was dependent on the starting point. This fact has not been verified for both methods.

The Nelder-Mead method is an iterative method that generates a sequence of feasible iterates whose objective function value is non-increasing. Also, the objective function is evaluated at a finite number of points on a mesh in order to try to find one that yields a decrease in the objective function value. Thus, the parameters defined to the mesh size and the admissible search directions determinate if the optimal solution is a local or a global one.

The GA application disclosed an optimal solution with a better value for the objective function. Nevertheless, there an aspect from applying this method that has to be taken into account, the randomness of this algorithm. In fact, at each simulation, the algorithm repeatedly modifies a population

of individual solutions, and at each step, the genetic algorithm randomly selects individuals from the current population and uses them as parents to produce the children for the next generation. Over successive generations, the population "evolves" toward an optimal solution. This means that the same simulation, with the same convergence parameters can depict different optimal solutions.

Table 6.25 compares the combination of optimal values from the two methods for all the decision variables. Both optimal solutions disclose a machine able to deliver, approximately, 3.0 kW$_{th}$ and 10.5 kW$_{el}$. However, despite both solutions disclose the same energy output, the application of different optimization methods leads to different optimal solutions in terms of decision variables.

The optimal solution from applying the PS algorithm with the GA method depict a thermal system working at lower mean pressure, with cylinders with higher capacity and requires higher values for the heat source temperature. Geometrically, the heater should have a lower number of tubes but with a higher diameter, whereas for the cooler, the best configuration leads to a lower number of cooler tubes with a smaller internal diameter. The results for the regenerator parameters are quite similar for both optimal solutions.

Table 6.25 Optimum values of the decision variables comparing different numerical methods (He)

Decision Variables	PS with Nelder-Mead	PS with GA method
P_{mean} , [bar]	75.06	62.13
V_{eng} , [cm³]	131.8	140.8
$d_{inner,h}$, [mm]	2.77	3.68
$d_{inner,k}$, [mm]	2.81	1.71
nt_h ,[-]	79	60
nt_k ,[-]	133	112
Φ_{matrix} ,[-]	0.77	0.78
d_{wire} , [mm]	0.303	0.307
T_h , [K]	784.1	811.7

There is a significant difference between the optimal solutions considering the configuration of the heat exchangers. Thus, the effectiveness of heater, regenerator and cooler was calculated in order to compare both solutions. The results for the effectiveness are presented in Figure 6.46. Comparing the effectiveness results, the optimal solution disclosed by the GA method allows a great improvement in the cooler effectiveness but heater effectiveness gets a worse result. The regenerator effectiveness, as expected, is similar for both solutions.
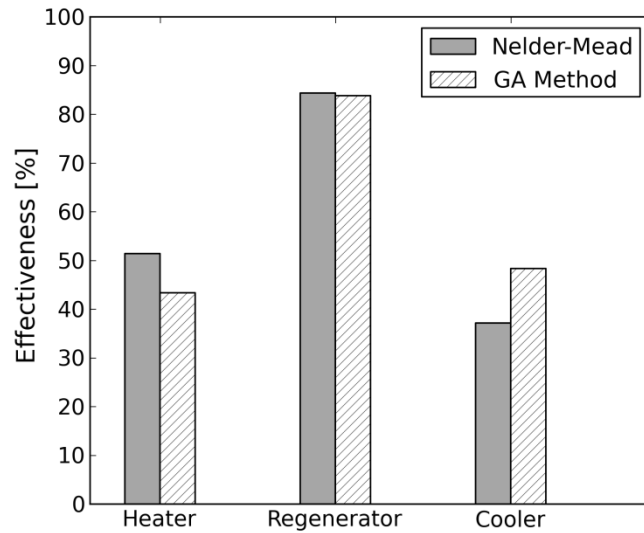
Figure 6.46 Effectiveness of the heat exchangers considering optimal solutions from both numerical methods.

The respective investment costs of the system and respective components for both solutions are presented in Figure 6.47. The total investment purchase cost disclosed by the PS algorithm applied with GA method optimal solution is lower than the one from the PS algorithm with Nelder-Mead method.
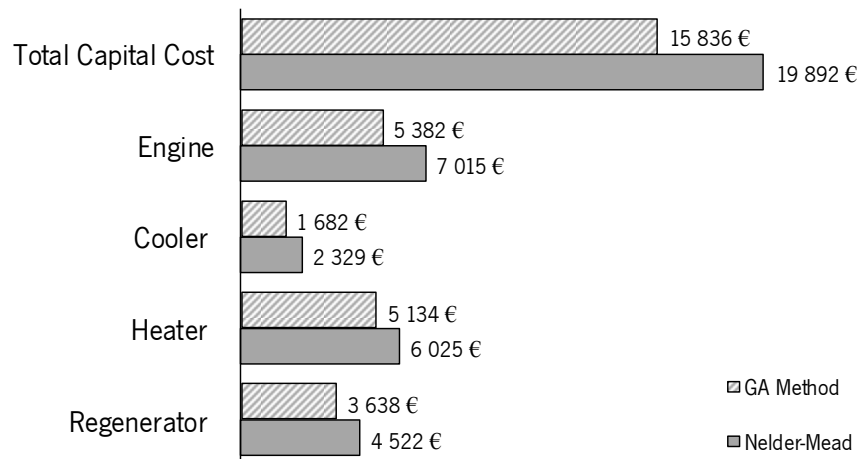
Figure 6.47 Comparison of purchase investment for both optimal solutions.

Therefore, the best system disclosed by the thermal-economic analysis leads to a thermal plant operating at 62 bar of mean pressure considering cylinders with a 141 cm³ of capacity, a heater constituted by 60 tubes with 3.68 mm of internal diameter, a cooler with 112 tubes and 1.71 mm of internal diameter. The tubular regenerator should contain a wired matrix with a porosity of 0.78 and the with a wire diameter of 0.307 mm. This system allows an annual profit of 1757 €/year and the purchase investment cos of this system correspond to 15 836 €.

Ahmadi, M. H., Sayyaadi, H., Dehghani, S., & Hosseinzade, H. (2013). Designing a solar powered Stirling heat engine based on multiple criteria: Maximized thermal efficiency and power. *Energy Conversion and Management*, *75*, 282–291. doi:10.1016/j.enconman.2013.06.025

Asnaghi, A., Ladjevardi, S. M., Saleh Izadkhast, P., & Kashani, a. H. (2012). Thermodynamics Performance Analysis of Solar Stirling Engines. *ISRN Renewable Energy*, *2012*, 1–14. doi:10.5402/2012/321923

Konrad, C., Obé, E., & Frey, H. (2009). Distributed generation potential in the German residential sector. *Cogeneration & On-Site Power Reviews*, 59–65. Retrieved from http://www.cospp.com/articles/article_display.cfm?ARTICLE_ID=361546&p=122

Thombare, D. G., & Verma, S. K. (2008). Technological development in the Stirling cycle engines. *Renewable and Sustainable Energy Reviews*, *12*(1), 1–38. doi:10.1016/j.rser.2006.07.001

Timoumi, Y., Tlili, I., & Ben Nasrallah, S. (2008). Performance optimization of Stirling engines. *Renewable Energy*, *33*(9), 2134–2144. doi:10.1016/j.renene.2007.12.012

Tlili, I., Timoumi, Y., & Nasrallah, S. Ben. (2008). Analysis and design consideration of mean temperature differential Stirling engine for solar application. *Renewable Energy*, *33*(8), 1911–1921. doi:10.1016/j.renene.2007.09.024

Urieli, I., & Berchowitz, D. M. (2010). Stirling Engine Simple Analysis. *Ohio University*. Retrieved February 10, 2010, from http://www.ohio.edu/mechanical/stirling/me422.html

Wu, F., Chen, L., Wu, C., & Sun, F. (1998). Optimum performance of irreversible stirling engine with imperfect regeneration. *Energy Conversion and Management*, *39*(8), 727–732. doi:10.1016/S0196-8904(97)10036-X

Zarinchang, J., & Yarmahmoudi, A. (2008). Optimization of Stirling Engine Heat Exchangers. In WSEAS (Ed.), *World Scientific and Engineering Academy and Society (WSEAS)* (pp. 143–150). Santander, Cantabria.

Zarinchang, J., & Yarmahmoudi, A. (2009). Optimization of Thermal Components in a Stirling Engine. In *WSEAS Transactions on Heat and Mass Transfer* (Vol. 4, pp. 1–10).

7

Sustainability and Economic viability of micro-CHP system

7.1 Economic and Technologic Challenges of CHP Systems

7.2 Sustainability of micro-CHP Systems

7.3 Economic Evaluation

Developing efficient energy generation technologies has become essential due to scarcity and high prices of fossil fuels and environmental concerns. The economic viability assessment of a micro-CHP system is of utmost importance in the decision making process when considering a new investment. The micro-CHP systems offer some benefits that underlie their economic viability: the capacity of producing heat and power at consumption place; the reduction of transmission and distribution losses; maximization of the primary energy savings and finally offers significant contribution to gas emissions reduction. In this chapter, the economic viability of micro-CHP system is discussed and analysed through different economic indexes.

7.1 Economic and Technologic Challenges of CHP Systems

Cogeneration is a capital-intensive opportunity, so investment has to be properly assessed and justified. Costs can be quantified relatively easily, but valuing the benefits from the heat and electricity that will be produced is more difficult. It is not possible to objectively divide the costs between electricity production and heat production; hence the value of the produced heat and electricity is normally calculated on the basis of avoided cost. The value of cogenerated heat is calculated from the avoided cost of producing heat in a boiler and the cogenerated electricity is determined from selling electricity to the grid.

The implementation of a residential cogeneration system can contribute significantly to the reduction of energy consumption. Yet, it requires additional expenses (namely, in terms of investment costs and

operation and maintenance costs), while providing environmental and, in many cases, also economic benefits. Most micro-CHP systems are currently heat-led, so the plants only operate when there is a heat demand, being the electricity a by-product. The most likely situation corresponds to a higher number of hours heat demand. According to Pehnt et al. (2004), micro-CHP power plants are economically viable if they operate at least for about 3,500 to 5,000 hours at full load, and if the electricity is used at the production site. Thus, applications with a rather constant heat demand and an electricity demand matching the CHP electricity production profile are particularly well suited for micro CHP installation. Moreover, the economic incentive to export electricity plus the improvement of system electrical efficiency, turn the micro-CHP systems into a more attractive investment. Also, micro-CHP units must meet the consumer expectations: similar in size when compared with the power devices they are trying to be a replaceable solution, quiet and free from excessive vibration.

The technical and economic challenges in the development of thermal plants are significantly higher for micro-CHP than for larger scale systems, because the costs per unit of power tend to rise exponentially as size reduces. The economic viability of the micro-CHP systems is associated with the capacity of design systems at a cost that can be recovered from the savings and incomes during its useful lifetime. The financial analysis depends on both the capital investment and the value of electricity produced by the unit, which represents the most valuable income from the systems operation (Barbieri, Spina, & Venturini, 2012). For any given system, the payback relies on the unit's operating hours and consequently the total electricity produced annually. Clearly, it is not only the system purchase costs that are important to calculate. The installation and the frequency of the maintenance service over the system-working lifetime have to be quantified. In fact, the capital cost of micro-CHP units is an essential parameter and fluctuates according to the system sizing. A general indication of the capital cost per kW_{el} of installed capacity is given in Figure 7.1.It reflects the specific capital cost of a cogeneration unit, including prime mover, generator and heat recovery equipment.
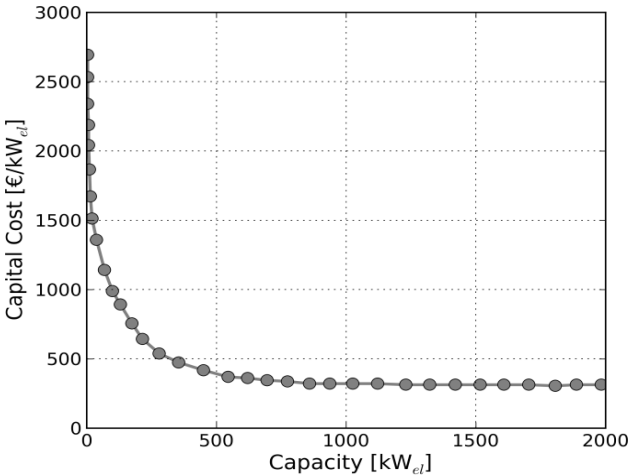
Figure 7.1 Specific capital cost as a function of cogeneration unit size. Adapted from (Smit, 2006).

Thus, the economic viability of micro CHP mainly depends on achieving savings to recover the investment costs, but it is evident that a more comprehensive assessment is required. Therefore, a cost-benefit analysis can be applied for the economic evaluation of micro-CHP systems by assessing the monetary socio-environmental costs and benefits of a capital investment over its useful lifetime.

7.2. Sustainability of Cogeneration Systems

According to Soliño, Prada and Vázquez (2009), when examining the potential of a cogeneration system for a small scale-application, both economic and environmental costs and benefits affects the decision-making process.

7.2.1. Growth Drivers and Markets Constraints

Assessing the sustainability of the micro cogeneration may be based on the balance between the growth drivers of these technologies and the market constraints they face. Therefore, the most relevant growth drivers for micro CHP are: the reduction of the external energy dependency, by reducing the fossil fuel imports; the favourable policies that ensure improved tariffs; the environmental concerns; the possibility to replace the heat production systems (e.g. boilers) by a system able to supply the thermal needs and additionally produce electricity where the surplus production can become an economic profit. The key market constraints that micro-CHP face are: the high manufacturing costs of these power plants; the lack of available money for risky investments; the competition from the conventional power production, as it's still the easier way to access energy; and, finally, fuel prices fluctuations which can be determinant in the determination of these plants profitability. Figure 7.2 summarizes the growth drivers and the most relevant constraints that micro-CHP units have to overcome.
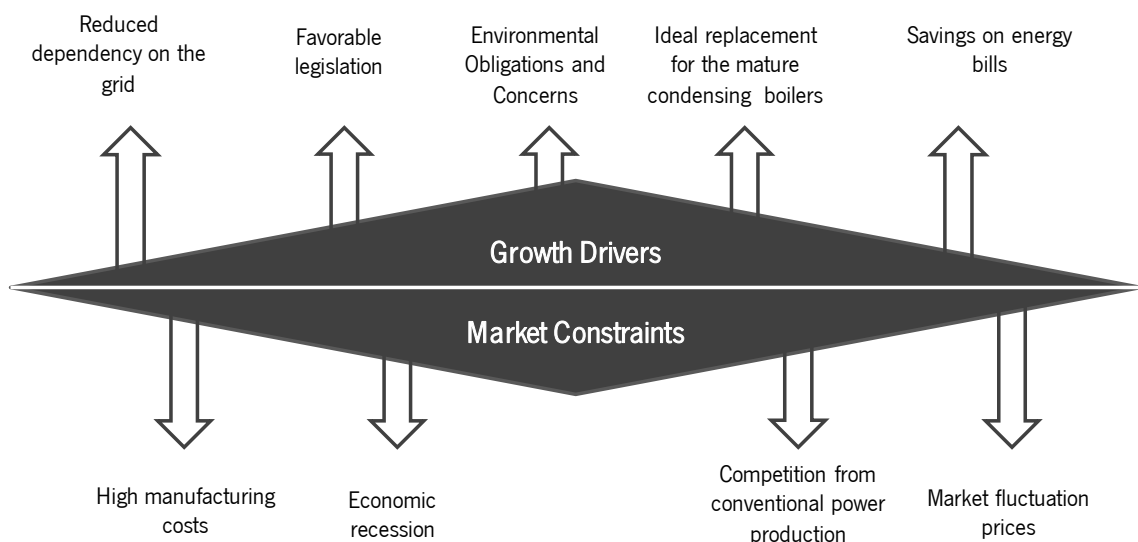
Figure 7.2 Growth drivers and the market constraints for micro-CHP units.

Costs are also subject to change over time – imposition of different interest rates, political changes, fluctuations of fuel and electricity tariffs – requiring a sensibility analysis of the payback period to the fuel price and feed-in-tariffs.

7.2.2. Sustainability Criteria Assessment

In the literature, it is very common the evaluation of CHP systems considering the comparison of different alternatives (Alanne, Salo, Saari, & Gustafsson, 2007; De Paepe & Mertens, 2007; Karger & Hennings, 2009). The available research investigates the advantages and the disadvantages of the alternative systems mostly on a hierarchically structure, based on sustainability criteria. The sustainability criteria used evaluate the alternative cogeneration systems can be summarized by a value tree analysis as shown by Figure 7.3. It is important to notice that, depending on the technical and economic boundary conditions, the advantages and the disadvantages from decentralized thermal plants are distinct and have different impacts. The criteria come from the information compilation, taking into account the sustainability evaluation of decentralized energy conversion systems. The criteria are mainly classified into four categories: environmental protection, security of supply, social and economic aspects.

In the field of environmental protection, the impacts of distributed generation are related to two criteria: the reduction of CO_2 emissions from households and the economical use of fuel and materials required during the construction, operation or dismantling of thermal power plants. The impacts in the security of energy supply sector are characterized by a number of conflicting influences and great uncertainty. For instance, there is an intensified dependence on NG even in the case of cogeneration power systems. This scenario has been changed mainly because of the incentives of applying renewable energy sources.

With respect to an evaluation of the diversification of supply sources, systems with a great versatility in terms of energy sources are more attractive. Also, if that versatility includes renewable and non-expensive energy sources with the same efficiency level, those systems are even more interesting regarding a possible investment.

Failure of small cogeneration systems has much less severe impacts than failure of large facilities. Nevertheless, when these power plants fail, the energy supply of the user is compromised. This issue raises the question of systems adaptability, which is a criterion highly valued regarding small-cogeneration systems.

With respect to social aspects, concerning that these power plants are usually installed within the residential building, one of the aspects that is largely valued is related to the visual impacts and the noise levels from the system operation. Systems with low noise levels, reduced visual impacts are evaluated positively by a consumer(Østergaard, 2009).
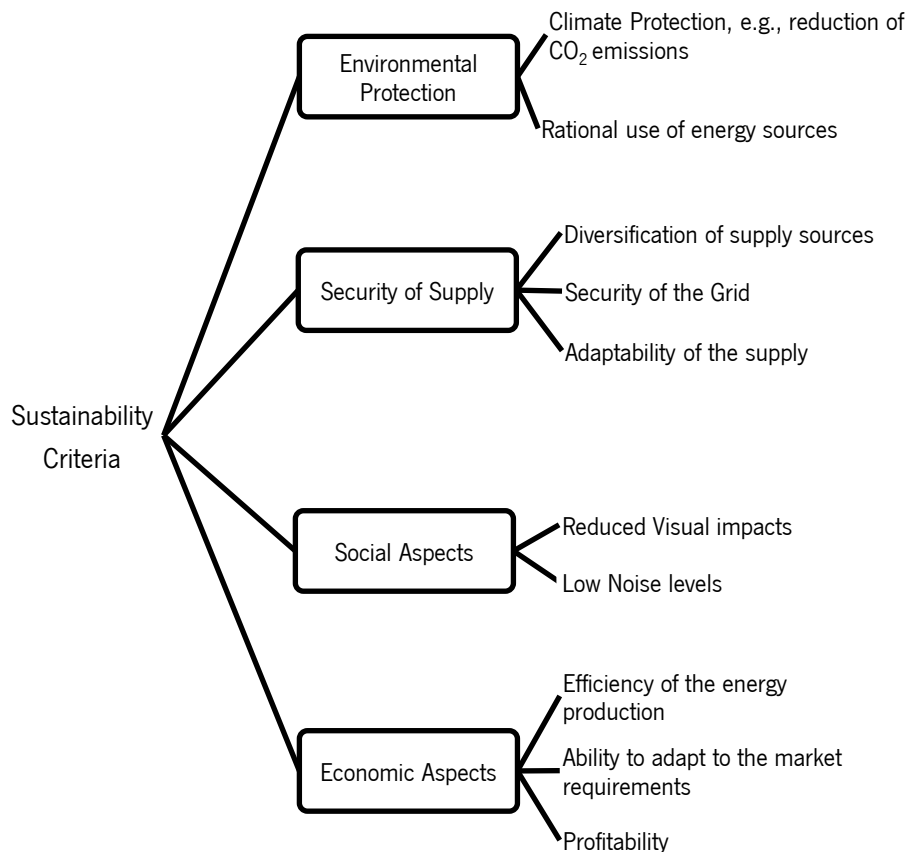
Figure 7.3 Sustainability criteria used in the cogeneration systems evaluation.

Regarding to economic aspects, investments in decentralized power plants are rated positively and have the greatest influence concerning its medium/long-term monetization (e.g. exporting total or part of the electricity to the electrical networks). On the other hand, there are the higher investment and maintenance costs of decentralized cogeneration systems, mainly if its acquisition is made by individual consumers.

7.2.3. Cost-effectiveness of Environmental Benefits

Cost effectiveness analysis is a well-known technique, frequently used in the implementation of environmental policies. The basic concept is simple: one can spend a euro only once (Commission, 2006). This means that the aim is to achieve highest environmental profit for each euro invested for environmental purposes. This is useful because the economic cost has to be balanced against the benefit that a cogeneration offers to the environment. The external impacts can be divided into costs (negative externalities) and benefits (positive externalities) depending on the impacts. The incorporation of environmental externalities into the assessment of cogeneration residential systems offers the advantage

of expressing all costs and benefits into a common measuring unit (i.e. monetary value), and thus provides a single measure of the attractiveness of an alternative energy supply option.

The performance of micro cogeneration technologies, regarding environmental aspects, depends mainly on the total conversion efficiency that can be achieved. Nevertheless, the emission reduction and potential of micro-CHP could partially be offset by a "rebound effect", implying that energy savings achieved by a more efficient technology are annulled, by an increase in energy demand. Micro-CHP systems have mainly relied on natural gas, although other fossil fuels, and in a limited extent, renewable energy sources, can be used with most technologies. One of the important questions that arise nowadays is if most micro-CHP systems, which operate on fossil sources, can compete with renewable energy supply systems, for example, solar collectors or biomass boilers. Although micro-CHP systems operating with solar collectors have particular requirements, they could improve the competitiveness of developing renewable-fuel-based technologies for operating micro CHP systems, particularly Stirling engines (Chicco & Mancarella, 2009). Therefore, several important advantages regarding to key sustainability criteria can be summarized: greenhouse emissions and fossil fuel consumption reduction when compared to the average energy supply and even when compared to efficient and state-of-the art separate production of electricity in conventional power plants and heat in condensing boilers. Regarding this, micro-CHP systems are part of the transformation process for power generation, since the use of micro CHP allows more flexibility solutions when compared to centralized power production (Pehnt, 2008; Pehnt et al., 2004).

The cost-benefit analysis can be used to estimate the social and environmental effects of an investment in thermal-power systems. The value attached to the visual impacts or the noise levels can be considered "priceless". The so-called high-efficient power plants, such as the cogeneration systems, generate a positive environmental externality given the decrease of air pollutants emissions. Pollutant emissions are difficult to account for the evaluation of the environmental externalities.

Considering that, several authors disclose that a strategic approach is needed to adequately embed the new technology, investment and operation practices in the expectations and living conditions of the potential users of micro-CHP systems. Pilavachi, Roumpeas, Minett, and Afgan (2006) defend that the development, construction and operation of small and micro-CHP systems must be evaluated according to economic, social and environmental aspects in an integrated way and the results of the evaluation should be compared by means of the sustainability scores. Huangfu, Wu, Wang, Kong, and Wei (2007) presented a study in which an analysis of a micro-scale combined cooling, heating and power system was performed. The economic efficiency of the system is discussed in terms of different criteria: payback period, initial costs, annual savings and profits, operating cost, calculation of the interest rate, payback time and net present value. Gulli (2006) presented a social cost-benefit analysis of small CHP distributed generation system. The analysis is based on the determination of internal (calculation of optimal electricity and fuel costs) and the external costs by applying the *ExternE* approach. The methodology of *ExternE*

approach includes the weighting of the external impacts using quantitative procedures in order to transform these impacts into monetary units. The author developed a comparison between the centralized and the decentralized energy supply concluding that, despite the optimism about decentralized power production, their implementation in the residential sector does not represent a competitive solution. The reported approach may represent a good approximation to determine the damages from pollutant emissions and the damage would be quantified as an "energy footprint". Alanne, Söderholm, Sirén, and Beausoleil-Morrison (2010) presented a techno-economic strategy to evaluate the performance of different configurations of a Stirling engine-based residential micro-cogeneration system. In the evaluation procedure, the variables considered were the annual costs, primary energy use and CO2 emissions. In this study, the economic viability of the system is based on the capacity to recover the capital investment costs by the annual savings during a certain period of time.

The environmental effects are usually grouped in order to identify the potential environmental effects (grouped into 7 topics: human toxicity (NO_x, SO_x emissions), global warming (CO_2, CH_4 emissions), aquatic toxicity, acidification (presence of NO_x, NH_3, and SO_x), eutrophication, ozone depletion, potential for photochemical ozone creation) provided for each of the pollutants, so that a wide range of pollutants can be directly compared or aggregated and expressed as an overall effect. The most common environment effects identified for the CHP residential system and analysed in this project are: reduction in emission of gas emissions and the reduction in primary energy consumption. In the specific case of this study, as it is intended to optimize a micro-CHP system based on Stirling engine with a renewable energy source, a solar collector, the challenge is apportioning costs (money) to the avoided emissions when compare to centralized energy production. Emissions from current Stirling engine burners can be ten times lower than those of ICE engines based on Otto or Diesel cycles without catalytic converters (Aliabadi et al., 2009).

So, the approach was to determine the cost effectiveness of the annual reduction of gas emissions by the micro-CHP system by attributing to it a monetary value. This could be a path to monetize an environmental benefit from the use of micro-CHP systems. Though, the evaluation of the environmental benefit can be made by two indexes: the reduction of total consumption of primary energy and the reduction in CO_2 emissions. Although the value of the monetization of carbon dioxide emissions is relatively low when compared with the other terms of the objective function (see results from Table 6.23), It contributes to the annual worth maximization. The results also prove that if the environmental benefits from using CHP technologies are accounted economically, this type of technologies will become more attractive as an effective alternative for energy supply. Obviously, the results of the optimal solution are deeply related with the constants assumed in the model, namely, the fuel and the electricity FIT. As matter of fact, the optimal solution is strongly correlated with the components performance/cost assumptions considered in the model (Ferreira, Nunes, Teixeira, & Martins, 2014).

It is important to be aware of whether or not the carbon dioxide emission costs have been included, as they might have a significant impact on the energy production costs if a life cycle cost analysis is considered (Fahlén & Ahlgren, 2010).

7.2.4. Primary Energy and Carbon Emission Savings

As a consequence of the primary energy saving, CHP systems can also be an effective means to pursue the objectives of the Kyoto's Protocol in terms of greenhouse gas emission reduction. However, on a country-wise basis these benefits are strongly related to the generation mix characteristics of the relevant power system. Hence, the adoption of cogeneration has been pushed forward from a regulatory point of view in several countries, above all in those ones where the power generation mix is mostly based on thermal plants, so that CHP production can also bring consistent CO_2 emission reduction. Besides the incentives available for cogeneration, CHP system profitability could be further improved by the possibility of accessing new energy-related markets (e.g., for green certificates, or emission allowances).

The Portuguese Decree-Law 23/2010 established the guidelines for high-efficiency cogeneration based on useful heat demand, which is considered a priority due to its potential PES and consequently reducing CO2 emissions, as well as, the remuneration scheme for the cogeneration production.

The energy and environmental benefits, in terms of primary energy saving of the CHP technology with respect to the separate production of electricity and heat can be evaluated through the PES index. The amount of primary energy provided by cogeneration production (in percentage) is calculated according to equation (7.1):

$$PES = \left(1 - \frac{1}{\dfrac{\eta_{th_{CHP}}}{\eta_{th_{ref}}} + \dfrac{\eta_{el_{CHP}}}{\eta_{el_{ref}}}} \right) \cdot 100 \qquad (7.1)$$

where $\eta_{th_{CHP}}$ is the cogeneration heat efficiency, defined as the annual useful heat output divided by the fuel energy input. The terms $\eta_{th_{ref}}$ and $\eta_{el_{ref}}$ are the efficiency reference values for the separate production of heat and electricity, respectively. Finally, $\eta_{el_{CHP}}$ is the electrical efficiency of the cogeneration production defined as annual electricity from cogeneration divided by the fuel input used to produce the sum of useful heat output and electricity from the cogeneration system.

The equivalent CO_2 avoided emissions can be calculated in order to estimate the reduction of gas emissions from using cogeneration systems to produce a certain amount of energy. Thus, CES allows estimating the carbon emission savings that are possible to achieve by a cogeneration unit, considering

the combined electric and thermal efficiencies, when compared with the conventional energy production process. This index can be calculated as in equation (7.2):

$$CES = \left(1 - \frac{\dfrac{1}{\eta_{el\,CHP}} FE_{CO_2,CHP}}{\sum y_i \dfrac{FE_{CO_2,i}}{\eta_i} + \dfrac{\lambda}{\eta_B} FE_{CO_2,CHP}} \right).100 \qquad (7.2)$$

where $\eta_{el\,CHP}$ is the electrical efficiency of the CHP unit, $FE_{CO_2,CHP}$ is the equivalent carbon dioxide emission factor from the fuel used by the cogeneration unit, and $FE_{CO_2,i}$ is the equivalent carbon dioxide emission factor from the conventional power production. The $FE_{CO_2,i}$ takes into account the specific CO_2 factor of the respective type of energy source multiplied by its fraction in energy mix. Correction factors relating to the average climatic situation was considered in the assumption of electric grid efficiency. The ambient temperature correction is based on the difference between the annual average temperature in a Member State and standard ISO conditions (15°C). A value of 0.1 % point efficiency is subtracted for every degree above ISO conditions. Correction factors for avoided grid losses for the application of the harmonised efficiency reference values were also accounted.

The values obtained for CES and PES considering different commercial systems based on Stirling Engine technologies and for the optimal solution from the thermal-economic model (OptSEA) is presented in Table 7.1. Notice that it was assumed that 100% of electricity exported to the grid and the technical data for the commercial systems was based on Table 2.3, Chapter 2.

Table 7.1 Primary Energy and Carbon emission savings for several micro-CHP systems

System	CES (%)	PES (%)
Whispergen	18.8	15.29
Baxi Ecogen	19.1	15.12
Sunmachine	21.6	15.95
SM5A	19.7	13.45
Solo 161	29.8	24.10
OptSEA	33.3	26.6

Cogeneration reduces the amount of primary energy used to produce the same energy output when compared with the conventional (separate) production and its quantification represents an environmental and economic benefit. CHP systems can contribute to the primary energy savings as well as for the reduction of carbon emissions, not only through higher efficiencies, but also through the use of renewable fuels. The most common fuel used by cogeneration systems is still the natural gas. For those systems, the

primary energy and the carbon emission savings are mainly due to the high efficiency of those systems in the energy conversion process.

For the systems that can use renewable energy sources, the environmental benefits are even higher since no fossil fuels are consumed by the power plant. This reality is translated by the results from CES and PES calculated at the Table. Despite all of the systems present positive values for both indexes, the best outcome was obtained for the OptSEA outcome, which was modelled to use a clean energy source, the solar radiation.

7.3 Economic Evaluation

The economic optimization in the design of CHP systems may be based on the analysis of investment criteria for project selection. Prior to the analysis of economic criteria, it is necessary to define two important aspects: the life time of the project analysis and the definition of the minimum attractive rate of the return. An assertive determination of the minimum attractive rate is decisive because it influences the result of the economic evaluation. According to Biezma & Cristóbal (2006), the economic analysis, separated from the technical, is usually performed via investment criteria in order to perform a comparison of project alternatives. Engineers need tools to make wise economic decisions. These tools can be applied to independent projects to determine whether or not to invest. The typical steps of an economic evaluation of a project include: (1) the establishment of the analysis period for economic study; (2) the specification of the attractive rate of return for that project; (3) the estimation of the project cash flow; (3) acceptation or rejection based on the established criteria.

Numerous criteria are available and the methods used in cogeneration systems selection can be categorized according to the information that each one provides about the project. The NPV method is used in capital budgeting to analyse the cash flows that an investment or a project will yield. Four economic criteria can be calculated: the present worth and future worth which give the cash flows of a project to one equivalent present and future data, respectively; the Annual Worth (AW) that converts all cash flows to a series of equal cash flows for the n number of years of the project lifetime; and the capitalized worth that represents the present worth evaluated over an infinite length of time. Concerning these methods, a project is accepted if the criteria have a positive value. The limitation of the NPV methods is a fair comparison can be made only when NPV values represent costs associated with equal service and assumes constant attractive rate throughout the analysis period.

The use of Rate of Return methods implies a positive present worth. These methods include the Internal Rate of Return (IRR) and the growth rate of return. The IRR is the rate that equates the present value of a project's cash outflow with the present value of its cash inflow. In other words, it concerns the interest rate for which the present value of a project is equal to zero.

The Payback Period methods returns the number of the years required to recover the amount of capital invested in the project. The main disadvantages of these methods are related to the fact that it ignores any benefits that occurs after the payback period, not measuring the project's profitability. In addition it does not take into account the time value of the money. All these economic evaluation methods provide valuable information about the projects. However, the NPV, IRR and the payback period indicators are the more common criteria used to evaluate the economic optimization of CHP systems and the three generally used to accept or reject a project (Biezma & Cristóbal, 2006; Larsson, Fantazzini, Davidsson, Kullander, & Höök, 2014). The economic criteria: NPV, IRR and payback period was calculated considering the investment on the optimal micro-CHP system based on Stirling engine disclosed by this study. After determining all the terms, the annual Cash Flows (CF) of the cogeneration plant can be calculated.

$$NPV = -|CF0| + \frac{CF1}{(1+i_e)} + \frac{CF2}{(1+i_e)^2} + ... + \frac{CFn}{(1+i_e)^n} \tag{7.3}$$

The project cash flow includes the annual payments (e.g. operational costs) and receipts (e.g. incomes from selling electricity to the grid, the economic bonification from CES and the avoided costs from producing heat) for the project lifetime. For our subject matter, CHP systems, n is considered to be 20 years. The term *CF0* (i.e. investment year) includes into the analysis the capital investment cost to purchase the CHP power plant and the costs of a solar collector. Notice that the price for solar collector includes installation and tank needed to energy storage. The solar collector cost estimation is presented in Annex III. The residual value of the thermal plant is also accounted at the end of the investment period.

IRR was also calculated as an indicator for the economics of the investment project. Expressing economic feasibility by means of IRR makes it easier to compare different power plants types or sizes. It is the current value of all actual or future cash flows over a given number of years at a predetermined interest rate. An investment is considered profitable if IRR is higher than the current interest rate, in order to take into account the risk of the investment. Considering the obtained economic output for the optimal solution, investment criteria like the VA, IRR and the payback period were calculated (Table 7.2).

Table 7.2 Economic indexes for the project evaluation

NPV, [€]	6 389
IRR, [%]	10.04
PP	8 years and 6 months

Results shows that the investment can be recovered over a period of 8 years and approximately 6 months, which is less than half of system life period considered in the study. The IRR obtained was of 10.04%, which suggests that the investment on the micro-CHP system with these performance characteristics is

economically attractive, once the interest rate was assumed to be 7%. Results disclosed a NPV of the 6389 € for an interest rate of 7% and a 20 years lifetime project. Despite the numerous investment criteria available, practically the only ones used without a specific criterion to evaluate the economic viability of a certain investment have been the NPV, IRR and payback period. However, in order to select a project it would be convenient to apply more than one scenario to obtain additional information to make a decision. A sensitivity analysis to the lifetime project period was considered and the NPV and IRR variation for different project lifetime periods is presented in Figure 7.4.
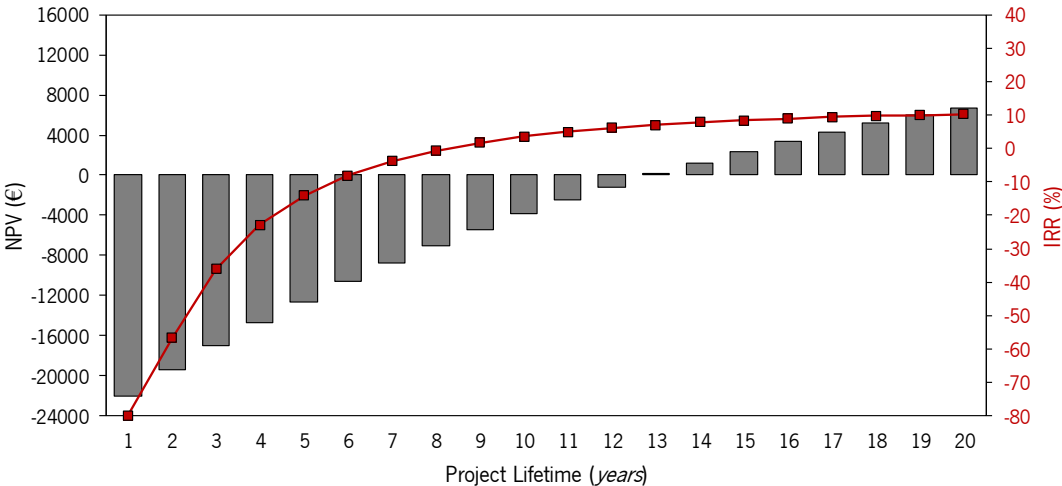
Figure 7.4 Variation of the NPV and IRR at the different number of years for the project lifetime.

According to the data, the economic viability of this micro-CHP system, taking into account all the technical and economic assumptions, presents a positive NPV for a lifetime period above 13 years. For a lifetime period equal or below 13 years, the internal rate of return is lower than the interest rate at which the present value of the future cash flows equals the investment cost. Considering the IRR variation, the investment is clearly profitable if the project is considered to be at least 14 years, once the IRR is above the interest rate defined. These results are due to the high investment with the thermal system and with the installation of the solar collector. Possibly, it is reasonable to include the solar collector in the thermal-economic optimization model in order to optimize this component, minimizing the costs from its installation. Due to the mutability of the economy, it would be also interesting to analyse the NPV if other interest rates were applied. Table 7.3 presents the NPV values considering different interest rates for the same lifetime period (20 years).

Table 7.3 Project NPV values considering different interest rates

	i_e [%]					
	3	4	5	6	7	8
NPV [€]	19785	15865	12431	9413	6389	4395

Data from Table 7.3 shows that the interest rate that is applied in the economic analysis has a great impact in the NPV. Interest rate is used to determine the present value of a stream of future cash flows and it has a significant impact on project feasibility, since the choice of the interest rate is one of the major cost factors for capital-intensive power generating technologies. In this regard, the reviewed studies differ considerably in their interest rate assumptions, making difficult a fair comparison of the results. This leads to generalize that the energy production costs are dependent on the used interest rate.

Alanne, K., Salo, A., Saari, A., & Gustafsson, S.-I. (2007). Multi-criteria evaluation of residential energy supply systems. *Energy and Buildings*, *39*(12), 1218–1226. doi:10.1016/j.enbuild.2007.01.009

Alanne, K., Söderholm, N., Sirén, K., & Beausoleil-Morrison, I. (2010). Techno-economic assessment and optimization of Stirling engine micro-cogeneration systems in residential buildings. *Energy Conversion and Management*, *51*(12), 2635–2646. doi:10.1016/j.enconman.2010.05.029

Aliabadi, A. a., Thomson, M. J., Wallace, J. S., Tzanetakis, T., Lamont, W., & Di Carlo, J. (2009). Efficiency and Emissions Measurement of a Stirling-Engine-Based Residential Microcogeneration System Run on Diesel and Biodiesel. *Energy & Fuels*, *23*(2), 1032–1039. doi:10.1021/ef800778g

Barbieri, E. S., Spina, P. R., & Venturini, M. (2012). Analysis of innovative micro-CHP systems to meet household energy demands. *Applied Energy*, *97*, 723–733. doi:10.1016/j.apenergy.2011.11.081

Biezma, M. V., & Cristóbal, J. R. S. (2006). Investment criteria for the selection of cogeneration plants—a state of the art review. *Applied Thermal Engineering*, *26*(5-6), 583–588. doi:10.1016/j.applthermaleng.2005.07.006

Chicco, G., & Mancarella, P. (2009). Distributed multi-generation: A comprehensive view. *Renewable and Sustainable Energy Reviews*, *13*(3), 535–551. doi:10.1016/j.rser.2007.11.014

Commission, E. (2006). *Economics and Cross-Media Effects* (pp. 1–175). European Commision.

De Paepe, M., & Mertens, D. (2007). Combined heat and power in a liberalised energy market. *Energy Conversion and Management*, *48*(9), 2542–2555. doi:10.1016/j.enconman.2007.03.019

Fahlén, E., & Ahlgren, E. O. (2010). Accounting for external costs in a study of a Swedish district-heating system – An assessment of environmental policies. *Energy Policy*, *38*(9), 4909–4920. doi:10.1016/j.enpol.2010.03.049

Ferreira, A. C., Nunes, M. L., Teixeira, S., & Martins, L. B. (2014). Technical-economic evaluation of a cogeneration technology. *International Journal of Sustainable Energy Planning and Management*, *XX*, 1–14.

Gulli, F. (2006). Small distributed generation versus centralised supply: a social cost–benefit analysis in the residential and service sectors. *Energy Policy*, *34*(7), 804–832. doi:10.1016/j.enpol.2004.08.008

Huangfu, Y., Wu, J. Y., Wang, R. Z., Kong, X. Q., & Wei, B. H. (2007). Evaluation and analysis of novel micro-scale combined cooling, heating and power (MCCHP) system. *Energy Conversion and Management*, *48*(5), 1703–1709. doi:10.1016/j.enconman.2006.11.008

Karger, C. R., & Hennings, W. (2009). Sustainability evaluation of decentralized electricity generation. *Renewable and Sustainable Energy Reviews*, *13*(3), 583–593. doi:10.1016/j.rser.2007.11.003

Larsson, S., Fantazzini, D., Davidsson, S., Kullander, S., & Höök, M. (2014). Reviewing electricity production cost assessments. *Renewable and Sustainable Energy Reviews*, *30*, 170–183. doi:10.1016/j.rser.2013.09.028

Østergaard, P. A. (2009). Reviewing optimisation criteria for energy systems analyses of renewable energy integration. *Energy*, *34*(9), 1236–1245. doi:10.1016/j.energy.2009.05.004

Pehnt, M. (2008). Environmental impacts of distributed energy systems—The case of micro cogeneration. *Environmental Science & Policy*, *11*(1), 25–37. doi:10.1016/j.envsci.2007.07.001

Pehnt, M., Praetorius, B., Schumacher, K., Berlin, D. I. W., Fischer, C., Schneider, L., ... Voß, J. (2004). *Micro CHP – a sustainable innovation?* (p. 32).

Pilavachi, P. a., Roumpeas, C. P., Minett, S., & Afgan, N. H. (2006). Multi-criteria evaluation for CHP system options. *Energy Conversion and Management*, *47*(20), 3519–3529. doi:10.1016/j.enconman.2006.03.004

Smit, R. (2006). Distributed Generation and Renewables. Arnhem, Netherlands: Copper Development Association Institution of Engineering and Technology Endorsed Training Provider. Retrieved from www.kema.com

Soliño, M., Prada, a., & Vázquez, M. X. (2009). Green electricity externalities: Forest biomass in an Atlantic European Region. *Biomass and Bioenergy*, *33*(3), 407–414. doi:10.1016/j.biombioe.2008.08.017

This page was intentionally left in blank

Numerical Optimization and Economic Analysis in the Design of a micro-CHP System with a Stirling Engine and a Solar Collector

8

Conclusions and Future Work |

8.1 Main Conclusions and Final Remarks

8.2 Suggestions of Future Work

The main objective of this project was to develop a methodology for the thermal-economic optimisation, at the design stage, of micro-CHP systems based on Stirling engine technology. In this research work, specific concepts and methodologies related to the thermal systems modelling, costing methodologies and application of numerical optimization methods were presented and discussed. Furthermore, general issues associated with the efficiency of computational methods to simulate real engineering problems were investigated. This chapter outlines the main conclusions and suggests possible lines of future work.

8.1. Main Conclusions and Final Remarks

The development of a model for a solar powered Stirling engine for micro-CHP applications integrated two main components: the definition of the thermodynamic model that described the Stirling engine operation and the definition of a set of cost equations able to describe the purchase cost of each system component. Both models were integrated in the optimization model in order to discover the optimal technical configuration for the system that will lead to the best possible economic output.

The possibility to use a renewable energy source is very important from the point of primary energy savings and reduction of carbon emissions. These features make the Stirling engine a suitable choice, as prime mover, tin the development of new cogeneration systems for the energy supply of residential buildings.

As imposed by an EU Directive, cogeneration plants are being sized and operated to match the thermal loads of the end-users. Micro-scale systems based on Stirling engines are typically designed to provide electricity in the range of 1-10 kW$_{el}$ and fairly larger heating loads, which appears to be a good opportunity

---

to meet the global energy needs of households. Thus, one of the most important aspects was to properly evaluate the thermal energy requirements of residential buildings.

A simplified methodology was defined to estimate the annual thermal power duration curve of a building that includes both the heating and the domestic hot water needs. Both thermal loads were calculated according to the Portuguese regulation for the thermal behaviour of buildings. The calculated peak thermal demand was approximately 7 kW$_{th}$ for a reference dwelling.

The research project led to an extensive study of the thermodynamic cycle of an alpha configuration Stirling engine. A mathematical model was defined assuming the engine as a set of five connected components, consisting of the compression space, cooler, regenerator, heater and the expansion space. Each engine component represents an entity endowed with its respective time-dependent volume, temperature, pressure and mass. The hot source temperature was assumed considering that the energy source is concentrated solar radiation and the engine cold sink is a mass flow of water that removes heat from the cooler to produce hot water.

Three approaches were considered for the thermodynamic analysis: isothermal, ideal adiabatic and a non-ideal analysis. The isothermal analysis assumes that the expansion and compression spaces are maintained at constant temperatures. In the ideal-adiabatic analysis, the compression and expansion spaces are considered adiabatic, and thus their temperatures are not constant, but all the heat-transfer processes are still considered as perfect. This is not the case with the non-ideal analysis that accounts for temperature differences both in the heater and cooler, a non-perfect regeneration process where the heat internally and reversely transferred suffers a reduction, and losses due to flow friction. From the comparative analysis it could be concluded that:

- The isothermal analysis is usually used as the classical approach to assess the theoretical maximum for the performance of a Stirling engine, given its size, geometry and gas operating pressure, although it considers all the heat transfer processes as perfect.

- In the isothermal and ideal adiabatic analysis, the engine power was proportional to mean pressure and engine rotational speed.

- The heat-transfer limitations strongly affect engine performance and the non-ideal effects of the regeneration are mainly due to the convective thermal resistance between the gas and the regenerator surface.

- The pumping losses refer to fluid friction associated with the flow through the three heat exchangers, resulting in a pressure drop between the compression and expansion spaces and thus to a reduction in the power output.

In addition to the analysis of the Stirling engine thermodynamics, a sensitivity analysis to the physical model was performed considering the non-ideal analysis. The effects of those parameters were mainly evaluated in terms of engine efficiency, power production and heat exchangers effectiveness. Moreover,

the results were analysed considering the use of different working fluids (i.e. helium and hydrogen). A few conclusions were disclosed from the analysis performed to the physical model:

- The pumping losses increase with operational mean pressure and engine rotational speed and the latter has a larger effect.

- The heat exchangers effectiveness is slightly higher for helium when compared with hydrogen. The fact may be explained through their thermal-physical properties. In fact, the thermal diffusivity of helium is higher than that of hydrogen, which improves heat transfer, but the density and viscosity are also higher. Hydrogen has better results in terms of power, efficiency and lower pressure drop.

- The heat source temperature has a great impact in the Stirling engine performance. The study of each geometric parameter of the Stirling engine thermal components provided an insight into the relations of those parameters with engine performance. Also, the individual analysis of the geometric parameters gave solid bases to decide which decision variables were the most relevant to be chosen for the thermo-economic optimization.

- The internal diameter and the number of the heater and cooler tubes, the wire diameter and the matrix regenerator porosity are the geometrical parameters with highest relevance in the heat exchangers effectiveness.

A costing methodology was developed to define the purchase cost equations of the system. The purchase cost equations relate the cost of the thermal components with the physical parameters that have relevance in the cost definition. The costing methodology evidenced a good correlation between the physical and cost coefficients in determining the total system cost. Moreover, the cost methodology was validated by using data from already available commercial systems.

The thermal-economic model was based on the definition of an economic objective function (i.e. the maximization of the annual worth) subject to the physical constraints. The results from the thermal-economic optimization disclosed that:

- The integration of physical and economic models allowed the identification of better combinations for the physical system parameters that resulted into lower investment and operational costs and in an increase in the engine performance and revenues.

- All the tested combinations of decision variables and optimization algorithms yielded optimal solutions with net profits.

- The objective function terms that most contribute to the positive balance of the annual profit, corresponds to revenue from selling electricity to the grid and the avoided costs in the production of heat. It is important to mention that the analysis assumed a fixed tariff for the electricity price. It must be recalled that the tariff can be very changeable over time and also depends on the legislation of the country. Other values may result in an unviable economic result. As expected, the thermal energy demand strongly influences CHP system profitability. An auxiliary boiler may be required to

meet the peak thermal demands when the prime mover in CHP configuration cannot achieve the thermal demand.

- The thermal-economic optimization disclosed a thermal system based on a Stirling engine prime mover, able to produce 3.0 kW_{el} and approximately 10.5 kW_{th}. Assuming a life time investment of 20 years with a fixed discount rate of 7%, it corresponds to an economic viable investment with a payback period of eight years and six months and with an internal rate of return of nearly 10%.

Regarding the economic evaluation and the analysis of the micro-CHP systems, it was concluded that:

- The economic aspect is, indeed, the most relevant when assessing this king of energy solutions. Yet, systems able to run with renewable and non-expensive energy sources are viewed positively.

- The possibility to use decentralized energy systems to supply the energy needs of residential consumers is seen as a positive fact, mainly if the systems are able to convert energy in a cleaner and efficient way.

- The monetization of the environmental benefits corresponds to an effective incentive to invest in this type of systems. This fact coupled with the current legislation that obliges additional measures to fulfil the environmental targets, may represent an advantage from purchasing and installing these CHP systems.

- The work has shown that different numerical methods may result in different optimal solutions. This outcome may be due on how the algorithm is implemented, the definition of the solution search domain and if the search algorithm is a local or a global optimization algorithm.

The model developed presents some limitations: the complexity of the thermodynamic cycle, the lack of technical data from the current commercial systems resulted in the adoption of some simplifications. Also, to correlate physical parameters and define reference cost coefficients requires a hard work and an extensive sensitivity analysis of the parameters. Nevertheless, the approach followed in this research project, provided information that is not available through the conventional energy analysis and economic evaluation, which is crucial to the design and operation of a cost-effective system. In fact, this methodology combined two types of optimization: thermodynamic and economic, where the thermodynamic optimization emphasizes the efficiency of the cogeneration system whereas, the economic one minimizes the levelized costs of the electricity and heat produced and assesses the profits.

In the design of complex thermal systems, the definition of representative models is a complex process. Also, even if all the required information is available, the definition of purchased-thermal system costs, as a function of the appropriate thermodynamic decision variables does not guarantee the mathematical model to be fully accurate. Nevertheless, there is a good correlation between the numerical models and the real thermal-economic output.

8.2. Suggestions of Future Work

There is ample scope for improving the work developed within this thesis. With regard to the field of numerical optimization, a more comprehensive sensitivity analysis could be made to the optimization model. These tests may include sensitivity studies of numerical parameters, by applying different optimization algorithms, for instance, heuristic methods such as the particle swarm algorithm. Other few suggestions can be made as future work:

- The solar collector is not yet included into the optimization model, being its costs only accounted in the final economic evaluation of the optimal solution. The inclusion of the solar collector in the optimization model could be an important improvement to the model. Also, the thermal-economic model could be tested considering different energy sources, e.g., biomass and evaluate the system performance.

- The influence of the cost variables and legislative restrictions (e.g. feed-in-tariffs) could be studied in order to evaluate the system feasibility in other markets.

- An additional suggestion for future work is to perform a comparative study of the results from this study to those from other alternative technologies, namely micro-gas turbines. Several thermal-economic studies were previously conducted for small-scale cogeneration systems based on micro-gas turbines for the building sector. A fair comparison could be performed to investigate the efficiency, the economic output and other few indexes (e.g. PES, CES) when covering the same energy demands for a reference building case.

- The maximization of a Stirling engine performance is limited by its correct conceptual design and optimal construction of all components. Computational Fluid Dynamics (CFD) models, describing real processes which occur in external heat supply engines, can be used to simulate the dynamics and heat transfer of Stirling engine components.

- Finally, the physical implementation of a test case/prototype to perform experimental tests would be useful and, therefore, to validate all the performed numerical studies.

This page was intentionally left in blank

Numerical Optimization and Economic Analysis in the Design of a micro-CHP System with a Stirling Engine and a Solar Collector

List of Publications |

International Journals

2014   Ferreira, A.C., Nunes, M.L., Teixeira, S., and Martins, L.B., Thermal Analysis and Cost Estimation of Stirling Cycle Engine, submitted to the Journal of World Scientific and Engineering Academy and Society (WSEAS) Transactions on Power Systems, March, 2014 (under review).

2014   Ferreira, A.C., Nunes, M.L., Teixeira, S., and Martins, L.B. Technical-economic evaluation of a cogeneration technology. International journal of Sustainable Energy Planning and Management, Vol. XX, (2014), 1–14 (accepted in edition).

2012   Ferreira, A. C. M., Nunes, M. L., Teixeira, S. F. C. F., Leão, C. P., Silva, Â. M., Teixeira, J. C. F., & Martins, L. A. S. B. (2012). An economic perspective on the optimisation of a small-scale cogeneration system for the Portuguese scenario. Energy, 45(1), 436–444. doi:10.1016/j.energy.2012.05.054.

2012   Ferreira, A. C. M., Rocha, A. M. A. C., Teixeira, S. F. C. F., Nunes, M. L., & Martins, L. A. S. B. (2012). On Solving the Profit Maximization of Small Cogeneration Systems. ICCSA 2012 - 12th International Conference on Computational Science and Its Applications - Lecture Notes in Computer Science Journal, 7335, 147–158. doi:10.1007/978-3-642-31137-6_11.

2011   Ferreira, A. C. M., Nunes, M. L., Leão, C. P., Teixeira, S. F. C., Silva, Â. M., Martins, L. A. S. B., & Teixeira, J. C. (2011). Thermo-Economic Optimization of CHP Systems: from large to small scale applications. International Journal of Engineering and Industrial Management, 3, 175–192.

Conference Proceedings

2014   Ferreira, A.C., Nunes, M.L., Teixeira, S., and Martins, L.B., Analysis of the Geometrical Parameters of Thermal Components in a Stirling Engine, submitted and accepted at World Congress on Computational Mechanics (WCCM XI), Barcelona, 2014.

2014   Ferreira, A.C., Oliveira, R., Nunes, M.L., Martins, L.B., & Teixeira, S.F. (2014). Modelling and Cost Estimation of Stirling Engine for CHP Applications. In A. Bulucea & E. M.Dias (Eds.), Proceedings of the International Conference on Power Systems, Energy, Environment (Vol. Energy, pp. 21–29). ISBN: 9781618042217

2013   Ferreira, A. C., Teixeira, S., Ferreira, C., Teixeira, J., Nunes, M. L., & Martins, L. B. (2013). Thermal-Economic Modelling of a Micro-CHP Unit Based on a Stirling Engine. In ASME (Ed.), Volume 6A: Energy (p. V06AT07A036). San Diego, California, USA: ASME. doi:10.1115/IMECE2013-65126

2013 Ferreira, A. C., Teixeira, S. F., Teixeira, J. C. F., Nunes, M. L., & Martins, L. B. (2013). Exergy Efficiency Optimization for Gas Turbine Based Cogeneration Systems. In ASME (Ed.), Volume 6A: Energy (p. V06AT07A064). San Diego, EUA: ASME. doi:10.1115/IMECE2013-65080

2013 Ferreira, A. C., Martins, L. B., Teixeira, S. F. C. F., & Nunes, M. L. (2013). Stirling micro-CHP based systems: a sustainable innovation? In 8th Conference on Sustainable Development of Energy, Water and Environment Systems – SDEWES (pp. 443–1; 443–12). Dubrovnik. ISSN: 1847-7178

2013 Ferreira, A.C., Teixeira, S. F., Martins, L. B., & Nunes, M. L. (2013). Techno-Economic Evaluation of Cogeneration Units Considering Carbon Emission Savings. In ICEE - 1st International Congress on Energy & Environment: bringing together Economics and Engineering (pp. 1209–1221). Oporto.

2013 Ferreira, A.C.M., Costa, J. M., Nunes, M. L., Teixeira, S. F. C. F., Teixeira, J. C. F., & Martins, L. a. S. B. (2013). Techno-Economical issues in the design of a heat-regenerator for Stirling engines. In 2° Encontro Nacional de Engenharia e Gestão Industrial (Vol. 45, pp. 1–2). Aveiro. ISSN: 03605442

2013 Ferreira, A., Nunes, L., Teixeira, S., Silva, A., Martins, L., & Teixeira, J. (2013). Techno-Economic and Exergy Analysis of a Small-Scale CHP Unit Based on a Micro-gas Turbine. In Proceedings of MICROGEN 3 International Conference on Microgeneration and Related Technologies. Naples, Italy

2012 Ferreira, A. C., Teixeira, S., Teixeira, J. C., Nunes, M. L., & Martins, L. B. (2012). Modelling a Stirling Engine for Cogeneration Applications. In Volume 6: Energy, Parts A and B (p. 361). Houston: ASME. doi:10.1115/IMECE2012-88183

2012 Ferreira, A. C., Nunes, M. L., Martins, L. B., & Teixeira, S. (2012). Innovation on Decentralised Power Production: The Sustainability of Micro-Cogeneration for the Portuguese Market. In C. Vivas & F. Lucas (Eds.), ECIE 2012: 7th European Conference on Innovation and Entrepreneurship (Vol. 2, pp. 217–227). Academic Publishing International. Retrieved from repositorium.sdum.uminho.pt /handle/1822/27989

2012 Ferreira, A. C. M., Nunes, M. L., Martins, L. A. S. B., & Teixeira. (2012). A Review of Stirling Engine Technologies applied to micro-Cogeneration Systems. In U. Desideri, G. Manfrida, & E. Sciubba (Eds.), ECOS 2012 - 25th International Conference on Efficiency, Cost, Optimization, Simulation and Environmental Impact of Energy Systems (Vol. I, pp. 1–11). Perugia, Italy. Retrieved from http://digital.casalini.it/9788866553229

2012 Ferreira, A. C. M., Martins, L. B., Teixeira, S. F., & Nunes, M. L. (2012). Techno-Economic Assessment of Micro-CHP Systems. In Proceedings of XVIII International Conference on Industrial Engineering and Operations Management (ICIEOM) (pp. 1–10). Guimarães. ISBN: 978-85-88478-43-5 Retrieved from repositorium.sdum.uminho.pt/handle/1822/27990

2012 Ferreira, A. C., Nunes, M. L., Martins, L. B., & Teixeira, S. (2012). Optimization of Small Scale Cogeneration Systems: Comparison of Nonlinear Optimization Algorithms. In H. V. (Eds.) A. Andrade-Campos, N. Lopes, R.A.F. Valente (Ed.), YIC 2012 - ECCOMAS Young Investigators Conference Proceedings (pp. 1–10). Aveiro. Retrieved from repositorium.sdum.uminho.pt /handle/1822/27988

2011 Martins, L. B., Ferreira, A. C. M., Nunes, M. L., Leão, C. P., Teixeira, S. F. C. F., Marques, F., & Teixeira, J. C. F. (2011). Optimal Design of Micro-Turbine Cogeneration Systems for the Portuguese Buildings Sector. In ASME (Ed.), Volume 4: Energy Systems Analysis, Thermodynamics and Sustainability; Combustion Science and Engineering; Nano engineering for Energy, Parts A and B (pp. 179–186). Denver: ASME. doi:10.1115/IMECE2011-64470

2011 Marques, F., Teixeira, S., Martins, L. B., Ferreira, A. C. M., Nunes, M.L., Leão, C.P., (2011). Optimization of a small-scale cogeneration system as a function of the thermal demand. In 4th International Congress on Energy and Environment Engineering and Management (4 pgs.). Merida. ISBN: 978-84-9978-014-6

2011 Ferreira, A. C. M., Martins, L. A. S. B., Nunes, M. L., & Teixeira, S. F. C. F. (2011). Development of a Cost-benefit Model for Micro CHP Systems. In Proceedings of ICOPEV '2011 1st International Conference on Project Economic Evaluation (pp. 1–7). Guimarães. ISBN: 978-989-97050-1-2. Retrieved from http://repositorium.sdum.uminho.pt/handle/1822/27990

2010 Ferreira, A. C. M., Madureira, F., Nunes, M. L., Leão, C. P., Teixeira, S. F. C. F., Teixeira, J. C. F., & Martins, L. B. (2010). Development and Evaluation of a Micro-Cogeneration Prototype for Residential Applications. In Volume 5: Energy Systems Analysis, Thermodynamics and Sustainability; Nano Engineering for Energy; Engineering to Address Climate Change, Parts A and B (pp. 1357–1364). ASME. doi:10.1115/IMECE2010-39192

This page was intentionally left in blank

Numerical Optimization and Economic Analysis in the Design of a micro-CHP System with a Stirling Engine and a Solar Collector

Annexes |

Annex I Schmidt Analysis

Table AI.1 Schmidt Analysis for Beta and Gama Configuration

Parameter	Beta Engine	Gama Engine
Expansion Space Volumes	$V_e = \dfrac{V_{sw,e}}{2}(1-cos\,\theta) + V_{d,e}$	$V_e = \dfrac{V_{sw,e}}{2}(1-cos\,\theta) + V_{d,e}$
Compression Space Volume	$V_c = \dfrac{V_{sw,e}}{2}(1-cos\,\theta) +$ $\dfrac{V_{sw,c}}{2}\left[1-cos(\theta-\omega)\right] + V_{d,c} - V_B$	$V_c = \dfrac{V_{sw,e}}{2}(1-cos\,\theta) +$ $\dfrac{V_{sw,c}}{2}\left[1-cos(\theta-\omega)\right] + V_{d,c}$
Total Volume	$V = V_e + V_r + V_c$	
Temperature	$T = \dfrac{T_c}{T_e}$	
Swept Volumes	$V = \dfrac{V_{sw,c}}{V_{sw,e}}$	
Dead Volumes	$X_{d,e} = \dfrac{V_{d,e}}{V_{sw,e}} \quad X_{d,c} = \dfrac{V_{d,c}}{V_{sw,e}} \quad X_r = \dfrac{V_r}{V_{sw,e}}$	
Total Mass	$M = \dfrac{PV_e}{RT_e} + \dfrac{PV_r}{RT_r} + \dfrac{PV_c}{RT_c}$	
Constants of the right-angled triangle for Schmidt Analysis	$\vartheta \sin\beta = \dfrac{V_{sw,e} \cdot \sin\omega}{2T_h}$ $\vartheta \cos\beta = \dfrac{V_{sw,e} \cdot \cos\omega}{2T_h} + \dfrac{V_{sw,c}}{2T_k}$ $\beta = \tan^{-1}\left(\dfrac{\dfrac{V_{sw,e} \cdot \sin\omega}{T_h}}{\dfrac{V_{sw,e} \cdot \cos\omega}{T_h} + \dfrac{V_{sw,c}}{T_k}} \right)$ $\vartheta = \dfrac{1}{2}\left(\left(\dfrac{V_{sw,e}}{T_h}\right)^2 + 2\dfrac{V_{sw,e}}{T_h}\dfrac{V_{sw,c}}{T_k}\cdot\cos\omega + \left(\dfrac{V_{sw,c}}{T_k}\right)^2 \right)^{1/2}$	
Mean Pressure	$p_{med} = \dfrac{1}{2\pi}\oint p\,d\theta = \dfrac{2M\,RT_c}{V_{pe}\sqrt{S^2 - B^2}}$	
Pressure	$P = \dfrac{M \cdot R}{s \cdot \left(1 + \dfrac{\vartheta}{s}\cdot\cos(\theta+\beta)\right)}$	

## Annex II Technical specifications of commercial Stirling CHP Systems

Table AII.1 Technical specifications, purchase costs of 5 commercial Stirling CHP systems

General Information					
Model Designation	EcoGen WGS 20.1	eVita 25s, eVita 28c	WhisperGen	5 - ZGM - 1 kW	SOLO Stirling 161
Manufacter	August Brotje GmbH	De Dietrich Remeha GmbH	Whispertech	ENERLYT NATUFEUER AG	SOLO Kleinmotoren
Engine Feature	Free Piston	Free Piston	4 Stirling Cycles-Motor (Siemens)	5 Stirling Cycles-Motor (Siemens)	V-2-Cylinder
Engine Configuration	beta	beta	alpha	alpha	alpha
Cylinder Capacity (cm^3)	-	-	-	328	160
Development Date	1995	1995 (engine), 2005 (full)	1993	2004	2004
Development Stage	Available	Available	Available	Experimental Phase	Available
Dimensins (L x A x P) (mm)	493 x 918 x 466	490 x 910 x 471	491 x 838 x 563	700 x 1500 x 520	1280x700x980
Weight (kg)	134	128	154	150	460
Noise (dB)	less than 46	≤ 46	< 46	< 40	-
Fuel	NG Biogás, GPL	NG	NG Biogás, GPL	NG	NG, LPG, pellets
Technical Specifications					
Thermal Output (kW)	3,3 - 20	3,5 - 23,7 (Stirling-Motor 3,5 - 5,5)	7,5 - 14,5	2.2	ago-26
Electric Output (kW)	0,31 - 1	0,7 - 1	1	1	2-9.5
CO Emission (mg/Nm^3)	29.6	37	< 100	2.9	50
NOx Emission (mg/m^3)	29.9	32	< 70	134.2	80-120
Total Efficiency (%)	107.4	98.6	95	91.4	92-96
Elect. Efficency (%)	15.0	13.9	12	28.6	22-24.5
Transmission	-	Free Piston	Wobble-Yoke	No gears	-
Rotational Speed (rpm)	3000	-	1500	1100	1500
Working Gas	Helium	Helium	Nitrogen	Nitrogen, Helium	Helium
Mean Pressure (bar)	23 bar a 25 °C no interior	23	28	6.5	150
Hot Heat Exchanger (°C)	-	530	-	800	700
Cold Heat Exchanger (°C)	-	-	-	70	30
max. temperature of heated water (°C)	70	65	70	65	65
Maintenance					
maintenance cycle (h)	.	8760	4000	6000	5800
Life time period (h)	50000	45000 - 50000	40000	> 100000	180000
Price					
Price (€)	13645	11950	8500	13000	25000

Solar collectors and thermal energy storage components are the two kernel subsystems in solar thermal applications. Solar collectors are usually classified into two categories according to concentration ratios: the non-concentrating collectors and concentrating collectors. A solar collector, the special energy exchanger, converts solar irradiation energy either to the thermal energy of the working fluid in solar thermal applications. For solar thermal applications, solar irradiation is absorbed by a solar collector as heat which is then transferred to its working fluid (air, water or oil). The heat carried by the working fluid can be used to either provide domestic hot water/heating, or to charge a thermal energy storage tank from which the heat can be drawn for use later (e.g. during the night periods). A non-concentrating collector has the same intercepting area as its absorbing area, whereas a sun-tracking concentrating solar collector usually has concave reflecting surfaces to intercept and focus the solar irradiation to a much smaller receiving area, resulting in an increased heat flux so that the thermodynamic cycle can achieve higher Carnot efficiency when working under higher temperatures. Regarding the concentrating collectors, they are usually equipped with sun-tracking devices and have much higher concentration ratio than non-concentrating collectors (Dascomb, 2009).

In the literature several dish-solar thermal collectors are reported to work in conjunction with Stirling engines for thermal-electrical power applications. Parabolic dish collectors use an array of parabolic dish-shaped mirrors (similar in shape to a satellite dish) to focus solar energy onto a receiver located at the common focal point of the dish mirrors. Heat transfer fluid contained in the receiver is then heated up to desirable working temperatures and pressures in order to generate electricity in the engine attached to the receiver. Parabolic dish-engine systems are characterized by high efficiency, low start-up losses and can be easily scaled up to meet the power needs in remote area, where centralised power supply is too expensive. Parabolic trough collectors can concentrate sunlight with a con- centration rate of around 40, depending on the trough size.
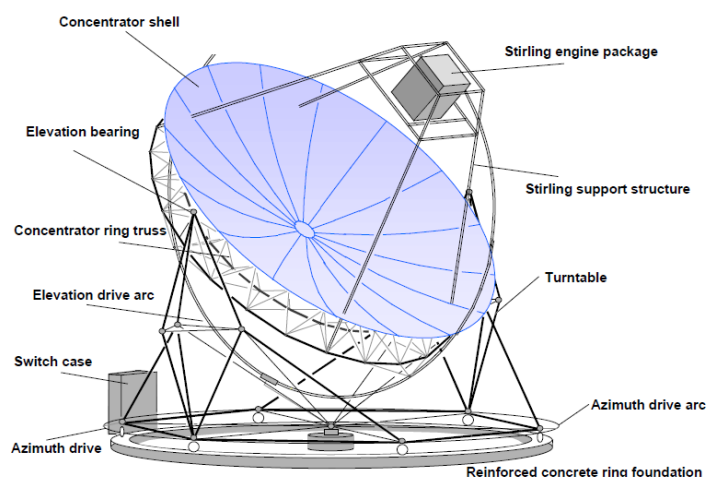
Figure AIII.1 Solar dish concentrator. Adapted from (Schlaich Bergermann & Partner GbR, 2001).

The key component of such collectors is a set of parabolic mirrors, each of which has the capability to reflect the sunlight that is parallel to its symmetrical axis to its common focal line. At the focal line, a black

metal receiver (covered by a glass tube to reduce heat loss) is placed to absorb collected heat. Parabolic trough collectors can be orientated through tracking the sun.

The parabolic collectors consist of solar collectors (mirrors), heat receivers and support structures. The parabolic-shaped mirrors are constructed by forming a sheet of reflective material into a parabolic shape that concentrates incoming sunlight onto a central receiver tube at the focal point. Since the concentrator always needs to be perfectly oriented towards the sun light, tracking system.

The receiver for this system acts as an absorber, boiler, and heat storage unit. The receiver is the part of the system that converts solar radiation to heat energy in a working fluid. The receiver consists of an absorber, heat exchanger and possibly heat storage. The absorber is the impinging surface for rejected solar radiation to strike. Radiation is absorbed into the absorber material as heat. The heat exchanger transfers the energy to a working fluid that carries the energy out of the receiver.

A methodology can be applied in order to calculate the area of the solar collector ($A_{collector}$) needed to provide the total energy based on the domestic hot water and heating needs, as in equation (AIII.1):

$$A_{collector} = \frac{Q_{dhw} + WHD}{Energy\ flow\ absorved} \Leftrightarrow A_{collector} = \frac{Q_{dhw} + WDH}{\eta_{collector}.\Gamma_0} \qquad \text{(AIII.1)}$$

where $\eta_{collector}$ is the average efficiency of the collector, Γ_0 the average solar irradiation. According to Nepveu, Ferriere and Bataille (2009), the direct solar irradiation is of 906 W/m². According to the implemented methodology, the peak thermal demand is about 7 kW$_{th}$. The efficiency of the collector is in fact a function of the exterior temperature, as disclosed by the equation (AIII.1), that was presented by Der Minassians and Sanders (2011):

$$\eta_{collector} = \eta_0 - \frac{U}{G}\left(T - T_{ref}\right) \qquad \text{(AIII.2)}$$

Where η_0 is the maximum collector efficiency, U is the thermal loss coefficient, G is the power density of the incident sun light, T is the mean temperature of the collector and T_{ref} is the ambient temperature.

The features and the cost per area of two commercial models are presented in Table AIII 1.

Table AIII 1 Market information about parabolic solar collectors

Collector Model	η_0 [%]	U [W/m².K]	Collector Cost per area [€/m²]
AOSOL CPC 1.5x	75	4.280	114.3
SOLEL CPC 2000 1.2x	91	4.080	309.6

Considering the SOLEL CPC 2000 model the reference case for calculations, the collector efficiency was calculated assuming the value of 515 W/m² for the variable G, as presented by the equations (AIII.3)

$$\eta_{collector} = 0.4778 \Leftrightarrow \eta_{collector} = 47.78\% \qquad \text{(AIII.3)}$$

Once the efficiency of the solar collector was determined, the area of the solar collector can be calculated assuming the peak thermal energy demand calculated in chapter 3. Then, and according to equation (AIII.4), the area of the collector is estimated to be:

$$A_{collector} = \frac{7.0 kW}{0.47 * 0.906 kW.m^{-2}.K^{-1}} = 16.44 m^2 \qquad \text{(AIII.4)}$$

Therefore, the cost of the solar collector can be estimated considering the cost per area of surface. The costs for a few commercial inverters and tracking system are reported at Table AIII 2. Note that the installations costs are usually accounted in the Recommended Retail Prices (RRP).

Table AIII 2 List of equipment costs for solar collector installation

Model	Price [€]
Tracking Systems	
SS2X_01 3M Metalogalva	4320
SS2X_O1 4M Metalogalva	4385
SS2X_01 5M Metalogalva	4485
Inverters	
AJ 400 – 48V Solar energias Renováveis Lda	333
AJ 500 – 12V Solar energias Renováveis Lda	579
AJ600 – 24V Solar energias Renováveis Lda	529

In the Table AIII 3, the assumed prices for the solar collector, inverters and tracking systems are presented. These values were used to define the cash flow maps of the investment.

Table AIII 3 List of equipment costs for solar collector installation

Model		Price [€]
Solar Collector (SOLEL CPC 2000 1.2x)		5090
Tracking system (SS2X_01 4M Metalogalva)		4385
Inverter (AJ 400 – 48V Solar energias Renováveis Lda)		333
	Total	9808

References

Dascomb, J. (2009). *Low-cost Concentrating Solar Collector for Steam Generation*. Florida State University.

Der Minassians, A., & Sanders, S. R. (2011). Stirling Engines for Distributed Low-Cost Solar-Thermal-Electric Power Generation. *Journal of Solar Energy Engineering*, *133*(1), 011015. doi:10.1115/1.4003144

Nepveu, F., Ferriere, A., & Bataille, F. (2009). Thermal model of a dish/Stirling systems. *Solar Energy*, *83*(1), 81–89. doi:10.1016/j.solener.2008.07.008

Schlaich Bergermann & Partner GbR. (2001). EuroDish - Stirling System Description. Stuttgarter, Germany: MERO-Raumstruktur GmbH&Co Mr.

Annex IV Economic Feasibility study

Table AIV 1 Cash flow map of the economic feasibility study for the CHP system

Data
Porject Lifetime   20 years
Discount Rate [%]   7%

	0	1	2	3	4	5	6	7	8	9	10	11	12	13	14	15	16	17	18	19	20
Solar Collector	-5090																				
Tracking System + Installation Costs	-4718																				
Initial Investment Costs	-15836																				
Fuel Costs		0	0	0	0	0	0	0	0	0	0	0	0	0	0	0	0	0	0	0	0
Cm		-180	-180	-180	-180	-180	-180	-180	-180	-180	-180	-180	-180	-180	-180	-180	-180	-180	-180	-180	-180
Rsell		1440	1440	1440	1440	1440	1440	1440	1440	1440	1440	1440	1440	1440	1440	1440	1440	1440	1440	1440	1440
Rres		0	0	0	0	0	0	0	0	0	0	0	0	0	0	0	0	0	0	0	436.2
RCES		73	73	73	73	73	73	73	73	73	73	73	73	73	73	73	73	73	73	73	73
C avoided		1680	1680	1680	1680	1680	1680	1680	1680	1680	1680	1680	1680	1680	1680	1680	1680	1680	1680	1680	1680
Cash Flow	-25644	3013	3013	3013	3013	3013	3013	3013	3013	3013	3013	3013	3013	3013	3013	3013	3013	3013	3013	3013	3449.2
NPV	6388.49																				
IRR	10.04%																				
Payback Period	-25644	-22631	-19618	-16605	-13592	-10579	-7566	-4553	-1540	1473	4486	7499	10512	13525	16538	19551	22564	25577	28590	31603	35052.2

The payback period corresponds to 8 years and approximately 6 months